UNIVERSIDAD COMPLUTENSE DE MADRID
FACULTAD DE CIENCIAS QUÍMICAS
Departamento de Bioquímica y Biología Molecular

TESIS DOCTORAL

Estudio del papel del epitelio pulmonar en la alergia: el polen de olivo como modelo experimental

Study of the role of the pulmonary epithelium in allergy: olive polen as an experimental model

MEMORIA PARA OPTAR AL GRADO DE DOCTOR

PRESENTADA POR

Juan Carlos López Rodríguez

Directoras

Eva Batanero Cremades
María Teresa Villalba Díaz

Madrid
Ed. electrónica 2019

© Juan Carlos López Rodríguez, 2019

UNIVERSIDAD COMPLUTENSE DE MADRID

FACULTAD DE CIENCIAS QUÍMICAS

Departamento de Bioquímica y Biología Molecular

ESTUDIO DEL PAPEL DEL EPITELIO PULMONAR EN LA ALERGIA. EL POLEN DE OLIVO COMO MODELO EXPERIMENTAL

STUDY OF THE ROLE OF THE PULMONARY EPITHELIUM IN ALLERGY. OLIVE POLLEN AS AN EXPERIMENTAL MODEL

TESIS DOCTORAL

Juan Carlos López Rodríguez

DIRIGIDA POR

Eva Batanero Cremades

María Teresa Villalba Díaz

Madrid, 2019

A quienes hicieron de su pasado mi presente,

A mis madres Nieves y Candelas, y a mis padres Cristóbal y Juan Manuel

La investigación presentada en esta *Tesis Doctoral* se ha realizado en el Departamento de Bioquímica y Biología Molecular, de la Facultad de CC. Químicas de la Universidad Complutense de Madrid (UCM), bajo la dirección de las Dras. Eva Batanero Cremades y María Teresa Villalba Díaz y la ayuda del Dr. Rodrigo Barderas Manchado.

Parte del trabajo experimental mostrado se ha llevado a cabo en colaboración con el grupo del Dr. Domingo Barber Hernández y la Dra. María Escribese Alonso del Centro de Excelencia en Metabolómica y Bioanálisis (CEMBIO, Universidad San Pablo-CEU, Madrid, España), con el grupo del Dr. Antonio Martínez Ruiz del Instituto de Investigación Sanitaria del Servicio de Inmunología del Hospital Universitario de La Princesa (Madrid, España), con el grupo de la Dra. Cristobalina Mayorga Mayorga del Instituto de Investigación Biomédica de Málaga (IBIMA, Málaga, España) y con el grupo del Dr. Jesús Pérez Gil de Biofísica de Membranas e Interfases Lipo-proteicas (BioMIL) de la Facultad de Ciencias Biológicas del Departamento de Bioquímica y Biología Molecular de la UCM.

El apoyo financiero principal para la realización de esta *Tesis Doctoral* ha sido proporcionado por el Ministerio de Educación, Cultura y Deporte bajo el Programa de Formación de Profesorado Universitario (FPU13/02393) y un contrato de investigación del Ministerio de Economía y Competitividad bajo la Red Temática de Investigación Cooperativa de Reacciones Adversas a Alérgenos y Fármacos en España (RIRAAF, Instituto de Salud Carlos III).

AGRADECIMIENTOS/ ACKNOWLEDGMENTS

El punto de partida se lo agradezco al Laboratorio 13, a María Antonia y Nieves y en especial al que considero mi “padre científico”, Javier, el cual me enseñó a atarme los “zapatos” y dar los primeros pasos en este mundo.

Una vez “puestas las botas”, el Laboratorio 1 me ofreció su “asfalto”. Gracias por confiar en mí para la puesta en marcha este bonito proyecto desde cero, por el cual sabéis que me he dejado el alma.

A Mayte, agradecerle su apuesta ciega en mí y en mi perfil desde el minuto uno. Espero contar con tu abrazo, ayuda, amistad y consejo siempre.

A Rodrigo por haberme dado tanto. Bien sabes tú que las cosas que uno siente en el corazón no suelen figurar en un papel.

Y a Eva por su amistad e incansable consejo, tanto dentro como fuera del laboratorio. Hoy soy lo que soy gracias a ti, a tu dedicación, tesón, cariño y a un sinfín de cosas que en 240 páginas no puedo agradecerte. El mejor regalo es dedicarte el resultado de estos años en forma de tesis.

Continuando con el Laboratorio 1, mencionar a la pieza angular de todo lo que somos hoy, a Rosalía, a quien admiro sin medida. Así mismo a Laura y Cristina por tantas risas (reguetón y ópera), a Pablo por permitirme conocer a un futuro Nobel de Química, a Sara Abián por ofrecerme una risa gratis cada mañana, llueva o haga sol, salga o no el ELISA, y a Sara Benedé por su ayuda incondicional y amistad durante estos dos años. También quiero acordarme del resto, Ana, María, Juliana, Guille y tantos otros con los que he compartido excelentes momentos.

Y en especial a Carmen, por escucharme y hacerme ver que todo es más auténtico si lo compartes con quien realmente quieres. Como ves, aún por complejo que sea el experimento se pueden obtener grandes resultados, ;).

No podría olvidarme de la ayuda recibida de esta, mi casa. En especial a Pepe, Paco, Belén, Inma, Álvaro, Nacho, Sara, Miriam, Clara, Laura, Rodrigo, Lucía, Javi, y sobre todo, a mi compañera y amiga Esperanza, la cual sé que se va a comer el mundo.

También agradecer este resultado a una larga lista de colaboradores, por su ayuda y cercanía, enriqueciendo mi espíritu científico y por abrirme las puertas de “vuestra casa” sin condiciones. Al Dr. Domingo Barber, a la Dra. María Escribese, al Dr. Antonio Martínez-Ruiz, a la Dra. Lina Mayorga, al Dr. Jesús Pérez-Gil y al Dr. Antonio Cruz por su atención, siempre cercana y constante.

Aquí quiero hacer un apartado especial a todos los componentes del grupo BioMil, en especial a Chiara, Raquel, Nuria, Alberto y Marta, por dejarme compartir tantos buenos ratos -profesionales y personales- a vuestro lado. Un placer realizar este viaje juntos.

Also, I would like to thank to Prof. Diefenbach’s group for welcoming me during three spectacular months in Mainz. Concretely, I would like to highlight the warm experimental support received from Irene, making me grow in a very short period of time. Also, I wanted to thank to Alica, Alina and Nadja (my German flatmates) for making me feel their home as mine.

Por último, a mis amigos, a Patricia, Alberto, Rebeca, José, Oscar, Diego, Rita, Aroa, Naomi, y a mi familia, tíos/tías y primos/primas, y a much@s más que seguro sentirán como propia esta tesis.

Índice
Index

Resumen
Summary

La **alergia respiratoria** es uno de los problemas de salud pública con mayor impacto social a nivel mundial, cuya prevalencia ha aumentado de forma alarmante durante los últimos años. Su etiología es compleja e implica la interacción de factores genéticos, factores ambientales y el estilo de vida de los países desarrollados. Este desorden clínico se caracteriza por un proceso inflamatorio de las vías respiratorias, dominado por una respuesta inmune en la que participan linfocitos tipo T-colaboradores 2 (Th2) y la presencia de elevados niveles de inmunoglobulina E específica en el suero frente a sustancias ambientales, denominadas aeroalérgenos, que normalmente son inocuas para la mayoría de los individuos. Cada vez hay más evidencias del importante papel del **epitelio respiratorio** como integrador y regulador de la respuesta alérgica.

Las vías aéreas inferiores humanas están revestidas por una capa de células epiteliales en forma de escutoide que contiene diferentes tipos celulares con funciones definidas. El epitelio respiratorio actúa como barrera física altamente selectiva, al representar la interfase entre el cuerpo y el ambiente externo, mediante la formación de una serie de uniones apicales intercelulares. Además, actúa como elemento integrador y coordinador de la respuesta inmune innata y adaptativa del pulmón, gracias a la presencia de receptores de patrones de reconocimiento y a la secreción de un amplio espectro de mediadores que regulan el desarrollo de la respuesta inmune subsecuente.

Dada la controversia existente sobre si la disfunción del epitelio es la causa o la consecuencia de la respuesta alérgica a un alérgeno, el objetivo principal de esta *Tesis Doctoral* ha sido profundizar en el estudio del papel del epitelio bronquial en la alergia respiratoria, utilizando como modelo **Ole e 1**, el aeroalérgeno más importante del **polen de olivo** (*Olea europaea*). Este polen representa una de las causas principales de polinosis en el área mediterránea y ciertas regiones de EE.UU., América del Sur, Sudáfrica, Japón y Australia, siendo la segunda causa de polinosis en España.

En el primer capítulo se ha estudiado la influencia del **estado de diferenciación** del epitelio bronquial en la respuesta inmune a Ole e 1. Para ello, se estableció y caracterizó un modelo *in vitro* de epitelio bronquial basado en cultivos primarios de células epiteliales bronquiales humanas (NHBE) crecidas en interfase aire-líquido (ALI). Para dicho estudio se utilizaron células NHBE procedentes de dos individuos sanos. Se analizó la respuesta a Ole e 1 a lo largo del proceso de diferenciación, los días 7 y 21 en ALI. Los resultados demostraron que Ole e 1 no afectaba a la formación de la barrera epitelial ni a la diferenciación celular. Sin embargo, si alteraba el patrón de citoquinas del secretado por estas células, en un proceso que era dependiente del estado de diferenciación celular y de las características propias del donante.

En el segundo capítulo se analizó el papel de las **proteasas ambientales** en la respuesta inmune del epitelio bronquial a Ole e 1, utilizando como modelo Der p 1, cisteín-proteasa del ácaro del polvo doméstico, siendo, además, su alérgeno más importante. En esta ocasión se utilizó un modelo *in vitro* de epitelio bronquial basado en la línea celular Calu-3 de células epiteliales bronquiales humanas inmortalizadas, para analizar el efecto de la co-exposición a Der p 1 los días 2 y 7 de cultivo en ALI. Estos dos días corresponden a un epitelio no diferenciado y diferenciado, respectivamente. La co-exposición a Der p 1 no incrementaba la permeabilidad epitelial a Ole e 1, sino que era el estado de diferenciación del epitelio bronquial el que regulaba la permeabilidad. Sin embargo, la exposición crónica a Der p 1 estaba asociada con una elevada permeabilidad a Ole e 1. Por otra parte, Ole e 1 era degradado por Der p 1, lo que generaba una serie de péptidos capaces de unir inmunoglobulina G y activar basófilos derivados de pacientes alérgicos al polen de olivo. El estudio metabolómico comparativo de las células Calu-3 expuestas a Ole e 1 y/o Der p 1 los días 2 y 7 de cultivo en ALI, indicó una gran dependencia del metaboloma del estado de diferenciación del epitelio en el momento de contacto con el alérgeno. Además, ha permitido identificar a la L-arginina, la kinurenina y el L-triptófano como posibles metabolitos implicados en la respuesta alérgica. Por último, también se demostró que la glutatión-S-transferasa pi (GSTpi) humana incrementaba la actividad cisteín-proteasa de Der p 1, pero no la isoenzima GSTmu de ácaro (Der p 8). Además, GSTpi se detectó en el medio apical de las células Calu-3 cultivadas en ALI.

De forma similar, en el tercer capítulo se estudió el efecto de la co-exposición al **humo del tabaco** en la respuesta del epitelio bronquial a Ole e 1. Para ello, se optimizó y estandarizó la preparación del extracto de humo de tabaco (CSE). Las células Calu-3 se expusieron a Ole e 1 en presencia de CSE al 10% durante 24 h, los días 2 y 7 de cultivo en ALI. La co-exposición a CSE incrementaba de forma significativa la permeabilidad de la barrera epitelial a Ole e 1 y la secreción apical de IL-6 de una manera dependiente del estado de diferenciación celular.

Finalmente, se estudiaron las propiedades interfaciales de Ole e 1 en el contexto del **surfactante pulmonar** y de modelos de membranas celulares, utilizando balanzas derivadas de Langmuir. Nuestros estudios han demostrado, por primera vez, que el aeroalérgeno Ole e 1 tiene actividad interfacial y es capaz de interaccionar de forma preferente con dominios lipídicos condensados y ordenados.

En conclusión, los datos obtenidos en esta *Tesis Doctoral* han demostrado que la respuesta del epitelio bronquial a un aeroalérgeno depende de su estado de

diferenciación en el momento de contacto, apoyando que la disfunción del epitelio es la causa y no la consecuencia de la respuesta alérgica. Además, la respuesta del epitelio a un alérgeno puede alterarse por agentes ambientales como proteasas y humo de tabaco. Estos estudios abren una nueva puerta para el entendimiento de los eventos que tienen lugar en las primeras etapas de la sensibilización y el desarrollo de los síntomas de la reacción alérgica en humanos.

Respiratory allergy is one of the public health problems with greatest social impact worldwide, whose prevalence has alarmingly increased in recent years. Allergy etiology is complex and involves the interaction of genetic, environmental factors and the influence of developed countries lifestyle. This clinical disorder is characterized by an exacerbated inflammatory process of the respiratory tract, dominated by an immune response T-helper type 2 (Th2) and the presence in the serum of high levels of specific immunoglobulin E against environmental substances, called aeroallergens, usually harmless to most individuals. In this sense, there is an increasing evidence of the crucial role of the **respiratory epithelium** as a main regulator of the allergic responses.

Human lower airways are continuously lined by a layer of epithelial cells that form a 'scutoid' epithelium containing different cell types with defined functions. Respiratory epithelium acts as a highly selective physical barrier by representing the interface between the body and the environment, throughout the formation of a set of intercellular apical junctions. In addition, it acts as an orchestrator of the innate and adaptive lung immune response thanks to the expression of recognition pattern receptors and the secretion of a broad spectrum of mediators that ultimately regulate the development of the incoming immune response.

Given the existing controversy about whether epithelial dysfunction is the cause or the consequence of the allergic response to an aeroallergen, the main objective of this *Doctoral Thesis* has been to get further insights into the role of bronchial epithelium in respiratory allergy, using as a model **Ole e 1**, the main aeroallergen of **olive pollen** (*Olea europaea*). This pollen represents one of the most important cause of pollinosis in the Mediterranean area and certain regions of USA, South America, South Africa, Japan and Australia, being the second cause of pollinosis in Spain.

In the first chapter, the influence of the **state of differentiation of the bronchial epithelium** on the immune response to Ole e 1 was studied. To this end, an *in vitro* model of bronchial epithelium based on primary cultures of human bronchial epithelial cells (NHBE) cultured at air-liquid interface (ALI) was established and characterized. NHBE cells from two healthy donors were used. The response to Ole e 1 was analysed throughout the differentiation process, on days 7 and 21 at ALI. Results showed that Ole e 1 did not affect the formation of the epithelial barrier and cell differentiation. However, Ole e 1 altered the cytokine pattern secreted by these cells, a process that was dependent on the state of cellular differentiation and donor characteristics.

In the second chapter, the role of **environmental proteases** in the immune response of the bronchial epithelium to Ole e 1 was analysed. Der p 1, which is the main house dust

mite cysteine protease and its most important allergen, was used as model. An *in vitro* model of bronchial epithelium based on the immortalized human cell line Calu-3 was used, in order to analyse the effect of co-exposure to Der p 1 on days 2 and 7 of culture at ALI. These two days correspond to an undifferentiated and differentiated epithelium, respectively. Co-exposure to Der p 1 did not increase the epithelial permeability to Ole e 1, but it was the state of differentiation of the bronchial epithelium that mainly regulated its permeability. Indeed, chronic exposure to Der p 1 was associated with a high permeability to Ole e 1. In addition, Ole e 1 was degraded by Der p 1, which generated a series of peptides capable of binding immunoglobulin G and activating basophils derived of patients allergic to olive pollen. The comparative metabolomics' study of Calu-3 cells exposed to Ole e 1 and/or Der p 1, on days 2 and 7 at ALI, which indicated a great dependence of the metabolome on the state of differentiation of the epithelium at the time of contact with the aeroallergen. L-arginine, kynurenine and L-tryptophan was highlighted as possible markers involved in the allergic process. Finally, it was also demonstrated that human Glutathione-S-transferase pi (GSTpi) increased the cysteine-protease activity of Der p 1, but not the mite-derived GSTmu isoenzyme (Der p 8). GSTpi was also detected in the apical medium of Calu-3 cells cultured at ALI.

Similarly, in the third chapter of this *Doctoral Thesis* we studied the effect of the co-exposure to **cigarette smoke** in the bronchial epithelium response to Ole e 1. For this purpose, the preparation of the cigarette smoke extract (CSE) was optimized and standardized. Calu-3 cells were exposed to Ole e 1 with the presence of 10% CSE for 24 h, on days 2 and 7 of culture at ALI. Co-exposure to CSE significantly increased the permeability of the epithelial barrier to Ole e 1 and the apical secretion of IL-6 in a dose- and cell differentiation state- manner.

Finally, the interfacial properties of Ole e 1 were studied in the context **of pulmonary surfactant** and cell membrane models, using Langmuir-derived balances. Our studies have demonstrated, for the first time, the interfacial activity of an aeroallergen (Ole e 1) and its preferential ability to interact with lipid condensed and ordered domains. Moreover, Ole e 1 was able to inhibit the interface adsorption of native pulmonary surfactant.

In conclusion, the data presented in this *Doctoral Thesis* have demonstrated that the response of the bronchial epithelium to an aeroallergen depends on its state of differentiation at the time of contact, indicating that the dysfunction of the epithelium may act as the cause and not the consequence of the allergic response. In addition, the response of the epithelium to an aeroallergen can be altered by certain environmental

agents such as proteases and for the cigarette smoke. These studies open a new door for understanding the events that take place in early stages of sensitization and the development of the symptoms of allergic reactions in humans.

Introducción
Introduction

EL EPITELIO PULMONAR: ORIGEN, ANATOMÍA Y FUNCIÓN

Hace unos 400 millones de años, en una atmósfera cada vez más enriquecida en oxígeno debido a la fotosíntesis, surgieron en el interior del organismo unas bolsas elásticas como evaginación del endodermo digestivo, los **pulmones**. En la evolución de los vertebrados, los pulmones han desempeñado un papel crucial en la conquista del medio terrestre, como necesidad en la sustitución de órganos relacionados con la ventilación acuática por otros relacionados con la aérea [1]. La gran diversidad estructural y funcional que muestran los pulmones hoy en día es el reflejo de la adaptación evolutiva de los vertebrados (peces pulmonados, anfibios, reptiles y mamíferos) a hábitats muy distintos, un desarrollo condicionado tanto por su constricción filogenética como por la adquisición de niveles adecuados de oxígeno molecular (O_2). Tan óptima es su adaptabilidad que hasta algunos invertebrados como los caracoles terrestres presentan estructuras respiratorias similares a las que hoy se observan en los anfibios.

Los pulmones de un individuo adulto son, en general, órganos pares que se comunican con el exterior por medio de la **tráquea**, la cual se divide en un par de **bronquios** (Figura 1). Cada bronquio se ramifica de manera sucesiva hasta dar lugar a una serie de pequeños **bronquiolos** que terminan en los **alveolos**, unos sacos diminutos muy irrigados donde se produce el intercambio gaseoso.

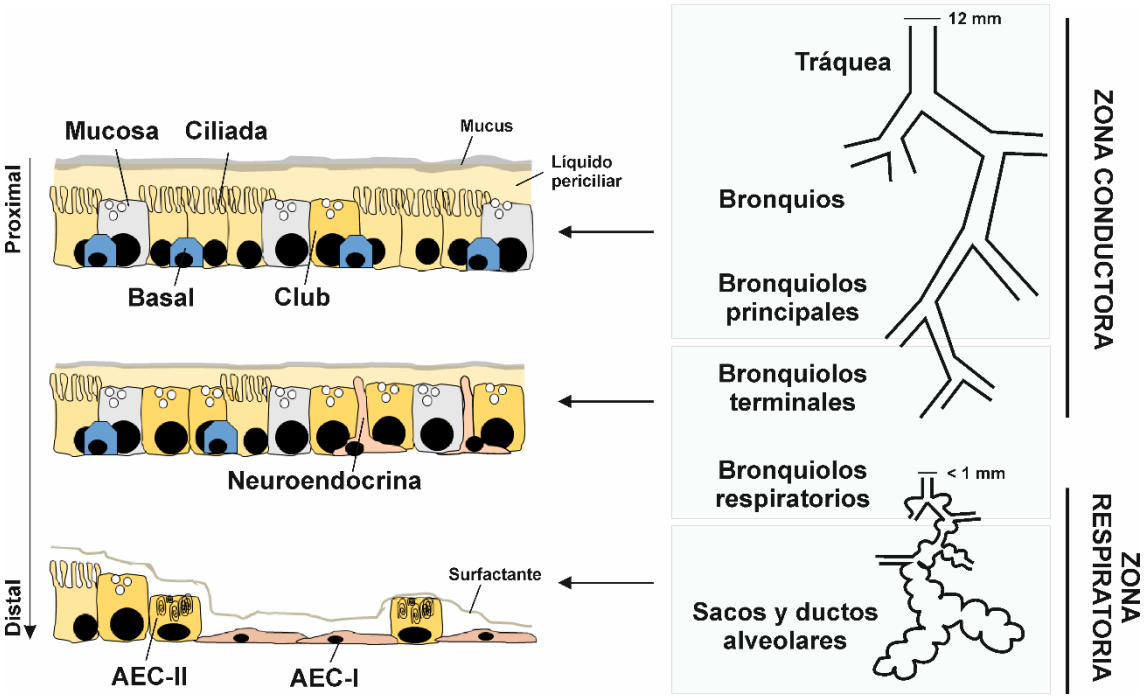

Figura 1. Esquema general de las principales regiones del epitelio pulmonar, indicando los tipos celulares más representativos y su distribución a lo largo de las zonas conductora y respiratoria del tracto respiratorio.

En humanos, los cinco lóbulos que componen este aparato -tres en el pulmón derecho y dos en el izquierdo- están recubiertos por una capa mesotelial, denominada pleura, que dota al pulmón de un entorno húmedo necesario para llevar a cabo el proceso respiratorio.

Atendiendo a su función principal, esta extensa red de tubos ramificados puede dividirse en dos grandes zonas: una zona conductora, encargada de dar direccionalidad al aire inhalado, y una zona respiratoria, donde se lleva a cabo el intercambio gaseoso (Figura 1) [2, 3]. La **zona conductora** es de aspecto cartilaginoso y mayor resistencia por el tono muscular, e incluye a la tráquea, bronquios, los bronquiolos principales y las segmentaciones que poco a poco confluyen en los bronquiolos terminales, aún carentes de alveolización. La **zona respiratoria**, de menor diámetro, comprende los bronquiolos respiratorios y toda una compleja red de sacos alveolares (ductos) que están recubiertos de finos capilares sanguíneos de hasta 10 μm, suficientes para albergar el paso de un eritrocito. Los sacos alveolares abarcan una extensa superficie de hasta 100 m^2 -equivalente al tamaño de un campo de tenis-, y reciben, aproximadamente, un 70% del total del aire inhalado.

Con hasta 6 litros de aire inhalado por minuto, los pulmones están expuestos a una gran variedad de agentes ambientales, tales como virus, bacterias, partículas contaminantes y alérgenos, entre otros. Por ello, la función respiratoria ha de ir acompañada por una eficaz función defensiva, la cual es desempeñada por las células del **epitelio pulmonar** que recubre de forma continua todas las vías respiratorias (Figura 1). La función principal del epitelio pulmonar es la de mantener la homeostasis del pulmón, promoviendo la expulsión del organismo de las sustancias inhaladas, sin inducir una respuesta inflamatoria [4, 5].

La gran variedad de señales a las que está expuesto el epitelio pulmonar hace que su composición sea muy compleja, presentando diferentes tipos celulares que se suceden a lo largo del tracto respiratorio. El **epitelio traqueo-bronquial**, localizado en la región proximal del tracto respiratorio, está formado por la tráquea y los bronquiolos principales, y se compone de una capa pseudoestratificada de células ciliadas y mucosas (en inglés *globet cells*), bajo la cual se distribuyen las células basales [6]. Recientemente, este tipo de disposición geométrica epitelial ha sido renombrada como “escutoide” (de *scutum*, parecido al tórax de los escarabajos) y se considera una adaptación energética del organismo [7]. El epitelio traqueo-bronquial también presenta células de origen no endodérmico, como las células neuroendocrinas.

A medida que se avanza hacia la región distal, el **epitelio bronquial** se hace más cuboideo o columnar y se enriquece en células Club, que secretan surfactante, entre otras sustancias [8]. Finalmente, en la región distal se encuentra el epitelio alveolar, una delgada capa celular compuesta en un 90% por **células alveolares de tipo I** (AEC-I) y un 10% de **células alveolares de tipo II** (AEC-II). Las AEC-I están implicadas en el intercambio gaseoso, mientras que las AEC-II están relacionadas con la producción y la secreción de surfactante pulmonar, así como con la regeneración del epitelio [9].

Las **células ciliadas** constituyen el 50% del total de células epiteliales de la región proximal. Presentan en el lado apical entre 200-300 cilios (de entre 3.6 a 6 μm de longitud), que forman parte del aparato muco-ciliar del epitelio pulmonar, junto con el moco [10]. Energéticamente, el elevado número de mitocondrias presentes en su citosol mantiene el batir coordinado de los cilios. El desarrollo de éstos (ciliogénesis) se encuentra regulado por el factor de transcripción FOXJ1, identificado como el marcador de este tipo celular [11-14]. Además, FOXJ1 regula la actividad de IκB-β, un inhibidor del factor de factor nuclear potenciador de las cadenas ligeras κ de las células B activadas (NFκB), que a su vez controla la expresión de varios genes inflamatorios [15]. El desarrollo del asma, ciertas infecciones víricas y otras enfermedades pulmonares como la enfermedad obstructiva crónica pulmonar (COPD, del inglés *Chronic Obstructive Pulmonary Disease*) han sido relacionadas con una disfunción de la actividad ciliar [16-18]. También la exposición a contaminantes ambientales como el humo de tabaco puede afectar a la función ciliar [19].

Las **células mucosas** son especialmente abundantes en la región proximal del tracto respiratorio, donde representan entre el 5-15% del total de células epiteliales. Se caracterizan por la acumulación apical de gránulos de secreción electro-claros ricos en mucinas ácidas [4, 20]. Las mucinas son glicoproteínas de masa molecular alta (hasta 200 kDa) que, una vez secretadas, forman el moco o *mucus*, una capa visco-elástica de carga negativa [21]. De las doce isoformas descritas en humanos, MUC5AC es la mucina característica de las células mucosas del epitelio pulmonar y se considera un marcador para este tipo celular [22]. La secreción de mucinas está regulada por diversos factores como los ciclos circadianos, la exposición al humo del tabaco o al dióxido de azufre [23-25]. Las células mucosas contribuyen con la secreción del moco al aparato muco-ciliar. La sobreexpresión de estas mucinas (denominada *hiperplasia globosa*) altera las propiedades visco-elásticas del moco, lo cual impide realizar una limpieza muco-ciliar efectiva. La *hiperplasia globosa* es una característica común de pacientes asmáticos o con bronquitis [23]. El moco se localiza en la superficie del **líquido periciliar**

(ELF, del inglés *Epithelial Lining Fluid*), una delgada capa acuosa de apenas 5-10 µm de espesor que cubre la superficie de las vías aéreas. El líquido periciliar contiene, además, moléculas de diferente naturaleza secretadas por las células epiteliales como lisozima, defensinas, lactoferrina, colectinas y glutatión (GSH). Numerosos autores sugieren que las células mucosas exhiben cierta pluripotencialidad, pudiéndose diferenciar incluso a células ciliadas [26, 27].

Las **células Club** -anteriormente denominadas células Clara- son células secretoras que presentan grandes gránulos electro-densos en su citoplasma [28]. Estos gránulos contienen proteínas del surfactante (SP) [29] e inhibidores de proteasas, entre otros [30]. La proteína de secreción de las células Club 10 (CC-10) se considera un marcador específico de este tipo celular [31]. Las células Club participan en procesos de detoxificación de xenobióticos y agentes oxidantes, a través de la expresión de la enzima citocromo P450 mono-oxigenasa [30, 32]. Las células Club también exhiben pluripotencialidad, pudiendo diferenciarse en células ciliadas y mucosas [8, 27].

Las **células basales** son células pequeñas, cuboides y con escaso citoplasma que descansan sobre la lámina basal [6]. Estas células son muy abundantes en la región proximal, donde representan hasta un 20% del total de células epiteliales [33]. Su función principal es el “anclaje” de las células ciliadas y mucosas a la lámina basal mediante la formación de hemidesmosomas. Además, las células basales participan en la regulación de la respuesta inflamatoria a través de la secreción de citoquinas y otros mediadores químicos [34]. Se caracterizan por su gran capacidad de auto-renovación y de trans-diferenciación, pudiendo dar lugar a células ciliadas, mucosas y Club, tanto en reposo [35] como en respuesta a daño severo [36-38]. Como marcador de las células basales se ha identificado a la proteína p63.

El **surfactante pulmonar** es una mezcla compleja de lípidos y proteínas que se localiza entre las capas de moco y de líquido periciliar, a lo largo del tracto respiratorio, siendo especialmente abundante en la región alveolar (Figura 1). El surfactante está presente en todos los mamíferos y es producido principalmente por las células AEC-II, aunque también por las células Club.

El surfactante pulmonar está compuesto en un 90% de lípidos, del tipo fosfolípidos en su mayoría, y el 10% restante por proteínas de las cuales cuatro son específicas: SP-A, -B, -C y -D (Figura 2) [39-41]. La fosfatidilcolina (PC), y en particular, la dipalmitoil-PC (DPPC) es la especie predominante, representando el 40% del total de fosfolípidos. Otros fosfolípidos de carácter aniónico presentes en el surfactante son fosfatidilglicerol (PG) y fosfatidilinositol (PI). Lípidos como fosfatidiletanolamina (PE), fosfatidilserina (PS), plasmalógenos y colesterol aunque también están presentes, son menos abundantes [42, 43].

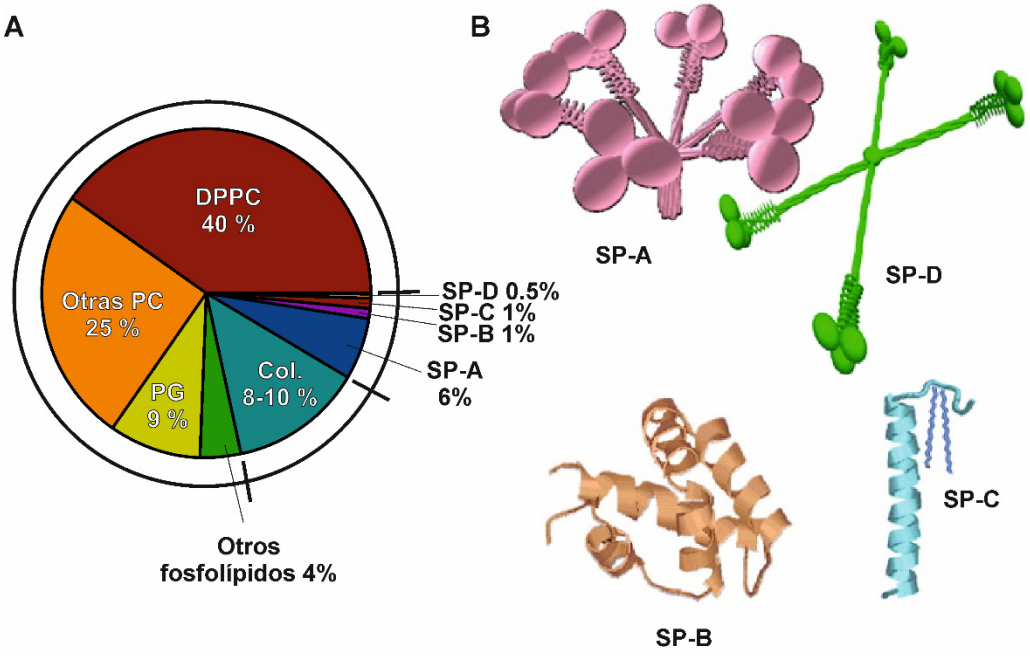

Figura 2. El surfactante pulmonar. A) Composición del surfactante. Se indica el porcentaje en peso de los lípidos y proteínas: Col, colesterol; DPPC, dipalmitoil-fosfatidilcolina; PC, fosfatidilcolina; PG, fosftidilglicerol; SP-A, -B, -C y -D, proteínas del surfactante A, B, C y D, respectivamente. B) Estructura tridimensional de las proteínas del surfactante SP-A, SP-B, SP-C y SP-D. Modelos espaciales compactos de SP-A y SP-D, y diagramas de cintas de SP-B y SP-C de Bauokina *et al.* [44].

El término surfactante proviene de la contracción de la expresión inglesa *surface active agent*, denominado así por su acción tensoactiva en los alveolos. Sus propiedades tensoactivas son clave para la función respiratoria, pues evita el colapso de las cavidades respiratorias durante la respiración al reducir la tensión superficial en la interfase aire-líquido del alvéolo, facilitando el intercambio gaseoso [41, 45]. Sin embargo, el surfactante también participa en los mecanismos de defensa innata del pulmón y exhibe propiedades inmunomoduladoras [40, 41].

La **tensión superficial (γ)** se define como la cantidad de energía necesaria para aumentar la superficie de un solvente por unidad de área y sus unidades son mN/m. Es un fenómeno físico que se genera en la interfase aire-líquido de ciertos solventes acuosos, como es el líquido alveolar. Las fuerzas cohesivas entre las moléculas situadas en la subfase poseen un efecto neto atractivo. Esto no ocurre en aquellas moléculas situadas en la interfase aire-liquido donde las fuerzas superficiales generan una fuerza atractiva neta perpendicular a la superficie del líquido, el cual acaba deformando. En el agua, estas fuerzas cohesivas son los puentes de hidrógeno intermoleculares, con valores de tensión superficial de aproximadamente 70 mN/m, en función de la temperatura. A nivel pulmonar, el surfactante reduce la tensión superficial que ocasionaría el colapso de los alveolos, hasta valores de 1-2 mN/m [46]**.** Los lípidos del surfactante, de naturaleza anfipática, son las moléculas responsables de reducir la tensión superficial, al situarse en la interfase aire-líquido formando una monocapa con la cabeza polar orientada hacia la subfase acuosa y las colas alifáticas apolares expuestas al aire (Figura 3).

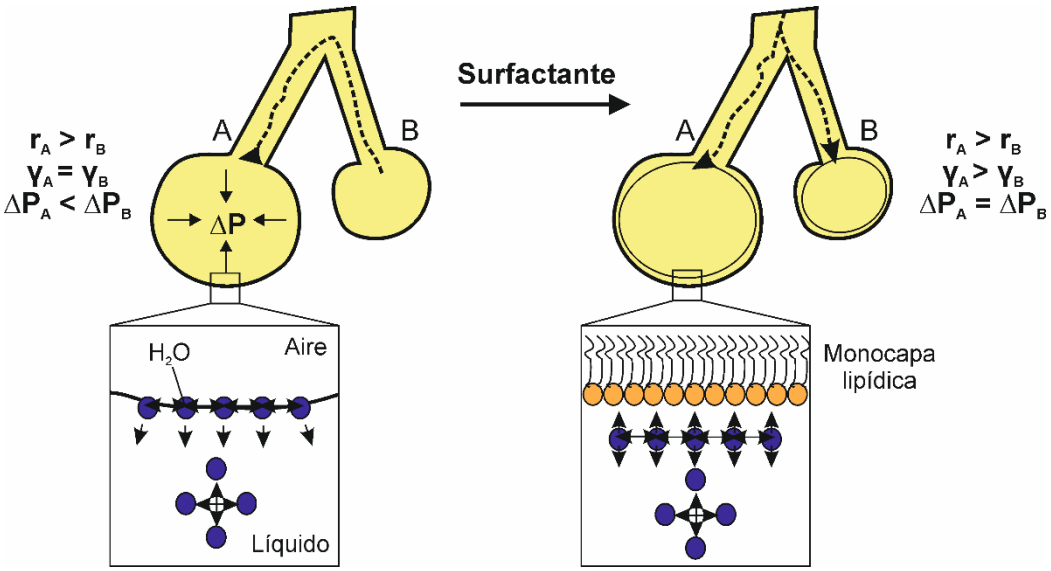

Figura 3. Esquema de la tensión superficial ejercida a nivel del alveolo pulmonar. Según la ley de *Laplace-Young* (ΔP = 2γ/r), en ausencia del surfactante pulmonar, el *alveolo B* de menor radio interno colapsaría en favor del *A* de mayor radio. En presencia del surfactante, el componente lipídico se dispone en la interfase aire-líquido formando una monocapa, ocasionando la reducción de la tensión superficial. Δ*P*, presión interna del alveolo; *γ*, tensión superficial; y *r*, radio interno del alveolo.

Las proteínas del surfactante también desempeñan un papel importante en sus propiedades biofísicas y son, en parte, responsables de sus propiedades inmunológicas [47]. Según su naturaleza polar, las proteínas del surfactante se dividen en dos grupos: proteínas hidrofílicas (SP-A y SP-D) e hidrofóbicas (SP-B y SP-C).

SP-A (28-36 kDa) y **SP-D** (40-48 kDa) son las proteínas más abundantes del surfactante, representando el 6 y 0.5% en masa, respectivamente. Son secretadas por las células AEC-II y las células Club [48]. SP-A y SP-D son proteínas oligoméricas [49] y pertenecen a la familia de las colectinas, denominadas así por contener estructuras proteicas tipo colágeno. Las colectinas participan en la defensa innata del pulmón a través de la opsonización y aglutinación de diferentes patógenos como *Streptococcus pneumoniae, Haemophilus influenzae, Klebsiella pneumoniae, Staphylococcus aureus, Mycoplasma sp.,* adenovirus, virus sincitial respiratorio y *Aspergillus sp*. [50], facilitando su eliminación por los macrófagos. Además, estas colectinas regulan la respuesta inflamatoria en el pulmón, mediante la interacción con células inmunes. Así, SP-D inhibe la desgranulación de mastocitos al agregar alérgenos [51]. SP-A y SP-D inhiben la desgranulación de basófilos [52], la maduración y activación de células dendríticas [53] y la proliferación de linfocitos T [54-56]. Finalmente, SP-A y SP-D unen alérgenos tanto glicosilados [51, 57] como con actividad proteolítica [58, 59].

SP-C y SP-B son proteínas de baja masa molecular: 4.2 y 8.7 kDa, respectivamente. Estas proteínas participan en las propiedades biofísicas del surfactante movilizando lípidos a la interfase aire-líquido desde los reservorios membranosos de la subfase [41, 60]. De esta manera, contribuyen a la reposición del material lipídico envejecido, así como del excluido de la interfase durante los ciclos continuos de compresión-expansión [45]. Por otra parte, SP-C participa en la respuesta inmune del pulmón al unir lipopolisacárido (LPS) bacteriano e interaccionar con receptores de superficie de macrófagos, contribuyendo a la eliminación de patógenos de una forma alternativa a las colectinas [61].

EL EPITELIO PULMONAR COMO BARRERA FÍSICA SELECTIVA

El epitelio respiratorio forma una barrera física continua, altamente selectiva, pues representa la interfase entre el organismo y el ambiente externo. La integridad de la barrera epitelial es crucial para su función y está determinada por el establecimiento de una serie de uniones apicales intercelulares, los denominados **complejos apicales de unión** (**AJC** del inglés *Apical Junction Complexes*) (Figura 4). Los AJC engloban dos tipos de uniones: las **uniones estrechas** (**TJ**, de inglés *Tight Junctions*), situadas en la parte más apical de las células, y las **uniones adherentes** (**AJ**, del inglés *Adherens Junctions*), localizadas bajo las anteriores [5, 62, 63]. Ambas uniones permiten la correcta polarización de las células epiteliales y se regulan mutuamente.

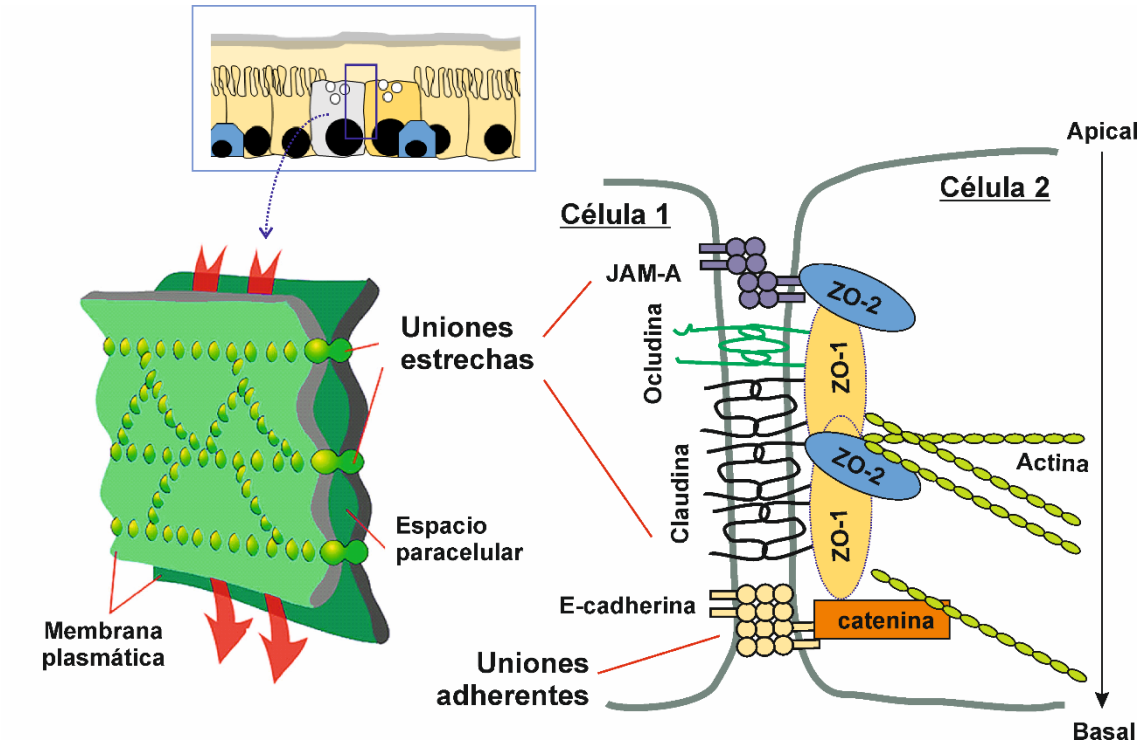

Figura 4. Representación esquemática de los complejos apicales de unión (AJC) que incluyen las uniones estrechas y las uniones adherentes. Adaptado de *Koval Lab* (http://kovallab.org/ic.html). *JAM-A,* del inglés *junctional adhesion molecule A; ZO-1,* proteína *zonula occludens 1*; *ZO-2,* proteína *zonula occludens 2.*

Las TJ están formadas por un complejo multiproteico de proteínas integrales de membrana de distintas familias, incluyendo ocludinas y claudinas, entre otras. Estas proteínas interaccionan con los filamentos de actina del citoesqueleto a través de las proteínas periféricas *zonula occludens* (ZO)-1, -2 y -3 [64]. Ocludinas y claudinas son proteínas homodiméricas, que controlan el transporte paracelular de iones y moléculas pequeñas. Las ocludinas están relacionadas con el ensamblaje *de novo* de las TJ, mientras que las claudinas modulan su expresión para permitir el paso selectivo de solutos [64]. Por ejemplo, las claudinas 1 y 8 tienen una expresión ubicua y regulan positivamente la robustez de las TJ [65]. La presencia de las claudinas 2 y 4 (entre otras isoformas) afecta negativamente a la permeabilidad de la barrera [66, 67], estando sobreexpresadas en pacientes con daño pulmonar severo [68-70]. Por otra parte, algunas proteínas de las TJ actúan como receptores de patógenos. Así, la claudina 1 se ha descrito como receptor del virus de la hepatitis C [71]. Las claudinas y ocludinas son dianas específicas de ciertas proteasas ambientales [72], y su expresión se ve afectada por la exposición a oxidantes ambientales como los presentes en el humo del tabaco [73].

Las AJ son cruciales para el correcto mantenimiento del cinturón de AJC, al regular la formación de las TJ [4] (Figura 4). La E-cadherina, una proteína transmembrana de la

superfamilia de las inmunoglobulinas, es el principal componente de las AJ [74]. La E-cadherina interacciona con los filamentos de actina a través de proteínas citosólicas del tipo cateninas, incluyendo p120-catenina, β-catenina y plakoglobina [75, 76]. La pérdida de la expresión de E-cadherina está relacionada con los procesos de transición epitelio-mesénquima (EMT) del pulmón como ocurre en los pacientes asmáticos [77], así como con la secreción de citoquinas pro-inflamatorias por las células epiteliales [78].

En condiciones normales (homeostasis), el epitelio forma una barrera epitelial casi impermeable y altamente regulada a través de las AJC y complementada por la acción del aparato mucociliar. La alteración de estas uniones resulta en una mayor penetración de partículas inhaladas en el espacio subepitelial, facilitando el muestreo de antígenos y el desarrollo de una respuesta inmune innata y adaptativa. Además, la disfunción de la barrera inicia una cascada de señalización que afecta a la activación y diferenciación de las células epiteliales. En conjunto, disfunción de AJC y señalización, conduce al daño tisular. La disfunción estructural y funcional de la barrera epitelial es una característica común de las enfermedades alérgicas: E-cadherina y ZO-1 están disminuidas en el epitelio de asmáticos [77].

Las AJC pueden alterarse directamente por sustancias inhaladas que atraviesan la capa de moco o indirectamente por ciertas citoquinas como interleuquina-4 (IL-4), IL-13, interferón-gamma (IFN-γ), factor de necrosis tumoral-alfa (TNF-α) y otros mediadores pro-inflamatorios como histamina o triptasa, creando un circuito de retroalimentación [64, 79].

EL EPITELIO PULMONAR COMO BARRERA INMUNOLÓGICA

El epitelio pulmonar actúa, además, como integrador y regulador clave de la respuesta inmune innata y adaptativa en el pulmón. Las células epiteliales son capaces de reconocer y de responder a multitud de estímulos ambientales gracias a la presencia de **receptores de patrones de reconocimiento** (PRRs, del inglés, *Pattern Recognition Receptors*) que se localizan en la membrana apical. Los PRRs reconocen patrones moleculares asociados a patógenos (PAMPs, del inglés *Pathogen Associated Molecular Patterns*) o asociados al daño celular (DAMPs, del inglés *Damage Associated Molecular Patterns*). Entre los PRRs se encuentran los receptores transmembranales de *tipo Toll* (TLRs, del inglés *Toll-like Receptors*), capaces de reconocer componentes bacterianos de la pared celular (TLR-1, -2, -4 y -6), RNA viral (TLR-3, -7 y -8) y motivos CpG no metilados de DNA bacteriano (TLR-9) [24, 80]. Los alérgenos también pueden ser reconocidos por las células epiteliales, tanto por receptores para proteasas (PAR, del

inglés *Protease-Activated Receptors*), como PAR-2, como a través de los receptores de dectina (p.e., dectina 1) que unen azúcares [81].

Como consecuencia de este reconocimiento, el epitelio pulmonar secreta un amplio espectro de moléculas que regulan el desarrollo de la respuesta inmune subsecuente [4, 5, 77].

Las células epiteliales de los pulmones son la principal fuente de las citoquinas **IL-25, IL-33 y linfopoyetina estromal tímica** (**TSLP**, del inglés *Thymic Stromal Lymphopoietin*) -denominadas *la triada-,* las cuáles actúan *upstream* de citoquinas tipo Th2, tales como IL-4, IL-5 e IL-13, que regulan la respuesta inflamatoria y frente a infecciones [82-85]. La desregulación de la triada, característica de pacientes con asma o COPD, podría estar ocasionada por la activación y reclutamiento de células dendríticas (DCs), células linfoides innatas de tipo 2 (ILC2s), mastocitos, eosinófilos, neutrófilos y basófilos [86] (Figura 5). Las células epiteliales también producen IL-1α, cuya acción autocrina induce la secreción de IL-33 y TSLP [87].

Las citoquinas IL-25 e IL-33 actúan como amplificadores de la respuesta inflamatoria [88-90], a través de sus receptores de membrana IL-17RA/IL-17RB e IL-33R, respectivamente [91, 92], los cuáles están presentes en ILC2s, mastocitos y basófilos [93-96]. Así, la IL-33 estimula la desgranulación de mastocitos [97], y la liberación de IL-1β, IL-6, IL-8, TNF-α y la quimioquina CCL-22 (del inglés *C-C motif ligand 22*) [98, 99]. Además, la IL-33 induce la expresión de IL-9 en basófilos y células T-CD4^{+} [100]. Por otra parte, la IL-25 es capaz de llevar a cabo acciones similares y a veces complementarias a las de la IL-33, induciendo la activación de células Th2 vía DCs [101] o promoviendo la proliferación de un subtipo de ILC2s inflamatorias [102].

TSLP es secretada en grandes cantidades por las células epiteliales bronquiales en respuesta a virus, partículas diésel, microbios, alérgenos y helmintos, vía TLRs [103]. La secreción de TSLP también aumenta tras la pérdida de E-cadherina ocasionada por el daño epitelial, así como por la exposición a citoquinas inflamatorias como IL-4 e IL-13 [104, 105]. TSLP actúa a través del receptor heterodimérico IL-7Rα/γc-*chain,* siendo capaz de inducir tanto la migración de DCs como la activación de ILC2s [106-108]. En combinación con IL-33 e IL-25, TSLP regula la secreción de IL-1β, IL-6 y TNF-α por células efectoras [109].

Además de esta triada de citoquinas, las células epiteliales secretan otras muchas moléculas con propiedades antimicrobianas y/o inmunomoduladoras, como antioxidantes, defensinas, inhibidores de proteasas, lactoferrina, lisozima, mediadores lipídicos, mucinas, péptidos antimicrobianos y quimioquinas [110]. Por ejemplo, en respuesta a proteasas ambientales, las células epiteliales secretan GM-CSF (en inglés *Granulocyte/Macrophage Colony-Stimulating Factor*), CCL2 y CCL20 [111], que inducen la quimiotaxis de mastocitos [112] y la activación de DCs y su migración hacia los nódulos linfáticos [113]. Otras moléculas de origen epitelial como las eotaxinas-1, -2 y -3 son capaces de inducir la activación de eosinófilos y de células Th2 en pacientes con asma [114]. Finalmente, las células epiteliales secretan alarminas en respuesta al estrés o a la muerte celular, tales como ATP, ácido úrico, HMGB1 (*High Mobility Group Box 1*) y la propia IL-33, cuyos niveles se encuentran aumentados en pacientes con asma alérgica [115, 116].

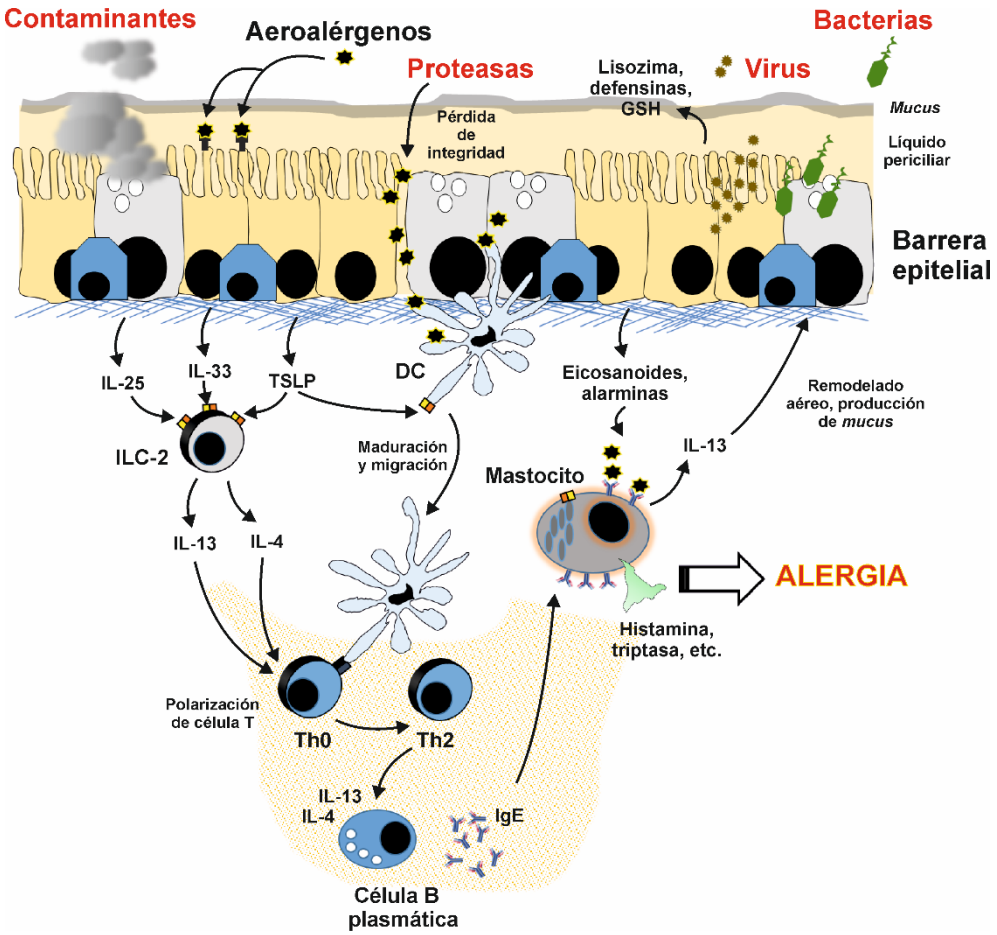

Figura 5. Esquema del mecanismo de la reacción alérgica frente a un aeroalérgeno y su relación con el epitelio pulmonar. Adaptado de López-Rodríguez *et al.* [117].

BIOLOGÍA REDOX EN EL EPITELIO PULMONAR

El epitelio pulmonar está constantemente expuesto a **oxidantes endógenos**, generados como subproductos durante los procesos metabólicos y la actividad de las células inflamatorias [118], así como a múltiples **oxidantes exógenos** de diferente procedencia, tales como el humo del tabaco, las radiaciones ionizantes, los metales y otros contaminantes ambientales [119, 120]. Los pólenes también representan una fuente importante de oxidantes exógenos como resultado de la actividad de enzimas tales como las NADPH-oxidasas, que contribuyen a los niveles de oxidantes del líquido periciliar una vez que alcanzan el epitelio pulmonar, favoreciendo el desarrollo de una reacción alérgica [121].

Los oxidantes endógenos y exógenos son generalmente sustancias muy pequeñas y altamente reactivas. En los organismos aeróbicos, las **especies reactivas de oxígeno (ROS)** derivadas del metabolismo del oxígeno constituyen la familia de oxidantes más relevantes, aunque también existen otras derivadas del nitrógeno (especies reactivas del nitrógeno, **RNS**), del azufre (especies reactivas de azufre) o del cloro (especies reactivas del cloro) [122]. A nivel fisiológico, las especies más relevantes son el anión radical superóxido (O_2^-), el radical hidroxilo (OH^-), el óxido nítrico (NO) y el peróxido de hidrógeno (H_2O_2). NO y O_2^- pueden reaccionar entre sí de forma espontánea y formar anión peroxinitrito ($ONOO^-$) [123].

Los organismos han desarrollado una serie de sistemas antioxidantes –tanto de naturaleza proteica como no proteica- para regular la generación y eliminación de estas especies reactivas. Sin embargo, bajo ciertas condiciones se produce un desequilibrio entre oxidantes y antioxidantes por ruptura de este control, ocasionando daño molecular. Esto es lo que se define como **estrés oxidativo** [124]. El daño oxidativo originado en el DNA, lípidos y proteínas inducido por estas especies reactivas hace que participen en numerosas enfermedades, bien iniciando el proceso patológico o contribuyendo a su progresión y exacerbación. Algunas de las enfermedades relacionadas con el estrés oxidativo son: cáncer, enfermedades cardiovasculares, enfermedades neurodegenerativas, diabetes, enfermedades autoinmunes y alergias, entre otras [125].

En respuesta al estrés oxidativo, las células epiteliales bronquiales y alveolares liberan ROS y RNS, moléculas que actúan como potentes activadores de cascadas de señalización implicadas en la respuesta inmune, generando un ambiente inflamatorio en el pulmón que favorece la sensibilización a aeroalérgenos [126, 127] (Figura 6). Los eosinófilos, macrófagos, y neutrófilos también contribuyen al daño pulmonar al producir elevados niveles de ROS y RNS en respuesta al estrés oxidativo inducido por los

oxidantes exógenos, debido a la actividad de enzimas, tales como la NADPH-oxidasa (gp91^{phox}-NOX2), peroxidasa eosinofílica (EPO), mieloperoxidasa (MPO) y óxido nítrico sintasa inducible (iNOS) [128].

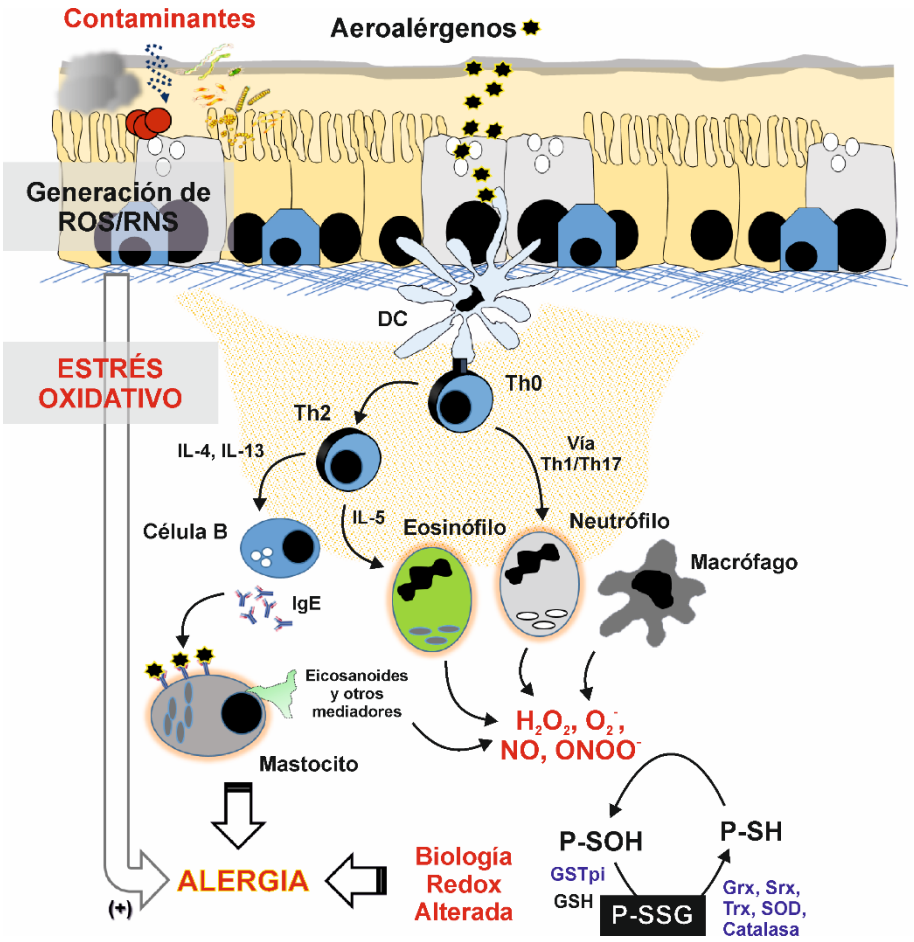

Figura 6. Biología redox en el epitelio pulmonar. Las células epiteliales e inflamatorias generan especies reactivas de oxígeno (ROS) y de nitrógeno (RNS) en respuesta al estrés oxidativo inducido por los oxidantes exógenos (contaminantes ambientales, entre otros), generando un ambiente inflamatorio que favorece la sensibilización a aeroalérgenos. La GSTpi cataliza la S-glutationilación de residuos de cisteína de la proteína diana, regulando su actividad. DC, célula dendrítica; Grx, glutarredoxina; GSTpi, glutatión-S-transferasa pi; H_2O_2, peróxido de oxígeno; O_2^-, superóxido; $ONOO^-$, peroxinitrito; NO, óxido nítrico; P-SH, grupo tiol proteico; P-SOH, grupo sulfonilo proteico; P-SSG, proteína S-glutationilada; SOD, superóxido dismutasa; Srx, sulforredoxina; Trx, tiorredoxina. Adaptado de López-Rodríguez *et al.* [117].

Diversos estudios han demostrado que los oxidantes exógenos también pueden favorecer la sensibilización a los aeroalérgenos al incrementar la permeabilidad de la barrera epitelial, inhibir la función del aparato mucociliar e inducir la secreción de mediadores pro-inflamatorios [129-133]. Otros estudios han indicado que estas moléculas pueden contribuir a la alergenicidad de un aeroalérgeno al actuar como vehículo de transporte [134] y/o alterar sus propiedades estructurales e inmunológicas [135-138].

Además de un efecto deletéreo, ROS y RNS endógenos desempeñan un importante papel en la señalización celular, en la transcripción génica y en varios procesos celulares al reaccionar con los sensores óxido-reducción presentes en proteínas y pequeñas moléculas [139]. En el pulmón, el tripéptido **GSH** -γ-glutamil-cisteinil-glicocola- y los grupos tioles de las proteínas son los principales sensores redox.

El GSH es el antioxidante más importante del epitelio pulmonar donde juega un papel central en el mantenimiento del homeostasis redox, definida como la relación [GSH]/[GSSG], siendo [GSH] y [GSSG] las concentraciones de las formas reducida y oxidada, respectivamente [140]. La concentración de GSH en el ELF es 140 veces superior (~ 429 μM) a la del plasma (~ 3 μM). En condiciones normales, la mayoría del GSH total en el ELF se encuentra en forma reducida (~ 99%) para funcionar como agente antioxidante [141, 142].

El metabolismo del GSH está estrechamente regulado y está implicado en numerosos procesos que son esenciales para la célula, tales como el mantenimiento de la homeostasis rédox, la señalización celular y la defensa contra el estrés oxidativo, entre otros. Su biosíntesis y degradación forma parte del ciclo del γ-glutamilo, que implica el transporte extracelular del GSH e intracelular de los γ-glutamil-aminoácidos. Además, el GSH intracelular se puede convertir en GSSG y viceversa mediante dos tipos de reacciones: 1) la reducción del H_2O_2 y otros peróxidos, catalizada por la glutatión peroxidasa; y 2) la reacción de trans-hidrogenación de GSSG a GSH, catalizada por la glutatión reductasa (Figura 7).

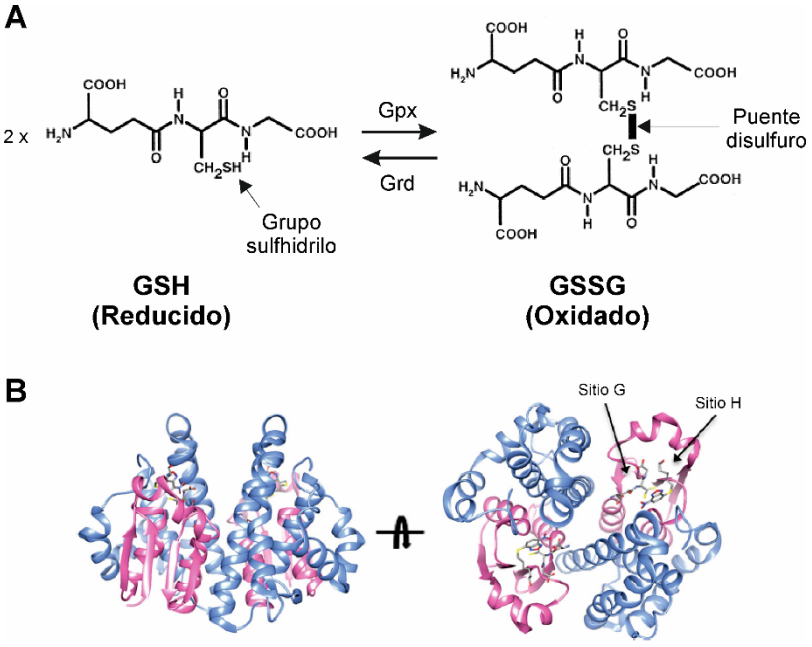

Figura 7. El glutatión (GSH) es el antioxidante más importante del epitelio pulmonar. A) Fórmulas estructurales de la pareja redox glutatión reducido (GSH) y oxidado (GSSG). Gpx = GSH Peroxidasa, Grd = GSH reductasa. B) Estructura tridimensional de la GSTpi humana formando complejo con el GSH (sitio G, color rosa) y con el inhibidor competitivo NBDHEX (sitio H, color azul). Diagrama de cintas adaptado de Allocati *et al.* [143].

Las alteraciones en la relación [GSH]/[GSSG], a favor de la forma oxidada, activan diferentes vías de señalización de las proteínas quinasas activadas por estrés, así como a factores de transcripción redox-sensibles, tales como AP-1 (Proteína activadora 1), NFκB y Nrf2 (del inglés, *Nuclear Factor (Erythroid-derived 2)- Related Factor-2*) que regulan la expresión de citoquinas pro-inflamatorias y de genes de enzimas antioxidantes y destoxificantes [120, 144]. Ciertas enfermedades pulmonares como asma, COPD y fibrosis pulmonar idiopática se caracterizan por un desequilibrio [GSH]/[GSSG] que suele ir asociado a una actividad disfuncional de enzimas antioxidantes pulmonares, como la superóxido dismutasa (SOD), catalasa y tiorredoxina (Trx) [144-146].

Una de las respuestas celulares al estrés oxidativo es la S-glutationilación de proteínas (P-SSG), una modificación postraduccional, covalente y reversible, que se caracteriza por la conjugación del GSH con una cisteína reactiva en la proteína diana a través de la formación de un puente disulfuro (Figura 7) [147, 148]. Esta modificación puede alterar la estructura, la función o la localización de la proteína diana, o puede servir para proteger los grupos tioles de una oxidación irreversible. La S-glutationilación modula la actividad de un número importante de proteínas que actúan como factores de transcripción, moléculas de adhesión, enzimas y citoquinas, así como procesos celulares en respuesta a señalización redox. Se han descrito más de 200 proteínas que

sufren esta modificación postraduccional, entre ellas la actina, la ATPasa de Na^+ y K^+, la proteína tirosina fosfatasa 1B, c-Jun, las subunidades p50 y p60 del NFκB, IKK y Fas [149-151].

En la célula, la enzima **glutatión-S-transferasa pi (GSTpi)** cataliza la reacción de S-glutationilación, mientras que la glutarredoxina (Grx) cataliza reacciones de deglutationilación [139].

GSTpi es miembro de la familia de las GSTs, enzimas multifuncionales, generalmente citosólicas, que se dividen en 7 clases (*alpha, zeta, theta, kappa, mu, pi, sigma y omega*) [143, 152, 153]. Los miembros de cada clase presentan una alta identidad de secuencia, entre el 60% y el 80%. Además, la expresión de las isoenzimas es específica de tejido. En humanos, por ejemplo, la isoforma predominante en pulmón, placenta y próstata, es GSTpi, mientras que GSTalpha es la isoenzima principal en hígado y riñón [153].

La mayoría de las GST son homodímeros, con masas moleculares entre 24 y 28 kDa por monómero (Figura 7). Todas las GSTs tienen una estructura 3-D similar en la que se distinguen dos dominios: el N-terminal, con el motivo estructural βαβαββα, que presenta el sitio de unión a GSH (sitio G), y el C-terminal en hélice α que contiene el sitio hidrofóbico (sitio H) que une diferentes substratos. El sitio G está muy conservado entre las diferentes clases de GSTs, mientras que el sitio H muestra una gran variabilidad ente las diferentes clases e incluso enzimas de una misma clase.

La función más conocida de las GSTs es la detoxificación celular y excreción de sustancias fisiológicas y xenobióticos [153]. Las GSTs catalizan la adición nucleofílica del tiol de GSH al centro electrofílico de un compuesto orgánico. El conjugado formado es más soluble en agua, lo que facilita su eliminación. Su papel clave en la detoxificación celular protege a los componentes celulares del ataque de las especies reactivas como ROS [154].

Además de su papel detoxificador, GSTpi exhibe otras funciones, tales como chaperona, regulador de las vías de señalización de las proteínas quinasas y de NO, y catalizador de la S-glutationilación de proteínas [152]. GSTpi interacciona con c-Jun, modulando la proliferación y la apoptosis. También regula la activación de NFκB, en las células del epitelio pulmonar expuestas a LPS [143, 152, 155, 156].

El gen que codifica para GSTpi es *GSTP1*, y exhibe polimorfismo como resultado de los cambios en Ile105Val y Ala114Val, lo que resulta en cuatro alelos *GSTP1* A, B, C y D que difieren estructural y funcionalmente [157]. Ciertos polimorfismos de *GSTP1* se ha asociado con asma, estrés oxidativo, metabolismo de xenobióticos y destoxificación de hidroperóxidos [158-161].

EL EPITELIO PULMONAR Y LA RESPUESTA ALÉRGICA

Cada vez hay más evidencia del importante papel del epitelio respiratorio como integrador y regulador de la respuesta inflamatoria en enfermedades como la alergia respiratoria [62, 162]. Sin embargo, en la actualidad, existe un intenso debate sobre si la disfunción del epitelio pulmonar es la causa o la consecuencia de la alergia respiratoria.

Durante las últimas décadas, la alergia respiratoria ha alcanzado proporciones pandémicas y su prevalencia continúa aumentando de forma alarmante, sobre todo en países industrializados, con un estilo de vida occidental: en Europa puede llegar a afectar a más del 25% de la población [163]. La elevada prevalencia y carácter crónico de esta enfermedad la convierte en un importante y caro problema de salud pública. Se estima que el tratamiento de los pacientes asmáticos consume entre el 1-2% del presupuesto destinado a la salud pública.

La **alergia respiratoria** es una enfermedad multifactorial que se caracteriza por una respuesta inflamatoria de tipo Th2 en las vías respiratorias, acompañada por la producción de altos niveles de IgE en suero, frente a sustancias inhaladas, generalmente inocuas para la mayoría de los individuos, denominadas aeroalérgenos [164-166].

Los mecanismos que subyacen a la reacción alérgica se pueden dividir de forma general en dos fases principales. Una primera **fase de sensibilización** y desarrollo de memoria celular, seguida por la **fase efectora** (Figura 5).

Durante la *fase de sensibilización*, el alérgeno entra en contacto con la superficie de las mucosas de un individuo susceptible, donde es capturado y procesado por las células presentadoras de antígeno, las DCs. Estas células migran a la zona de las células T de los ganglios linfáticos donde presentan los péptidos derivados del alérgeno, en el contexto del complejo mayor de histocompatibilidad de clase II (MHC-II en ratón y HLA en humanos), a las células $CD4^+$T *naïve* (Th0) que expresan receptores (TCR) específicos, las cuales se diferencian a células Th2 productoras de IL-4, IL-5 e IL-13. Estas citoquinas son igualmente secretadas de forma antígeno-independiente por los ILC2s, residentes en el tejido pulmonar [167]. Las citoquinas IL-4 e IL-13 son responsables de la activación de las células B en células plasmáticas productoras de IgE específica que liberan a la sangre, mientras que la IL-5 promueve la eosinofilia. Las IgE circulantes se unen a receptores de IgE de alta afinidad (FcƐRI) presentes en la superficie de las células efectoras (mastocitos y basófilos), lo que provoca la sensibilización de los individuos a un determinado alérgeno. Las IgE presentes en el

suero tienen una vida media corta (2 días) en comparación con otros anticuerpos, como IgG (21-23 días) pero una vez unidos al receptor su vida media aumenta hasta los 10 días.

La *fase efectora* es la fase sintomática y se produce cuando el individuo entra de nuevo en contacto con el alérgeno, el cual se une a los complejos IgE-FcƐRI presentes en la superficie de las células efectoras. Esta unión provoca el entrecruzamiento de los receptores, activándose una cascada de señalización que deriva en la desgranulación de las células, con la consiguiente liberación al entorno de mediadores inflamatorios, incluyendo histamina, prostaglandinas, leucotrienos, triptasa, citoquinas y quimioquinas, entre otros. Las acciones de estos mediadores sobre los tejidos diana son responsables de la aparición de los síntomas clínicos que caracterizan a la enfermedad, tales como congestión, rinitis o algunos síntomas más severos como la broncoconstricción y el asma. Aunque las alergias respiratorias se clasifican como enfermedades inflamatorias de tipo Th2, numerosos estudios han demostrado el importante papel de las células epiteliales respiratorias y de otros tipos celulares como los ILC2s en la patogénesis de la reacción alérgica (Figura 5).

A pesar de los numerosos estudios realizados, se desconoce por qué unas personas desarrollan alergia y otras no. En este sentido, diversos estudios epidemiológicos han indicado que la etiología de las reacciones alérgicas es compleja y está influenciada no sólo por factores genéticos y las características intrínsecas del alérgeno, sino también por factores ambientales, denominados factores de riesgo [168]. La contaminación, las proteasas ambientales, infecciones víricas o bacterianas y el humo del tabaco, pueden aumentar el riesgo de desarrollar alergia o exacerbar los síntomas (Figura 5).

- **Aeroalérgenos y el polen de olivo**

Los **aeroalérgenos** son los principales antígenos responsables de las alergias respiratorias, que acceden al organismo, frecuentemente, a través de las vías aéreas superiores.

En general, los aeroalérgenos son proteínas o glicoproteínas de baja masa molecular (5-70 kDa) que poseen una elevada solubilidad y estabilidad en los fluidos corporales. Estas moléculas viajan comúnmente asociadas a partículas de mayor tamaño que tras ser inhaladas se depositan a lo largo de la mucosa respiratoria, donde se encuentran con la primera barrera defensiva del organismo, el epitelio de las vías respiratorias.

Las fuentes de aeroalérgenos son muy variadas en la naturaleza (www.eaaci.org/GlobalAtlas): pólenes de árboles, arbustos y hierbas; ácaros del polvo

doméstico (HDM); epitelios de perros, gatos y otros animales domésticos; y esporas de hongos [169]. Sin embargo, los **pólenes** representan la fuente de aeroalérgenos de mayor relevancia clínica en la actualidad, a nivel mundial, sobrepasando a los de HDM en ciertas regiones.

En el área mediterránea, y ciertas regiones de EE.UU. (California), América del Sur (Chile, Perú y Argentina), Sudáfrica, Japón y Australia, el **polen de olivo** (*Olea europaea*) representa una de las causas más importantes de alergia respiratoria estacional, siendo la segunda causa de polinosis en España (Figura 8). Sin embargo, en zonas donde existe un cultivo intenso de este árbol se llega a convertir en la primera causa de polinosis [170, 171].

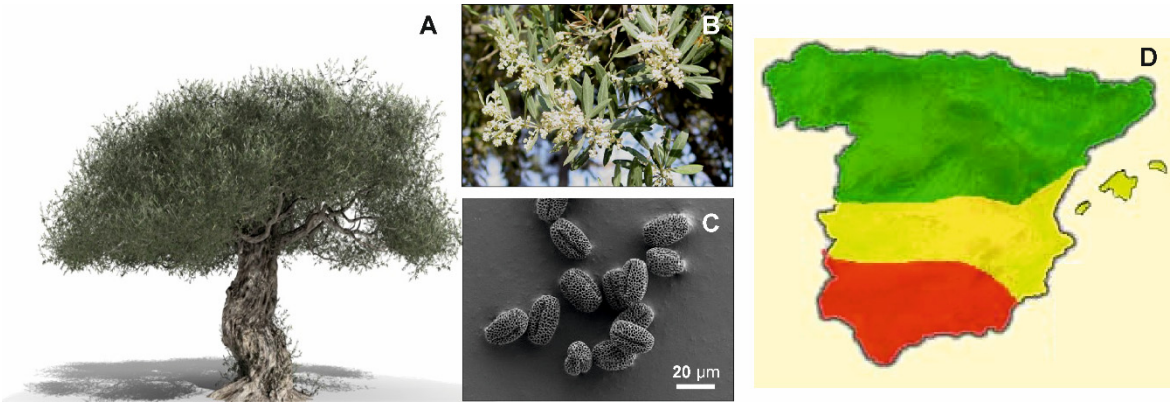

Figura 8. El polen de olivo (*Olea europaea*) como fuente de aeroalérgenos. A) Árbol del olivo. B) Detalle de las hojas, flores y frutos. C) Micrografía electrónica de barrido de los granos de polen de olivo. D) Mapa de la incidencia polínica de olivo en España. Niveles de pólenes (granos/m^3): Rojo, muy alto (>200); amarillo, moderado (100-200); y verde, bajo (<100). Fuente: www.uco.es.

De los 14 alérgenos del polen de olivo identificados hasta la fecha, **Ole e 1** es el más relevante y el agente de sensibilización más frecuente, siendo también la proteína más abundante en el extracto (Figura 8) [172]. Dependiendo del área geográfica estudiada, el alérgeno muestra una prevalencia entre el 55% y el 90% entre los pacientes alérgicos a este polen [173, 174].

Ole e 1 es una glicoproteína de 145 residuos aminoacídicos que exhibe un alto grado de polimorfismo, tanto a nivel de secuencia de aminoácidos como del N-oligosacárido del único sitio de glicosilación que posee [175, 176]. Esta proteína presenta un patrón complejo en PAGE-SDS, caracterizado por la presencia de dos bandas mayoritarias: la forma glicosilada, con una masa molecular aparente de 20 kDa, y la forma no glicosilada de 18.5 kDa. Además, en algunas preparaciones se detectan dos formas minoritarias

de 22 y 40 kDa, correspondientes a la forma hiperglicosilada y al dímero de la forma glicosilada, respectivamente.

Ole e 1 es el alérgeno más importante de la familia de alérgenos a la que da nombre (Ole e 1-*like*) [172]. Todos los miembros son proteínas que se expresan específicamente en el polen [177, 178] y aunque su función no se conoce con exactitud, parecen estar implicados en la hidratación y/o germinación del polen [179-181].

Ole e 1 exhibe alta reactividad cruzada a nivel de IgE e IgG con los miembros de la familia de las Oleáceas: Fra e 1, Lig v 1 y Syr v 1 de los pólenes de fresno (*Fraxinus excelsior*), aligustre (*Ligustrum vulgare*) y lila (*Syringa vulgaris*), respectivamente. Estos alérgenos muestran una identidad de secuencia mayor del 85% con Ole e 1. Sin embargo, con otros miembros de esta familia, Ole e 1 presenta escasa reactividad cruzada debido a la baja identidad de secuencia: por ejemplo, Pla a 1 de polen del llantén menor (*Plantago lanceolata),* Che a 1 del polen de cenizo blanco *(Chenopodium album)* y Sal k 1 del polen de la barrilla borde *(Salsola kali)* [182-184].

Los estudios de mapeo epitópico han permitido la identificación de dos epítopos T inmunodominantes en la molécula de Ole e 1, localizados en las posiciones 91-102 y 109-130; así como varias regiones de unión a IgG e IgE [185, 186].

- **Proteasas como agentes adyuvantes de la respuesta alérgica**

Las **proteasas** son enzimas que hidrolizan los enlaces peptídicos en las proteínas. Estas enzimas están presentes en todas las fuentes de alérgenos descritas como HDM [187], cucarachas [188], pólenes [73] y hongos [189], donde llevan a cabo funciones que son cruciales para los organismos, desde la simple hidrólisis de proteínas hasta la regulación de procesos fisiológicos.

Diversos estudios han demostrado que las proteasas ambientales actúan como adyuvantes en la respuesta alérgica, siendo muchas de ellas alérgenos de relevancia clínica (Tabla 1) [190]. La mayoría de las proteasas alergénicas descritas pertenecen a la clase de las serín-proteasas (p.e., Der p 3, Der p 6 y Der p 9), sin embargo, también se han identificado alérgenos con actividad aspartil- (p.e., Bla g 2), cisteín- (Der p 1) y metalo-proteasa (Asp f 5).

Tabla 1. Algunas proteasas alergénicas descritas.

Fuente	Alérgeno	Tipo de Proteasa
Ácaro	Grupo 1 (Der p 1)	Cisteín-proteasa
	Grupo 3 (Der p 3)	Serín-proteasa
	Grupo 6 (Der p 6)	Serín-proteasa
	Grupo 9 (Der p 9)	Serín-proteasa
Cucaracha	Bla g 2	Aspartil-proteasa
	Per a 10	Serín-proteasa
Hongo	*Cladosporium* Grupo 9	Serín-proteasa
	Curvularia Grupo 1	Serín-proteasa
	Penicillium Grupo 18	Serín-proteasa
	Aspergillus Asp f 13	Serín-proteasa
	Penicillium Pen ch 13	Serín-proteasa
	Rhodotorula Grupo 2	Serín-proteasa
	Epicoccum Grupo 1	Serín-proteasa
	Aspergillus Asp f 5	Metalo-proteasa
Pólen	*Cryptomeria* CPA63	Aspartil-proteasa
	Phleum Grupo 1	Cisteín-proteasa
	Lolium Grupo 1	Cisteín-proteasa

Los **HDM** constituyen una de las fuentes más importantes de proteasas alergénicas de relevancia clínica, pues más del 20% de los pacientes alérgicos a nivel mundial están sensibilizados a sus alérgenos [191, 192].

Los HDM son miembros de la clase *Arachnida* y cohabitan con los humanos (www.eaaci.org/GlobalAtlas). Son artrópodos microscópicos que miden entre 0.2 y 0.5 mm de longitud, y tienen ocho patas (Figura 9A). Se alimentan de escamas de la piel, hongos y otros restos orgánicos.

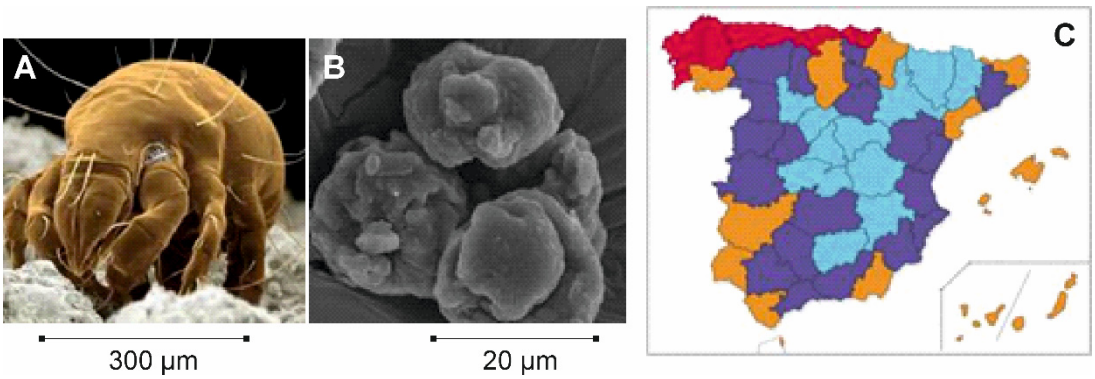

Figura 9. A) Micrografía electrónica de barrido coloreada de un ácaro del polvo doméstico (*D. pteronyssinus*). Fuente: www.taringa.net. B) Micrografía electrónica de barrido de las heces de *D. pteronyssinus*. Imagen adquirida en el Centro de Microscopía electrónica (UCM, Madrid). C) Mapa de los niveles de exposición a *D. pteronyssinus* en España. Niveles de exposición (ácaros/gramo de polvo): Rojo, muy alta (> 1000); naranja alta (> 500); azul oscuro, moderada (> 100); y azul claro, baja (< 100). Fuente: www.leti.com.

Para su crecimiento requieren de un ambiente cálido (20-25ºC) y húmedo (70-75%), de ahí su alta incidencia en zonas costeras o cercanas a los cursos de los ríos. Los alérgenos de HDM son principalmente excretados en las heces, las cuáles se acumulan en el polvo doméstico [193]. Las heces son partículas con un tamaño comprendido entre los 10-35 μm (similar al de un grano de polen) que están compuestas de restos de alimentos, proteasas y moco (Figura 9B). Las especies de HDM más comunes son *Dermatophagoides pteronyssinus* y *D. farinae*, siendo la primera la más relevante en España desde el punto de vista clínico (Figura 9C) [194].

Hasta la fecha se han identificado 23 alérgenos en *D. pteronyssinus* [195, 196], siendo la mayor parte de ellos proteasas implicadas en el proceso digestivo del ácaro [197, 198].

Der p 1 es el alérgeno principal de *D. pteronyssinus*, con una prevalencia de hasta el 80% en los pacientes alérgicos a HDM [198]. Der p 1 es una glicoproteína polimórfica de 25 kDa de masa molecular que pertenece al grupo 1 de alérgenos con actividad cisteín-proteasa. De forma similar a otras proteasas, Der p 1 se expresa como un pre-zimógeno inactivo (pre-proDer p 1), compuesto por un péptido señal esencial para su secreción, un pro-péptido N-terminal de 80 residuos aminoácidos necesario para su plegamiento, y un dominio de 222 residuos aminoacídicos que corresponden a la proteasa madura [199]. Der p 1 se activa por autocatálisis a pH ácido y a su vez, puede activar otras moléculas de pro-Der p 1, así como a otras pro-proteasas de ácaro como Der p 3, Der p 6 y Der p 9 [200].

La estructura tridimensional de Der p 1 se ha determinado mediante cristalografía de rayos X con una resolución de 1.9 Å [194]. Der p 1 presenta el plegamiento cisteín-proteasa típico de la familia de la papaína que consiste en dos dominios plegados en forma de “V”. Los residuos catalíticos Der p 1 son la cisteína 34 (Cys34) y la His170, junto con la Gln28 y la Asn190. La Cys34 y la His170, que forman el par iónico tiolato-imidazol, son probablemente los residuos más críticos para la actividad de la enzima y está conservado en otras cisteín-proteasas. Der p 1 presenta además otros 6 residuos de cisteína, los cuales se encuentran implicados en la formación de tres puentes disulfuro: Cys4-Cys117, Cys31-Cys71, y Cys65-Cys103 [194].

Numerosos estudios han señalado el posible papel de la actividad cisteín-proteasa de Der p 1 en la respuesta alérgica a HDM [187]. Der p 1 es capaz de alterar la permeabilidad del epitelio bronquial mediante la ruptura de las TJ, al degradar las proteínas ocludina, claudina y ZO-1 [201-203]. Además, Der p 1 degrada a las colectinas SP-A y SP-D [59], y a los inhibidores de proteasas α1-antitripsina, elafina y SLPI (anti-

leucoproteasa, del inglés *Secretory LeukoProtease Inhibitor*) [204, 205]; todas ellas son moléculas implicadas en la protección del pulmón frente a la inflamación. Hammad *et al.* demostraron que Der p 1 degrada al receptor de baja afinidad de IgE (CD23) presente en la membrana de las células B, aumentando así la producción de IgE [206]. El mismo grupo demostró que Der p 1 también degrada a CD40 de la superficie de las DCs, ocasionando una disminución en la producción de IL-12 que juega un papel clave en la polarización Th1 [206]. En un estudio realizado por Schulz *et al*. se demostró que Der p 1 rompe la subunidad α del receptor de IL-2 de la superficie de las células T, lo que inhibe la producción de IFN-γ y favorece la respuesta Th2 [207]. Otros estudios han demostrado que Der p 1 induce la secreción de mediadores pro-inflamatorios como IL-6, IL-8, eotaxina y GM-CSF, tanto a través de la activación de los receptores de membrana TLRs y PAR-2 [208, 209] como mediante la generación de especies reactivas de oxígeno (ROS) [210]. Der p 1 también induce la secreción de IL-4 e IL-13 en basófilos y mastocitos, a través de un mecanismo independiente de IgE [211]. Recientemente, Cayrol *et al.* han demostrado que Der p 1 puede regular el proceso inflamatorio al inducir la secreción de IL-33 y modular su actividad biológica [212].

- **El humo del tabaco y las enfermedades alérgicas**

El consumo de tabaco **o tabaquismo** se define como una intoxicación crónica producida por el abuso del tabaco. Se estima que, a nivel mundial, unos mil millones de personas consumen tabaco de forma regular y su prevalencia está aumentando de forma alarmante en los países desarrollados debido, principalmente, al aumento de factores socioeconómicos desfavorables (*WHO Global Report on Trends in Prevalence of Tobacco Smoking*, 2015). Según la Organización Mundial de la Salud (OMS), el tabaquismo es una de las principales causas de mortalidad a nivel mundial, situándose por encima del consumo de alcohol, la hipertensión arterial y el sobrepeso. El tabaquismo se ha asociado con enfermedades como artritis reumatoide, cáncer, enfermedad coronaria, infarto de miocardio, enfermedad de Crohn, así como con un conjunto de patologías que afectan al tracto respiratorio (bronquitis obstructiva crónica, asma y las alergias respiratorias) [213, 214].

En la actualidad, la principal forma de consumo del tabaco se realiza mediante inhalación de las sustancias generadas por la combustión del cigarrillo (humo del tabaco) que son captadas por el fumador activo o pasivo (Figura 10). Para fabricar un cigarrillo, las hojas secas, fermentadas y trituradas de la planta *Nicotiana tabacum* -una especie tropical de la familia de las solanáceas, originaria de América- se mezclan con diferentes aditivos (como etilenglicol y amoniaco) para formar la *liga*, a la que se añade una *salsa* -responsable de sus propiedades aromáticas y gustativas- que puede

contener cacao, miel, regaliz y resinas disueltas en agua o en alcohol. Muchos de los 700 aditivos que se utilizan en la preparación del tabaco no están permitidos por la FDA (*Food and Drug Administration*).

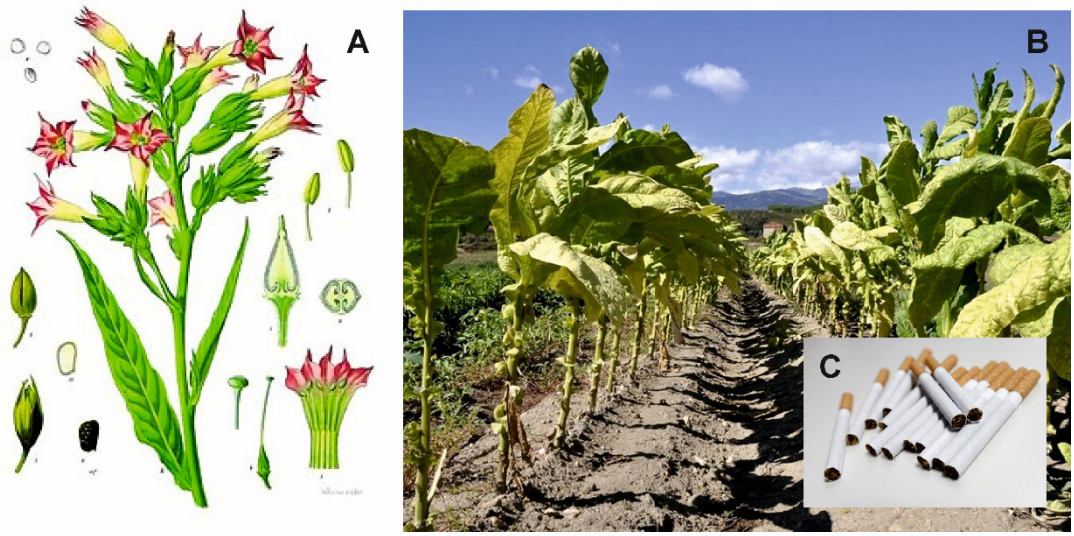

Figura 10. A) Planta del tabaco (*Nicotiana tabacum L.*), según una lámina de cromolitografía recogida en Köhler's Medizinal-Pflanzen, vol. I, 1887. Fuente: www.redaccionmedica.com. B) Cultivo de la planta de tabaco. Fuente: www.extremadura7dias.com. C) Cigarrillos.

El **humo del tabaco** es un aerosol complejo y heterogéneo compuesto por una fase gaseosa de compuestos volátiles y una fase de partículas semi-volátiles y no volátiles, cuya composición viene determinada por el modo de fumar de cada individuo [215]. La temperatura, cercana a los 900ºC, que se alcanza en la zona incandescente del cigarrillo cuando el fumador aspira, trasforma numerosos componentes originales del mismo, dado lugar a las más de 7000 sustancias presentes en el humo [216-218]. El gradiente de temperatura que se genera arrastra, con la aspiración, compuestos de baja masa molecular hasta los pulmones, donde pueden desencadenar una reacción inmune. Por otra parte, las partículas del humo de tamaño inferior a 1 micra, llegan a los alveolos gracias a su coeficiente de difusión, donde contactan de forma directa con las células inmunes. Entre las sustancias presentes en el humo del tabaco existen numerosos compuestos perjudiciales para la salud: i) carcinógenos, como metilcolantreno, benzopirenos o acroleína; ii) toxinas, como monóxido de carbono, hidroquinona, acetonas, amonio o nicotina; y iii) oxidantes, como superóxido, peróxido de hidrógeno u óxidos de nitrógeno.

Al entrar en contacto con el epitelio respiratorio, estos compuestos pueden contribuir de forma efectiva al daño tisular y a la inducción de estrés oxidativo al potenciar la rápida oxidación del GSH pulmonar hacia su forma oxidada e inactiva (GSSG) [216, 217]. La pérdida de GSH promueve la activación de NFκB y la liberación inmediata de un amplio

set de moléculas proinflamatorias como IL-5, IL-6, IL-8, IL-13 e IL-33, entre otras, que afectan a la migración y activación de numerosas células inmunes como DCs, neutrófilos, basófilos, mastocitos y linfocitos B y T [219-224]. Además, las células inflamatorias adyacentes poseen una gran variedad de mecanismos enzimáticos que amplifican la respuesta inflamatoria desencadenada por el epitelio y el estrés oxidativo iniciado por los oxidantes exógenos, lo que aumenta más si cabe el daño en el pulmón al promover una mayor liberación de interleuquinas pro-inflamatorias y quimioquinas, potenciando en último término el desarrollo y mantenimiento de una respuesta inmune Th2 [127, 128]. Además, el humo del tabaco tiene un efecto deletéreo sobre la estructura, organización y estado de diferenciación del epitelio pulmonar. Este daño de la barrera epitelial dificulta la eliminación de las sustancias inhaladas como los patógenos [225, 226], y favorece su penetración al alterar la permeabilidad, lo que promueve una respuesta inflamatoria [227].

Por último, aunque existen aún pocos estudios al respecto, la planta de tabaco puede causar alergia ocupacional en los trabajadores de las plantaciones de tabaco y en los empleados de las tabacaleras que requieren su continua manipulación [228, 229]. La alergia al tabaco parece ser más frecuente entre los fumadores asmáticos que están sensibilizados a pólenes de *Lolium* y *Artemisia*, o al látex (*Hevea brasiliensis*), debido seguramente a fenómenos de reactividad cruzada [228, 229].

CULTIVOS EN INTERFASE AIRE-LÍQUIDO (ALI): UNA HERRAMIENTA IDEAL PARA ESTUDIAR LA FISIOLOGÍA DEL EPITELIO RESPIRATORIO HUMANO

Los cultivos celulares *in vitro* son esenciales en investigación biomédica para estudiar la interacción del epitelio con distintos agentes ambientales, tales como los aeroalérgenos. Estos ofrecen la posibilidad de utilizar células humanas en lugar de utilizar modelos animales que, aunque útiles, introducen los problemas asociados a las diferencias entre especies [230, 231].

De todos los modelos utilizados, los modelos *ex vivo* de pulmón – obtenidos de biopsias, explantes de pulmón y necropsias- son los que más se aproximan a la situación *in vivo*. Sin embargo, aunque se han utilizado como modelos de infecciones y ensayos de fármacos, presentan una serie de inconvenientes, como son el bajo rendimiento celular, los explantes proceden generalmente de individuos con enfermedades pulmonares y las muestras *post mortem* con frecuencia están dañadas, entre otros.

Frente a los modelos *ex vivo*, existen dos alternativas (Tabla 2):

- **Cultivos primarios** derivados de individuos sanos. Estos modelos son útiles, pero presentan varios inconvenientes, tales como tener una expansión limitada, ser difíciles de transfectar, la disponibilidad de tejidos y la variabilidad entre donantes y experimentos. Existen cultivos primarios disponibles comercialmente como los de las células humanas normales del epitelio traqueo-bronquial (NHBE) derivadas de biopsias de tráquea que exhiben el característico fenotipo de epitelio pseudoestratificado compuesto por células ciliadas, mucosas y basales, tras su diferenciación *in vitro*. Sin embargo, los cultivos de células NHBE presentan varias desventajas: 1) soportan un número de pases reducido, lo que limita el número de experimentos que pueden llevarse a cabo con un donante dado; 2) son cultivos difíciles de manipular; 3) exhiben un alto grado de variabilidad entre donantes, experimentos y pases, lo que afecta la reproducibilidad de los resultados; y 4) carecen de células neuroendocrinas. Estos cultivos no se suelen utilizar para estudios de transporte, al estar formados por una población heterogénea.
- **Líneas celulares.** Son células inmortalizadas, generalmente aisladas de tumores o generadas por transformación de cultivos primarios usando vectores virales. Las líneas celulares son más consistentes y permiten seguir protocolos establecidos. La ventaja es que son genéticamente homogéneas y los resultados obtenidos reproducibles, sin embargo, muestran con frecuencia características que se han modificado comparadas con los cultivos primarios. Hay varias líneas celulares humanas disponibles comercialmente, tanto traqueo-bronquiales como bronquiales y alveolares (Tabla 2).

Una vez que se ha elegido el tipo celular, hay que establecer las condiciones de cultivo (densidad celular, tiempo de cultivo, presencia de nutrientes y otros factores de crecimiento, etc.) puesto que éstas van a afectar significativamente a la diferenciación celular y, por lo tanto, a los resultados obtenidos.

Durante los últimos años, la comunidad científica ha visto necesario el desarrollo de modelos *in vitro* que mimeticen el complejo microentorno de las vías respiratorias humanas con el fin de disponer de una herramienta útil para el estudio de la patogénesis de enfermedades respiratorias y el desarrollo de nuevos tratamientos.

Los cultivos tradicionales son cultivos bidimensionales, donde las células se crecen sumergidas en el medio. Los **cultivos sumergidos** han sido utilizados ampliamente en investigación debido a su fácil manipulación, bajo coste y alta reproducibilidad experimental [232], sin embargo, no reflejan las condiciones *in vivo* de las células del epitelio pulmonar que por el lado apical están en contacto directo con el aire. Por ello se han desarrollado los **cultivos en ALI**, donde las células se crecen sobre un soporte

poroso que divide la cámara en dos compartimentos para mimetizar las condiciones fisiológicas: *apical*, en contacto con el aire y *basolateral,* en contacto con el medio de cultivo (Figura 11). La principal ventaja de los cultivos primarios de células NHBE en ALI es que permiten obtener un modelo de epitelio traqueo-bronquial fisiológicamente relevante: un epitelio pseudoestratificado polarizado, compuesto por células basales, secretoras y ciliadas. Los cultivos en ALI permiten un metabolismo más oxidativo -debido a la mayor exposición de O_2-, la formación de uniones intercelulares mejor organizadas, la expresión polarizada de ciertos receptores de membrana y un aparato muco-ciliar funcional [232-234]. Además de las similitudes estructurales, existe una buena correlación entre la expresión global de genes de los cultivos *in vitro* de células NHBE y de las obtenidas de biopsias de individuos sanos. Los cultivos en ALI son también sistemas muy versátiles, pues permiten el co-cultivo con otros tipos celulares no epiteliales como las células endoteliales [235-237], lo cual reproduce de forma más cercana la situación que ocurre *in vivo*. Numerosos estudios han utilizado cultivos en ALI con una gran variedad de células primarias y líneas celulares, cuyas características más relevantes se recogen en la Tabla 2.

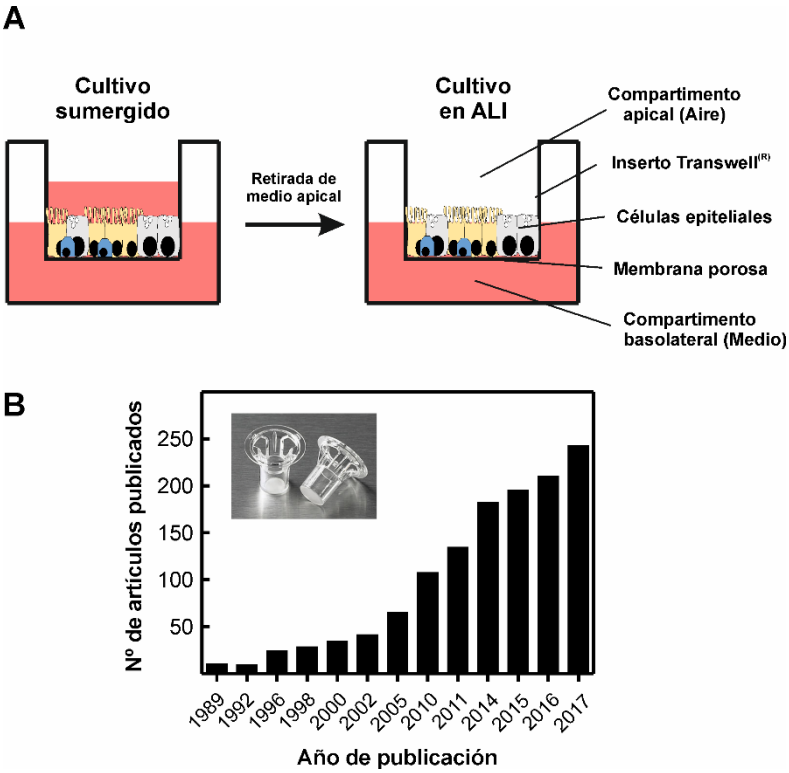

Figura 11. A) Esquema del protocolo de establecimiento de un cultivo en interfase aire-líquido (ALI). B) Gráfico del número de estudios publicados en revistas indexadas que han utilizado los cultivos en ALI desde 1999 hasta 2017. Fuente: PubMed (https://www.ncbi.nlm.nih.gov), usando como criterios de búsqueda "*ALI*", "*epithelial*" y "*cell culture*".

Tabla 2. Cultivos celulares de epitelio pulmonar empleados más frecuentemente en investigación biomédica.

Células	Origen	Morfología	Funcionalidad	ALI	Referencias
NHBE	Biopsias traqueo-bronquiales No inmortalizadas	Epitelio estratificado con células ciliadas, basales y secretoras	Altos valores de TEER (400-4000 $\Omega \cdot cm^2$) Forman TJ y AJ Secretan citoquinas y mucinas	SÍ	Bhowmick R *et al*. 2016 Prytherch ZC *et al*. 2014 Klein SG *et al*. 2011 Papazian D *et al*. 2016 Berubé K *et al*. 2010
Calu-3	Epitelio de adenocarcinoma bronquial Tumoral	Epitelio columnar con propiedades secretoras, con microvellosidades y cilios (algunos autores)	Altos valores de TEER (1000-2000 $\Omega \cdot cm^2$) Forman TJ y AJ Secretan citoquinas y mucinas	SÍ	Grainger CI *et al*. 2006 Papazian D *et al*. 2016 Berubé K *et al*. 2010 Prytherch ZC *et al*. 2014 Kreft ME *et al*. 2015
16HBE14o$^-$	Epitelio bronquial sano Inmortalizada (SV40)	Epitelio cuboideo, a veces estratificado, carente de células ciliadas	Altos valores de TEER (700-2500 $\Omega \cdot cm^2$) Forman TJ y AJ Secretan citoquinas y no mucinas	SÍ	Papazian D *et al*. 2016 Berubé K *et al*. 2010 Prytherch ZC *et al*. 2014 Forbes B *et al*, 2003
BEAS-2B	Epitelio bronquial sano Inmortalizada (SV40)	Epitelio escamoso	Bajos valores de TEER (150-200 $\Omega \cdot cm^2$) No forman TJ ni AJ Secretan citoquinas	NO	Bhowmick R *et al*. 2016 Klein SG *et al*. 2011 Papazian D *et al*. 2016 Berubé K *et al*. 2010 Park YH *et al*. 2015
A549	Epitelio de adenocarcinoma alveolar Tumoral	Epitelio de tipo AEC-II, carente de AEC-I	Muy bajos valores de TEER (0-150 $\Omega \cdot cm^2$) No forman TJ ni AJ Secretan surfactante y mucinas	NO	Bhowmick R *et al*. 2016 Prytherch ZC *et al*. 2014 Klein SG *et al*. 2011 Berubé K *et al*. 2010 Wu J. Braz *et al.* 2017

AEC, célula epitelial alveolar; AJ, uniones adhrentes; TEER, Resistencia eléctrica transepitelial; TJ, uniones estrechas.

Objetivos

Objectives

Dado el actual debate que existe sobre si la disfunción del epitelio actúa como causa o consecuencia de la reacción alérgica frente a un alérgeno particular, el objetivo principal de esta *Tesis Doctoral* ha consistido en profundizar en el **estudio del papel del epitelio bronquial en la alergia respiratoria, utilizando como modelo Ole e 1, el alérgeno más importante del polen de olivo.**

Con este fin, el objetivo general se ha desglosado en cuatro capítulos diferenciados con los siguientes objetivos específicos:

- ***Capítulo I. Estudiar la influencia del estado de diferenciación del epitelio bronquial en la respuesta inmune a Ole e 1.***

    - Establecer y caracterizar un modelo *in vitro* de epitelio bronquial basado en cultivos primarios de células epiteliales bronquiales humanas (NHBE) crecidas en ALI obtenidas de dos donantes sanos.
    - Analizar la respuesta inmune a Ole e 1 en cultivos primarios de células NHBE crecidas en ALI, a lo largo del proceso de diferenciación usando el modelo establecido.

- ***Capítulo II. Analizar el papel de las proteasas ambientales en la respuesta inmune del epitelio bronquial a Ole e 1.***

    - Establecer y caracterizar un modelo *in vitro* de epitelio bronquial basado en la línea de células epiteliales bronquiales humanas inmortalizadas (Calu-3), crecidas en ALI. Este modelo se ha utilizado para analizar el efecto de la co-exposición a proteasas en la respuesta inmune a Ole e 1. Der p 1, cisteín-proteasa del ácaro del polvo doméstico, se ha empleado como modelo de proteasa.
    - Determinar el efecto de la co-exposición de Der p 1 sobre la permeabilidad del epitelio bronquial a Ole e 1.
    - Estudiar los cambios en el metaboloma como consecuencia de la co-exposición a Ole e 1 y Der p 1.
    - Evaluar el efecto de Der p 1 en las propiedades estructurales e inmunológicas de Ole e 1.
    - Analizar el efecto del GSH y la GSTpi sobre la actividad proteolítica de Der p 1.

- ***Capítulo III. Estudiar el efecto de la co-exposición al humo del tabaco en la respuesta inmune del epitelio bronquial a Ole e 1.***

    - Preparar, caracterizar y estandarizar el extracto de humo del tabaco a partir de cigarrillos comerciales.
    - Determinar el efecto de la exposición al humo de tabaco del modelo *in vitro* de epitelio bronquial basado en Calu-3.
    - Analizar el efecto de la co-exposición al humo de tabaco en la respuesta inmune a Ole e 1.

- ***Capítulo IV. Estudiar las propiedades interfaciales de Ole e 1 en el contexto del surfactante pulmonar y modelos de membranas celulares modelo.***

    - Caracterizar la actividad interfacial de Ole e 1 y evaluar su efecto sobre las propiedades interfaciales del surfactante pulmonar.
    - Analizar la interacción lípido-proteína utilizando modelos de monocapas lipídicas modelo y balanzas de tipo Langmuir-Blodgett y Langmuir-Wilhelmy.

Materiales y Métodos

Materials and Methods

MATERIALES

Células

NHBE (*Normal Human Bronchial Epithelial cells*): Células humanas de epitelio bronquial de individuos sanos. Fueron suministradas por Lonza (Ref. CC-2540S, Lotes 307177 y 340483). Las células se aislaron de dos donantes sanos, mujeres no fumadoras, de 40 y 44 años.

Calu-3: Línea inmortalizada de células epiteliales bronquiales humanas derivada de un adenocarcinoma pulmonar. Fue obtenida de *American Type Culture Collection* (ATCC, Ref. HTB-55, Lot. 614499062).

Proteínas

Ole e 1: Alérgeno principal del polen de olivo. Se purificó a homogeneidad a partir de polen de olivo (*Olea europaea* variedad *picual*) suministrado por IberPolen (Ref. A-022.10, Lote 014), siguiendo el método descrito por Villalba *et al.* [175].

Der p 1: Alérgeno principal del ácaro del polvo doméstico (*Dermatophagoides pteronyssinus*). Fue suministrado libre de endotoxina (≤ 0.03 EU/µg) por Indoor Biotechnologies (Ref. LTN-DP-1-1, Lot. 38190).

GSTpi: Glutatión-S-transferasa pi de placenta humana. Se obtuvo de Sigma (Ref. G8642, Lote SLBB8465V).

Der p 8: Alérgeno minoritario del ácaro del polvo doméstico. Se purificó a partir del extracto de las heces de ácaro según el protocolo descrito por Simons *et al.* [238], con algunas modificaciones. Las heces de ácaro fueron amablemente cedidas por ALK-Abelló. Der p 8 es una GST isoforma mu (GSTmu).

Pacientes e individuos control

Los pacientes ($n = 5$) se diagnosticaron en función de la historia clínica de alergia al polen de olivo y valores de IgE específica a Ole e 1 y Der p 1, mediante ImmunoCAP-FEIA, según las instrucciones de la casa comercial (Thermo Fisher Scientific). Como controles ($n = 5$) se utilizaron individuos no atópicos (Tabla 3). Para todos los pacientes se obtuvo un valor de IgE específica a Der p 1 < 0.35 kU/L. Los pacientes fueron reclutados en el Hospital Regional Universitario de Málaga y firmaron un consentimiento de cesión de muestras al Biobanco de dicho hospital. El estudio se aprobó por el Comité Ético del Instituto de Salud Carlos III, así como por el Comité de Ética asociado al Biobanco del Hospital Regional Universitario de Málaga.

Tabla 3. Características clínicas de los individuos reclutados para los ensayos celulares.

No.*	Diagnosis	Síntomas	Fumador/a	Sexo[1]	Edad[2]	sIgE [3]
P1	RC severa persistente estacional	Obstrucción nasal, estornudo, nariz mocosa, picor naso-ocular, rojez ocular, lagrimeo	No	M	28	1.93
P2	RC moderada intermitente estacional	Estornudo, nariz mocosa, picor naso-ocular, lagrimeo	Exfumador (hace 5 años)	F	36	18.4
P3	RC moderada persistente permanente	Obstrucción nasal intermitente, estornudo, nariz mocosa, picor naso-ocular y oral, lagrimeo	Exfumador (hace 5 años)	F	58	1.55
P4	RC moderada persistente estacional y asma	Estornudo, nariz mocosa, picor naso-ocular, lagrimeo y dipnea	No	M	44	17.2
P5	RC moderada persistente estacional y asma	Obstrucción nasal, estornudo, nariz mocosa, picor naso-ocular, dipnea, jadeo, tos	Sí	F	48	1.07
C1	Negativo	Negativo	No	M	26	<0.35
C2	Negativo	Negativo	No	M	69	<0.35
C3	Negativo	Negativo	No	F	49	<0.35
C4	Negativo	Negativo	No	F	38	<0.35
C5	Negativo	Negativo	No	M	29	<0.35

RC; Rinoconjuntivitis

*Número de individuo reclutado; P, paciente alérgico; C, control no atópico

[1] Sexo; M: Masculino, F: Femenino

[2] Edad; años

[3] sIgE, IgE específica a Ole e 1(kU/L)

Anticuerpos monoclonales y policlonales

Los anticuerpos primarios y secundarios utilizados en el estudio se detallan en las Tablas 4 y 5, respectivamente.

Tabla 4. Anticuerpos primarios comerciales utilizados en el estudio.

Antígeno	Especie	Clon	Dilución		Casa comercial
			IF	ID	
Anti-Ole e 1	Conejo	C5	N/E	1:5000	[1]
Anti-Der p 1	Conejo	N/E	N/E	1:5000	[2]
E-Cadherina	Ratón	36	1:75	1:2500	BD-Bioscience
Vinculina	Ratón	hVIN-1	N/E	1:2000	Sigma
ZO-1	Conejo	N/E	1:75	1:500	Invitrogen

IF: inmunofluorescencia; ID, inmunodetección; N/E: No especificado/ensayado;

ZO-1, Zonula Occludens protein 1.

[1] Producido en el laboratorio del Dr. Fernando Vivanco, Fundación Jiménez Díaz (Madrid).

[2] Amablemente cedido por ALK-Abelló.

N/E, No especificado/ensayado.

Tabla 5. Anticuerpos secundarios comerciales utilizados en el estudio.

Anticuerpo	Especie	Dilución		Molécula conjugada	Casa comercial
		IF	ID		
Anti-IgG de ratón	Cabra	N/E	1:2500	HRP	Pierce
Anti-IgG de conejo	Cabra	N/E	1:3000	HRP	Bio-Rad
Anti-IgG de ratón	Cabra	1:450	N/E	Alexa 488	Invitrogen
Anti-IgG de conejo	Cabra	1:450	N/E	Alexa 647	Invitrogen

HRP, peroxidasa de rábano; IF: inmunofluorescencia; ID, inmunodetección.

N/E: No especificado/ensayado;

Soluciones de uso general

Tampón fosfato salino (PBS): KH_2PO_4 1.5 mM, Na_2HPO_4 8.1 mM, NaCl 140 mM y KCl 2.7 mM, pH 7.4.

Tampón Tris salino (TBS): Tris-HCl 25 mM y NaCl 125 mM, pH 8.0.

Tampón de transferencia a membranas de nitrocelulosa: Tris-Base 48 mM, SDS al 0.0375% (p/v), glicocola 39 mM y metanol 20% (v/v).

Tampón RIPA: Tris 10 mM, NaCl 150 mM, pH 7.35, conteniendo Triton X-100 al 1% (v/v) (Sigma), SDS al 0.1% (v/v) (Merck) y desoxicolato sódico al 0.1% (v/v) (Sigma). A este tampón, utilizado para la lisis y la solubilización de proteínas, se le añade una mezcla de inhibidores de proteasas (*Protease inhibitor cocktail* 10X, Sigma), justo antes de su uso.

Soluciones para electroforesis en geles de agarosa

Tampón para el desarrollo de la electroforesis (TAE): Tris-base 40 mM, ácido acético 20 mM y EDTA 1 mM, pH 8.5.

Tampón de aplicación de DNA: glicerol al 30% (v/v) y azul de xilencianol al 0.25% (p/v).

Tampón de revelado: Bromuro de etidio 1 µg/mL en H_2O-MilliQ.

Soluciones para electroforesis en geles de acrilamida en presencia de SDS (PAGE-SDS)

Tampón para el desarrollo de la electroforesis: Tris-Base 25 mM, pH 8.4, glicocola al 0.14% (p/v) con/sin SDS al 0.1% (p/v).

Tampón de aplicación de proteínas: Tris-HCl 50 mM, pH 6.8, glicerol al 10% (v/v), azul de bromofenol al 0.01% (p/v) con/sin SDS al 0.1%(p/v).

Solución de teñido de proteínas: Brilliant Blue R-250 al 0.25% (p/v), metanol al 45% (v/v) y ácido acético glacial al 9% (v/v).

Solución de desteñido: Ácido acético glacial al 7.5% (v/v).

Tampones para los ensayos de inmunoabsorción ligado a enzima (ELISA)

Tampón de lavado: Tween-20 al 0.5% (v/v, Sigma-Aldrich) en PBS.

Tampón de saturación: Leche en polvo desnatada, libre de calcio al 3% (p/v) y Tween-20 al 0.1% (v/v) en PBS.

Tampones para los ensayos de inmunodetección en membrana

Tampón de lavado: Se utilizaron dos tampones de lavado según el anticuerpo primario empleado: (1) *PBS-T*, PBS con Tween-20 al 0.1% (v/v); (2) *TBS-T,* TBS con Tween-20 al 0.1% (v/v).

Tampón de bloqueo: Se usaron dos soluciones según el anticuerpo primario empleado: (1) *PBS-T-leche*, PBS-T con leche en polvo desnatada, libre de calcio, al 3% (p/v) o al 5% (p/v); (2) *TBS-T-BSA*, TBS-T con albúmina de suero bovino (BSA, Sigma-Aldrich) al 3% (p/v).

Medios de cultivo

B-ALI-G (*Bronchial-ALI-Growth medium*)**:** Medio de crecimiento suplementado con factores de crecimiento, hormonas y antibióticos, suministrado por Lonza. Estos incluyen extracto de pituitaria bovina, hidrocortisona, factor de crecimiento epitelial humano (hEGF), adrenalina, transferrina, insulina, ácido retinoico, triyodotironina, gentamicina-anfotericina, de acuerdo a las especificaciones de la casa comercial.

B-ALI-D (*Bronchial-ALI-Differentiation medium*)**:** Medio de diferenciación celular compuesto por B-ALI-G suplementado con ácido retinoico (Lonza) como inductor de la diferenciación.

HEPES-BSS (*HEPES Buffered Saline Solution)*: fue suministrado por Lonza.

DMEM completo: Medio basal Eagle modificado por Dulbecco (*Dulbecco's modified Eagle medium*) suplementado con suero fetal bovino al 5% (v/v) (FBS, Hyclone), L-Glutamina 2 mM (Sigma), penicilina 100 µg/mL (Lonza) y estreptomicina 100 µg/mL (Lonza).

DMEM/F12 completo: Medio basal Eagle modificado por Dulbecco (*Dulbecco's modified Eagle medium*) con F12 (*Nutrient mixture F12*, Gibco), suplementado con FBS al 10% (v/v) (FBS, Hyclone), L-Glutamina 2 mM (Sigma), penicilina 100 µg/mL (Lonza) y estreptomicina 100 µg/mL (Lonza).

RPMI completo: RPMI 1640 (Thermo Fisher Scientific) suplementado con FBS al 10% (v/v), L-Glutamina 2 mM (Sigma), penicilina 100 µg/mL (Lonza) y estreptomicina 100 µg/mL (Lonza).

PBS: Tampón fosfato salino compuesto por Na_2PO_4 67 mM, sin calcio ni magnesio y libre de endotoxina (≤ 0.1 EU/mL), pH 7.3, suministrado por Lonza.

Solución de tripsinización: Solución para despegar las células adheridas a la superficie de crecimiento -proceso conocido como tripsinización- para posteriormente realizar un subcultivo. Se utilizaron dos protocolos diferentes según el tipo de cultivo:

Cultivos primarios de células NHBE: tripsina al 0.05% (p/v, Lonza) y EDTA 0.5 mM (Sigma-Aldrich) en tampón HEPES-BSS. Tras el tratamiento durante un tiempo de 5 minutos con 5 mL de solución de tripsinización, la actividad de la tripsina se detiene añadiendo una solución de neutralización (1:1 v/v, Lonza).

Cultivos de células Calu-3: tripsina al 0.25% (p/v) y EDTA 0.5 mM en HEPES-BSS. Tras 3 incubaciones de 10 min cada una con 5 mL de solución de tripsinización, la actividad enzimática se inhibe mediante la adición de DMEM/F12 completo (1:1 v/v).

Solución de colágeno: Colágeno de tipo I de cola de rata (0.06 mg/mL, Sigma) en PBS. Los *transwell* (filtros de membrana de poliestireno de 6.5 mm de diámetro con 0.4 µm de tamaño de poro y 0.33 cm^2 de superficie de crecimiento, Corning), se incubaron con la solución de colágeno durante 45 min a 37ºC y se esterilizaron con luz

UV durante 45 min. Antes de su uso, los *transwell* se lavaron 3 veces con PBS con el fin de eliminar el exceso de colágeno.

Lípidos y soluciones

Lípidos: 4-colesten-3-ona (CNE) fue suministrada por Sigma-Aldrich; 1,2-dihexadecanoil-sn-glicero-3-fosfocolina (DPPC), esfingomielina (SM, cerebro de cerdo), 1-hexanodecanoil-2-(9Z-octadecenoil)-sn-glicero-3-fosfocolina (POPC), colesterol (CHO) y 1,2-dioleil-sn-glicero-3-fosfoetanolamina-N-(lisamina sulfonil rodamina B) (Rho-PE) se obtuvieron de Avanti Polar Lipids. Los lípidos se disolvieron en cloroformo:metanol (2:1, v/v, Scharlab), empleando las siguientes combinaciones: DPPC, POPC:SM:CHO (2:1:1, ratio molar), POPC:CHO (2:1, ratio molar), SM:CHO (2:1, ratio molar) y POPC:SM:CNE (2:1:1, ratio molar).

Tampón de monocapas: Tris-HCl 5 mM, pH 7.4, conteniendo NaCl 0.15 M, en H_2O doblemente destilada en presencia de permanganato.

MÉTODOS

Cultivos primarios y de líneas celulares en ALI

Cultivo primario de células NHBE en ALI

Las células NHBE (pase 1, vial criopreservado con $5 \cdot 10^5$ células) se crecieron inicialmente en una botella de 75 cm^2 (Corning), en 20-25 mL de medio B-ALI-G, a 37ºC y bajo condiciones de CO_2 al 5%, hasta alcanzar el 80% de confluencia (Figura 12). El medio de cultivo se cambió, 2 o 3 veces por semana. Una vez alcanzado el 80% de confluencia y tras lavar las células con HEPES-BSS, las células se tripsinizaron. Después de centrifugar a 1200 *g* durante 5 min, las células se resuspendieron en medio B-ALI-G y se contaron con una cámara de Neubahuer bajo el microscopio óptico Eclipse TS100 (Nikon), verificándose su viabilidad con una disolución de azul tripán (Sigma). Finalmente, se ajustaron a la densidad deseada en medio B-ALI-G y se sembraron nuevamente en una botella de 75 cm^2.

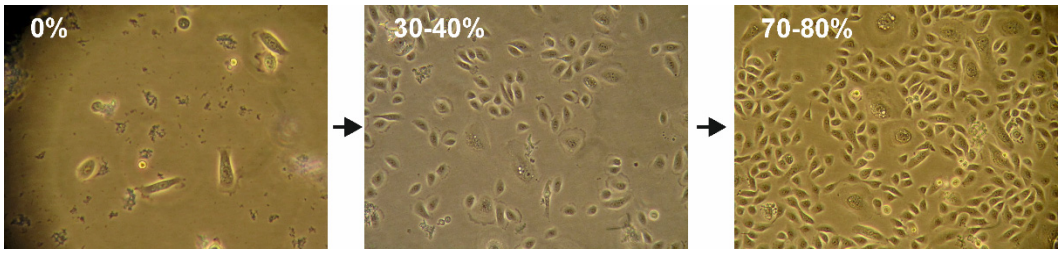

Figura 12. Cultivo en monocapa de células NHBE monitorizado por microscopía óptica. Aumento: 100x. Microscopio Nikon Eclipse TS-100. Se indica la confluencia del cultivo (%).

Tras un nuevo pase (pase 3), las células se cultivaron, a una densidad de $1.5 \cdot 10^5$ células/cm^2, en *transwell* previamente tapizados con una solución de colágeno. Se añadieron 100 µL y 500 µL de medio B-ALI-D en el lado apical y basolateral, respectivamente. Una vez alcanzado el 80% de confluencia (aproximadamente 3 días), el medio apical se retiró mediante aspiración y el basolateral se reemplazó por medio B-ALI-D con ácido retinoico. De esta forma se estableció el cultivo en ALI, siendo éste el día 0. El medio se cambió cada 2 días, y la acumulación de moco en el lado apical se evitó mediante lavados con PBS (200 µL por pocillo). El estado de diferenciación y el establecimiento de una barrera epitelial se evaluaron mediante diferentes técnicas: medidas de resistencia transepitelial (TEER), microscopía electrónica de barrido (SEM) y de transmisión (TEM), microscopía confocal de fluorescencia (CLSM), inmunodetección (*Western Blot*) y PCR semicuantitativa (sqPCR). Los días 7 y 21 de cultivo en ALI se seleccionaron para el estudio como representativos de un epitelio no diferenciado y diferenciado, respectivamente.

Con el fin de estudiar la influencia del estado de diferenciación del epitelio bronquial en la respuesta inmune a Ole e 1, las células se expusieron por el lado apical al alérgeno (25 µg/mL) en medio B-ALI-D los días 7 y 21 de cultivo en ALI (Figura 13).

Transcurridas 16 h después de la exposición, se analizó la integridad de la barrera epitelial por inmunodetección, TEM, SEM y CSLM. El estado de diferenciación de las células NHBE se determinó mediante RT-PCR semicuantitativa. Además, se recogió el sobrenadante de los cultivos para evaluar la producción de citoquinas mediante un *microarray* de anticuerpos. En el estudio se establecieron 2 grupos experimentales: *grupo 1*, células expuestas a Ole e 1; y *grupo 2*, células tratadas con PBS (control).

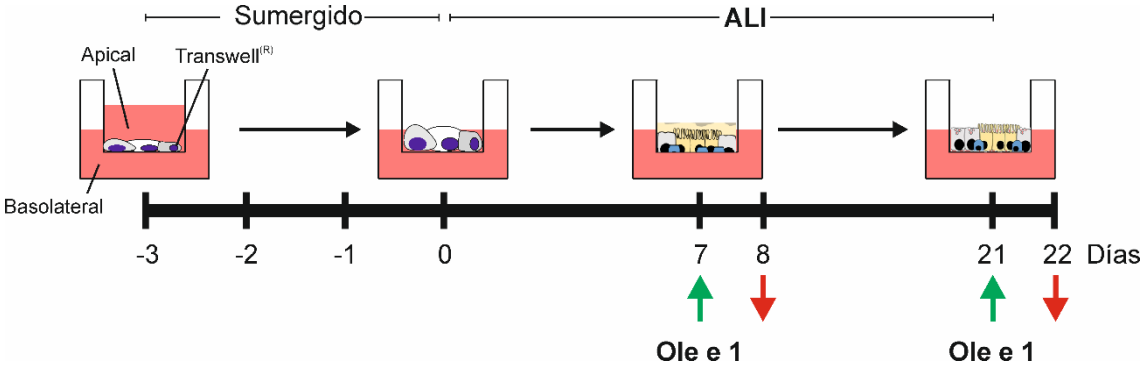

Figura 13. Esquema del protocolo experimental empleado para analizar la influencia del estado de diferenciación en la respuesta de las células NHBE a Ole e 1. Las flechas verdes indican los días de exposición por el lado apical al alérgeno Ole e 1 (25 µg/mL); y las rojas, el momento de la recogida de muestras. ALI, interfase aire-líquido.

Cultivos de la línea celular Calu-3 en ALI

Las células Calu-3 (entre los pases 23-28) se cultivaron, a una densidad de $5 \cdot 10^4$ células/cm^2, en 25 mL de DMEM/F12 completo en botellas de 75 cm^2, a 37ºC y en una atmósfera húmeda con CO_2 al 5% (Figura 14). El medio de cultivo se renovó cada 2 días. Una vez alcanzado el 80% de confluencia, las células se tripsinizaron y tras centrifugación a 1200 *g* durante 5 min, se resuspendieron en medio completo y, finalmente, se cultivaron, a una densidad de $3 \cdot 10^5$ células/cm^2, en *transwell*, añadiendo 100 µL y 500 µL de medio completo en el lado apical y basolateral, respectivamente. Al llegar al 80% de confluencia, se retiró el medio del lado apical, reemplazando el basolateral por DMEM/F12 suplementado con FBS al 5% con el fin de establecer las condiciones de cultivo en ALI. El medio basolateral se renovó cada 2 días, y el lado apical se lavó con 100 µL de PBS, para eliminar el exceso de moco secretado.

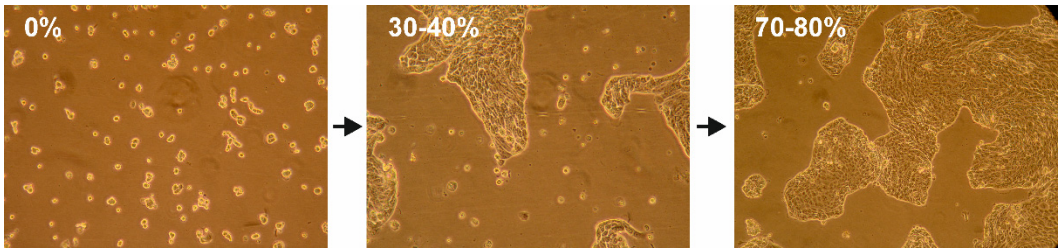

Figura 14. Cultivo en monocapa de células Calu-3 monitorizado por microscopía óptica. Aumento: 100x. Microscopio Nikon Eclipse TS-100. Se indica la confluencia del cultivo (%).

Para el estudio del **efecto de la co-exposición a la proteasa Der p 1** en la respuesta del epitelio bronquial a Ole e 1, las células se expusieron apicalmente al alérgeno Ole e 1 (25 µg/mL) en PBS, conteniendo GSH 0.1 mM, en presencia o ausencia de Der p 1 (10 µg/mL), los días 2 y 7 de cultivo en ALI (Figura 15).

En los experimentos de *exposición aguda*, las células fueron co-expuestas a Ole e 1 y Der p 1 durante 24 h. En los experimentos de *exposición crónica* las células fueron tratadas con Der p 1 durante 5 días consecutivos (días 2-6), renovando la solución de proteasa cada 24 h. El día 7 fueron co-expuestas a Ole e 1 y Der p 1 durante 24 h. En todos los experimentos, se activó Der p 1 mediante su incubación en PBS con GSH 0.1 mM durante 15 min a 37ºC.

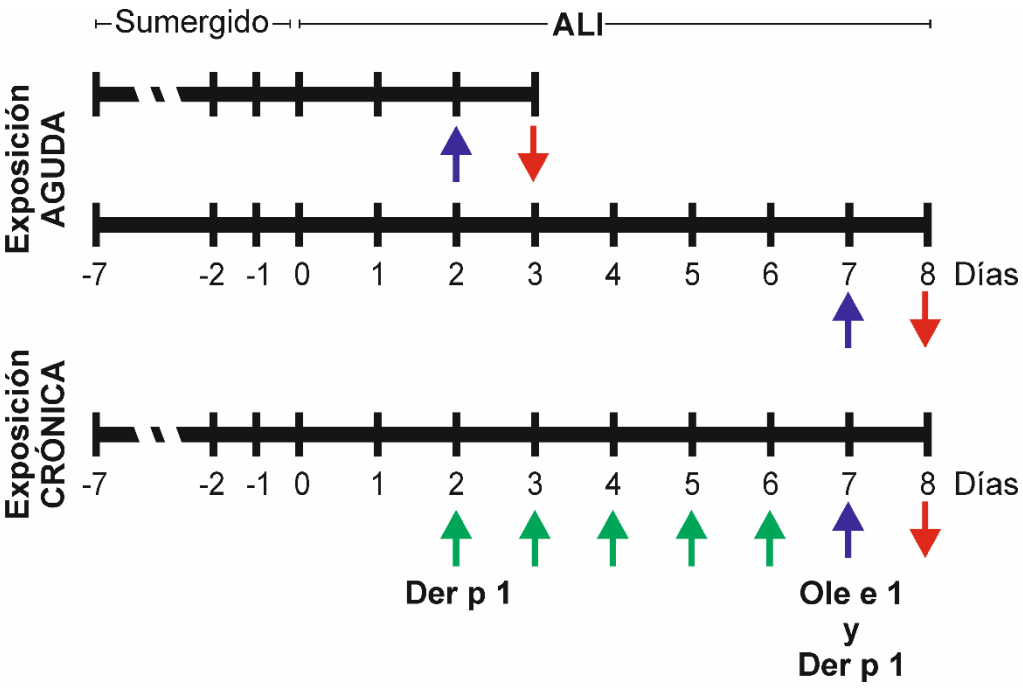

Figura 15. Esquema del protocolo experimental empleado para analizar el efecto de la co-exposición, *aguda* y *crónica*, a la proteasa Der p 1 en la respuesta de las células Calu-3 a Ole e 1. Las flechas verdes indican los días de exposición por el lado apical a Der p 1 (10 µg/mL); las azules, los días de co-exposición al alérgeno Ole e 1 (25 µg/mL) y Der p 1; y las rojas, el día de la recogida de muestras.

En ambos casos se establecieron 4 grupos experimentales: *grupo 1*, células expuestas a Ole e 1; *grupo 2*, células expuestas a Der p 1; *grupo 3*, células co-expuestas a Ole e 1 y Der p 1; y *grupo 4,* célula*s* control tratadas con PBS/GSH.

Después de la co-exposición, se analizó la permeabilidad del epitelio a Ole e 1 y la integridad de la barrera epitelial mediante inmunodetección, microscopía electrónica y microscopía confocal. Además, en los experimentos de *exposición aguda* se recogió el sobrenadante de los cultivos para determinar la producción de metabolitos, así como para los ensayos de activación *in vitro* de basófilos.

El efecto de la co-exposición al extracto de humo de tabaco (CSE) en la respuesta del epitelio bronquial a Ole e 1, requirió el establecimiento de un modelo *in vitro* de epitelio bronquial dañado por la exposición al CSE. Con este fin, las células Calu-3 se expusieron apicalmente a diferentes concentraciones de CSE (0-50% v/v) en 300 µL de PBS, los días 2 y 7 de cultivo en ALI. Se ensayaron distintos tiempos de exposición. La validez del modelo se evaluó mediante el análisis de diferentes parámetros: viabilidad celular, integridad de la barrera epitelial, producción de IL-6 y expresión de genes implicados en la respuesta al estrés oxidativo y en la producción de citoquinas pro-inflamatorias. Esto permitió establecer las condiciones óptimas para los estudios de co-exposición. Dado el carácter volátil de algunos componentes del CSE, las células expuestas al CSE se cultivaron en una placa separada de las tratadas con PBS (grupo control).

Con el fin de analizar el efecto de la co-exposición a CSE en la respuesta del epitelio bronquial al alérgeno, las células Calu-3 fueron tratadas apicalmente con CSE al 10% (v/v) en 300 µL de PBS, los días 2 y 7 de cultivo en ALI. Transcurridas 24 h, las células fueron co-expuestas a Ole e 1 (25 µg/mL) y CSE al 10% durante otras 24 h (Figura 16).

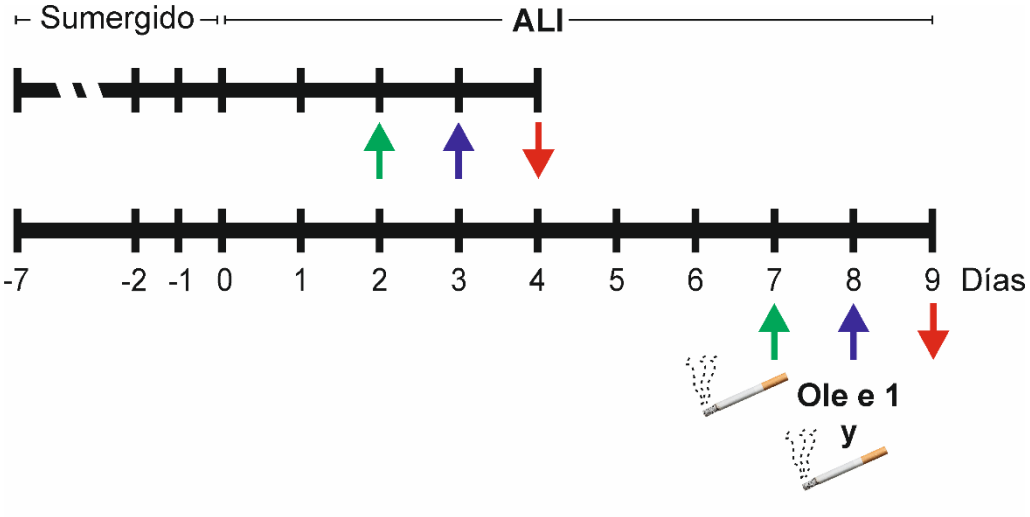

Figura 16. Esquema del protocolo experimental empleado para analizar el efecto de la co-exposición al extracto del humo de tabaco (CSE) en la respuesta de las células Calu-3 a Ole e 1. Las flechas verdes indican los días de exposición por el lado apical al CSE al 10%; las azules, los días de co-exposición al alérgeno Ole e 1 (25 µg/mL) y CSE; y las rojas, el día de la recogida de muestra.

El efecto de la co-exposición se determinó analizando los parámetros indicados anteriormente: permeabilidad del epitelio a Ole e 1, integridad de la barrera epitelial y expresión de genes implicados en la respuesta al estrés oxidativo y en la producción de citoquinas pro-inflamatorias.

En el estudio se establecieron 4 grupos experimentales: *grupo 1*, células expuestas a Ole e 1; *grupo 2*, células expuestas a CSE; *grupo 3*, células co-expuestas a Ole e 1 y CSE; y *grupo 4,* células tratadas con PBS (control).

Preparación de extractos celulares y cuantificación de proteínas

Tras lavar con PBS, las células se levantaron por raspado y se centrifugaron a 1600 *g* durante 10 min a 4ºC. El sedimento celular se resuspendió en tampón RIPA y se homogeneizó con una jeringa de insulina y una aguja de 25G (BD Biosciences). La suspensión se incubó durante 1 h a 4ºC y tras centrifugar a 16000 *g* durante 10 min a 4ºC para eliminar el material celular no solubilizado, el sobrenadante se congeló y se almacenó a -20ºC hasta su utilización.

La concentración de proteína total presente en los extractos se determinó mediante el método colorimétrico del ácido bicinconiníco (BCA), con el *kit Micro BCA Protein Assay* (Thermo Scientific). Este *kit* permite valorar cantidades de proteína comprendidas entre 25 y 2000 µg/mL, utilizando BSA como proteína patrón.

Preparación del extracto de humo de tabaco

El CSE se preparó según el protocolo descrito por Higashi *et al.* [239], con pequeñas modificaciones. El humo de la combustión en 5 min de un cigarrillo de la marca Marlboro® (Lote 2047642) se burbujeó en 15 mL de PBS estéril (previamente atemperado a 37ºC), utilizando una bomba peristáltica GP1000 (Fisher Scientific) a un flujo constante de 50 rpm y a 37ºC (Figura 17). La fase gaseosa se dejó reposar durante 10 min y a continuación, el CSE se filtró a través de un filtro de nylon de 0.45 µm de poro (Millipore). Se hicieron alícuotas que se conservaron a -80ºC hasta su uso. El CSE se estandarizó tomando como referencia la concentración de nicotina determinada en un espectrofotómetro Beckman DU-7 en el UV lejano, utilizando un coeficiente de extinción molar a 260 nm de 3020 $mol^{-1} \cdot L \cdot cm^{-1}$ [240]. La ausencia de endotoxina en la muestra (≤ 0.005 EU/mL, datos no mostrados) se confirmó mediante el uso del kit THP1-Blue Cells, siguiendo las indicaciones de la casa comercial (Invivogen).

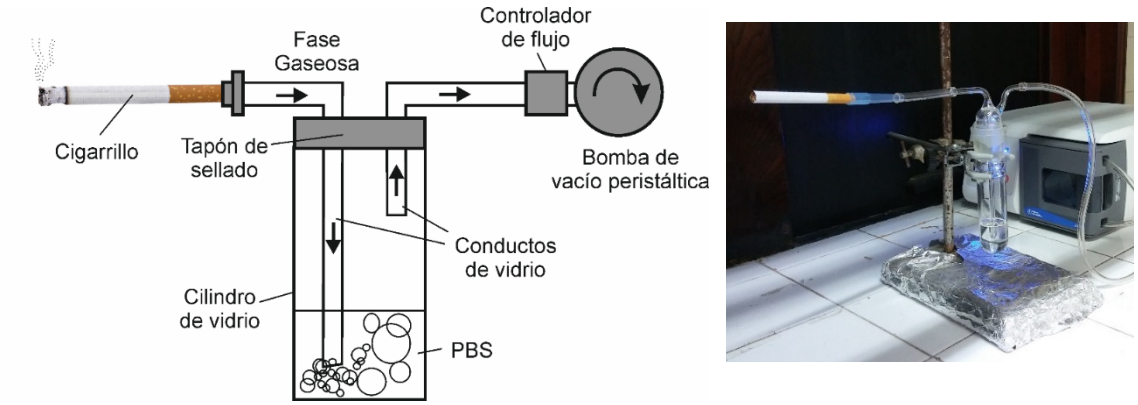

Figura 17. Esquema e imagen del dispositivo utilizado para la obtención del extracto de humo de tabaco, basado en Higashi *et al.* [239].

La composición del CSE se determinó en el Centro de Apoyo a la Investigación de Espectrometría de Masas (CAI-UCM), utilizando un cromatógrafo de gases 3800 acoplado a un espectrómetro de masas *Varian Saturn 2200* con inyector automático *CombiPal* (Saturn). Se utilizaron las condiciones experimentales indicadas en la Tabla 6.

Tabla 6. Condiciones experimentales utilizadas en la caracterización del CSE.

Cromatografía de Gases (GS)	
Columna	ZB-5MSplus (30 m x 0.25mm x 0.25 µm) de fase polisilarileno al 5%/dimetilpolisiloxano al 95%
Inyección	Automática
Modo de inyección	*Splitless*
Flujo de gas portador	1 mL/min
Temperatura del inyector	250ºC
Energía de ionización	70 eV
Programa de Tª del horno	40ºC (1 min), 6ºC/min hasta 250ºC (38 min)
Espectrometría de masas (MS)	
Retraso del solvente	0 min
Relación masa/carga (m/z)	40 - 650

Aislamiento y purificación de surfactante pulmonar

El surfactante pulmonar se aisló a partir de pulmones de cerdo frescos suministrados por el Matadero de Madrid, según el protocolo descrito por Taeusch *et al.* [241], con pequeñas modificaciones. Tras canular manualmente la tráquea los pulmones se lavaron con 2.5 L de NaCl al 0.9% (p/v) en tampón de monocapas. El lavado se filtró por una gasa para descartar los posibles restos celulares y otros contaminantes presentes en la muestra y se centrifugó utilizando un rotor flotante SW40Ti (Beckman Coulter) a 710 *g* durante 5 min a 4ºC. El sobrenadante se filtró de nuevo por una gasa y se centrifugó a 170000 *g* durante 1 h a 4ºC. El sobrenadante se eliminó y el sedimento se resuspendió con ayuda de un *potter* en NaBr al 16% (p/v) en NaCl al 0.9% (p/v) en hielo con el fin de realizar una centrifugación en gradiente NaBr. Para ello, la muestra (4 mL) se depositó en el fondo de un tubo de centrífuga y sobre ella se aplicaron 6 mL de NaBr al 13% en NaCl 0.9% y, finalmente, 2.5 mL de NaCl al 0.9%. La muestra se centrifugó a 120000 *g* en el mismo rotor durante 2 h a 4ºC. La fracción correspondiente al surfactante se recolectó con ayuda de una pipeta *Pasteur*, se homogenizó con un *potter* en NaCl al 0.9% y tras hacer alícuotas, se conservó hasta su uso a -80ºC.

La cantidad de surfactante se estimó determinando la concentración de fosfolípidos totales mediante el método de valoración de fósforo [242]. La muestra se desecó y se incubó en ácido perclórico puro durante 30 min a 260ºC, en un baño de arena. A continuación, se añadieron 3.5 mL de H_2O bidestilada, 0.5 mL de molibdato de amonio al 2.5% (p/v) y 0.5 mL de ácido ascórbico al 10% (p/v), y la mezcla se incubó durante 7 min a 100ºC. Tras enfriar en hielo, se midió la absorbancia a 820 nm en un espectrofotómetro Beckman DU-7 (Beckman), utilizando una solución de fosfato inorgánico de concentración conocida como patrón.

Marcaje fluorescente de Ole e 1

El marcaje de Ole e 1 con Alexa 488 Fluor® Succinimidyl Ester (Alexa 488, Thermo Fisher Scientific) se realizó de acuerdo a las instrucciones de la casa comercial. La proteína marcada con Alexa 488 se purificó mediante un sistema de ultrafiltración *Nanosep®-10K* (Pall Corporation). El grado de marcaje (DOL, 1) y la concentración (2) de la proteína se determinaron según las fórmulas:

$$(1)\ DOL = (Abs_{\lambda 1} \cdot MM_{proteína})/(C_{proteína} \cdot \varepsilon_{\lambda 1}^{sonda})$$

$$(2)\ C_{proteína} = (Abs_{\lambda 2} - Abs_{\lambda 1} \cdot CF)/\varepsilon_{\lambda 2}^{proteína}$$

siendo:

$Abs_{\lambda 1}$ y $Abs_{\lambda 2}$ = absorciones de la proteína marcada a λ1 y λ2.

CF = factor de corrección de la sonda.

$C_{proteína}$ = concentración molar de proteína.

$MM_{proteína}$ = masa molecular de la proteína.

$\varepsilon_{\lambda 1}^{sonda}$ y $\varepsilon_{\lambda 2}^{proteína}$ = coeficiente de extinción molar de la sonda a λ1 y de la proteína a λ2, respectivamente.

λ1 y λ2 = longitudes de ondas correspondientes al máximo de absorción de la sonda y de la proteína, respectivamente.

Marcaje fluorescente del surfactante

El surfactante (0.5 mg/mL) se resuspendió en tampón de monocapas conteniendo BODIPY-PC (2-(4,4-difluoro-5,7-dimetil-4-bora-3a, 4a-diazo-s-indaceno-3-pentanoil)-hexadeca-noil-sn-glicero-3-fosfocolin, Invitrogen), a una relación molar sonda:surfactante de 1:100, y se incubó durante 1 h a 37ºC, con ciclos de 5 min de agitación a 1200 rpm y 10 min de reposo. Finalmente, la muestra se diluyó a una concentración de 25 µg/µL en tampón de monocapas y se conservó a -20ºC hasta su uso.

Medición de la resistencia eléctrica transepitelial (TEER)

El TEER es un parámetro que aporta información sobre la integridad del epitelio, tanto de la confluencia e integridad celular como de la formación de uniones intercelulares [243]. El TEER de los cultivos en ALI se determinó utilizando un voltímetro *EVOM2* (World Precision Instruments, WPI) con electrodos STX2, según las instrucciones de la casa comercial (Figura 18).

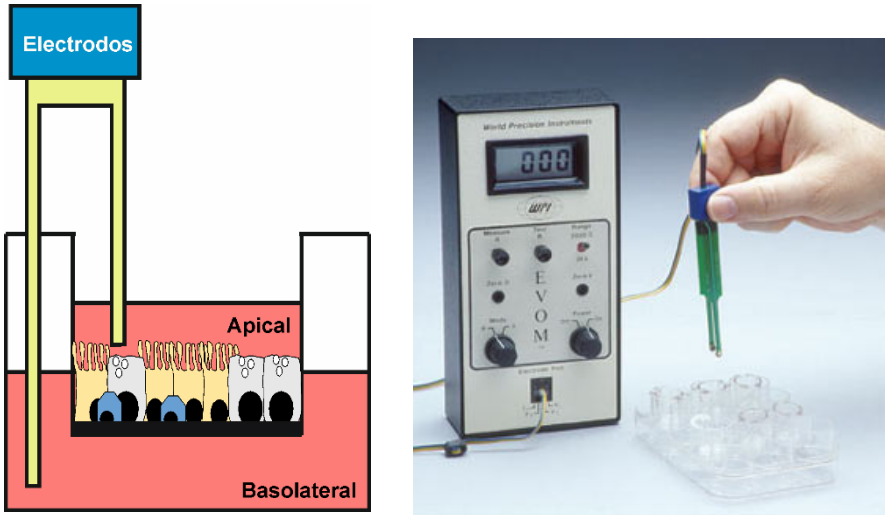

Figura 18. A) Esquema del dispositivo empleado para la medición de la resistencia eléctrica transepitelial de los cultivos celulares crecidos en placas tipo *transwell*. B) Voltímetro EVOM con electrodos STX2 (Fuente: https://www.wpiinc.com).

Se realizaron medidas por triplicado de cada pocillo (*n = 5-8*), a distintos tiempos. Los valores de TEER se expresaron en $\Omega \cdot cm^2$ tras su corrección usando un blanco (membrana sin células para evaluar la resistencia intrínseca) y el área efectiva de crecimiento (0.33 cm^2).

Ensayo de citotoxicidad

La toxicidad celular del CSE se determinó utilizando el ensayo MTT (bromuro de 3-(4,5-dimetiltiazol-2-il)-2,5-difeniltetrazolio) descrito por Denizot *et al.* [244], con pequeñas modificaciones. Este ensayo se basa en la reducción metabólica del MTT (compuesto de color amarillo, Sigma-Aldrich) a su forma insoluble formazán (compuesto de color púrpura), catalizada por la enzima succinato-deshidrogenasa mitocondrial, funcional de las células tratadas (Figura 19).

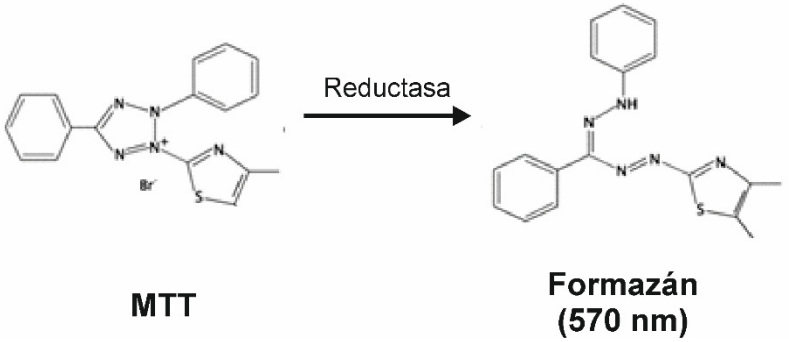

Figura 19. Esquema de la reducción metabólica del MTT (compuesto de color amarillo) a formazán (color morado), catalizada por la enzima succinato-deshidrogenasa mitocondrial funcional de las células tratadas. Se incluye la longitud de onda de absorción máxima del formazán (570 nm).

Para ello, se sembraron $2 \cdot 10^4$ células/cm^2 en placas de 96 pocillos (Corning) en medio DMEM/F12 completo y por triplicado. Una vez alcanzado el 80% de confluencia, las células se trataron con diferentes concentraciones de CSE (1.25%-50% (v/v)) en DMEM con FBS al 5%, durante 24 y 48 h a 37ºC. A continuación, se añadió el MTT (0.5 mg/mL) en PBS y se incubó durante 4 h más a 37ºC. Tras aspirar el sobrenadante, los cristales de formazán formados se disolvieron con metanol/dimetilsulfóxido (DMSO, Sigma) a una relación 1:1 (v/v) y se cuantificaron midiendo la absorbancia a 570 nm (con filtro de referencia a 650 nm) en un espectrofotómetro *iMark Microplate Absorbance Reader* (Bio-Rad). El porcentaje de células viables es proporcional a la cantidad de formazán producido.

La viabilidad se determinó según la siguiente fórmula:

$$\% \text{ Viabilidad} = (Abs_{\text{células tratadas}}/Abs_{\text{células control}}) \cdot 100$$

Ensayo de la permeabilidad epitelial *in vitro*

La función de la barrera epitelial se monitorizó *in vitro* mediante el análisis de la permeabilidad paracelular a Ole e 1 (25 µg/mL) conjugado con Alexa 488, en presencia o ausencia de Der p 1. Para ello, las células Calu-3 fueron expuestas apicalmente al alérgeno, en las condiciones indicadas anteriormente, los días 2 y 7 de cultivo en ALI. Este momento se consideró como tiempo 0 y a partir de entonces se tomaron alícuotas de 10 µL del medio apical y 200 µL del basolateral, cada 30-60 min durante un total de 24 h. La intensidad de la fluorescencia de cada muestra fue determinada en un lector de placas FLUOstar OPTIMA (λ_{exc} = 485 nm y λ_{em} = 520 nm). La permeabilidad de Ole e 1 se calculó como el cambio relativo en la intensidad de fluorescencia del grupo control y de soluciones de Ole e 1-Alexa 488, equivalentes a un 100% de proteína presente en los medios apical y basolateral.

De forma paralela, la permeabilidad paracelular a Ole e 1 también se analizó mediante inmunodetección usando el anticuerpo policlonal anti-Ole e 1 (Tabla 4).

Microscopía electrónica de barrido (SEM)

Tras retirar el medio, las células se lavaron con HEPES-BSS, se fijaron en paraformaldehído (PFA) al 4% (v/v, sigma) y glutaraldehído al 2.5% (p/v, Sigma), en H_2O-MilliQ, durante 3 h, y se post-fijaron con tetraóxido de osmio al 1% (v/v) y ferricianuro potásico al 1.5% (v/v), en H_2O-MilliQ, durante 1 h. Tras dos lavados con H_2O-MilliQ, las muestras se deshidrataron mediante inmersiones de 10 min en una serie de concentraciones crecientes de etanol (35, 50, 70, 80, 90, 95 y 100% (v/v), Merck). Finalmente, las membranas se retiraron con un escalpelo estéril, se montaron sobre un

soporte de aluminio empleando cinta adhesiva de doble cara, se desecaron en un sistema de punto crítico de CO_2 (EM CPD300, Leica) y se metalizaron con oro-paladio. Las muestras se examinaron en un microscopio *JEOL 6400 JSM* en el Centro Nacional de Microscopía Electrónica (CNME-UCM), utilizando el programa INCA para la captura y procesamiento de las imágenes. Las muestras se prepararon y analizaron por duplicado. Todas las incubaciones se realizaron a temperatura ambiente.

Microscopía electrónica de transmisión (TEM)

Una vez lavadas, las células se fijaron, post-fijaron y deshidrataron siguiendo el protocolo descrito para el análisis mediante SEM. A continuación, las muestras se transfirieron gradualmente a resina de epóxidos (25, 50 y 75% en etanol puro, Agar Scientific) y se incubaron en resina pura durante 16 h a temperatura ambiente. Una vez retiradas las membranas de los *transwells* con un escalpelo estéril, se depositaron sobre un molde de resina polimerizada, se cubrieron con resina fresca y se incubaron durante 4 días a 65ºC. Las secciones ultrafinas (micras) obtenidas con un crioultramicrotomo *Leica Ultracut S* se contrastaron con acetato de uranilo y citrato de plomo, y se examinaron en un microscopio de transmisión *JEOL JEM 1010* en el CNME-UCM. Las muestras se prepararon por duplicado.

Inmunolocalización de proteínas para microscopía confocal láser de fluorescencia (CLSM)

Después de tres lavados con PBS, las células se fijaron en PFA al 4% (p/v) en PBS, durante 15 min. Tras varios lavados con PBS-T y permeabilizar la membrana celular con Triton X-100 al 0.5% (v/v) en PBS durante 10 min, las muestras se incubaron con BSA al 3% en PBS-T durante 1 h. A continuación, se incubaron con el anticuerpo primario correspondiente (Tabla 4) en tampón de bloqueo durante 1 h. Tras los lavados, las muestras se incubaron con el anticuerpo secundario correspondiente (Tabla 5) en PBS-T conteniendo BSA al 0.05% (p/v), durante 1 h en oscuridad. Tras un lavado final en PBS, se extrajeron las membranas de los *transwell* con la ayuda de un escalpelo, y se montaron en portaobjetos con la solución protectora de fluorescencia *Prolong Gold* (Thermo Fisher Scientific), y DAPI (4',6-diamidino-2-fenilindol, Invitrogen) como marcador de núcleos, para su análisis en un microscopio láser confocal *OLYMPUS FV1200* en el Centro de Citometría y Microscopía de Fluorescencia (UCM). La captura y procesamiento de las imágenes se realizó con el programa *Fiji-ImageJ*. Las muestras se prepararon por duplicado y todas las incubaciones se realizaron a temperatura ambiente.

PAGE-SDS

Las electroforesis se realizaron en un sistema discontinuo, según el método descrito por Laemmli *et al.* [245]. La preparación de los geles y el desarrollo de la electroforesis se llevaron a cabo en un sistema *Mini-Protean III* (Bio-Rad). Se prepararon geles al 10% (p/v) y al 15% (p/v) de poliacrilamida con un gel concentrante al 4% (p/v). Los geles de 8 cm·7.3 cm y 0.75 mm de espesor se preformaron con peines de 10 o 15 pocillos. Las muestras se diluyeron en tampón de aplicación con/sin β-mercaptoetanol al 5% (v/v) (Sigma-Aldrich) y se calentaron a 90ºC durante 15 min. La intensidad de corriente utilizada fue de 25 mA por gel, aplicándose hasta que el marcador del frente (azul de bromofenol) alcanzó el extremo del gel.

Tras la electroforesis, el gel se tiñó con una solución de azul de Coomassie R-250 durante 5-10 min, para una visualización directa de las proteínas, o bien, se transfirió a membranas de nitrocelulosa para los ensayos de inmunodetección. Para eliminar el exceso de colorante del gel se utilizó una solución de ácido acético glacial al 7.5% (v/v) y metanol al 20% (v/v).

Transferencia a membranas de nitrocelulosa

La transferencia de proteínas a membranas de nitrocelulosa (Amersham) se llevó a cabo según el protocolo descrito por Towbin *et al*. [246], utilizando 2 condiciones diferentes. La transferencia de proteínas de baja masa molecular (≤ 80 kDa) se realizó en un sistema semi-seco *Transfer-Blot SD Semi-Dry Transfer Cell* (Bio-Rad) en tampón Tris-Base 48 mM, SDS al 0.0375% (p/v), glicocola 39 mM y metanol al 20% (v/v), aplicando una intensidad de corriente de 1 mA/cm^2 durante 1 h. La transferencia de proteínas de alta masa molecular (> 80 kDa) se llevó a cabo en un sistema húmedo *Mini-Protean II* (Bio-Rad), aplicando un voltaje de 100 V durante 90 min. La eficacia de la transferencia se comprobó mediante visualización directa de las proteínas patrón preteñidas con un rango de masas moleculares conocidas: 17.5-105 kDa (Ref. 161-0309) y 46.9-202 kDa (Ref. 161-0305), ambos suministrados por Bio-Rad.

Inmunodetección de proteínas transferidas a membranas de nitrocelulosa

Después de la transferencia, la membrana de nitrocelulosa se hidrató con PBS o TBS, y se incubó con la solución de saturación adecuada durante 1 h: PBS-T-leche o TBS-T-BSA. Seguidamente, la membrana se incubó, durante 16 h a 4ºC, con el anticuerpo primario correspondiente diluido en el mismo tampón de saturación (Tabla 4). Tras realizar 3 lavados de 10 min cada uno en PBS-T o TBS-T, la membrana se incubó con el anticuerpo secundario correspondiente (Tabla 5), diluido en PBS-T o TBS-T con leche

desnatada al 1.5% (v/v), durante 1 h. Tras una nueva etapa de lavado, la membrana se reveló con el *kit Pierce ECL Western Blotting Substrate* (Thermo Scientific) según las instrucciones de la casa comercial, y se reveló en un analizador de imágenes *LAS-3000 mini* (Fuji-film). Todas las incubaciones, menos aquellas en las que se indican, se realizaron a temperatura ambiente y con agitación.

ELISA de inhibición

Los ensayos se llevaron a cabo en placas de 96 pocillos, fondo plano y alta capacidad de unión (Costar), realizándose cada uno de ellos por duplicado. Todas las incubaciones, menos las indicadas, se realizaron a temperatura ambiente.

Las placas se tapizaron con 100 µL/pocillo de una solución de Ole e 1 (1 µg/mL) en PBS y se incubaron toda la noche a 4ºC. Tras 4 lavados en PBS-T, los sitios de unión inespecífica se bloquearon mediante incubación con tampón de saturación durante 1 h. Transcurrido este tiempo, los pocillos se incubaron con los sueros de pacientes alérgicos al polen de olivo (*n = 3*, dilución 1:10, facilitados generosamente por el Dr. Miguel Blanca) que previamente habían sido preincubados con distintas cantidades de las muestras de Ole e 1 tratadas con Der p 1 en tampón de saturación durante 2 h. Como controles positivos y negativos se utilizaron cantidades equivalentes de Ole e 1 sin digerir y el producto de hidrólisis de Ole e 1 con HCl 2 N, respectivamente. Tras una nueva etapa de lavado, los pocillos se incubaron con un anticuerpo monoclonal anti-IgE humana (dilución 1:5000) durante 1 h. Después de otra etapa de lavado, los pocillos se incubaron con un anticuerpo de cabra anti-IgG de ratón conjugado con peroxidasa de rábano (HRP) (Tabla 5). Tras una etapa final de lavado, el revelado de los pocillos se llevó a cabo con el cromógeno *o*-fenilendiamina (0.63 mg/mL) y H_2O_2 al 0.03% (v/v) en citrato sódico 0.1 M, pH 5.0 y metanol al 4% (v/v) (100 µL/pocillo). La reacción se detuvo mediante la adición de ácido sulfúrico 3 N (100 µL/pocillo). Las medidas de absorbancia a 492 nm se realizaron en un lector *iMark Microplate Absorbance Reader* (Bio-Rad). El porcentaje de inhibición se calculó según la fórmula:

$$\% \text{ Inhibición} = [1 - (Abs_{\text{con inhibidor}}/Abs_{\text{sin inhibidor}})] \cdot 100$$

Algunos experimentos se llevaron a cabo con el anticuerpo policlonal anti-Ole e 1 (dilución 1:100.000 en tampón de saturación), utilizando en esta ocasión un anticuerpo de cabra anti-IgG de conejo conjugado con HRP (Tabla 5).

Determinación de los niveles de interleucina 6 (IL-6)

La determinación de los niveles de IL-6 en los sobrenadantes de los medios apicales y basolaterales de los cultivos de células Calu-3 se realizó mediante ELISA en sándwich,

utilizando el *kit Human IL-6 ELISA Set* (BD Biosciences), siguiendo las instrucciones de la casa comercial.

Microarrays de anticuerpos

El patrón de citoquinas secretadas por las células NHBE estimuladas con el alérgeno Ole e 1 se analizó con un *microarray* de anticuerpos *RayBio® Human Cytokine Antibody Array 5* (Ray-Biotech), siguiendo las instrucciones de la casa comercial. Para los ensayos se utilizaron los sobrenadantes de los medios apicales (dilución 1:2 en tampón de bloqueo 1) y basolaterales (sin diluir), obtenidos tras centrifugar a 1600 *g* durante 10 min a 4ºC con el fin de eliminar el material insoluble. Las imágenes se adquirieron con un sistema *LAS-3000 Mini Imaging System* (Fujifilm) y se analizaron con el *software GenePix Pro 7.1* (Molecular Devices). Todos los valores se corrigieron y normalizaron respecto a los *spots* negativos y positivos del *microarray*. La normalización entre *microarrays* se llevó a cabo usando la mediana de los *spots* referidos como positivos. Los resultados se expresaron como "cambio de expresión" respecto al nivel basal, considerando positivos cambios en la expresión ≥ 2.

Espectros de dicroísmo circular (CD)

Los espectros de CD se obtuvieron en un dicrógrafo *Jasco J-715*, equipado con lámpara de Xenón de 150 W. Se utilizó una cubeta cilíndrica de cuarzo de 0.1 cm de paso óptico y una concentración de proteína de 0.2 mg/mL en tampón fosfato sódico 50 mM, pH 7.4, en presencia o ausencia de GSH o Cys. Se registraron 6 espectros en el ultravioleta (UV)-lejano (200-260 nm), a una velocidad de 50 nm/min.

Todos los espectros se corrigieron mediante la sustracción de la línea base correspondiente obtenida para el tampón en las mismas condiciones. Los valores de elipticidad, expresados como elipticidad molar por residuo de aminoácido (grados x cm^2 x $dmol^{-1}$), se calcularon según la fórmula:

$$[\theta]^{MWR} = 3300 \cdot S \cdot H \cdot MWR / l \cdot C$$

siendo:

$[\theta]^{MWR}$ = elipticidad molar por residuo.
S = sensibilidad de detección del aparato.
H = diferencia en mm entre la línea base y el espectro de la muestra.
MWR = masa molecular promedio para cada aminoácido.
l = paso óptico en cm.
C = concentración de proteína en mg/mL.

El cálculo teórico del porcentaje de contribución de cada una de las estructuras secundarias básicas a la estructura global de la proteína se realizó con el *software* de deconvolución CDNN CD (Applied Photophysics) que emplea como referencia hasta 33 espectros de CD de proteínas conocidas.

Aislamiento de RNA total y síntesis de cDNA

El RNA total se aisló a partir de los sedimentos celulares, tras homogenizarlos en *TRIzol Reagent* (Ambion), utilizando el kit *RNeasy Mini* (Qiagen), siguiendo las instrucciones de la casa comercial. La concentración, pureza e integridad del RNA se determinaron en un *Bioanalyzer 2100B* (Agilent Technology) en la Unidad de Genómica del Parque Científico de Madrid (UCM).

El RNA total aislado se empleó para la síntesis de cDNA monocatenario utilizando el *kit Superscript III First-Strand Synthesis System* (Thermo Fisher Scientific), según las indicaciones de la casa comercial. Este cDNA se utilizó como molde en la reacción en cadena de la polimerasa (PCR) semicuantitiva y cuantitativa.

Electroforesis de DNA

El análisis de los fragmentos de DNA se realizó en geles de agarosa (Pronadisa) al 1 o 2% (p/v) en tampón TAE. Las muestras se diluyeron en tampón de aplicación y la electroforesis se desarrolló en tampón TAE, a 100 V y a temperatura ambiente. Las bandas de DNA se visualizaron por tinción del gel con una solución de bromuro de etidio y posterior iluminación con luz UV con un equipo *Molecular Imager Gel Doc XR System 170-8170* (Bio-Rad).

Análisis de la expresión génica mediante PCR

PCR semi-cuantitativa (sqPCR)

Las reacciones de PCR semi-cuantitativa se llevaron a cabo en un termociclador *Mastercycler Thermal Cycler* (Eppendorf). Una vez diseñados, los oligonucleótidos fueron sintetizados por Sigma (Tabla 7). Las amplificaciones por PCR se realizaron con 25 µL de una mezcla de reacción conteniendo los componentes del *kit Advantage® 2 PCR Enzyme System* (Clontech) y los oligonucleótidos específicos (0.25 µM). Se emplearon dos condiciones diferentes, tras una primera etapa de desnaturalización a 95ºC durante 5 min: *Condición A*, 30 ciclos de desnaturalización a 95ºC durante 30 seg, hibridación a 60ºC durante 30 seg y extensión a 72ºC durante 30 seg; *Condición B*, 30 ciclos de desnaturalización a 95ºC durante 30 seg, seguidos por ciclos de hibridación y extensión simultánea a 68ºC durante 1 min. Por último, y en ambos casos, se realizó

una extensión a 72ºC durante 10 min. Los productos de PCR se analizaron en geles de agarosa al 2% (p/v) y visualizaron con luz UV tras tinción durante 10 min en una solución de bromuro de etidio. Las imágenes obtenidas se analizaron con el *software Gel Doc-XR System* (Bio-Rad). Para la normalización de los datos y calcular los niveles de expresión relativa de los genes analizados, se utilizaron los niveles de expresión del gen de la enzima gliceraldehído-3-fosfato deshidrogenasa (GAPDH). Se realizaron al menos 3 réplicas experimentales y 2 biológicas por cada condición.

Tabla 7. Secuencias y características de los oligonucleótidos empleados para el estudio de las distintas poblaciones celulares presentes en los cultivos de células NHBE.

Gen	Población Celular	Primer	Secuencia (5'-3')	Tm[1] (ºC)	pb[2]	Condición[3]
CC10	Club	*sense*	TCCACCATGAAACTCGCTGT	59.6	150	A
		antisense	AAGTTCCATGGCAGCCTCAT	59.6		
FOXJ1	Ciliadas	*sense*	CACGTGAAGCCTCCCTACTC	63.8	594	A
		antisense	TTTGAGGGGTTCCAGCTCAC	59.8		
GAPDH	Constitutiva	*sense*	AAGGTGAAGGTCGGAGTC	59.2	226	A
		antisense	AAGATGGTGATGGGATTTC	58.7		
MUC5AC	Globosas	*sense*	TGCAGTAGGGCAGCTTTGTT	60.2	237	A
		antisense	TCCGAGTACCTTCCCGACAT	60.0		
NKX2.1	Progenitoras	*sense*	GGGCTAAAACAAACGCGAGG	60.1	242	B
		antisense	GGAGTCGTGTGCTTTGGACT	60.3		
P63	Basales	*sense*	AGCCAGAAGAAAGGACAGCA	59.2	274	A
		antisense	TAGTCGGTGTTGGAGGGGAT	60.0		

CC10, *club cell secretory protein* ; FOXJ1, *forkhead box protein J1* ; MUC5AC, *mucin 5AC* ; NKX2.1, *NK2 homeobox 1* : P63, *tumour protein p63* .

[1]Tm, temperatura de fusión.

[2]pb, pares del amplicón resultante.

[3]Condición, método PCR empleado.

PCR cuantitativa en tiempo real (RT-PCR)

La amplificación mediante RT-PCR del cDNA sintetizado a partir del RNA total se realizó en un termociclador *7900HT Fast Real Time PCR* (Applied Biosystems), usando oligonucleótidos específicos (Tabla 8). La normalización de los datos se llevó a cabo utilizando los niveles de expresión del mRNA de GAPDH y los niveles relativos de expresión del mRNA de cada uno de los genes analizados se calcularon mediante el método del $\Delta\Delta C_T$ [247]. Las amplificaciones por RT-PCR se realizaron en la Unidad de Genómica del Parque Científico de Madrid (UCM).

Tabla 8. Secuencias y características de los oligonucleótidos empleados para el estudio por qPCR de la expresión de distintos genes susceptibles de alteración en los cultivos Calu-3.

Gen	Primer	Secuencia de nucleótidos (5'→3')	Tm[1] (ºC)	pb[2]
CDH1	*sense*	CGTCCTGGGCAGAGTGAAT	59.4	79
	antisense	TTTGAATCGGGTGTCGAGGG	60.0	
GAPDH	*sense*	CCCCGGTTTCTATAAATTGAGCC	59.4	100
	antisense	TGGCTCGGCTGGCGAC	62.3	
GSTP1	*sense*	CGGGCAACTGAAGCCTTTTG	60.3	87
	antisense	TCAGCGAAGGAGATCTGGTC	58.9	
IDO-1	*sense*	AGCCCTTCAAGTGTTTCACCA	60.1	92
	antisense	TGCCTTTCCAGCCAGACAAA	60.1	
JUN	*sense*	GCAAAGAACTTTCCCGGCTG	60.0	92
	antisense	GGAGAAGCCTAAGACGCAGG	60.2	
NFKB	*sense*	CGCTGCATCCACAGTTTCC	59.5	99
	antisense	GGGGTTGTTGTTGGTCTGGA	60.1	
NRF2	*sense*	CACGGTCCACAGCTCATCAT	60.1	75
	antisense	CAAATCCATGTCCTGCTGGG	58.8	
TJP1	*sense*	AGAGAAAGGTGAAACACTGCTGA	60.1	97
	antisense	ATCACAGTGTGGTAAGCGCA	59.9	
XOR	*sense*	AGCACTAACACTGTGCCCAA	59.8	91
	antisense	TGGTCTGACAAGCCGCATAG	60.1	

CDH, *cadherin 1* ; GAPDH, *glyceraldehyde-3-phosphate dehydrogenase* ; GSTP1, *glutathione S-transferase pi;* IDO-1, *indoleamine 2,3-dioxygenase* 1; JUN, *Jun proto-oncogene* ; NFKB, *Nuclear factor kappa B subunit* ; NRF2, *nuclear factor (erythroid 2)-like 2* ; TJP1, *tight junction protein 1* ; XOR, *xanthine dehydrogenase.*

[1]Tm, temperatura de fusión.

[2]pb, pares del amplicón resultante.

Determinación de la actividad cisteín-proteasa

La actividad cisteín-proteasa de Der p 1 se determinó mediante fluorimetría, según el protocolo descrito por Schulz *et al.* [248]**,** utilizando como sustrato el péptido fluorogénico N-tert-butoxicarbonil-Gln-Ala-Arg-AMC [AMC=7-amino-4-metilcoumarino] (Boc-QAR-AMC) a una concentración de 75 µM. La hidrólisis enzimática libera el fluoróforo AMC, lo que permite correlacionar el incremento en la intensidad de fluorescencia en el tiempo, con la actividad proteolítica de la enzima (Figura 20). La cantidad de AMC producidos (micromoles) se determinó con una curva de calibrado de concentraciones crecientes de este reactivo (0.78-12.5 µM).

Los ensayos se realizaron por duplicado en placas de 96 pocillos *Nunclon Delta Surface* (Thermo Fisher), en 0.2 mL de PBS a 37ºC. Previamente, Der p 1 (25 nM) fue incubado con el agente reductor GSH (0-2 mM), durante 15 min, con el fin de regenerar el grupo tiol de la cisteína catalítica. Tras la adición del sustrato, los cambios en la intensidad de fluorescencia (λ_{exc} = 355 nm y λ_{em} = 460 nm) se registraron en un lector de placas *FLUOstar OPTIMA* (BMG LabTech), durante 90 min. La hidrólisis no enzimática se

determinó reemplazando la solución de enzima por PBS. En algunos experimentos se utilizó cisteína (L-Cys, 0-2 mM) como agente reductor en lugar de GSH.

El efecto de la enzima GST sobre la actividad cisteín-proteasa de Der p 1 se analizó añadiendo diferentes concentraciones de GST (0-2.5 µM) a la mezcla de reacción. Los parámetros cinéticos aparentes (Km, $V_{máx}$, K_{cat}/Km) se calcularon empleando el *software Hyper32 1.0*. En ciertos experimentos se utilizó como fuente alternativa de GST el sobrenadante del medio apical (25 µL/pocillo) recogido tras 24h de exposición en células Calu-3 a día 7 en ALI. En los experimentos de inhibición, el sobrenadante fue pre-incubado con el inhibidor específico de GSTpi TLK199 (0.5 mM, Ezatiostat, Sigma-Aldrich), durante 15 min a 37ºC, para permitir la formación del complejo.

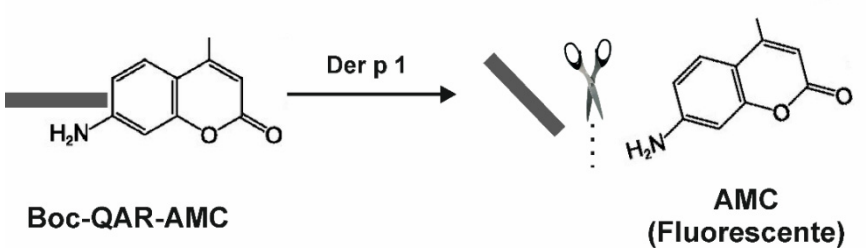

Figura 20. Esquema de la determinación de la actividad cisteín-proteasa utilizando como sustrato el péptido fluorogénico Boc-QAR-AMC. La hidrólisis enzimática libera el fluoróforo AMC, lo que permite correlacionar el incremento en la intensidad de fluorescencia en el tiempo, con la actividad proteolítica de la enzima.

Determinación de la actividad glutatión-S-transferasa

La actividad GST de las enzimas GSTpi de placenta humana y GSTmu de ácaro se determinó mediante colorimetría con el *kit Glutathione S-Transferase (GST) Assay* (Sigma) que utiliza como sustrato el 1-cloro-2,4-dinitrobenceno (CNDB). El ensayo se basa en la medida del incremento de la absorbancia a 340 nm por la formación del producto GS-DNB como resultado de la reacción de conjugación del grupo tiol del GSH al CDNB, catalizada por la GST (Figura 21). La actividad GST de la enzima GSTpi de placenta humana fue inhibida empleando el inhibidor específico TLK199 (0-0.5 mM).

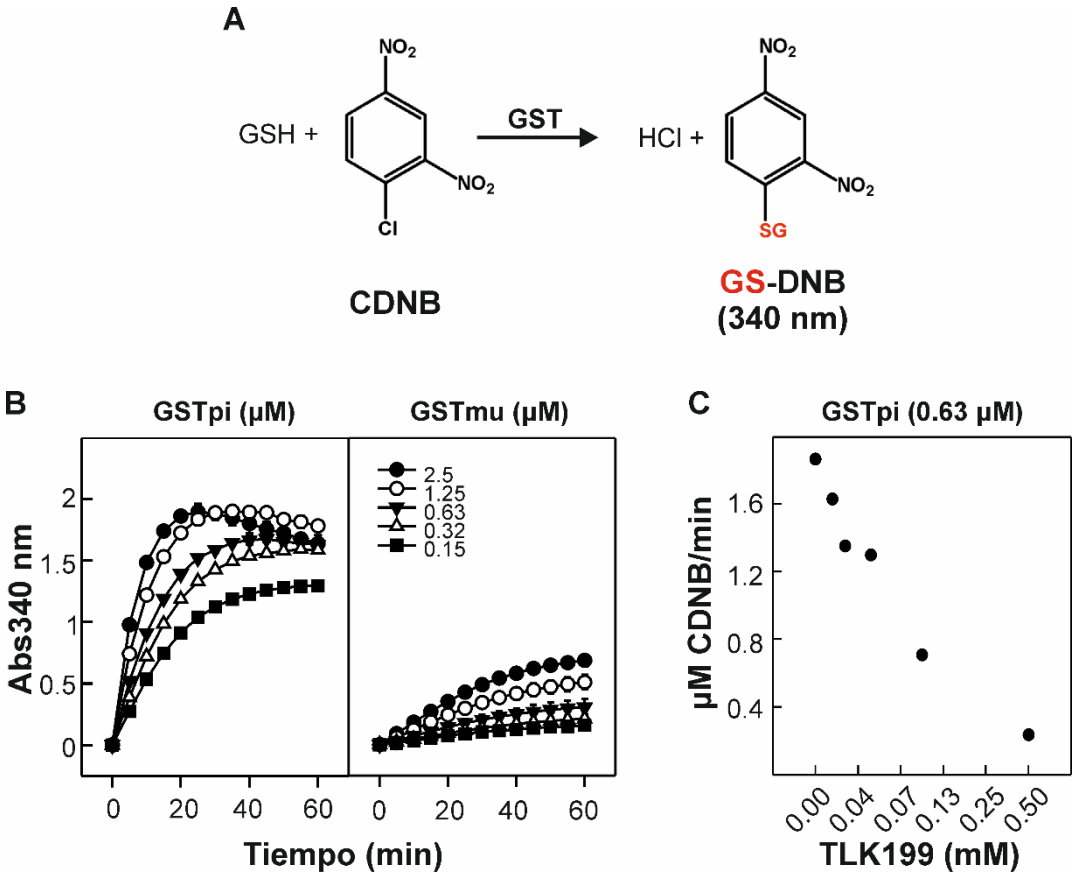

Figura 21. A) Esquema de la formación del conjugado GS-DNB catalizada por GST, a partir del sustrato CDNB y GSH. La formación del conjugado se monitorizó mediante el incremento de la absorción a 340 nm, siendo este valor directamente proporcional a la actividad GST. B). Actividad catalítica de la GSTpi humana y la GSTmu de ácaro. La enzima (0.2-2.5 µM) se incubó con CDNB 1 mM y GSH 1 mM en PBS a 37ºC. La formación del producto GS-DNB se registró con medidas de Abs340 nm durante 60 min. C). TLK199 (0-0.5 mM) inhibe la actividad GSTpi (µM CDNB/min) hasta un 80%. Para la inhibición se utilizó una concentración de GSTpi de 0.63 µM.

La reacción se monitorizó durante 60 minutos en un lector de placas *FLUOstar OPTIMA*. Los ensayos se llevaron a cabo en placas de 96 pocillos *Nunclon Delta Surface*, realizándose cada determinación por duplicado.

Ensayo RFS

El ensayo RFS (del inglés *Redox Fluorescence Switch*) se realizó según el protocolo descrito por Izquierdo-Álvarez *et al.* [249], con pequeñas modificaciones. Dicho ensayo se basa en el uso de maleimida fluorescente para la visualización directa de cambios en el estado redox de la muestra mediante PAGE-SDS en geles de poliacrilamida al 10% (Figura 22).

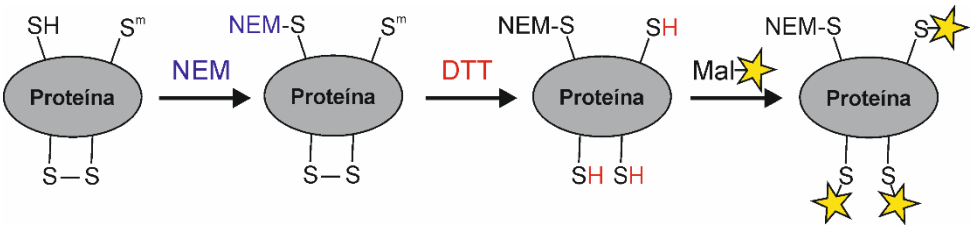

Figura 22. Esquema del ensayo RFS. Tras bloquear los grupos tioles (-SH) con N-etilmaleimida (NEM), los puentes disulfuro (S-S) y los grupos modificados de forma reversible (S^m) se reducen con ditiotreitol (DTT). Finalmente, los grupos tioles generados se bloquean con BODIPY- FL N-(2-aminoetil)-maleimida, antes de su análisis mediante PAGE-SDS.

Con este fin, Der p 1 (1 µg/tratamiento) se pre-activó con GSH 1 mM en PBS durante 30 min a 37ºC y la muestra se diluyó en TENS (Tris 50 mM, EDTA 1 mM, neocuproina 100 mM, SDS 1% (v/v), pH 7.5). Seguidamente, se precipitó añadiendo 3 volúmenes de acetona sobre la muestra tras su incubación durante 10 minutos a -20ºC y centrifugación durante 5 min a 4ºC. El precipitado se lavó con 1 volumen de acetona al 100% a -20ºC y se sometió a 3 tipos de tratamiento: *Tratamiento A*, la muestra se incubó con la sonda fluorescente BODIPY-FL N-(2-aminoetil)-maleimida 40 µM (Invitrogen) en TENS durante 30 min a 37ºC y en oscuridad; *Tratamiento B*, la muestra se incubó con N-etilmaleimida (NEM) 100 mM en TENS durante 30 min a 37ºC y en oscuridad con el fin de bloquear los grupos tioles (-SH) y, a continuación con DTT 2.5 mM en TENS, para reducir los puentes disulfuro (-S-S-). *Tratamiento C,* la muestra se incubó con NEM utilizando las mismas condiciones del *Tratamiento B,* pero en esta ocasión no se redujo con DTT antes de su análisis mediante PAGE-SDS.

Todas las muestras se analizaron mediante PAGE-SDS al 10%, tras ser precipitadas con acetona. Tras incubar el gel con la sonda fluorescente SYPRO Ruby (Invitrogen), según las indicaciones de la casa comercial, la visualización de las bandas se realizó en un sistema *Kodak Image Station 4000MM* (BODIPY-FL, λ_{exc} = 470 nm y λ_{em} = 535 nm y SYPRO Ruby, λ_{exc} = 430 nm y λ_{em} = 600 nm). Las imágenes se analizaron con el *software* PDQuest 2-D gel.

Determinación del metaboloma

Este análisis fue realizado por la Dra. Alma Villaseñor del Centro de Metabolómica y Bioanálisis (CEMBIO) de la Universidad San Pablo (CEU). El perfil de los metabolitos liberados por las células Calu-3 en los medios apicales y basales como consecuencia de la co-exposición a Ole e 1 y Der p 1 (*n* = *3*) se analizó por electroforesis capilar acoplado a un espectrómetro de masas (CE-MS/TOF) (Agilent Technologies). La extracción de los metabolitos presentes en los sobrenadantes de los medios se llevó a cabo según el protocolo de Canuto *et al.* [250]. Los datos obtenidos fueron procesados

mediante el *software MassHunter Profinder B.08.00* (Agilent Technologies). La identificación de los metabolitos se realizó utilizando las bases de datos KEGG, METLIN, LipidMaps y HMDB, a través del buscador *CEU Mass Mediator*. La confirmación de la identidad de estos metabolitos se llevó a cabo usando estándares comerciales. Los datos fueron analizados con el *software* estadístico univariante *UVA Mas Profiler Professional MPP v14.9.1* (Agilent technologies). La calidad de los datos, la detección de *outliers* y la identificación de patrones muestrales se realizaron de forma no supervisada mediante análisis de componentes principales (PCA) [251]. La significancia estadística entre grupos de muestras se analizó mediante la prueba no paramétrica *U de Mann-Whitney*, fijando un intervalo de confianza del 95% ($p < 0.05$).

Espectrometría de masas (MS) y secuenciación de proteínas

La determinación de la masa molecular de los productos resultantes del tratamiento de Ole e 1 con Der p 1 se llevó a cabo mediante espectrometría de masas MALDI-TOF-TOF. Ole e 1 se incubó con Der p 1 pre-activado (relación sustrato:enzima, 1:1 p/p), en PBS con GSH 0.1 mM, a 37ºC durante 0, 0.5, 8 y 24 h. La reacción se detuvo mediante adición del inhibidor específico de cisteín-proteasas E-64 (100 µM, Sigma). Para los ensayos con células y ELISA de inhibición, los productos de la digestión se separaron en 2 fracciones (≤ 3 kDa y > 3 kDa) en función de su masa molecular, utilizando un sistema *Nanosep®-3K* (Pall Corporation) y se analizaron alternativamente mediante espectrometría de masas e inmunodetección utilizando los anticuerpos policlonales anti-Ole e 1 y anti-Der p 1 (Tabla 4).

Las muestras (~1 µg) se mezclaron con una disolución saturada de ácido α–ciano-4-hidroxicinámico (Bruker Daltonics) en acetonitrilo acuoso al 30% y se analizaron en un espectrómetro de masas *Auto Flex III MALDI-TOF-TOF* (Bruker Daltonics). Para la calibración del sistema se utilizó *Protein Calibration Standard I* (Bruker), el cual cubría el rango de masas moleculares de 1000 a 5000 Da ó de 5000 a 20000 Da, según el caso. Estos ensayos se realizaron en el Servicio de Proteómica y Genómica del Centro de Investigaciones Biológicas (CIB-CSIC, Madrid).

La secuenciación N-terminal de la proteína digerida 0.5 h se determinó mediante degradación automática de Edman, en un secuenciador *Procise 494 HT Sequencing System* (Applied Biosystems), en el Servicio de Química de Proteínas del CIB-CSIC. Para ello, los productos de la digestión se separaron mediante PAGE-SDS al 15%, se transfirieron a membranas de PVDF (Immobilon-P) y se tiñeron con una solución de *Coomasie Brilliant Blue* R-250 al 0.1% (p/v) en metanol al 40% (v/v) y ácido acético al 1% (v/v) durante 1 min. El exceso de colorante se eliminó con una solución de metanol

al 50%. Las bandas proteicas se recortaron y se aplicaron directamente en el secuenciador según el protocolo descrito por LeGendre *et al.* [252].

Cromatografía líquida acoplada a espectrometría de masas (LC-MS/MS)

La proteína Der p 1 se incubó con GSTpi en presencia o ausencia de GSH 1 mM, durante 30 min a 37ºC, a una relación sustrato:enzima 1:1 (p/p). Posteriormente, la muestra se incubó con NEM 150 mM durante 15 min a 37ºC y en oscuridad, y se separaron en PAGE-SDS al 12%. Las bandas se cortaron y se digirieron con tripsina (Promega) y quimotripsina (Roche), en ausencia de DTT y yodoacetamida, según el protocolo descrito por Pérez *et al.* [253]. Los péptidos resultantes de la digestión se separaron mediante cromatografía líquida en fase reversa acoplada a un espectrómetro de masas *Easy-nLC II/LTQ-Orbitrap-Velos-Pro* (Thermo Scientific, modo de exclusión dinámica) en el Servicio de Proteómica del Centro de Biología Molecular Severo Ochoa (CBMSO). Los espectros se contrastaron frente a la base de datos *SEQUEST* (*Proteome Discoverer 1.4*, Thermo Scientific). La búsqueda en las bases de datos de las proteínas en función del espectro de fragmentación se llevó a cabo con el *software Peaks 8.0* considerando los siguientes parámetros: (i) oxidación de las metioninas, como modificación variable, (ii) carbamidación de cisteínas como modificación fija y (iii) incorporación de GSH y NEM en cisteínas [254].

Test de activación *in vitro* de basófilos

El test de activación de basófilos fue realizado por el Dr. Miguel González en el Hospital Regional Universitario de Málaga. Se tomaron muestras de sangre periférica de individuos alérgicos a Ole e 1 (n = 5) e individuos no atópicos (n = 5) (Tabla 3). Las células sanguíneas se incubaron con IL-3 (0.2 µg, R&D Systems) y anti-CCR3-APC (1 µg, Bio-Legend) en 20 µL de tampón de estimulación [HEPES 1 M, NaCl al 0.78% (p/v), KCl al 0.037% (p/v), $CaCl_2$ al 0.078% (p/v), $MgCl_2$ al 0.033% (p/v) y BSA al 0.1% (p/v)], durante 10 min a 37ºC. A continuación, se incubaron durante 30 min a 37ºC, con 100 µL de los medios apicales (diluciones 1:50-1:10.000) o basolaterales (diluciones 1:5-1:10.000) procedente de los cultivos celulares y de fracciones de ≤ 3 kDa y > 3 kDa derivadas del tratamiento de Ole e 1 con Der p 1 durante 24 h. Como control negativo y positivo se emplearon PBS (activación basal) y anti-IgE humana (0.5 mg/mL, BD Biosciences), respectivamente. El proceso de degranulación se interrumpió mediante incubación en hielo durante 5 min. La activación de basófilos se expresó en porcentaje $CD63^+$, en base al triple marcaje con los anticuerpos anti-CD203c-PE (Bio-Legend), anti-CCR3-APC (Bio-Legend) y anti-CD63-FITC (Bio-Legend), analizado mediante

citometría de flujo en un citómetro *FACSCalibur* (BD Biosciences), usando el *software FlowJo* (Tree Star). Se adquirieron al menos 500 basófilos por muestra.

Balanzas de Langmuir

La balanza de Langmuir y sus derivadas (*Langmuir-Wilhelmy* y *Langmuir-Blodgett*) permiten simular de forma controlada las condiciones fisiológicas de temperatura y compresión a las que se encuentran sometidas las películas interfaciales biológicas [255]. Así mismo, este sistema permite evaluar la interacción lípido-proteína en el contexto de una monocapa interfacial [45].

Balanza Langmuir-Wilhelmy

La adsorción interfacial de Ole e 1 se determinó tras inyectar, en agitación constante, cantidades crecientes de proteína (0.05-2.78 μM) en 1.8 mL de subfase acuosa (tampón de monocapas), utilizando una cubeta de teflón termostatizada de una balanza de adsorción *Langmuir-Wilhelmy* (NIMA Technologies). Los cambios de presión superficial (ΔΠ) se registraron en función del tiempo (t): isotermas Π *versus* t.

Para analizar el comportamiento de Ole e 1 con monocapas lipídicas preformadas, se depositó el tampón de monocapas (1.8 mL, subfase acuosa) en la cubeta y, sobre éste, se distribuyó el material lipídico (0.1 mg/mL) para formar una monocapa interfacial (*película de Langmuir*). Una vez alcanzada la presión superficial inicial requerida (Π_i), y tras esperar 10 min para permitir la evaporación del disolvente orgánico, se monitorizaron los ∆Π tras la inyección de Ole e 1 (0.55 μM). El incremento máximo de presión ($\Delta\Pi_{max}$) a los 20 min y la presión de exclusión (Π_c) se calcularon gráficamente (Figura 23). Como modelos de surfactante pulmonar y de membrana eucariota genérica se utilizaron mezclas de DPPC y de POPC:SM:CHO (relación molar 2:1:1), respectivamente.

Balanza de Langmuir-Blodgett

La balanza de *Langmuir-Blodgett* permite la trasferencia de una monocapa a un soporte sólido para su visualización bajo un microscopio de epifluorescencia [256]. El material lipídico (0.1 mg/mL) se distribuye por toda la superficie de la subfase acuosa (~ 300 mL) y queda confinado en un área determinada (A), donde puede ser sometido a ciclos de compresión-expansión debido a la presencia de una barrera móvil (Figura 24A). La sonda fluorescente Rho-PE (relación molar sonda:lípido 1:100) se incluyó en las preparaciones de lípido [257, 258]. Los cambios de presión superficial que se producen como consecuencia de la compresión-expansión de la monocapa, a temperatura constante, se denominan *isotermas de compresión* y se registran con una bandera de

papel acoplada a un sensor de tensión superficial. La presión superficial resultante (Π, mN/m) se calcula como la diferencia entre la tensión superficial generada por el H_2O en ausencia de lípidos (~ 70 mN/m) y la generada por el agente tenso-activo. En una isoterma de compresión típica de DPPC se pueden identificar hasta 5 fases bidimensionales: Colapso, Líquido Condensado (LC), Transición Líquido Expandido (LE)/LC, LE y Gas (Figura 24B).

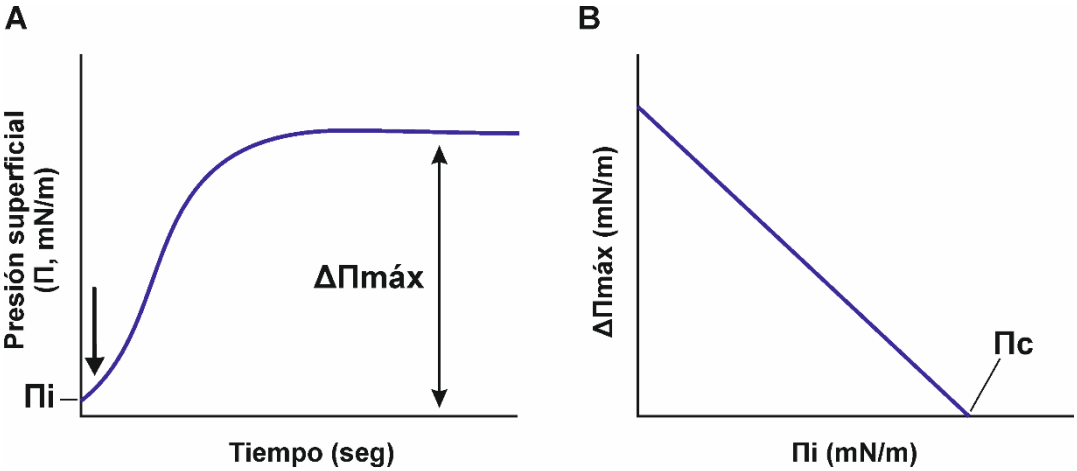

Figura 23. A) Isoterma de compresión en función del tiempo (Π *vs* t). La flecha indica la inyección del agente tenso-activo. La presión inicial (Π_i) es la presión alcanzada por la monocapa lipídica estabilizada en interfase antes de la inyección del agente tenso-activo. B) La presión de exclusión (Π_c) se corresponde al corte con el eje de abscisas de la recta obtenida al representar $\Delta\Pi_{max}$ *vs* Π_i.

Las monocapas se comprimieron a una velocidad constante de 25 cm^2/min hasta alcanzar un valor de presión superficial de 2 mN/m, utilizando una balanza de *Langmuir-Blodgett* (NIMA Technologies). Tras 5 min de equilibrado a esta presión, se inyectó Ole e 1 marcado con Alexa 488 (15 µg) en la subfase acuosa y el material se transfirió a un portaobjetos deslipidizado. La interacción proteína-monocapa se registró como cambios de presión durante 10 min. Las *isotermas de compresión* equivalentes se registraron al comprimir la monocapa a una velocidad mayor de 65 cm^2/min, hasta alcanzar la presión de colapso. Las monocapas formadas se analizaron en un microscopio Leica DM4000B (Leica Microsystems), usando una cámara *Hamamatsu C10600-10B ORCA-R2*.

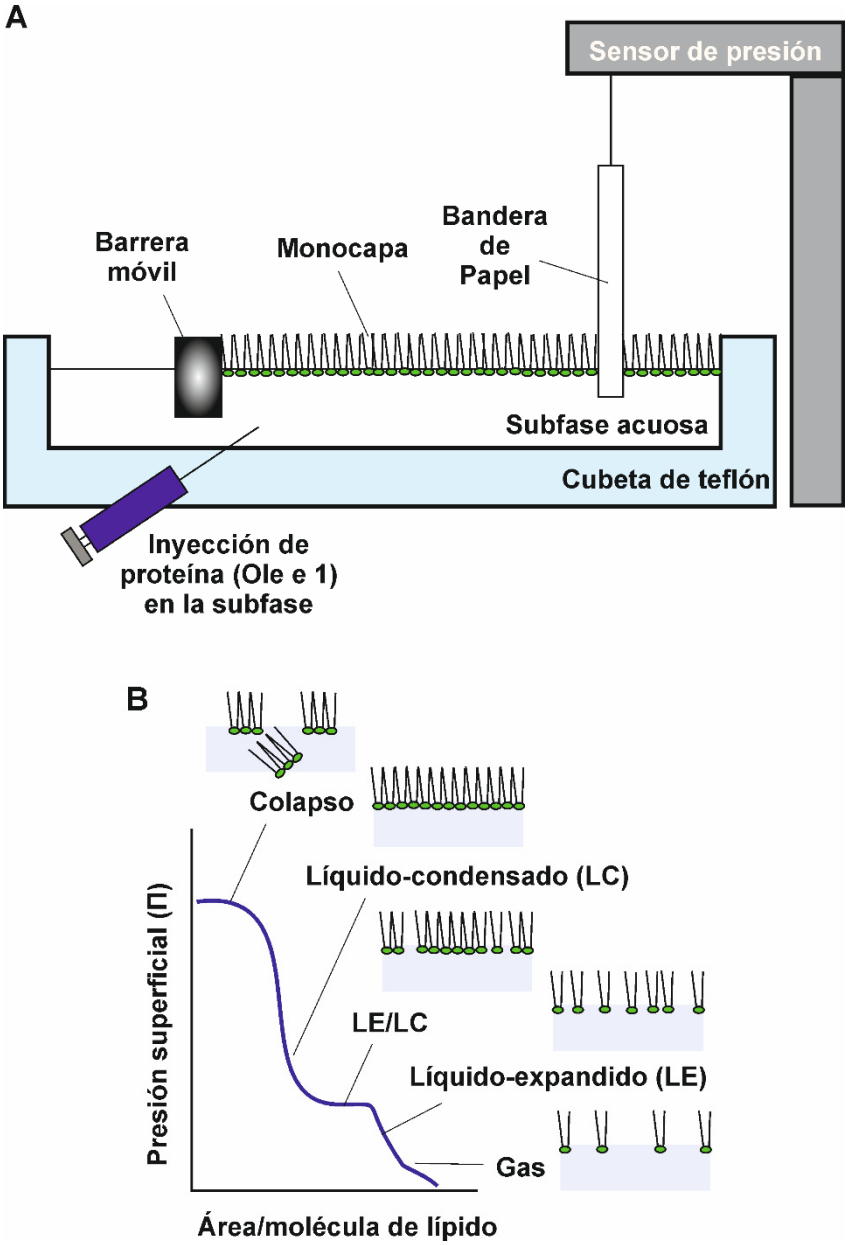

Figura 24. A) Esquema representativo de una balanza de *Langmuir-Blodgett*. A) Una vez preformada la monocapa interfacial se inyecta la proteína (Ole e 1) en la subfase acuosa (tampón de monocapas). Los cambios de presión superficial (ΔΠ) son registrados a través de la bandera de papel vez acoplada a un sensor. B) Isoterma de compresión de DPPC a 25ºC con las 5 fases bidimensionales asociadas: Colapso, Líquido Condensado (LC), Transición Líquido Expandido (LE)/LC, LE y Gas.

Análisis de la adsorción interfacial del surfactante pulmonar mediante *Brilliant Black*

El efecto inhibitorio de Ole e 1 sobre la adsorción interfacial del surfactante pulmonar se analizó mediante el método descrito por Ravasio *et al.* [259], basado en la capacidad del compuesto *Brilliant Black* de absorber luz y bloquear cualquier paso de luz transmitida a través de la subfase acuosa. Así, solo las moléculas marcadas con una sonda fluorescente situadas en la interfase aire-líquido pueden emitir fluorescencia

(Figura 25). Para ello, el surfactante pulmonar marcado con BODIPY-PC se inyectó en la subfase acuosa de *Brilliant Black* (5 mg/mL, Sigma) en presencia o ausencia de Ole e 1 (1 y 50 µg/mL). Las medidas de fluorescencia (λ_{exc} = 485 nm, λ_{em} = 540 nm) se registraron utilizando un lector de placas *FLUOstar OPTIMA*, utilizando como control positivo concentraciones equivalenes de BSA. El ensayo se realizó en placas hidrofílicas de 96 pocillos *MaxiSorp* (Nunc) por duplicado.

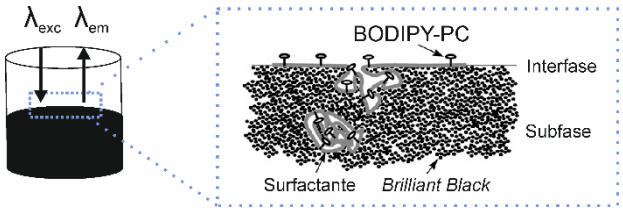

Figura 25. Esquema del análisis de la adsorción interfacial del surfactante pulmonar mediante *Brilliant Black*. El surfactante marcado con BODIPY-PC se inyecta en la subfase acuosa de *Brilliant Black* y se registra la emisión de fluorescencia de las moléculas de la interfase air-líquido.

Análisis estadístico

El análisis estadístico general se realizó usando el método *T de Student*. Los datos se expresan como media y desviación estándar (SD), excepto donde se indique. Un valor $p < 0.05$ se consideró como significativo. La significancia se muestra como (*), $p < 0.05$; (**), < 0.01 y (***), $p < 0.001$.

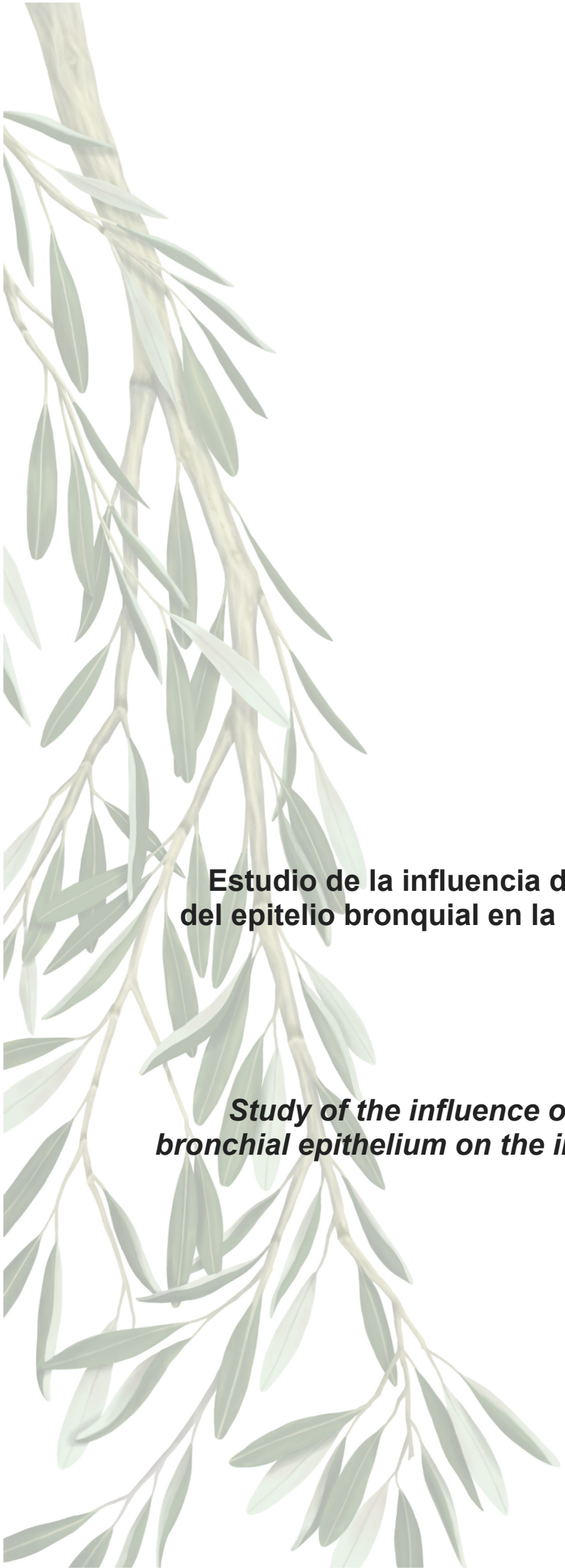

Capítulo I

Estudio de la influencia del estado de diferenciación del epitelio bronquial en la respuesta inmune a Ole e 1

Chapter I

Study of the influence of the differentiation state of bronchial epithelium on the immune response to Ole e 1

Airway epithelium constitutes the first line of defence against inhaled substances including respiratory viruses, air pollutants, cigarette smoke and aeroallergens, and acts as a key orchestrator of immune response in the lung. Several studies suggest that airway epithelium state may ultimately influence the host immune response and clinical outcome. In this first chapter, we analyse the **effect of Ole e 1, the main allergen of olive pollen, in primary NHBE cells along the differentiation process**.

NHBE cells from two healthy donors were used as an *in vitro* model of the airway epithelium. NHBE cells cultured at ALI allows obtaining a pseudostratified barrier with mucociliary phenotype, constituting one of the best cell *in vitro* models that mimics the complexity of existing factors in human airways. The effects of Ole e 1 exposure were evaluated both on days 7 and 21 of differentiation.

Exposure of differentiating NHBE cells to Ole e 1 did not impair epithelial barrier formation, as assessed by transepithelial electrical resistance measurements, ultrastructural studies using electron microscopy, and junctional protein expression by immunofluorescence and western blotting. Moreover, Ole e 1 did not significantly change the mRNA levels of cell type specific markers in differentiating NHBE. However, Ole e 1 exposure altered the cytokine profile secreted by NHBE cells, a process that seems highly dependent on the cell differentiation state and donor features.

Our results suggested that the cytokine secretion in response to Ole e 1 exposure is associated with the differentiation state of NHBE cells at ALI. Usage of ALI-cultured primary cells and the impact of the epithelial functional state in the development of allergic responses will be discussed.

Primary NHBE cells develop TEER during differentiation when cultured at ALI

Primary NHBE cells (2 donors) were cultured at ALI and TEER monitored every 2 days for 35 days (Figure 26). All experiments were performed at passage 3 from frozen vials. The starting point of differentiation at ALI was designated as day 0. NHBE cells from both donors developed increasing TEER values until reaching a plateau (600 and 1000 $\Omega \cdot cm^2$ for donor 1 and donor 2, respectively), being maintained above these values for more than 20 days. Values started to decline around day 30. Therefore, to study how the differentiation state of NHBE cells influences the response to Ole e 1, two time points were selected: days 7 and 21, which correspond with those typically of an undifferentiated and a differentiated epithelium, respectively.

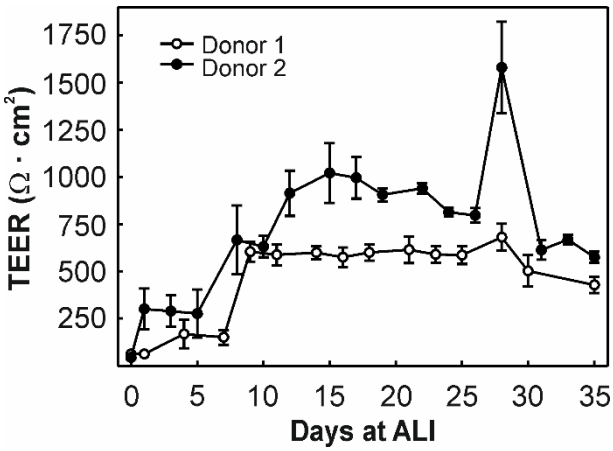

Figure 26. Time course of TEER values of NHBE cells from two donors on ALI culture over 35 days of differentiation. TEER was measured every 2 days. Data shown is the average TEER ± standard deviations (SD) of triplicate determinations.

Ole e 1 exposure does not impair epithelial barrier establishment during NHBE cell differentiation

To investigate whether Ole e 1 affects bronchial epithelium barrier establishment, differentiating NHBE cells were exposed to the aeroallergen on days 7 and 21 of culture at ALI. After 16 h of exposure, changes in TEER values -an indirect measure of AJC formation- were examined. No significant changes in TEER values were observed in response to Ole e 1 exposure, neither on day 7 nor on day 21 at ALI (Figure 27).

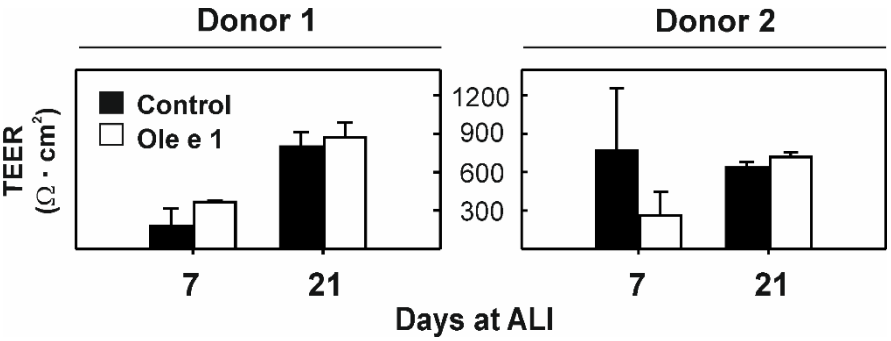

Figure 27. Ole e 1 exposure did not alter TEER values during NHBE differentiation on ALI (for days 7 and 21). TEER values are the average ± SD of triplicate determinations.

Ultrastructural analysis by TEM revealed a normal epithelium structure in differentiating NHBE cells exposed to Ole e 1, showing 2-3 layers of cells with scattered microvilli at the apical surface at day 7 (Figure 28). On day 21 at ALI, the epithelial barrier of exposed NHBE cells was always founded to be intact, which was associated with the characteristic axonemal formation of ciliated cells as well as the vesicle-enriched cytosol from secretory cells.

Further ultrastructural analysis using SEM supported that Ole e 1-exposed of differentiating NHBE cells did no alter epithelial integrity (Figure 28). No gaps or spaces were observed on cell surface topography after aeroallergen exposure.

Collectively, our data showed that Ole e 1 does not impair the establishment of the epithelial barrier in differentiating NHBE cells.

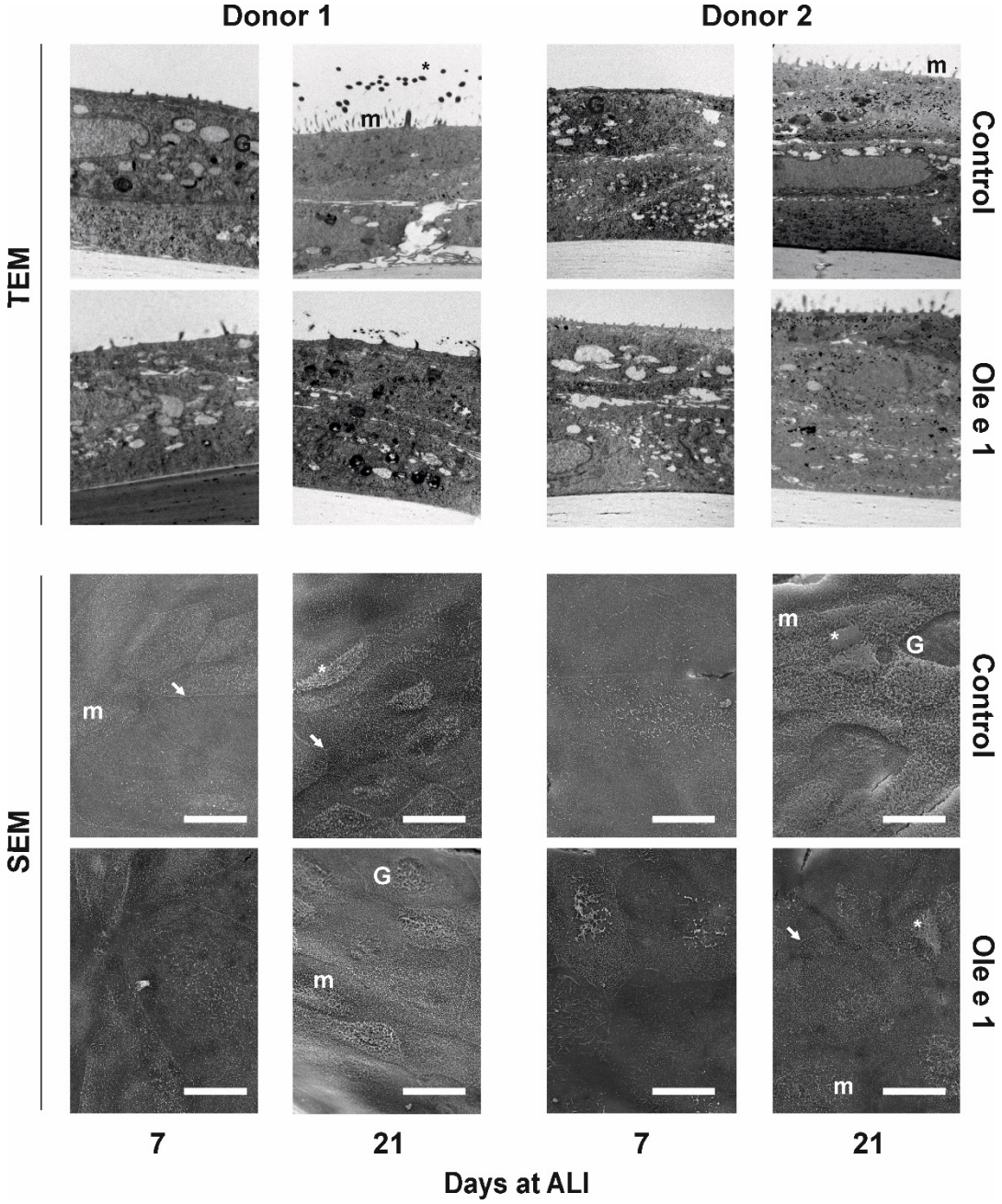

Figure 28. Ole e 1 exposure did not impair the epithelial barrier establishment during NHBE differentiation at ALI (on days 7 and 21). TEM representative micrographs show the axoneme formation with cilia presence (*). Microvilli (m), mucus (M) and globet (G) cells are also highlighted. Magnification 10-20Kx; SEM micrographs show the mucociliary epithelial surface. Microvillus covering (m) and raised microvillus borders delineating cells (arrow) are also indicated. Scale bar = 15 µm.

Ole e 1 exposure does not disrupt AJC structures in differentiating NHBE cells

To assess whether the exposure of differentiating NHBE cells to Ole e 1 had an effect on AJC formation, immunofluorescence labelling was used. We focused on E-cadherin and ZO-1 proteins as canonical proteins of AJ and TJ, respectively. On day 7 at ALI, E-cadherin and ZO-1 were diffusely organized within the cytoplasm, and at the plasma membrane in control NHBE cells (Figure 29).

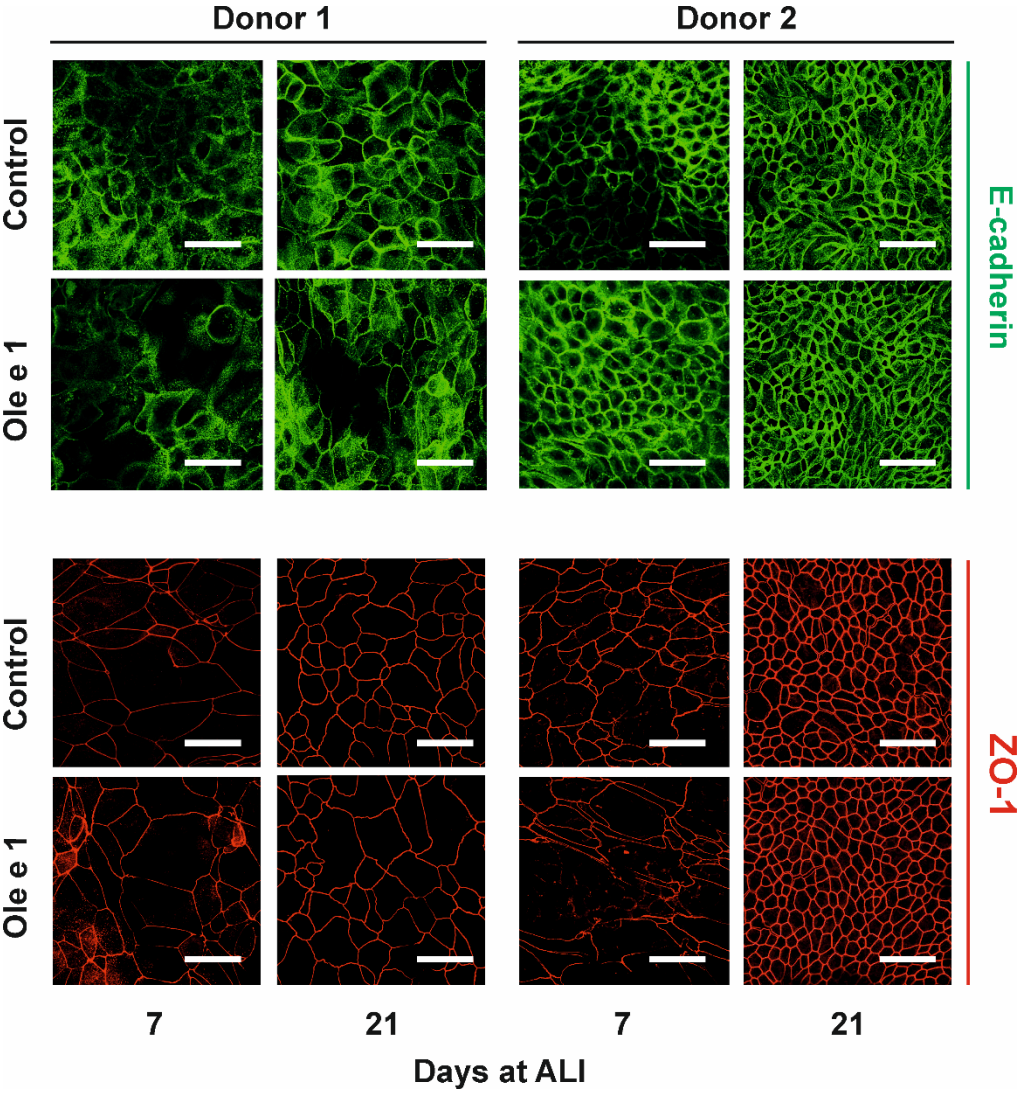

Figure 29. Ole e 1 exposure did not disrupt apical junctional complex structures in differentiating NHBE cells at ALI culture (on days 7 and 21). CLSM analysis for E-cadherin (green) and ZO-1 (red) proteins. Representative Z-stacks are shown. Scale bar = 25 µm.

On day 21 at ALI, both proteins became localized to the plasma membrane at the cell-cell contact sites, and thus indicating the formation of AJC. This pattern, which matches the healthy and expected pattern, was not impaired after Ole e 1 exposure over the variations between donors. Western blotting analysis confirmed these results; no

significant changes in the expression of AJC proteins were detected in Ole e 1-exposed NHBE cells compared to control (Figure 30).

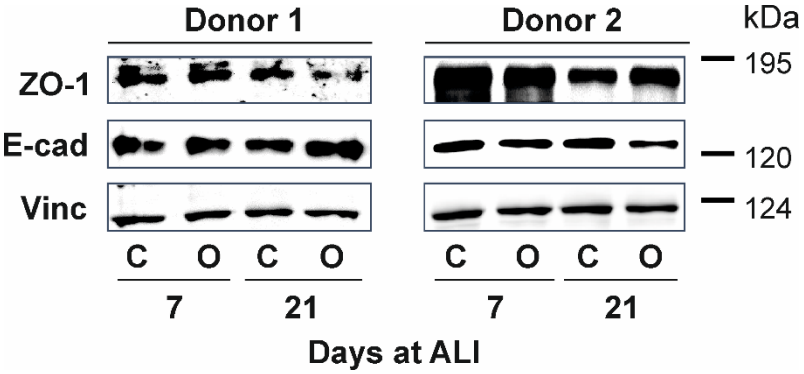

Figure 30. Western blotting analysis for the expression of E-cadherin (E-cad) and ZO-1 in differentiating NHBE cells after Ole e 1 exposure (O) compared to control cells (C), at ALI on day 7 and 21. Vinculin (Vinc) was used as lane loading control. Molecular masses of proteins are indicated in kDa. Representative Western blot of 2 replicates are shown.

Collectively, we concluded that Ole e 1 exposure did not impair AJC formation in differentiating NHBE cells.

Ole e 1 exposure does not significantly alter NHBE differentiation

The effect of Ole e 1 exposure on the emerging epithelial cell populations from differentiating NHBE cells at ALI was determined by PCR using specific cell type markers: *CC-10* for Club cells, *FOXJ1* for ciliated cells, *MUC5AC* for globet cells, and *NKX2.1* as a lung-committed marker and P63 for basal cells (Figure 31). In control NHBE cells, the expression levels of *FOXJ1*, *MUC5AC* and *NKX2.1* mRNA changed in the course of differentiation at ALI. Overall, we did not observe significant alterations in any of the transcript levels studied upon Ole e 1 exposure, besides the decrease in *NKX2.1* mRNA levels on day 21 at ALI in donor 1.

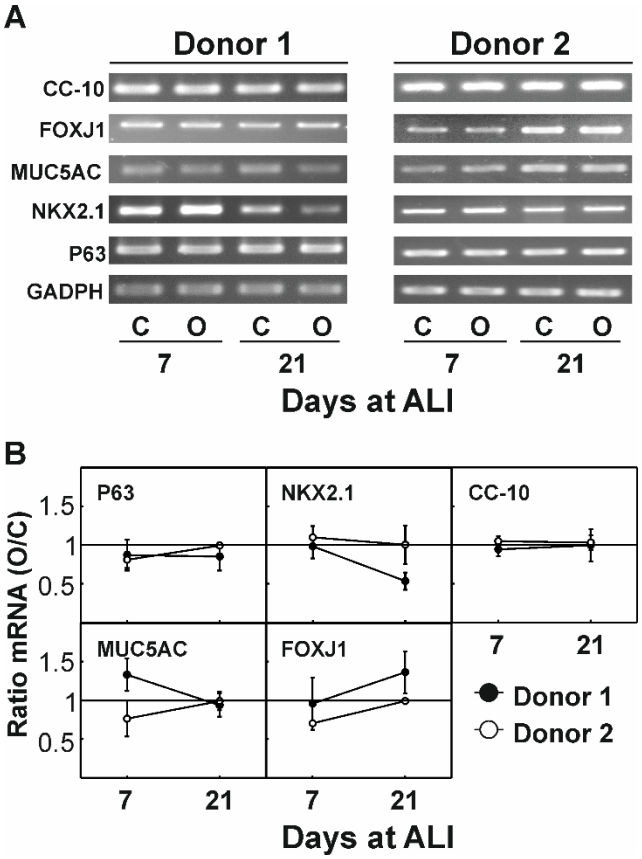

Figure 31. Ole e 1 exposure did not alter mRNA levels of epithelial markers in differentiating NHBE cells on day 7 and 21 of culture at ALI. The cells treated with Ole e 1 (O) and the control cells (C) are shown in comparison. A) An agarose gel electrophoresis (2%) representative image of 3 independent experiments is shown. B) Relative mRNA levels of *CC-10* (Club cell), *FOXJ1* (ciliated cells), *MUC5AC* (goblet cells), *NKX2.*1 (progenitor cells), and *P63* (basal cells) were determined by semi-quantitative reverse transcription polymerase chain reaction and expressed as a fold-change of control values after normalization using *GAPDH* as a housekeeping control. A ≥ 2-fold change was considered significant. Data shown are mean (SD) of 3 replicates.

Ole e 1 exposure alters the cytokine secretion pattern in differentiating NHBE cells

Finally, an antibody microarray analysis was performed to assess whether Ole e 1 exposure affected the levels of cytokine secreted from differentiating NHBE cells in the apical and basal medium (Figure 32).

Interestingly, Ole e 1-exposed undifferentiating NHBE cells (day 7 at ALI) from donor 1 and 2 had 45 and 26 cytokines, respectively, which were up- or down-regulated as compared to control cells: apically (Donor 1, 3 cytokines up-regulated and 9 cytokines down-regulated; Donor 2, 13 cytokines up-regulated and 1 cytokines down-regulated) and basolaterally (Donor 1, 30 cytokines up-regulated and 3 cytokines down-regulated; Donor 2, 9 cytokines up-regulated and 3 cytokines down-regulated). On the other hand, the exposure of differentiating cells (day 21 at ALI) to Ole e 1 only altered significantly 2

and 8 cytokines in donor 1 and 2, respectively. This suggests that cytokine outcomes may be related to cellular state of differentiation at the time of aeroallergen exposure.

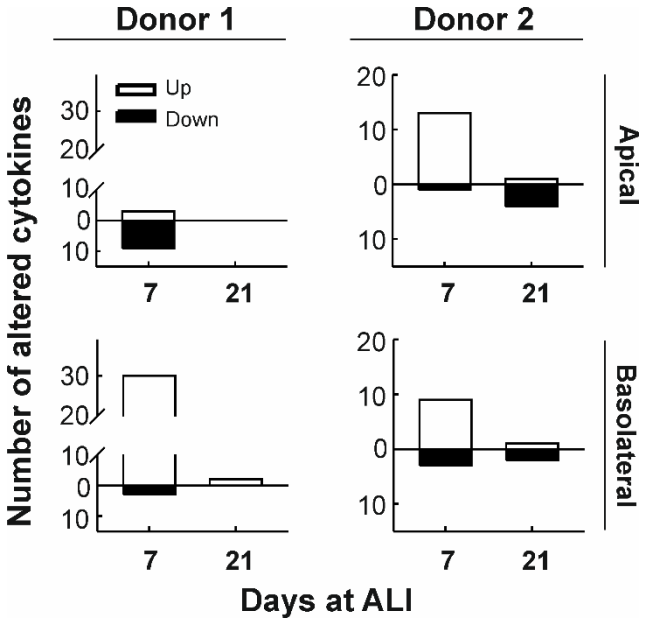

Figure 32. Ole e 1 exposure altered cytokine secretion pattern in differentiating NHBE cells on days 7 and 21 at ALI. Bar graphs indicate the number of significantly altered cytokines that displayed ≥ 2-fold changes compared to control cells in the apical and basolateral compartments as determined by microarray analysis.

Furthermore, important differences in the cytokine patterns were observed between the two donors, both in the number and the cytokine secreted, indicating that response outcome was strongly influenced by the donor features. Just two cytokines were commonly secreted from both donor 1 and 2 cells: Insulin-like growth factor binding protein 4 (IGFBP-4) and MIG (CXCL9). The full list of altered cytokine is showed in Tables 9, 10 and 11. Some of them have been previously described in asthma and allergic inflammation, including interferon gamma-induced protein 10 (IP-10, CXCL10) [260], tumour necrosis factor superfamily 14 (TNFS14, LIGHT) [261], monocyte chemotactic protein-4 (MCP-4, CCL13) [262], osteopontin (OPN) [263], RANTES (CCL5) [264], MCP-3 (CCL7) [265], macrophage inflammatory protein MIP-3α [111], and leptin [266, 267]. In addition, OPN [268] and LIGHT [261] have also been associated with remodelling processes of the airways. Following to microarray data analysis, three cytokines (CXCL9, IGFBP-4 and leptin) were selected for validation by conventional sandwich ELISA; however, no cytokines levels were detected in media of none groups. The discrepancy between data obtained with the 2 techniques may be explained in terms of differences in sensitivity. Microarray detection assays (>10.000 of fluorescence arbitrary units) display higher sensitivity than ELISA (from 0 to 3 optical density scale): ≤ 30 pg/mL and 500 fg/mL, respectively, for the examined cytokines [269, 270].

Table 9. Differentially expressed cytokines in culture media of NHBE cells exposed to Ole e 1 on day 7 at ALI from Donor 1 .

Cytokine	Description	Gen ID	UniProt Ref	Alternative name*	Media compartment	Fold Change[1]
ANG	Angiogenin (EC 3.1.27.-)	283	P03950	ANG, RNASE5	Apical	0.49
BDNF	Brain-derived neurotrophic factor	627	P23560	Abrineurin	Basolateral	5.36
CCL23	Myeloid progenitor inhibitory factor 1	6368	P55773	MPIF, MIP3	Basolateral	2.05
Flt-3Ligand	Fms-related tyrosine kinase 3 ligand	2323	P49771	Flt3L	Basolateral	>10
Fracktalkine	Fractalkine (C-X3-C motif chemokine 1)	6376	P78423	CX3CL1, FKN	Basolateral	5.39
FGF4	Fibroblast growth factor 4	2249	P08620	HST-1	Apical	2.24
FGF6	Fibroblast growth factor 6	2251	P10767	HST2, HBGF-6	Basolateral	2.32
FGF7	Fibroblast growth factor 7	2252	P21781	KGF,HBGF7	Basolateral	2.95
FGF9	Fibroblast growth factor 9	2254	P31371	GAF, HBGF-9	Basolateral	4.23
GCP-2	Granulocyte chemotactic protein 2 (C-X-C motif chemokine 6)	6372	P80162	CXCL6	Basolateral	2.53
G-CSF	Granulocyte colony-stimulating factor (Pluripoietin)	1440	P09919	CSF3, C17orf3	Basolateral	0.01
HGF	Hepatocyte growth factor (Hepatopoietin-A)	3082	P14210	HPTA	Apical	0.5
IGFBP4	Insulin-like growth factor-binding protein 4	3487	P22692	IBP4	Apical/Basolateral	2.04/4.98
IL-1β	Interleukin-1 beta (IL-1 beta) (Catabolin)	3553	P01584	IL-1B, IL-1 F2	Basolateral	2.54
IL-5	Interleukin-5	3567	P05113	TRF	Apical/Basolateral	0.37/0.25
IL-7	Interleukin-7	3574	P13232		Apical/Basolateral	0.01/0.24
IL-15	Interleukin-15	3600	P40933		Basolateral	2.45
IL-16	Interleukin-16	3603	Q14005	LCF	Basolateral	3.16
IP-10	C-X-C motif chemokine 10 (10 kDa interferon gamma-induced protein)	3627	P02778	CXCL10, INP10	Basolateral	7.82
LEPTIN	Leptin (Obese protein)	3952	P41159	LEP	Basolateral	7.05
LIF	Leukemia inhibitory factor	3976	P15018	HILDA	Basolateral	8.08
LIGHT	Tumor necrosis factor ligand superfamily member 14	8740	O43557	TNFSF14	Basolateral	9.52
M-CSF	Macrophage colony-stimulating factor 1	1435	P09603	CSF1	Apical	0.32
MCP-1	Monocyte chemoattractant protein 1	6347	P13500	CCL2, MCAF	Basolateral	2.53
MCP-4	Monocyte chemoattractant protein 4	6357	Q99616	CCL13	Basolateral	3.74
MDC	Macrophage-derived chemokine (C-C motif chemokine 22)	6367	O00626	CCL22	Apical	0.21
MIG	C-X-C motif chemokine 9 (Monokine induced by interferon-gamma)	4283	Q07325	CXCL9	Apical/Basolateral	0.29/>10
MIP-1δ	C-C motif chemokine 15 (Chemokine CC-2)	6359	Q16663	CCL15, MIP5	Apical	0.5
OPG	Tumor necrosis factor receptor superfamily member 11B (Osteoprotegerin)	4982	O00300	TNFRSF11B	Basolateral	5.89
OPN	Osteopontin (Bone sialoprotein 1)	6696	P10451	SPP1, BNSP	Basolateral	5.21
PARC	Pulmonary and activation-regulated chemokine	6362	P55774	CCL18, AMAC-1	Apical/Basolateral	2.63/6.02

* Alternative names are used for a protein (*UniProt accession number*).

[1] Values over 2-fold changes were considered biologically relevant.

Table 9. *(Continuation)* Differentially expressed cytokines in culture media of NHBE cells exposed to Ole e 1 on day 7 at ALI from Donor 1.

Cytokine	Description	Gen ID	UniProt Ref	Alternative name*	Media compartment	Fold Change[1]
PDGF BB	Platelet-derived growth factor subunit B	5155	P01127	PDGFB, PDGF2	Basolateral	4.33
PLGF	Placenta growth factor	5228	P49763	PGF, PGFL	Basolateral	3.73
RANTES	C-C motif chemokine 5 (Eosinophil chemotactic cytokine)	6352	P13501	CCL5	Apical	0.45
SDF-1	Stromal cell-derived factor 1 (C-X-C motif chemokine 12)	6387	P48061	CXCL12 alpha	Basolateral	2.38
TARC	Thymus and activation-regulated chemokine (C-C motif chemokine 17)	6361	Q92583	CCL17, SCYA17	Basolateral	2.25
TGFβ1	Transforming growth factor beta-1	7040	P01137	LAP	Basolateral	2.45
TGFβ2	Transforming growth factor beta-2	7042	P61812	BSC-1, G-TSF	Basolateral	3.07
TGFβ3	Transforming growth factor beta-3	7043	P10600		Basolateral	2.55
VEGF	Vascular endothelial growth factor A	7422	P15692	VEGFA	Basolateral	2.07

* Alternative names are used for a protein (*UniProt accession number*).

[1] Values over 2-fold changes were considered biologically relevant.

Table 10. Differentially expressed cytokines in culture media of NHBE cells exposed to Ole e 1 on day 7 at ALI from Donor 2.

Cytokine	Description	Gen ID	UniProt Ref	Alternative name*	Media compartment	Fold Change[1]
I-309	C-C motif chemokine 1 (Small-inducible cytokine A1)	6346	P22362	TCA3, CCL1	Apical	3.83
IGFBP4	Insulin-like growth factor-binding protein 4	3487	P22692	IBP4	Apical/Basolateral	2.80/6.46
IFNγ	Interferon gamma	3458	P01579	IFNG	Apical/Basolateral	2.04/5.53
IL-1α	Interleukin-1 alpha (Hematopoietin-1)	3552	P01583	IL-1A, IL-1 F1	Apical	3.57
IL-2	Interleukin-2	3558	P60568	TCGF	Basolateral	2.6
IL-4	Interleukin-4	3565	P05112	BSF1, Pitrakinra	Apical/Basolateral	2.12/2.70
IL-5	Interleukin-5	3567	P05113	TRF	Basolateral	2.58
IL-6	Interleukin-6	3569	P05231	BSF2, CDF	Basolateral	2.84
IL-7	Interleukin-7	3574	P13232		Basolateral	2.23
IL-10	Interleukin-10	3586	P22301	CSIF	Apical/Basolateral	>10/3.92
IL-12p40/70	Interleukin-12 subunit alpha	3592	P29459	NKSF1, IL-12A	Apical	4.33
IL-13	Interleukin-13	3596	P35225	NC30	Basolateral	4.53
IL-15	Interleukin-15	3600	P40933		Apical	4.41
LEPTIN	Leptin (Obese protein)	3952	P41159	LEP	Apical	4.77
MCP-1	Monocyte chemoattractant protein 1	6347	P13500	CCL2, MCAF	Apical	4.83
MCP-2	Monocyte chemoattractant protein 2	6355	P80075	CCL8	Apical/Basolateral	3.30/0.44
MCP-3	Monocyte chemoattractant protein 3	6354	P80098	CCL7, MARC	Apical	3.18
MIG	C-X-C motif chemokine 9 (Monokine induced by interferon-gamma)	4283	Q07325	CXCL9	Apical/Basolateral	0.39/0.02
MIP-1δ	C-C motif chemokine 15 (Chemokine CC-2)	6359	Q16663	CCL15, MIP5	Apical	3.57
SDF-1	Stromal cell-derived factor 1 (C-X-C motif chemokine 12)	6387	P48061	CXCL12 alpha	Basolateral	0.15

* Alternative names are used for a protein (*UniProt accession number*).

[1] Values over 2-fold changes were considered biologically relevant.

Table 11. Differentially expressed cytokines in culture media of NHBE cells exposed to Ole e 1 on day 21 at ALI from Donors 1 and 2.

Cytokine	Description	Gen ID	UniProt Ref	Alternative name*	Media compartment	Fold Change[1]
IGFBP1†	Insulin-like growth factor-binding protein 1	3484	P08833	IGF1, IBP1	Basolateral	2.16
MIP-3α†	Macrophage inflammatory protein 3 alpha	6364	P78556	CCL20, LARC	Basolateral	2.52
FGF7‡	Fibroblast growth factor 7	2252	P21781	KGF,HBGF7	Apical	0.5
GROα‡	Growth-regulated alpha protein (C-X-C motif chemokine 1)	2919	P09341	CXCL1, NAP3	Basolateral	0.37
I-309‡	C-C motif chemokine 1 (Small-inducible cytokine A1)	6346	P22362	TCA3, CCL1	Basolateral	0.46
IL-4‡	Interleukin-4	3565	P05112	BSF1, Pitrakinra	Apical	0.35
IL-6‡	Interleukin-6	3569	P05231	BSF2, CDF	Basolateral	>10
MCP-1‡	Monocyte chemoattractant protein 1	6347	P13500	CCL2, MCAF	Apical	0.38
MIG‡	C-X-C motif chemokine 9 (Monokine induced by interferon-gamma)	4283	Q07325	CXCL9	Apical	4.32
TGFβ1‡	Transforming growth factor beta-1	7040	P01137	LAP	Apical	0.48

* Alternative names are used for a protein (*UniProt accession number*).

† Donor 1 y ‡ Donor 2.

[1] Values over 2-fold changes were considered biologically relevant.

DISCUSSION

In the present study, we analysed the effect of Ole e 1 on bronchial epithelial cells, and assessed if there was a differential response to the aeroallergen between undifferentiated and differentiated NHBE cells from healthy donors.

We tried to *in vitro* reproduce the differentiation process of primary NHBE cells taking advantage of ALI cultures, which provide the most accurate model to study human airway epithelium. At day 7, NHBE cells were not fully differentiated as indicated by lower TEER values, the absence of cilia, and the diffuse expression of E-cadherin and ZO-1 proteins. At this initial stage, undifferentiated cells could also mimic a damaged epithelium. At day 21, NHBE cells were fully differentiated with higher TEER values, well-defined cilia and AJC, indicating a good epithelial barrier function.

Since cytokines play a central role in the development of allergic airway inflammation, mediators secreted apically and basolaterally in differentiating NHBE cells after Ole e 1 exposure were evaluated -in comparison to control cells- using this *in vitro* model. Interestingly, the number of altered cytokines secreted by undifferentiated cells exposed to Ole e 1 was higher when compared to differentiated NHBE cells, which had lower secretion from both the apical and the basolateral side of the culture.

These findings on the differences in the cytokine profile could be attributed to the significant changes in gene expression that take place during the differentiation process of NHBE cells [271, 272]. In addition, there was also variability in the profile of altered cytokines in undifferentiated NHBE cells induced by Ole e 1 exposure between donor's airway epithelia. The observed heterogeneity on the cytokines secreted by airway epithelial cells upon aeroallergen interaction would provide a variety of microenvironments that would support the activation/maturation of different immune cells, and consequently, the final host's immune response. Previous reports have shown the high degree of variability between individual NHBE cell donors [234, 273, 274]. Inter-donor variability is one of the main disadvantages of the use of primary NHBE cells cultured at ALI for research as it hinders results interpretation. Thus, our study supports the idea that both the donor and the state of differentiation of bronchial epithelial cells have a major influence in the immune response to Ole e 1. Other studies have reported that the level of differentiation of NHBE cells has a profound effect on the expression of sialic acid receptor, and, in consequence, in the host's immune response to influenza H5N1 and H1N1 virus [275]. Krunkosky *et al*. [276] have also showed that *Mycoplasma pneumoniae* infection is influenced by the differentiation state of NHBE cells [110].

Airway epithelial AJC disruption by environmental proteases could facilitate allergens penetration through the epithelium and their access to immune cells, contributing to the initiation and exacerbation of allergic diseases [162, 277]. A number of studies have shown that protease allergens from house dust mite, cockroaches, fungal, and pollens disrupt the epithelial barrier by cleaving junctional proteins such as occludin or ZO-1 [72, 73, 278, 279], or by interacting with PARs, which induce the loss of junctional protein expression [280, 281]**.** In the present study, we showed that Ole e 1 did not alter epithelial barrier establishment and integrity as supported by the absence of effect on TEER values and ultrastructure in these cells. Ole e 1 disrupted neither the expression nor the localization of ZO-1 and E-cadherin proteins during differentiation of NHBE cells. In addition, Ole e 1 has been shown not to change transcript levels of epithelial cell markers, supporting ultrastructural data. Moreover, Ole e 1 modified the cytokine release pattern of NHBE cells but no disrupted the epithelial barrier integrity. It is likely that a protease-independent mechanism is involved in the sensitization and/or the development of an allergic reaction to this aeroallergen; thus creating the optimal microenvironment for immune cells and ultimately influencing the overall outcome of the host's immune response. A protease-independent mechanism has been described for several allergens, including those from HDM [282, 283] and pollens [284].

Finally, this study emphasized the usefulness of primary NHBE cells cultured at ALI conditions, as a more accurate model of human airway epithelium. In contrast to submerged cultures, ALI system has a higher oxygen availability thus promoting full differentiation of NHBE cells that form a tight and polarized multilayer composed of ciliated cells, basal and globet cells [232, 285-287]. Moreover, NHBE cells cultured at ALI present a gene expression profile similar to that described for *in vivo* cells [271, 272]. However, primary NHBE cultures have several disadvantages such as a high cost, short lifespan, and a high degree of variation between donors, passage or experiments [232]. In this sense, immortalized bronchial epithelial cell lines represent an alternative for a stable model of epithelial barrier such as Calu-3 cells [288-291]. Therefore, further studies using these cells might give more light to the effects of Ole e 1 on bronchial epithelial cells.

In conclusion, in this work we have demonstrated that Ole e 1 aeroallergen induced the release of a plethora of cytokines from NHBE cells cultured at ALI, which is affected both by the differentiation state of the bronchial epithelial cells at the moment of exposure and donor features. Additionally, this work highlights the importance of using a well characterized model of human airway for allergy related-research.

Capítulo II

Análisis del papel de las proteasas ambientales en la respuesta inmune del epitelio bronquial a Ole e 1

Chapter II

Analysis of the role of environmental proteases on the immune response of the bronchial epithelium to Ole e 1

The early event of allergic sensitization involves the allergen transport across the epithelial barrier. The precise mechanism of how the allergen overcomes the airway epithelial barrier is not completely understood, and for that reason has been the target of an exhaustive investigation. Numerous evidences have suggested that a dysfunction of the airway epithelium may be behind the origin of respiratory allergies [162]. Among other environmental substances, proteases such those derived from HDM [187], cockroach [188], molds [189] and pollens [73], have been reported to disrupt and activate the airway epithelium through multiple mechanisms, thus contributing to allergen sensitization and/or exacerbation of allergic response.

In this chapter, we analysed **the role of environmental proteases on the response of bronchial epithelium to Ole e 1**, the main aeroallergen of olive pollen. We focused on the cysteine-protease Der p 1 from *D. pteronyssinus* because it is recognized as a major cause of respiratory allergic diseases. In *Part I*, we analysed the contribution of the co-exposure to Der p 1 in the bronchial epithelial-permeability to Ole e 1. In *Part II*, a comparative analysis of the metabolome of the bronchial epithelium co-exposed to Der p 1 was performed in order to understand the role of this cysteine-protease in the initiation of allergic response to Ole e 1. Finally, in *Part III*, the regulation of Der p 1-protease activity in the bronchial epithelium by host components was also analysed.

This study required the use of a functional *in vitro* model. Calu-3 cell line derived from human bronchial carcinoma was selected for this purpose because it is one of the few airway epithelial cell lines that form TJ and exhibit high TEER values *in vitro*. Thus, Calu-3 cells were cultured under ALI conditions, allowing to obtain a functional and polarized bronchial epithelium that mimics the *in vivo* one [234]**.**

ALI-cultured Calu-3 cells were exposed to Ole e 1 (25 µg/mL) in the absence or presence of Der p 1 cysteine-protease (10 µg/mL), on days 2 and 7 of culture. These time points correspond to undifferentiated and differentiated epithelium, respectively. In *Part I,* we demonstrated that the bronchial epithelium state *per se* regulates the barrier permeability to Ole e 1, while the exposure to Der p 1 protease did not cause a significant increase in this parameter. However, chronic exposure to Der p 1 was associated with an increase permeability to Ole e 1. Moreover, we found that Ole e 1 was cleaved by Der p 1, and more importantly, that products derived from Der p 1-treated Ole e 1 may exhibit immunogenic activity as indicated by both IgG-reactivity and activation of human basophils from patients allergic to olive pollen. This study provides several important insights about how proteases can contribute to allergen sensitization.

***Part I*. Epithelial permeability to the olive pollen aeroallergen Ole e 1 strongly depends on bronchial epithelium state but no on Der p 1 protease activity**

Der p 1 decreases TEER and disrupts TJ in a bronchial epithelium state-dependent manner

Calu-3 cells were apically exposed to Ole e 1, Der p 1, or the combination of both proteins, for 24 h on days 2 and 7 at ALI, and after removing the challenge, incubated for another 2 h. TEER values were determined at different time points over the ALI-culture (Figure 33A). TEER values of non-treated Calu-3 cells increased above baseline after 3 days at ALI, indicating that Calu-3 cells have started to establish AJC. TEER reached a value above 600 $\Omega \cdot cm^2$ on day 8. For ALI-cultured Calu-3 cells, TEER values above 300 $\Omega \cdot cm^2$ indicate an established barrier. Ole 1 exposure for 24 h did not significantly altered TEER values compared to non-treated Calu-3 cells over time, indicating that physical barrier is not impaired after exposure to Ole e 1. In contrast, Der p 1 exposure for 24 h caused a markedly decrease in TEER values (about 2-3 folds) on day 2 at ALI, compared to control cells. Moreover, this effect was not modified by the exposure to the combination of Der p 1 and Ole e 1. Interestingly, the decrease in TEER caused by Der p 1 was almost immediately restored after removing the protease, reaching control values in 10 min, showing the exceptional regenerative capacity of the bronchial epithelium. Unexpectedly, the protease exposure did not alter TEER values of Calu-3 cells on day 7 at ALI, when the epithelial barrier is completely functional. Thus, these results suggested that the impairment of the barrier integrity by Der p 1 cysteine-protease is dependent of the differentiation state of the bronchial epithelium.

The integrity of TJ formed by ALI-cultured Calu-3 cells was analysed by CLSM for ZO-1 immunostaining (Figure 33B). As expected, exposure to Ole e 1 for 24 h either on days 2 or 7 at ALI, did not altered the localization and distribution of ZO-1, which was similar to the non-treated cells: a ring surrounding each cells. Only exposure to Der p 1 alone or in combination with Ole e 1 for 24 h on day 2 similarly reduced (in a time-dependent manner) the intensity of ZO-1 staining and disrupted its pattern, which appeared as discontinuous ring (zipper-like pattern) caused by a loss of protein from TJ. Again, no TJ disruption was observed in cells exposed to Der p 1 on day 7 at ALI. These results correlated with the decrease in TEER measurements reported above. Overall, these data suggest that Der p 1 protease may increase the epithelial barrier permeability by TJ disruption.

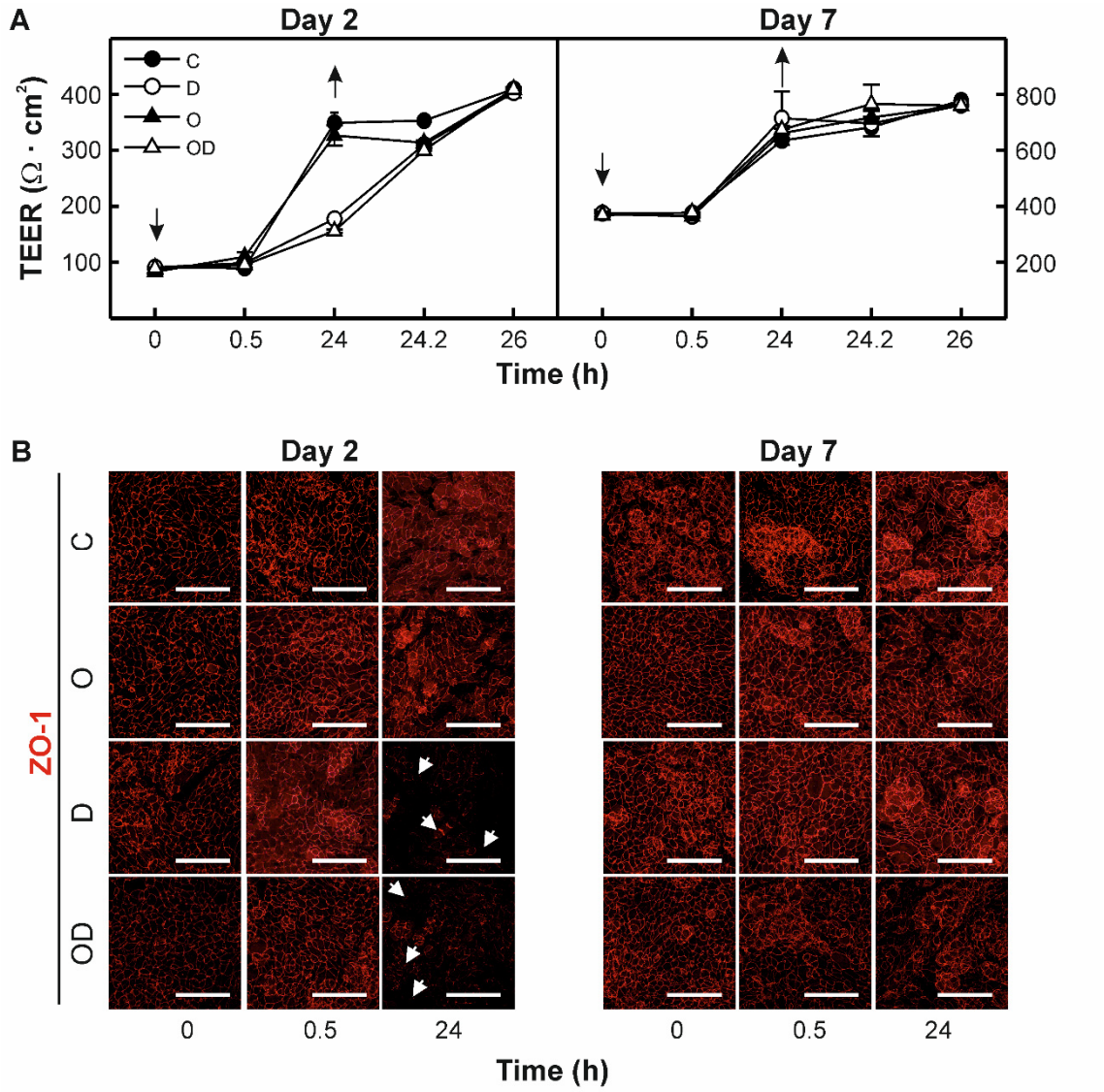

Figure 33. Effect of Der p 1 on the epithelial barrier integrity of Calu-3 cells, on days 2 and 7 at ALI. A) Time course of TEER values of Calu-3 cells over 26 h of ALI culture on the indicated day, after aeroallergen and/or protease exposure, compared to untreated cells. TEER was measured at the indicated time points. Data shown are the mean ± SD of triplicate determinations. Arrows indicate the time of addition and removal of the aeroallergen and/or protease. B) CLSM analysis of ZO-1 (red) expression over time of exposure. Representative Z-stacks are shown. White arrows indicate TJ disruptions. Scale bar = 25 µm. C, non-treated cells (control); O, cells exposed to Ole e 1 aeroallergen alone; D, cells exposed to Der p 1 protease alone; OD, cells exposed to the combination of Ole e 1 and Der p 1.

Epithelial permeability to Ole e 1 strongly depends on the state of bronchial epithelium but not on the protease action

Epithelial permeability to Ole e 1 was analysed to determine whether the protease effect on TJ was associated with a dysfunction on the physical barrier. For this purpose, the permeability to Ole e 1 of ALI-cultured Calu-3 was measured in absence and presence of Der p 1, at different time points on days 2 and 7.

Figure 34A shows the results of Ole e 1 detection in culture media by Western blot, using a specific pAb. ALI-cultured Calu-3 cells formed a physical barrier on day 7 that exhibited low permeability to Ole e 1 compared to day 2, where the aeroallergen was detected on the basolateral medium after 0.5 h of culture being its levels increased over the time of incubation. Surprisingly, and despite of the disruption of TJ, co-exposure to Der p 1 did not seem to further increase cell permeability to Ole e 1. The markedly decrease on the aeroallergens levels observed at the apical side could be due to the proteolytic cleavage of Ole e 1 as it was suggested by the modification of its electrophoretic pattern by Der p 1 co-exposure: Ole e 1 from non-protease treated cells has two majority bands with apparent molecular masses of 18 and 20 kDa; following 0.5 h co-exposure to Der p 1 on day 2, the intensity of the bands were slightly decreased and after 24 h, faint bands were detected. Changes on the electrophoretic pattern at this time also were detected on day 7.

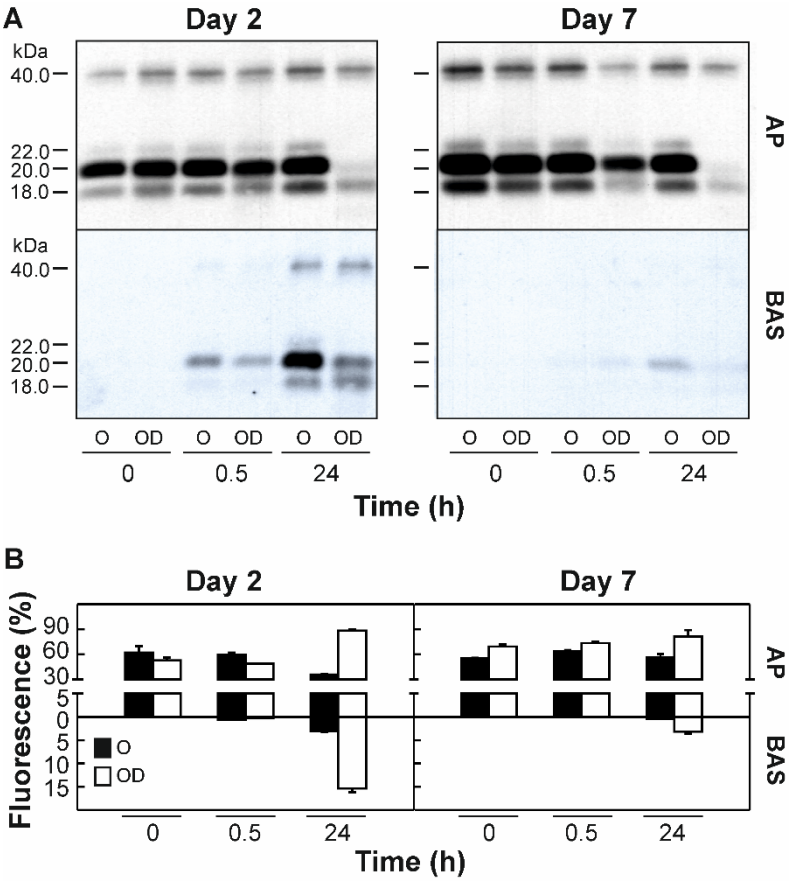

Figure 34. Effect of Der p 1 cysteine-protease on bronchial epithelial permeability to Ole e 1. ALI-cultured Calu-3 cells were co-exposed to Ole e 1 and Der p 1 on days 2 and 7, and the presence of the aeroallergen was determined in the medium at different time points (0 h, 0.5 h and 24 h). A) Immunodetection of Ole e 1 in the media using a specific pAb. Molecular masses of Ole e 1 forms in kDa are indicated. B) Aeroallergen distribution was also monitored by recording the fluorescence emission of Alex488-labeled Ole e 1. Data are expressed as percentage of fluorescence relative to control. AP, apical medium; BAS, basolateral medium; O, exposure to Ole e 1; and OD, exposure to Ole e 1 in combination with Der p 1.

These results were confirmed by studies with Alexa488-labeled Ole e 1 (Figure 34B). As expected, on day 2 cells exhibited high permeability to Ole e 1, as indicated by the decrease of the apical fluorescent signal (up to 60%) by 24 h of culture, accompanied with a slight increase at the basolateral side. This was not observed on day 7 at ALI. Interestingly, following co-exposure to Der p 1 for 24 h an unexpected increase on the fluorescence signal was found on both apical and basolateral sides, on either day 2 or day 7 at ALI. This was explained by the proteolytic cleavage of Ole e 1 by Der p 1. The intrinsic fluorescence quenching of the molecule was disrupted by the proteolytic cleavage of Alexa488-labeled Ole e 1, as indicated by the increase of fluorescence (Figure 35).

Thus, our results supported the hypothesis that the epithelial permeability to Ole e 1 aeroallergen dependent on bronchial epithelium state, but not protease activity.

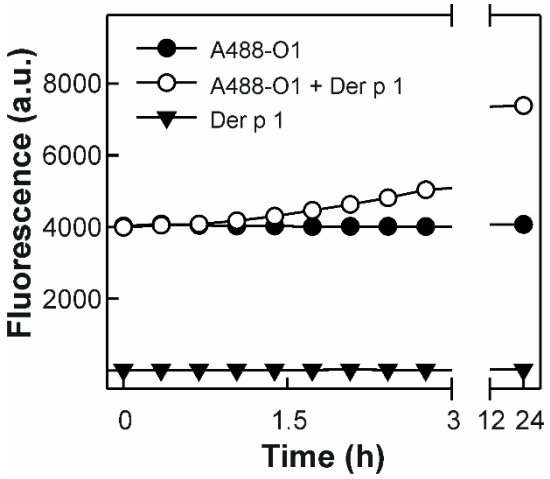

Figure 35. Kinetic of the increase of fluorescence due to the proteolytic cleavage of Alexa488-labeled Ole e 1 (A488-O1, 25 µg/mL) by Der p 1 (10 µg/mL) for 24 h at 37°C. Fluorescence is expressed in arbitrary units (a.u.).

Chronic exposure to Der p 1 alters the integrity of the bronchial epithelium in a time-dependent manner

To analyse whether the effect of Der p 1 on epithelial barrier integrity was time-dependent, ALI-cultured Calu-3 cells were daily exposed to Der p 1 (10 µg/mL) for 5 days (120 h), starting on day 2 of culture and ending on day 7. Some cultures were exposed daily to Ole e 1 alone and others were kept unexposed. Then, all groups of cells were exposed to either Ole e 1 or Der p 1 for another 24 h.

First, changes on TEER values were analysed at different time-points (Figure 36A). As indicated above, TEER values of non-treated Calu-3 cells (C*) increased above basal one (about 100 $\Omega \cdot cm^2$) after 3 days at ALI, reaching a plateau of 300-400 $\Omega \cdot cm^2$,

indicating the barrier establishment. Ole e 1-exposed cells (O*) for 5 days exhibited similar behaviour to non-treated cells. However, chronic exposure to Der p 1 (D*) maintained TEER basal values all over the culture.

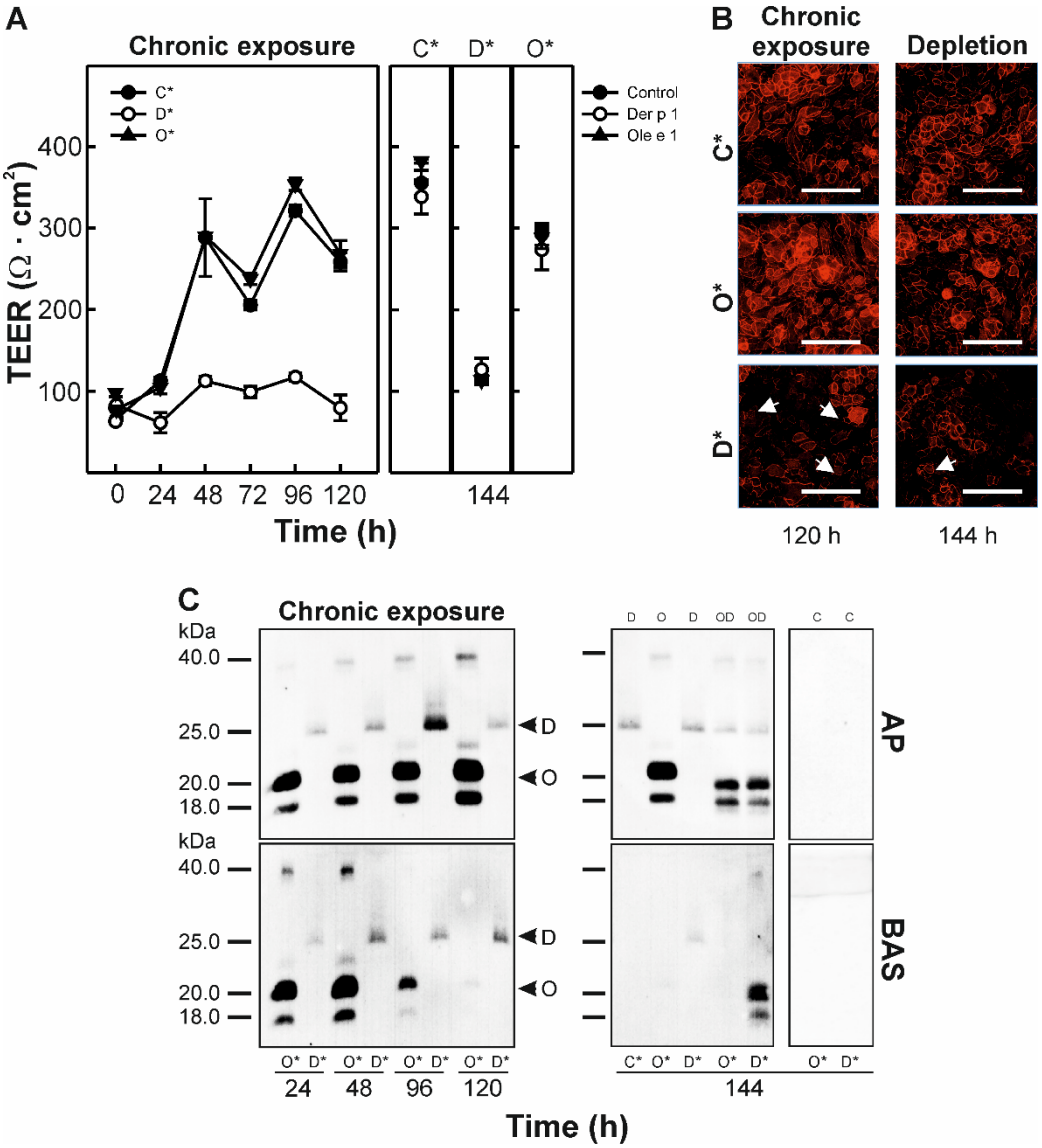

Figure 36. Effect of chronic exposure to Der p 1 on the epithelial barrier integrity of Calu-3 cells on day 2 at ALI. A) Time course of TEER values of Calu-3 cells over 120 h of ALI culture, after exposure to either Ole e 1 or Der p 1, compared to non-treated cells (left side). TEER was measured at the indicated time points. Data shown are the mean ± SD of triplicate determinations. (Right side) TEER values of Calu-3 cells after re-exposure to Ole e 1 or Der p 1 for 24 h on day 7 at ALI, compared to control. Data shown are the mean ± SD of triplicate determinations. B) CLSM analysis of ZO-1 (red) expression after chronic exposure and re-exposure on day 7 to Der p 1 or Ole e 1, compared to non-treated cells. Representative Z-stacks are shown. White arrows indicate TJ disruptions. Scale bar = 25 µm. C) Immunodetection of Ole e 1 and Der p 1 in the apical and basolateral media, using specific pAbs, at different time points (24 h, 48 h, 96 h and 120 h) during chronic exposure and at 24 h after re-exposure on day 7. Black arrows indicated the position of Ole e 1 and Der p 1 bands. Molecular masses in kDa are indicated. AP, apical medium; BAS, basolateral medium; C control cells; D, exposure to Der p 1; and O, exposure to Ole e 1. ∗, chronic exposure.

Twenty-four hours after removing the protease, TEER values of D* cells did not recover those of C* cells, as indicated by TEER values of non-exposed D* cells at 144 h post-exposure. Again, exposure of cells to Der p 1 for 24 h on day 8 at ALI (when epithelial barrier is formed) did not alter TEER values (see 144 h post-exposure). These results showed that the effect of protease exposure on TEER values is time-dependent.

The effect of chronic exposure on the integrity of TJ formed by ALI-cultured Calu-3 cells was analysed by CLSM for ZO-1 immunostaining (Figure 36B). Again, only chronic exposure to Der p 1 protease disrupted TJ in a time-dependent manner, as indicated by the marked reduction on ZO-1 staining and its zipper-like pattern, compared to control cells.

Finally, the effect of the chronic co-exposure to Der p 1 on the epithelial barrier permeability to Ole e 1 was analysed by Western blot, using a specific pAb, at different time points (Figure 36C). In addition, the presence of Der p 1 was also analysed in both media using a specific pAb. In absence of Der p 1, the permeability of ALI-cultured Calu-3 cells decreased over the 5 days of culture, as indicated by the reduction of Ole e 1 content in the basolateral media. No Ole e 1 was detected on the basolateral medium by 120 h, which corresponds to day 7 at ALI where the epithelial barrier is completely formed. This decrease was correlated with an increase of Ole e 1 content in the apical media. In contrast, Der p 1 was detected in both media over the time of cultured. These results correlated with the low TEER values and TJ disruptions. Re-exposure to Der p 1 for 24 h did not affect permeability to Ole e 1 of cells chronic treated with this aeroallergen: no Ole e 1 was detected on the basolateral medium. Only cells that were chronic exposure to the protease exhibited an increased permeability to Ole e 1. Overall, these data supported that bronchial epithelial permeability to Ole e 1 strongly depends on bronchial epithelium state.

Der p 1 cleaves Ole e 1 aeroallergen

Studies of co-exposure of cells to the combination Der p 1 and Ole e 1, suggested that the aeroallergen was proteolytic cleaved by Der p 1. Thus, Ole e 1 was incubated with Der p 1 for 24 h, and aliquots were analysed by Western blot and MS at different time points (0 h, 0.5 h, 8 h and 24 h) (Figure 37). At 0 h, MS spectrum of Ole e 1 showed two peaks at 16197.4 and 17518.4 m/z, corresponding to MH^+ species of the non-glycosylated and glycosylated form of Ole e 1, respectively. Also, MH_2^{+2} species of these forms were detected (8285.3 and 8612.2 m/z). The size of the 17518.4 m/z-peak decrease over incubation time with Der p 1, which was associated to both an increase in

the peak of 16197.4 m/z and the area with m/z < 12500. No peaks were detected in HCL-hydrolysed Ole e 1 used as a control. Similar results were found by Western blot.

Edman degradation of 0.5 h-treated Ole e 1 rendered 2 N-terminal sequences: EDVP, which corresponded to the N-terminal of the full-length aeroallergen; and FHIQ, which corresponded to a shorter-length form that lacked the first 10 amino acid residues.

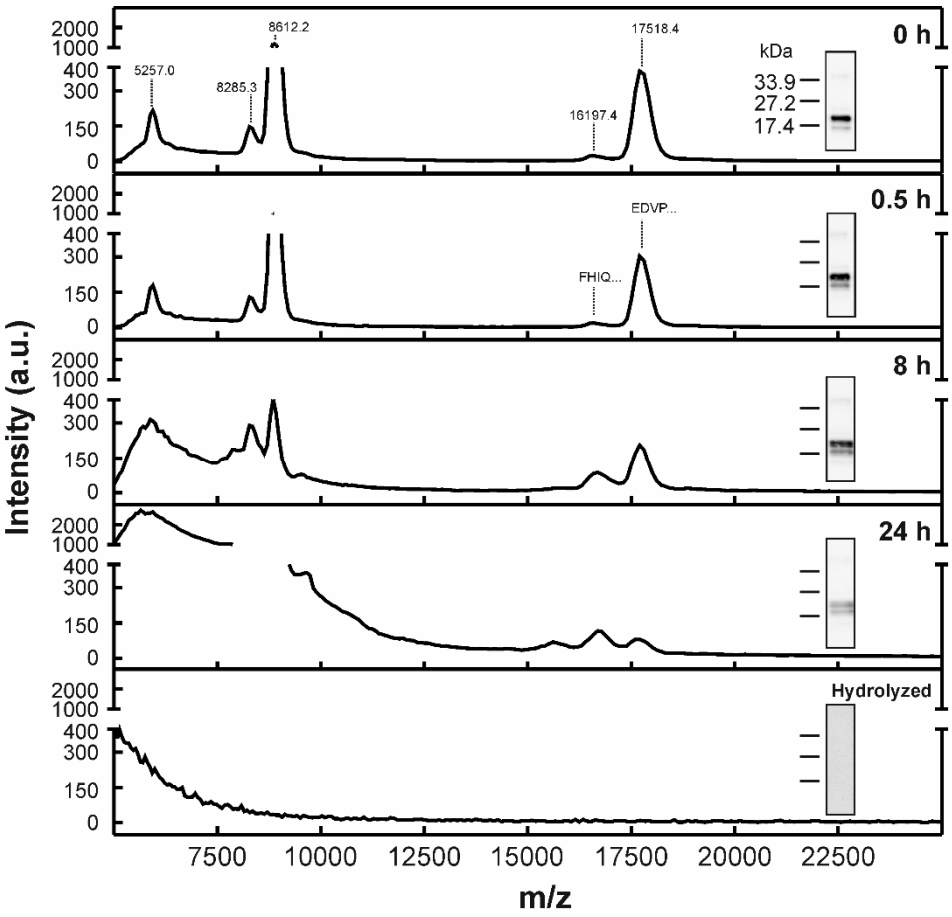

Figure 37. MS analysed of Ole e 1-cleavage by Der p 1 protease at different time points. The mass/charge ratio (*m/z*) is shown. The N-terminal sequence of full- and short-length forms of Ole e 1 after protease-treatment for 0.5 h are shown. *Insert*, immunodetection of Ole e 1 with a specific pAb, after treatment with Der p 1. Molecular masses in kDa are indicated.

Der p 1-treated Ole e 1 exhibits reduced IgE-reactivity but maintains IgG-binding capacity

To address whether cleavage by Der p 1 affects the immunological properties of Ole e 1, inhibition ELISA were performed. First, proteolytic products derived from Der p 1-treated Ole e 1 were separated in 2 fractions based on their molecular masses by using a Nanosep®-3K: ≤ 3 kDa and > 3 kDa fractions. The ion mass spectrum of ≤ 3 kDa-

fraction obtained after treatment of Ole e 1 with Der p 1 for 24 h showed that it was enriched in low-molecular mass peptides, below 2 kDa (Figure 38).

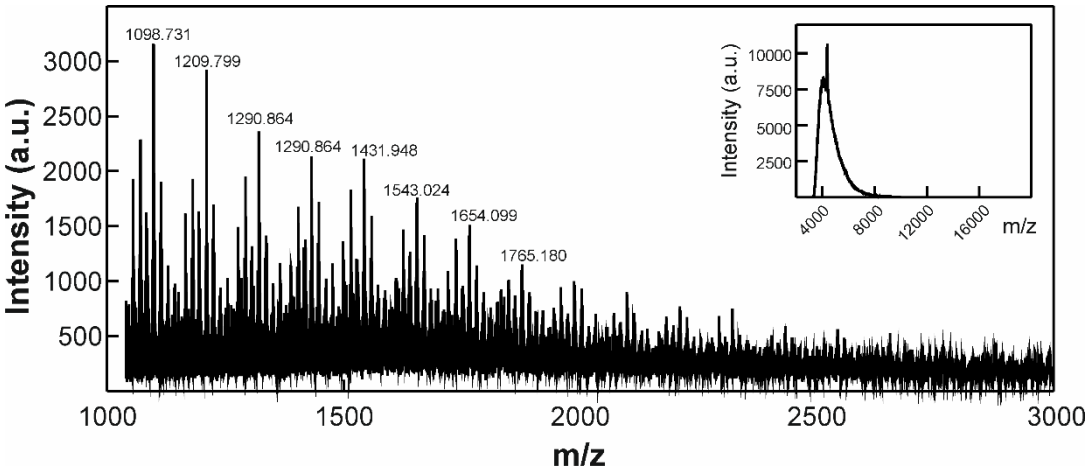

Figure 38. MS spectrum of ≤ 3 kDa-fraction derived from Ole e 1 treated with Der p 1 for 24 h. *Insert*, ion mass spectrum ranging from 2500 to 20,000 m/z. The mass/charge ration (m/z) is shown, and *m/z* values of the most abundant peaks are indicated.

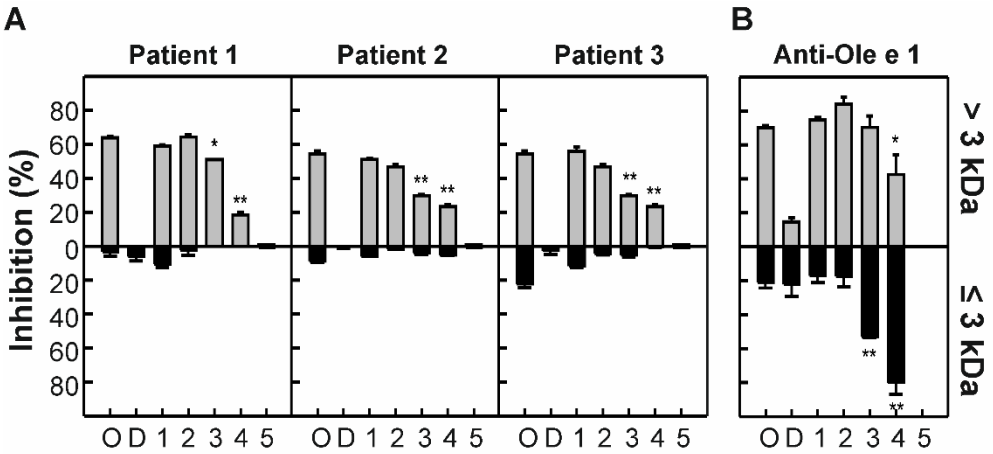

Figure 39. Immunological analysis of Ole e 1 after Der p 1-treatement. Proteolytic products were separated based on the molecular mass using a Nanosep®-3K, and assayed by inhibition ELISA. A) Inhibition ELISA of IgE-binding of 3 individual sera from olive pollen patients allergic to Ole e 1 coated-wells by soluble proteolytic products, as inhibitors. B) Inhibition ELISA of IgG-binding of a specific pAb is shown. Data are expressed as inhibition percentage (%) respect to control, and are the mean ± SD of duplicate determinations. Der p 1-treatments: 1, 0 h; 2, 0.5 h; 3, 8 h; and 4, 24 h; and 5, HCl-hydrolysed Ole e 1. O, Ole e 1; D, Der p 1. Significant differences are indicated by: *p < 0.05, **p < 0.01.

The IgE-reactivity of both ≤ 3 kDa and > 3 kDa fractions derived from Der p 1-treated Ole e 1 at different times points was analysed by inhibition ELISA using individual sera from 3 olive-pollen allergic patients (Figure 39A). As controls, equivalent amount of non-treated Ole e 1, HCl-hydrolysed Ole e 1 and Der p 1 were used. The IgE-reactivity of > 3 kDa fractions for each of the tested sera (with variations among allergic individuals) was significantly reduced (up to 40%) by the time of protease-treatment, in comparison

to that of non-treated Ole e 1. This was due to the reduction of both the amount and the length of full-length aeroallergen. No IgE-reactivity was exhibited by ≤ 3 kDa fractions, in agreement with the presence of peptides below 2 kDa as indicated by MS.

Also, the IgG-reactivity of ≤ 3 kDa and > 3 kDa fractions was analysed by inhibition ELISA using a specific anti-Ole e 1 (Figure 39B). This time, 3 of the > 3 kDa fractions (from *1* to *3*) exhibited an IgG-reactivity comparable to that of non-treated aeroallergen; nevertheless, fraction *4* maintained a 40% of IgG-reactivity. Interestingly, ≤ 3 kDa fractions, in particular number *4* and *5*, showed a significantly IgG-reactivity. Thus, suggesting that Ole e 1-derived peptides could be potentially immunogenic, being able to play an important role in the development of an immune response.

Overall, these data showed that Der p 1-treatment of Ole e 1 led to a significant reduction of its IgE-reactivity but maintained its IgG-binding capacity.

Der p 1-treated Ole e 1 induces activation of basophils from allergic patients

In order to obtain the potential clinical relevance of Der p 1-treated Ole e 1, basophil activation assays were performed with peripheral blood cells of 5 olive pollen-allergic patients (Figure 40). Cells from 5 non-atopic individuals were used as negative controls.

With this aim, ≤ 3 kDa and > 3 kDa fractions derived from Der p 1-treated Ole e 1 for 24 h were used in the basophil activation assays. Also, the apical and basolateral media collected from ALI-culture Calu-3 cells co-exposed to Ole e 1 and Der p 1 for 24 h on day 2 of culture, were used in theses assays. All tested samples were analysed by Western blot using both specific anti-Ole e 1 and anti-Der p 1 pAbs (Figure 40A).

In 4 of our of 5 patients tested, apical products derived from Der p 1-treated Ole e 1 induced activation of basophils in a dose-dependent manner, with variations among allergic individual responses. No significant differences were detected on the activation percentage between Ole e 1 and its apical-derived products. Similar results were obtained when > 3 kDa fraction were used in the assays. Basophils from both patient *2* and non-atopic controls did not respond to either Ole e 1 or its derived products (Figure 40B).

Once again, basolateral products derived from Der p 1-treated Ole e 1 induced activation of basophils from 4 patients in a dose-dependent manner, comparable to that obtained with Ole e 1, with variations among allergic individual responses. Percentages of basophil activation were significant lower with ≤ 3 kDa fraction than with basolateral products in 3 out of 5 patients. Interestingly, in all cases, Der p 1-treatement caused a

slight increase in basophil activation compared to non-treated samples. These data suggested that mediators secreted by Calu-3 cells exposed to Der p 1-treated Ole e 1 may also contribute to basophil activation by an IgE-independent mechanism, thus supporting the crucial role of the airway epithelium in the development of allergy.

Overall, our data suggest that products from Der p 1-treated Ole e 1 may exhibit immunogenic activity as indicated by their IgG-binding capacity and their ability to activate human basophils from patients allergic to olive pollen.

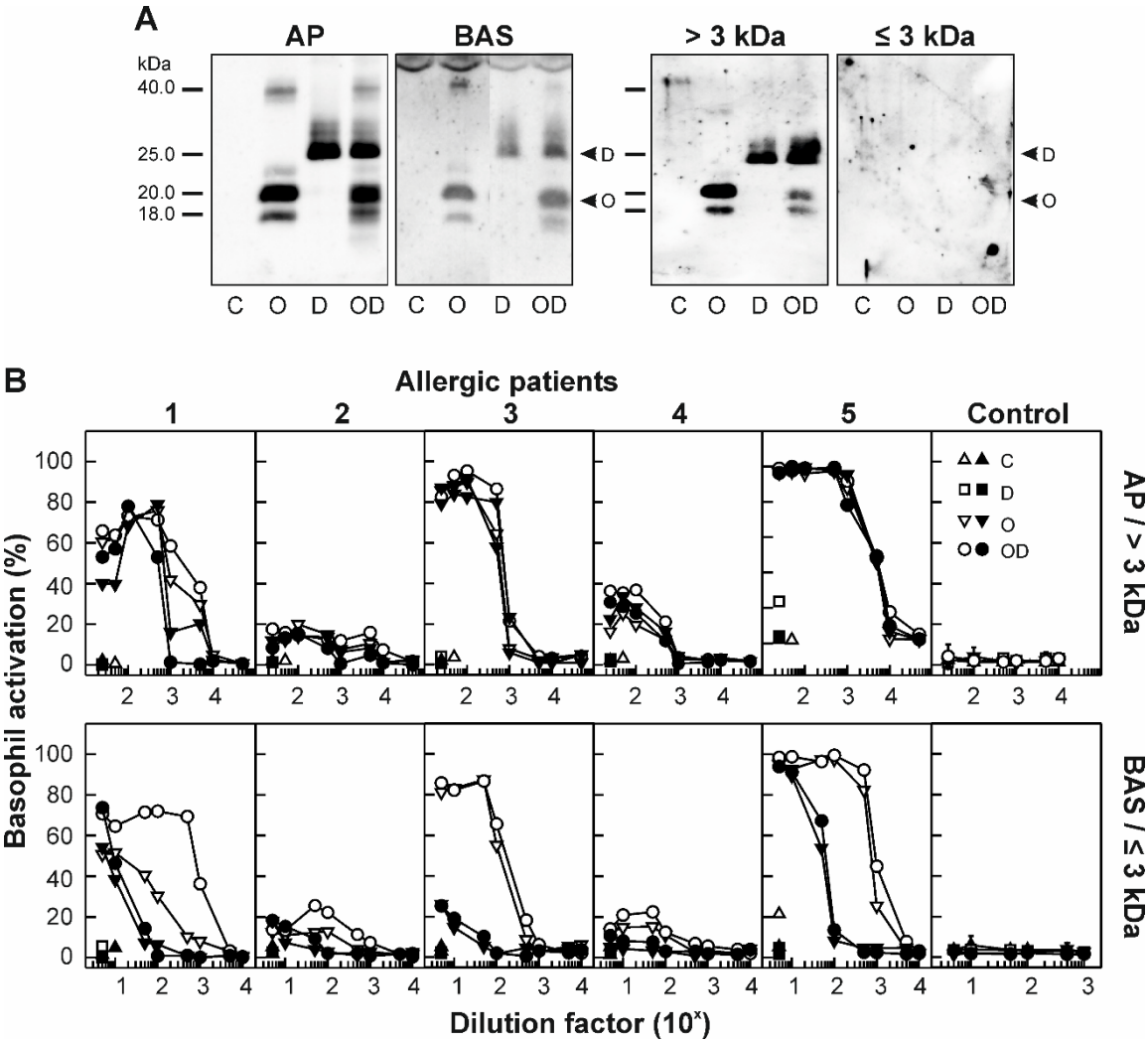

Figure 40. Effect of products derived from Der p 1-treated Ole e 1 on basophil activation from olive pollen-allergic patients (*n* = 5). Cells from non-atopic individuals (*n* = 5) were used as negative control. A) Immunodetection of products derived from Der p 1-treated Ole e 1 in the culture media (apical and basolateral) and in the Nanosep®-3K-fractions (≤3 kDa and >3 kDa), using specific anti-Ole e 1 and anti-Der p 1 pAbs. Black arrows indicated the position of Ole e 1 and Der p 1 bands. Marker molecular masses in kDa are indicated. B) Percentage (%) of activation of basophils determined by FACS. Basophils were incubated with different doses of derived products. Results are given as percentage of CD63 expression. AP, apical medium; BAS, basolateral medium; C control cells; D, Der p 1; and O, Ole e 1. White symbols, products derived from ALI-cultured Calu-3 cells co-exposed to Ole e 1 and Der p 1; black symbol, products derived from Der p 1-treated Ole e 1.

DISCUSSION

Several evidences support the important contribution of environmental proteases in the sensitization to allergens and the exacerbation of allergic diseases by disruption and activation of airway epithelium [209, 292-294]. However, the complete understanding of the underlying mechanism by which allergens overcome epithelial barrier, which is essential for allergic sensitization, is not completely defined. In this study we have used as a model HDM, a clinically relevant source of allergens, which contains proteases including the cysteine-protease Der p 1 [198, 295].

We have focused on the role of co-exposure to Der p 1 protease in the immune response of the bronchial epithelium to Ole e 1 aeroallergen. Our data support that: (i) Co-exposure to Der p 1 did not cause a significant increase in the epithelial permeability to Ole e 1, only chronic-Der p 1 exposure lead to its increase; (ii) Epithelial permeability to Ole e 1 was strongly depended of bronchial epithelium state *per se*; and (iii) the aeroallergen was cleaved by Der p 1, and its products exhibited immunogenic activity.

Der p 1 exposure of ALI-cultured Calu-3 cells for 24 h caused a marked decrease in TEER values associated with the disruption of TJ (indicated by reduction in ZO-1 levels) on day 2 of culture but not on day 7 when the barrier was well established. This effect was not further enhanced by the presence of Ole e 1. The possible importance of protease activity on allergic sensitization has been suggested in multiple studies. However, our findings suggested a novel link between deleterious effect of Der p 1 protease and bronchial epithelial state. Evidences have shown that Der p 1 cleaves AJC proteins, (including occludins, claudins, cadherins and ZO-1), leading to an impaired epithelial barrier [72, 201, 280]. It is well established that TJ play an important role in the control of the epithelial permeability [296, 297]. The disruption of the epithelial barrier has been associated with asthma and allergic diseases, and discussed as requirement for the allergic sensitization event [298-302]. In addition, we demonstrated that permeability to Ole e 1 was strongly dependent on bronchial epithelium state. On day 2 at ALI, when TJ establishment was on process, Ole e 1 passage across the epithelial barrier is higher than on day 7. In addition, the co-exposure to Der p 1 protease seemed not to lead to a further increase on the aeroallergen-permeability. These data suggested that the early events of immune response to an aeroallergen such as Ole e 1 could be mainly conditioned by the state of the epithelium at the time of contact.

Another important aspect of our study was that, after removal of Der p 1, initial TEER values were recovered, thus indicating that TJ were re-established. The high regenerative capacity of human bronchial epithelial has also been demonstrated by Wan

et al. [72], which found that 16HBE14o cells recovered from Der p 1 exposure via de *novo* synthesis of occludins. Furthermore, Jeong *et al.* have reported that mite exposure induced a delay in the skin barrier recovery via PAR-2 activation [294].

We showed that, in contrast to Ole e 1, chronic exposure to Der p 1 altered the integrity of the bronchial epithelium in a time-dependent manner, as indicated by baseline TEER values and the disruption of ZO-1. Interestingly, the impairment of epithelial barrier was maintained at least 24 h after removal of Der p 1. Moreover, only cells that were chronically exposed to the protease exhibited an increased permeability to Ole e 1. The maintenance of the dysfunctional epithelium could constitute the basis of the chronic inflammatory processes observed in asthmatic patients, where recurrent inflammatory episodes lead to structural epithelium abnormalities, that evolves in chronic airway remodelling [303, 304]. This study represents a simple 'proof of concept' that certain environmental substances, such as proteases, would act as a 'foot in the door', maintaining a dysfunctional epithelial barrier state. They would favour the passage of an aeroallergen as well as others inhaled molecules, and thus contributing to the primary sensitization to aeroallergens and the exacerbation of allergic diseases.

For the first time, we demonstrated that Ole e 1 is a novel protein target for Der p 1, and more interesting that Ole e 1-derived products exhibited immunogenic properties as analysed by ELISA inhibition and basophil activation tests. As MS data showed, short-term treatment with Der p 1 cleaved the peptide bond located between residues 10 and 11 of Ole e 1 sequence, rendering a shorter-length protein: EDIPQPPVSQ↓FHIQ […] (Figure 41). Although the N-terminal of the main Ole e 1 isoform did not display the consensus proteolytic specificity sequence of Der p 1 defined by Jacquet *et al.* [305], who indicated that the nature of the residues at position 1, 2, 4 and 5 upstream (P) and 1, 2 and 3 downstream (P') of the cleavage site are important, the aeroallergen can be efficiently cleaved by this protease. Similar controversial data have been reported for human thrombin, which is able to cleavage natural substrates displaying only from 1% to 30% of the optimal consensus specificity [306]. Thus, these data suggested that other factors in addition of specific sequence requirements, may be involved in the protease cleavage [305, 307]. In agreement with our results, Furmonaviciene *et al.* [308] showed that Der p 1 cleaved cell surface DC-SIGN and DC-SIGNR, which do not display protease optimal consensus profile. In addition, Wan *et al*. [72] suggest that Der p 1, like papain, exhibit preference for hydrophobic residues and small, uncharged polar residues at P1' (Leu) and P2 (Ser), respectively, which are presented in its natural substrates occludin and claudin. While Ole e 1 presented a Phe11 and a Ser9 as the P1' and P2 residues, respectively; two conservative substitutions.

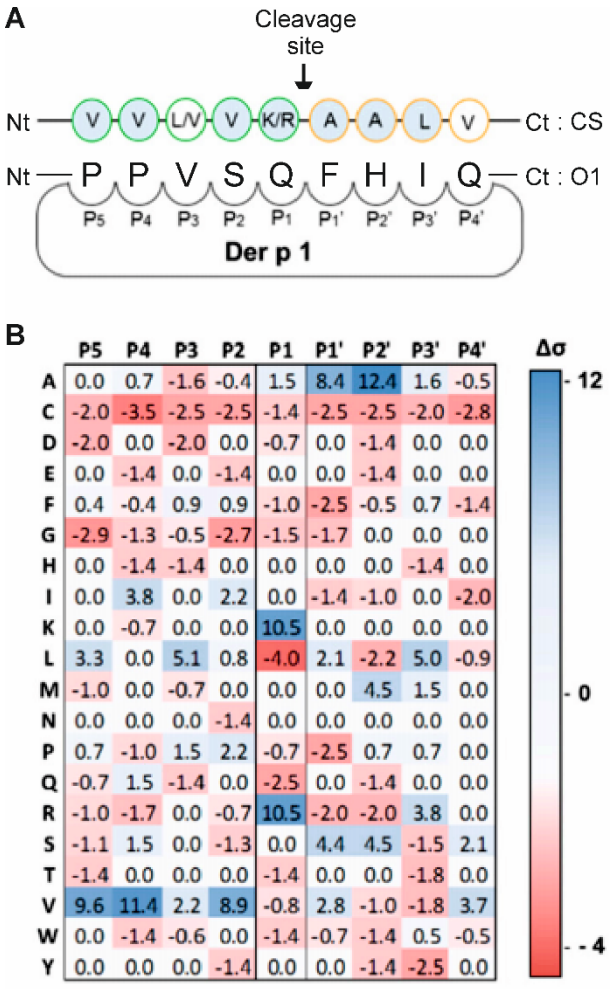

Figure 41. Ole e 1 is specifically cleaved by Der p 1 protease. A) Representation of the targeted cleavage site by Der p 1 on the N-terminal sequence of Ole e 1 (O1) versus the consensus proteolytic specificity profile (CS). The black arrow indicated the position of the peptide bond cleaved by the cysteine-protease. P and P' represents Ole e 1 residues located upstream and downstream of the cleavage site, respectively. B) Matrix of Der p 1-substrate specificity for P5 to P4' positions based on standard deviations (Δσ) calculated for each amino acid residue. Positive and negative Δσ correspond to scores attributed to positively and negatively selected residues, respectively. Adapted from Jacquet *et al*. [305]. Nt, N-terminal part of the sequence; Ct, C-terminal part of the sequence.

Our data showed that Der p 1 presented an early cleavage site located at positions 10-11 of Ole e 1, as supported by the new N-terminal sequence detected by MS at 0.5 h of digestion. Other cleavage sites on the molecule became more accessible to the protease once this first site was cleaved. Thus, the number of peptides increased with the time of proteolysis, being the protein almost completely disrupted by 24 h.

Der p 1-proteolytic treatment of Ole e 1 rendered a peptide cluster, which comprised B cell epitopes as show by ELISA inhibition. Der p 1-treated Ole e 1 exhibited IgG-reactivity but not IgE-reactivity. Five IgG-epitopes were identified in Ole e 1 using overlapping short-synthetic peptide (12 amino acid residues) covering the full polypeptide chain [186].

In addition, IgE epitopes were identified by these authors, regardless of the faint recognition of these peptides by individual sera of allergic patients to olive pollen. The absence of IgE-reactivity with ≤ 3 kDa fraction could be explained in part by the sensitivity of the assay. To demonstrate the biological relevance of our data, basophil activation tests were performed. We found that ≤ 3 kDa fraction –where neither Ole e 1 nor Der p 1 were presented- induced basophil activation in a dose-dependent manner. In agreement with our data, it has been shown that the N-oligosaccharide of Ole e 1, a small molecule of above 1.3 kDa, was able to induce basophil histamine release [173]. Thus, peptides of ≤ 3 kDa fraction have the right molecular masses for containing at least the 2 epitopes required to promote FcƐR-cross-linking. More interestingly, the basophil activation levels of basophil were higher when basolateral media were used, either those derived from cells expose to Ole e 1 alone or the combination of the allergen with Der p 1. Our data suggested an IgE-independent mechanism for basophil activation. The observed activation of basophils appeared not only to be the result of Ole e 1-derived peptides (IgE-dependent mechanism) but Der p 1 as well as Ole e 1 can activate epithelial cells and induce the release of a plethora of mediators [209, 292, 293, 309]. These mediators may be involved in the establishment of the optimal Th2-promoting milieu that leads to an allergic response, thus acting as a linkage between the initial innate response and the subsequent adaptive immune response. An IgE-independent mechanism for basophil activation has been previously described [211, 310-313].

Indeed, T cell epitopes may be generated by Der p 1-cleavage of Ole e 1. In this sense, Wildner *et al*. [314] have reported that the degradation of Ole e 1 and other relevant allergens from Ole e 1-like family by the endolysosomal cathepsin S –a cysteine-protease- from JAWS DC line. These cells generated similar peptide profiles, which substantially overlapped with the T cell epitopes of Ole e 1 [185] in spite of the differences in susceptibility to endolysosomal degradation, and thus, suggesting that endolysosomal degradation assay provided information on the immunogenic properties of a protein.

Collectively, these small peptides could easily be transported across the airway epithelial barrier, gaining access to APC and other immune cells such as mast cells, basophils and T cells, and thus, inducing an allergic response. Therefore, it is tempting to speculate that a similar mechanism could be activate by other environmental proteases such as those present in the *Olea europaea* pollen [73]. These findings open a new dimension in the understanding of both early events in allergic sensitization and exacerbation of the disease.

***Part II*. A metabolomics' study delineating lung epithelial response caused by Ole e 1 and Der p 1 co-exposure: preliminary results by CE-MS analysis**

Metabolomics is a potent *omic* technique able to unravel the metabolic fluctuations associated to particular cell situations. It has been widely applied in numerous fields, including the identification of disease biomarkers such as asthma, diabetes mellitus and cancer, the drug discovery in plants and bacteria, nutrition and certain environment approaches [315]. To obtain the *metabolite footprinting*, common analytical techniques can be used, including chromatography -gas or liquid- coupled to MS, nuclear magnetic resonance spectroscopy and Raman spectroscopy. Recently, CE coupled to MS has emerged as a novel promising approach to separate and detect ionic compounds based on the different migration rates of charged metabolites [316, 317]. Thus, the combination of CE-MS, LC-MS and GC-MS could expand the coverage of metabolites. The analysis of general metabolic changes is achieved by using an unsupervised dimensionality reduction method such as *principal component analysis* (PCA), and a supervised discriminant analysis method of *partial least squares* (PLS) [318].

Our previous data suggested that mediators released by ALI-cultured Calu-3 cells exposed to Der p 1 and Ole e 1 could be involved in the activation of basophils from patient allergic to olive pollen. Here, we used the ALI-cultured Calu-3 cells exposed to Der p 1, Ole e 1 and the combination of both for 24 h, on days 2 and 7 of culture, to obtain the comparative metabolite footprinting using CE-MS, to identify key metabolites involved in allergy. To our knowledge, this is the first comparative metabolomics' study reported on the response of human bronchial epithelium cells to aeroallergen co-exposure up to date. Our data showed the strong dependence of metabolic responses to aeroallergen exposure on epithelium state at the time of contact, as indicate by the day of culture at ALI (day 2 *versus* day 7). In addition, the metabolic pathways of particular SDM that could be involved in the allergic response (L-Arg, Kyn and L-Trp), were also discussed.

Metabolite profiling using CE-MS

CE-MS was used to obtain the metabolite footprinting of apical and basolateral media of ALI-cultured Calu-3 cells exposed to Der p 1 and/or Ole e 1, on days 2 and 7 of culture. Electropherograms from CE-MS in cationic mode are shown in Figure 42. Those of apical samples were similar to those of basolateral ones, suggesting an effective transfer of metabolites between both cell compartments. However, several differences were detected in the metabolic profiles when comparing days 2 and 7 at ALI.

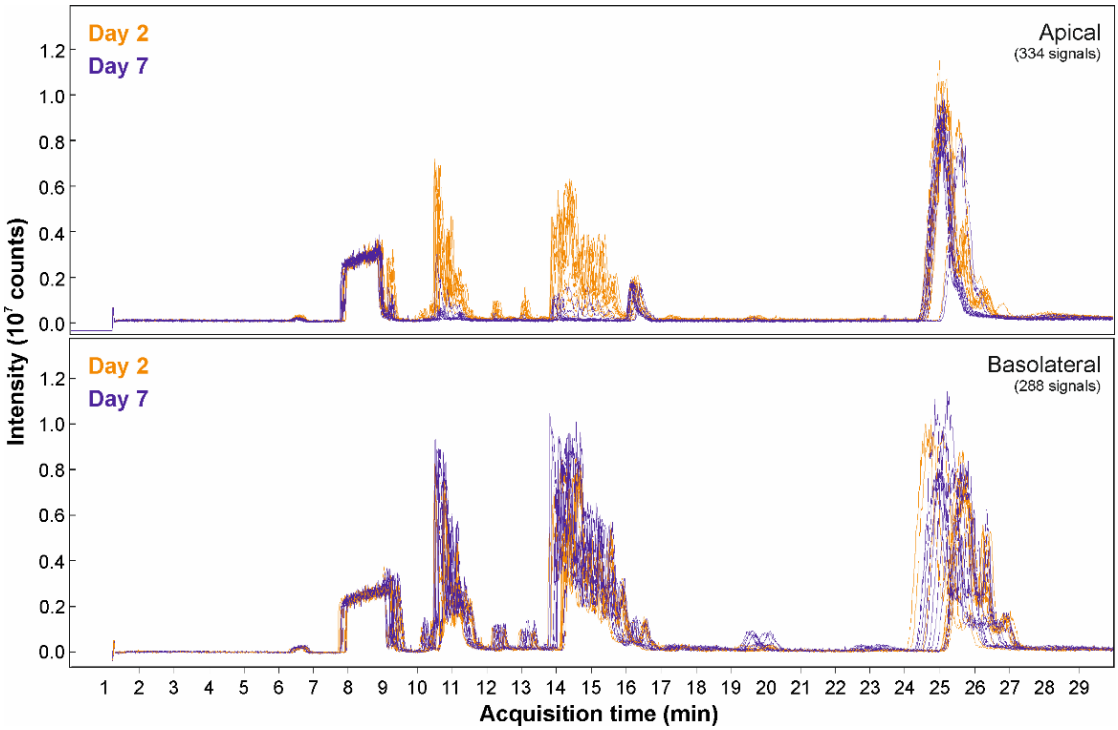

Figure 42. Multiple extracted ion electropherograms of the apical and basolateral media, obtained with CE-MS using a cationic capillary coating. ALI-cultured Calu-3 cells were exposed to Der p 1, Ole e 1 and the combination of them, on days 2 and 7 of culture. After 24 h media were analysed. Experimental conditions: Background electrolyte, 0.8 M formic acid in 10% methanol; separation voltage, 30 kV; sample injection, 50 mbar in 50 s. (n = 3).

A total of 334 and 288 peaks were obtained on apical and basolateral media, respectively. An unsupervised PCA analysis of the metabolites was performed to visualize the effect of both, the time of exposure and the challenge with allergens on Calu-3 cell metabolism (Figure 43). The PCA score plots allowed to detect sample patterns and outliers. Plots are showed in a 2-dimensional space by reducing the high variables number into the first and second principal components: PC [1] and PC [2], respectively, where PC indicates the maximum variation achieved within the data.

The PCA score plots showed a clear separation of cell metabolites in 2 clusters according to the time of exposure (days 2 and 7 at ALI), irrespective of the medium

compartment. No outliers went beyond the 95% Hotelling's T-square ellipse. This model explained and predicted about the 80% and 40% of the total variations on the apical and basolateral samples, respectively. This is reflected by a high goodness of fit and predictability indicated by R^2 value of 0.797 and Q^2 value of 0.752, respectively, for the apical media; while at the basolateral, the R^2 and Q^2 values were 0.714 and 0.468, respectively. This lower Q^2 value at the basolateral compartment could be attributed to the behaviour of one of the samples, and it may be solved by increasing the number of replicates. These data showed the strong dependence of the metabolic response on the epithelium state, as indicated by the time of exposure: day 2 *versus* day 7.

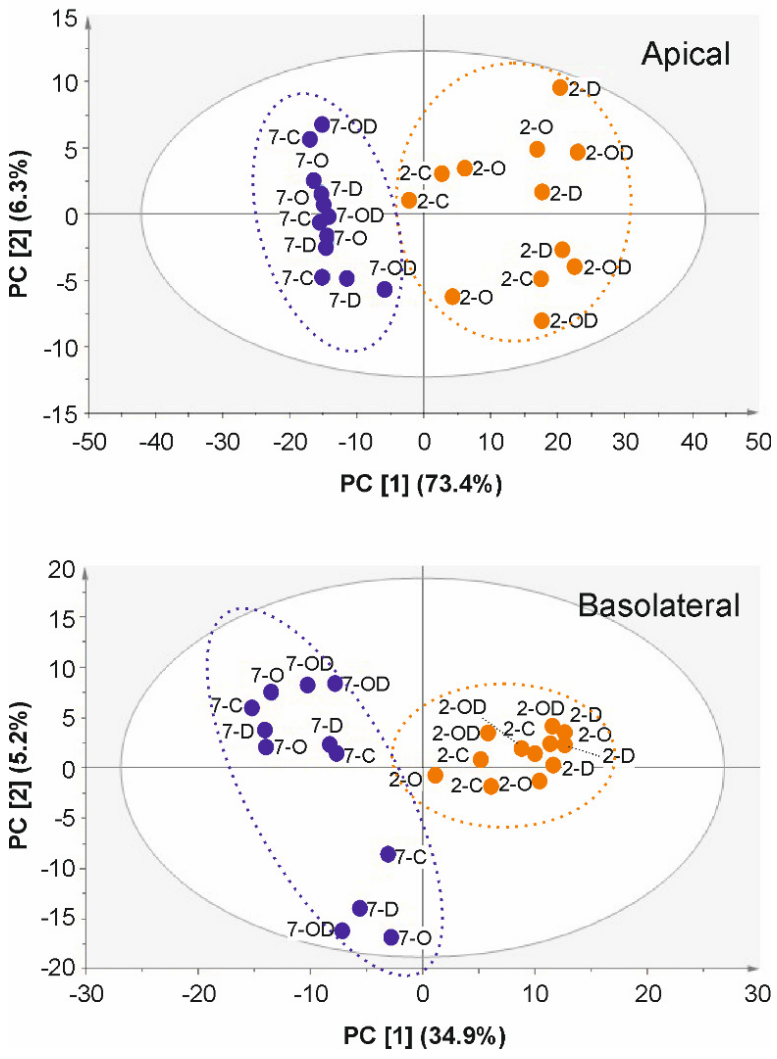

Figure 43. PCA score plot of media metabolites from ALI-cultured Calu-3 cells exposed to Der p 1 and/or Ole e 1, on days 2 (orange dots) and 7 (blue dots) of culture. PC [1] and PC [2], the first and second principal components, respectively. Samples (*n = 3*) are represented by dots, and are grouped according to the day of aeroallergen exposure. Component variability is indicated as percentage (%) of the total. D, cells exposed to Der p 1; O, cells exposed to Ole e 1; OD, cells co-exposed to Ole e 1 1 and Der p 1; C, unexposed cells.

In addition, the PLS discriminant analysis (DA) was performed to analyse the influence of the challenger in the cell metabolic response on days 2 and 7 at ALI, in both apical and basolateral media. PLS-DA indicated the separation of cell metabolites in 2 clusters: Cluster 1, samples derived from cells exposed to Der p 1 alone (D) and their combination (OD); cluster 2, media derived from non-treated cells (C) and cells exposed to Ole e 1 alone (O). Analysis of the correlation coefficients showed that significant metabolite changes occurred on day 2 at ALI, being almost unaltered on day 7, when the epithelial barrier is well established (Table 12). However, no significant models were obtained when comparing cluster 1 and 2: cells exposed (D *versus* OD) and unexposed to Der p 1 (O *versus* C), respectively.

Table 12. Correlation coefficients of the PLS-DA.

Treatment	Apical				Basolateral			
	Day 2		Day 7		Day 2		Day 7	
	R^2	Q^2	R^2	Q^2	R^2	Q^2	R^2	Q^2
D *vs* C	0.63	0.51	-	-	0.88	0.53	-	-
D *vs* O	0.97	0.77	-	-	0.99	0.55	-	-
D *vs* OD	-	-	-	-	0.99	0.66	-	-
O *vs* C	-	-	-	-	-	-	-	-
O *vs* OD	0.97	0.83	0.99	0.54	0.94	0.34	-	-
OD *vs* C	0.65	0.55	0.97	0.81	0.97	0.6	-	-

C, non-treated cells; D, cells exposed to Der p 1;

O, cells exposed to Ole e 1; OD, cells exposed to both allergens

R^2 and Q^2 represents the coefficients of fit and predictability, respectively

(-), absence of predicted model.

Identification of significantly different metabolites (SDM)

A non-parametric Mann-Whitney U ($p < 0.05$) test was carried out to define the variables associated with the time of exposure at ALI. A total of 241 and 152 significantly different metabolites (SDM) were detected in the apical and basolateral media, respectively, as shown in the Venn diagrams (Figure 44). Moreover, 133 out of 241 SDM were equally detected in the apical medium on both days 2 and 7, but only 19 out of 152 SDM were present in the basolateral media on both days of ALI culture.

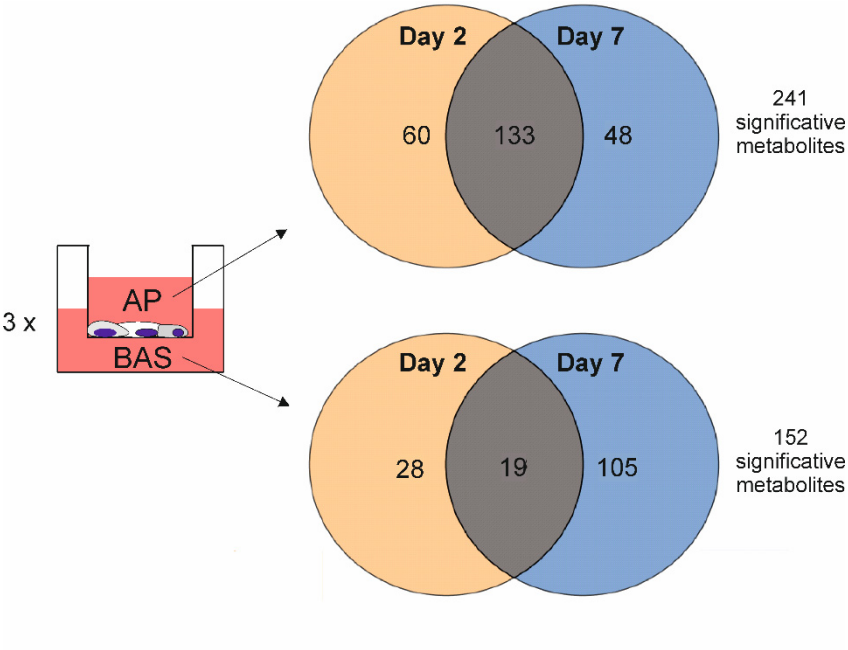

Figure 44. Venn diagrams of Mann-Whitney U test ($p > 0.05$), defining the significantly different metabolites (SDM) detected in the media of ALI-cultured Calu-3 cells on days 2 and 7 of culture, and showing their interaction. AP, apical medium; BAS, basolateral medium. The number of biological replicates ($n = 3$) and significant metabolites are indicated.

A total of 39 and 19 metabolites were identified by matching with MS public libraries, and 25 and 13 were verified using commercial standards, in the apical and basolateral media, respectively, of ALI-cultured Calu-3 cells exposed to Der p 1 and/or Ole e 1. Further information of SDMs is shown in Tables 13-16.

SDM belonging to the categories of L-amino acids and other carbonyl compounds derived from nitrogen metabolism were abundant in both media. The presence in the samples of protein amino acids such as L-histidine, L-lysine, L-methionine, L-phenylalanine, L-threonine, L-tryptophan, and L-valine, could be observed by the proteolytic activity of Der p 1. Also, SDM belonging to carbohydrates, purine and pyridine derivatives, dipeptides and vitamins (including pantothenic acid, niacinamide and folic acid) were detected in the media. Moreover, Der p 1 exposure seemed to increase the apical SDM levels on day 2 at ALI, but not on day 7, compared to either Ole e 1 exposed or non-exposed cells.

Table 13. Significantly different metabolites identified in the apical media of ALI-cultured Calu-3 cells exposed to Der p 1 and/or Ole e 1, on day 2 of culture.

Metabolite	HMDB[1]	KEGG[1]	m/z	MM[2]	MT[3]	Formula	ppm[4]	Biochemical Class	Abundance[A]							
									C		O		D		OD	
									Mean ± SD		Mean ± SD		Mean ± SD		Mean ± SD	
Acetylgalactosamine	HMDB0000212	C01074	222.097	221.090	26.29	$C_8H_{15}NO_6$	0.5	Hexose	528704	22825	613012	99177	624359	75131	526315	3391
Asymmetric dimethylarginine	HMDB0003334	N/A	203.149	202.142	11.61	$C_8H_{18}N4O_2$	-4.0	Amino acid	38323	14963	46613	8516	58938	8825	60718	13133
Betaine*	HMDB0000043	C00719	118.086	117.079	15.64	$C_5H_{11}NO_2$	-1.7	Amino acid	90245	35800	109671	43026	134591	9330	166254	85736
Creatine*	HMDB0000064	C00300	132.077	131.070	12.91	$C_4H_9N_3O_2$	0.0	Amino acid	189822	38995	211769	44652	231745	23054	242608	13802
Cysteinylglycine disulfide	HMDB0000709	N/A	298.052	297.045	13.71	$C_8H_{15}N_3O_5S_2$	-1.0	Peptide	338541	101086	294320	93424	424525	15729	379806	46694
Deoxyfructosyl leucine	HMDB0037840	N/A	294.155	293.148	18.23	$C_{12}H_{23}NO_7$	0.7	Amino acid	67563	31750	82487	22973	124519	23630	127288	21273
Folic acid*	HMDB0000121	C00504	442.147	441.140	18.62	$C_{19}H_{19}N_7O_6$	0.7	Vitamin	128705	66231	142186	32122	214065	20916	227501	48297
Fructoselysine	HMDB0034879	C16488	309.167	308.160	12.96	$C_{12}H_{24}N_2O_7$	4.9	Carbohydrate	63734	49154	95199	48920	178105	68639	156200	36258
Glutaminylglutamic acid	HMDB0029147	N/A	276.119	275.112	17.34	$C_{10}H_{17}N_3O_6$	-0.4	Dipeptide	180316	128308	199395	118569	308885	36921	302001	11470
Glycerophosphocholine	HMDB0000086	C00670	258.110	257.103	24.96	$C_8H_{20}NO_6P$	1.2	Glycerophosphocholine	295103	6900	282849	20223	216406	35974	241308	47856
Glycine*	HMDB0000123	C00037	76.040	75.033	12.26	$C_2H_5NO_2$	10.7	Amino acid	3160845	1728799	3840323	1040660	4864655	622315	5104222	300482
Hydroxy-tryptophan	HMDB0000472	C00643	221.093	220.086	17.40	$C_{11}H_{12}N_2O_3$	4.5	Amino acid	152325	73901	171211	30484	237989	11268	268212	50967
Indoleacetaldehyde	HMDB0001190	C00637	160.076	159.069	11.98	$C_{10}H_9NO$	0.6	Indole	68267	3329	71053	4633	72416	6827	78469	6533
L-Alanine*	HMDB0000161	C00041	90.055	89.048	13.07	$C_3H_7NO_2$	5.6	Amino acid	3094766	2077645	4250857	1252478	5987126	722208	6088354	238340
L-Arginine*	HMDB0000517	C00062	175.119	174.112	10.93	$C_6H_{14}N_4O_2$	1.7	Amino acid	11875552	8500347	14848175	4960639	22234610	684519	22553276	1596932
L-Asparagine	HMDB0000168	C00152	133.060	132.053	14.64	$C_4H_8N_2O_3$	-7.6	Amino acid	84354	35184	112158	14600	160227	40551	156925	21806
L-Cystine*	HMDB0000192	C00491	241.032	240.025	15.35	$C_6H_{12}N_2O_4S_2$	4.6	Amino acid	1488631	796311	1737847	551085	2562233	360396	2582539	500516
L-Glutamic acid*	HMDB0000148	C00025	148.061	147.054	15.27	$C_5H_9NO_4$	6.8	Amino acid	17331	5917	8408	8515	62010	37863	23877	9042
L-Glutamine*	HMDB0000641	C00064	147.077	146.070	14.98	$C_5H_{10}N_2O_3$	4.1	Amino acid	14766029	10106960	18129950	6303558	26347365	1270438	27149807	1964311
L-Histidine*	HMDB0000177	C00135	156.077	155.070	11.15	$C_6H_9N_3O_2$	0.6	Amino acid	3394381	3401509	4125139	1896916	7920193	232996	7840547	554417
L-Kynurenine*	HMDB0000684	C00328	209.092	208.085	14.32	$C_{10}H_{12}N_2O_3$	0.0	Carbonyl compounds	35768	44280	43293	38196	102013	14699	101175	16524
L-Leucine/L-Isoleucine*	HMDB0000687	C00123	132.102	131.095	14.46	$C_6H_{13}NO_2$	0.8	Amino acid	23293186	30145769	28998908	23567806	70362290	5223951	69468307	9253466
L-Lysine*	HMDB0000182	C00047	147.113	146.106	10.61	$C_6H_{14}N_2O_2$	3.4	Amino acid	17557900	9946017	22254823	5924685	30015234	1785231	30826565	2548198
L-Methionine sulfoxide*	HMDB0002005	N/A	166.054	165.046	16.11	$C_5H_{11}NO_3S$	1.8	Amino acid	1464138	1905255	1733459	1478684	4517277	245185	4499248	640237
L-Methionine*	HMDB0000696	C00073	150.059	149.052	14.88	$C_5H_{11}NO_2S$	7.4	Amino acid	1099500	837916	1401847	535745	2120399	123850	2183257	150098
L-Phenylalanine*	HMDB0000159	C00079	166.087	165.080	15.29	$C_9H_{11}NO_2$	6.7	Amino acid	8283612	10310038	9920159	7999768	24047395	1194853	24076785	3429826
L-Proline*	HMDB0000162	C00148	116.070	115.063	15.05	$C_5H_9NO_2$	-0.9	Amino acid	1150868	573827	1367891	600831	1645470	197270	1663581	319827
L-Threonine*	HMDB0000167	C00188	120.064	119.057	14.69	$C_4H_9NO_3$	-8.4	Amino acid	10838168	6281479	14152211	3710415	18984123	2328188	19479375	1638584
L-Tryptophan*	HMDB0000929	C00078	205.098	204.090	15.23	$C_{11}H_{12}N_2O_2$	2.4	Amino acid	621825	782217	735062	575739	1870717	133844	1863360	277415
L-Tyrosine*	HMDB0000158	C00082	182.081	181.074	15.61	$C_9H_{11}NO_3$	1.1	Amino acid	5300559	6202758	6879874	4811664	14430181	949024	14676971	1792311
L-Valine*	HMDB0000883	C00183	118.087	117.080	14.14	$C_5H_{11}NO_2$	5.1	Amino acid	11703904	12171081	15309328	8486521	28415699	1593601	28714891	2744556
Methylnicotinamide	HMDB0000699	C02918	137.071	136.064	11.07	$C_7H_{10}N_4O$	-1.5	Pyridines derivatives	410597	18952	439986	22276	332139	29877	341360	6732
N-Formyl-4-amino… (FAMP)	N/A	C19872	167.092	166.085	12.44	$C_7H_{10}N_4O$	-1.8	Thiamine metabolism	229348	55167	250311	35147	276072	13713	297345	11646
Niacinamide (Vit B3)	HMDB0001406	C00153	123.056	122.048	11.27	$C_6H_6N_2O$	2.5	Vitamin	1308220	98566	1338551	156021	1469128	161396	1456575	102594
Pantothenic acid*	HMDB0000210	C00864	220.118	219.111	25.29	$C_9H_{17}NO_5$	1.8	Vitamin	659965	220689	752018	147206	973284	57666	1002972	133326
Prolylphenylalanine	HMDB0011179	N/A	263.139	262.132	12.29	$C_{14}H_{18}N_2O_3$	-0.8	Peptide	64811	31529	106509	48099	131100	50154	104569	8722
Pyridoxine*	HMDB0000239	C00314	170.081	169.074	12.65	$C_8H_{11}NO_3$	1.8	Vitamin	404383	96825	436878	24988	575702	115077	567301	90271
Serine*	HMDB0000187	C00065	106.050	105.043	14.12	$C_3H_7NO_3$	0.0	Amino acid	2379120	1553610	3056753	775271	4688987	608966	4734171	560474
Xanthine*	HMDB0000292	C00385	153.041	152.034	23.62	$C_5H_4N_4O_2$	2.0	Purine derivatives	74572	12872	84931	3673	73579	20654	68817	8507

*SDM confirmed with commercial standard.

[1]Human Metabolome Database Number (HMDN) or Kyoto Encyclopedia of Genes and Genomes (KEGG) Accesion Number. N/A, Not available.

[2]MM, molecular mass in dalton (Da).

[3]MT, migration time in min.

[4]ppm, MM tolerance.

[A]Data are represented as area of the peak (abundance), and the mean ± standard deviation (SD) ($n = 3$). C, non-exposed cells; D, cells exposed to Der p1; O, cells exposed to Ole e 1; OD, cells exposed to Der p 1 and Ole e 1.

Table 14. Significantly different metabolites identified in the apical media of ALI-cultured Calu-3 cells exposed to Der p 1 and/or Ole e 1, on day 7 of culture.

Metabolite	HMDB[1]	KEGG[1]	m/z	MM[2]	MT[3]	Formula	ppm[4]	Biochemical Class	Abundance[A]							
									C		O		D		OD	
									Mean ± SD		Mean ± SD		Mean ± SD		Mean ± SD	
Acetylgalactosamine	HMDB0000212	C01074	222.097	221.090	26.29	$C_8H_{15}NO_6$	0.5	Hexose	83183	66312	82789	52973	104033	49458	118437	52201
Asymmetric dimethylarginine	HMDB0003334	N/A	203.149	202.142	11.61	$C_8H_{18}N4O_2$	-4.0	Amino acid	8819	7144	13340	3250	55608	32494	49281	23857
Betaine*	HMDB0000043	C00719	118.086	117.079	15.64	$C_5H_{11}NO_2$	-1.7	Amino acid	20791	11418	38607	17285	46487	33439	48471	29017
Creatine*	HMDB0000064	C00300	132.077	131.070	12.91	$C_4H_9N_3O_2$	0.0	Amino acid	266464	210777	377513	128317	391633	48775	392642	86181
Cysteinylglycine disulfide	HMDB0000709	N/A	298.052	297.045	13.71	$C_8H_{15}N_3O_5S_2$	-1.0	Peptide	7122	1277	28906	15141	42370	17309	61636	53053
Deoxyfructosyl leucine	HMDB0037840	N/A	294.155	293.148	18.23	$C_{12}H_{23}NO_7$	0.7	Amino acid	1093	412	1433	1131	2398	4153	6278	10874
Folic acid*	HMDB0000121	C00504	442.147	441.140	18.62	$C_{19}H_{19}N_7O_6$	0.7	Vitamin	5090	488	5189	4789	13754	12962	26991	40922
Fructoselysine	HMDB0034879	C16488	309.167	308.160	12.96	$C_{12}H_{24}N_2O_7$	4.9	Carbohydrate	0	0	0	0	1968	3409	9922	7376
Glutaminylglutamic acid	HMDB0029147	N/A	276.119	275.112	17.34	$C_{10}H_{17}N_3O_6$	-0.4	Dipeptide	0	0	0	0	9489	16435	19151	33171
Glycerophosphocholine	HMDB0000086	C00670	258.110	257.103	24.96	$C_8H_{20}NO_6P$	1.2	Glycerophosphocholine	893117	555112	1162990	292522	1178250	234044	1264853	86240
Glycine*	HMDB0000123	C00037	76.040	75.033	12.26	$C_2H_5NO_2$	10.7	Amino acid	150264	28646	207630	81450	953934	1150525	799319	810359
Hydroxy-tryptophan	HMDB0000472	C00643	221.093	220.086	17.40	$C_{11}H_{12}N_2O_3$	4.5	Amino acid	7165	8376	8122	5988	12816	5763	20582	17455
Indoleacetaldehyde	HMDB0001190	C00637	160.076	159.069	11.98	$C_{10}H_9NO$	0.6	Indole	40635	35151	53722	16993	56191	11971	54524	16693
L-Alanine*	HMDB0000161	C00041	90.055	89.048	13.07	$C_3H_7NO_2$	5.6	Amino acid	81605	43897	107647	40293	855905	1050112	757566	819765
L-Arginine*	HMDB0000517	C00062	175.119	174.112	10.93	$C_6H_{14}N_4O_2$	1.7	Amino acid	172026	140202	236123	88772	1505966	1714124	2732106	3676714
L-Asparagine	HMDB0000168	C00152	133.060	132.053	14.64	$C_4H_8N_2O_3$	-7.6	Amino acid	21711	19143	30970	18854	211820	215132	143693	49146
L-Cystine*	HMDB0000192	C00491	241.032	240.025	15.35	$C_6H_{12}N_2O_4S_2$	4.6	Amino acid	65024	4662	78170	14429	239887	212007	351412	432071
L-Glutamic acid*	HMDB0000148	C00025	148.061	147.054	15.27	$C_5H_9NO_4$	6.8	Amino acid	186823	109129	200031	97845	408347	180843	330874	73647
L-Glutamine*	HMDB0000641	C00064	147.077	146.070	14.98	$C_5H_{10}N_2O_3$	4.1	Amino acid	183806	119975	248651	26918	2543422	3504746	4320662	6551697
L-Histidine*	HMDB0000177	C00135	156.077	155.070	11.15	$C_6H_9N_3O_2$	0.6	Amino acid	45879	23203	60729	21421	376260	444272	874158	1259906
L-Kynurenine*	HMDB0000684	C00328	209.092	208.085	14.32	$C_{10}H_{12}N_2O_3$	0.0	Carbonyl compounds	539	933	331	574	3892	957	5605	2662
L-Leucine/L-Isoleucine*	HMDB0000687	C00123	132.102	131.095	14.46	$C_6H_{13}NO_2$	0.8	Amino acid	111605	37353	163478	62140	1701588	2184858	5384525	8239000
L-Lysine*	HMDB0000182	C00047	147.113	146.106	10.61	$C_6H_{14}N_2O_2$	3.4	Amino acid	306549	251058	441177	110867	2833540	3404745	3993006	5303552
L-Methionine sulfoxide*	HMDB0002005	N/A	166.054	165.046	16.11	$C_5H_{11}NO_3S$	1.8	Amino acid	18605	7671	24921	11235	183964	215618	475514	693266
L-Methionine*	HMDB0000696	C00073	150.059	149.052	14.88	$C_5H_{11}NO_2S$	7.4	Amino acid	1414	2449	2943	4010	19645	25714	47454	69468
L-Phenylalanine*	HMDB0000159	C00079	166.087	165.080	15.29	$C_9H_{11}NO_2$	6.7	Amino acid	47291	23384	64672	26403	626984	798974	1868547	2857536
L-Proline*	HMDB0000162	C00148	116.070	115.063	15.05	$C_5H_9NO_2$	-0.9	Amino acid	180249	54014	263194	85978	598191	252197	659700	140975
L-Threonine*	HMDB0000167	C00188	120.064	119.057	14.69	$C_4H_9NO_3$	-8.4	Amino acid	200179	104423	271870	78873	1753503	2167646	1317392	1360739
L-Tryptophan*	HMDB0000929	C00078	205.098	204.090	15.23	$C_{11}H_{12}N_2O_2$	2.4	Amino acid	8679	1880	11542	4214	82690	99859	206202	302644
L-Tyrosine*	HMDB0000158	C00082	182.081	181.074	15.61	$C_9H_{11}NO_3$	1.1	Amino acid	40894	15918	50521	14583	440832	573160	1134963	1750300
L-Valine*	HMDB0000883	C00183	118.087	117.080	14.14	$C_5H_{11}NO_2$	5.1	Amino acid	57342	33091	74740	25858	954482	1290628	2456795	3835952
Methylnicotinamide	HMDB0000699	C02918	137.071	136.064	11.07	$C_7H_{10}N_4O$	-1.5	Pyridines derivatives	484166	162894	620247	39448	600383	57626	602669	101608
N-Formyl-4-amino… (FAMP)	N/A	C19872	167.092	166.085	12.44	$C_7H_{10}N_4O$	-1.8	Thiamine metabolism	61090	47810	91665	39006	95350	16697	95219	17650
Niacinamide (Vit B3)	HMDB0001406	C00153	123.056	122.048	11.27	$C_6H_6N_2O$	2.5	Vitamin	775977	592633	1411586	97941	1228373	232653	1379614	94201
Pantothenic acid*	HMDB0000210	C00864	220.118	219.111	25.29	$C_9H_{17}NO_5$	1.8	Vitamin	76369	41346	95482	14540	128459	49623	170012	127093
Prolylphenylalanine	HMDB0011179	N/A	263.139	262.132	12.29	$C_{14}H_{18}N_2O_3$	-0.8	Peptide	0	0	824	209	12409	11182	9181	15901
Pyridoxine*	HMDB0000239	C00314	170.081	169.074	12.65	$C_8H_{11}NO_3$	1.8	Vitamin	119859	90139	163623	47124	183699	48174	214946	56136
Serine*	HMDB0000187	C00065	106.050	105.043	14.12	$C_3H_7NO_3$	0.0	Amino acid	45732	20436	50742	8970	410201	475302	577579	724517
Xanthine*	HMDB0000292	C00385	153.041	152.034	23.62	$C_5H_4N_4O_2$	2.0	Purine derivatives	177354	147942	244621	72544	263287	72592	239775	84578

*SDM confirmed with commercial standard.

[1]Human Metabolome Database Number (HMDN) or Kyoto Encyclopedia of Genes and Genomes (KEGG) Accesion Number. N/A, Not available.

[2]MM, molecular mass in dalton (Da).

[3]MT, migration time in min.

[4]ppm, MM tolerance.

[A]Data are represented as area of the peak (abundance), and the mean ± standard deviation (SD) ($n = 3$). C, non-exposed cells; D, cells exposed to Der p1; O, cells exposed to Ole e 1; OD, cells exposed to Der p 1 and Ole e 1.

Table 15. Significantly different metabolites identified in the basolateral media of ALI-cultured Calu-3 cells exposed to Der p 1 and/or Ole e 1, on day 2 of culture

Metabolite	HMDB[1]	KEGG[1]	m/z	MM[2]	MT[3]	Formula	ppm[4]	Biochemical Class	Abundance[A]							
									C		O		D		OD	
									Mean ± SD		Mean ± SD		Mean ± SD		Mean ± SD	
Acetylgalactosamine	HMDB0000212	C01074	222.097	221.090	26.64	$C_8H_{15}NO_6$	0.0	Hexose	601523	166207	510521	21922	618173	127407	548063	123668
Folic acid*	HMDB0000121	C00504	442.148	441.140	18.76	$C_{19}H_{19}N_7O_6$	-1.6	Vitamin	315955	7871	341218	26731	346246	40879	334342	18527
L-Glutamine*	HMDB0000641	C00064	147.074	146.067	15.08	$C_5H_{10}N_2O_3$	13.7	Amino acid	4708258	161352	4826080	47386	4976701	147594	4947398	196597
Glutaminylglutamic acid	HMDB0029147	N/A	276.119	275.112	17.48	$C_{10}H_{17}N_3O_6$	0.4	Dipeptide	299014	41756	279514	41082	237140	54776	210376	57485
Glycerophosphocholine	HMDB0000086	C00670	258.112	257.105	25.19	$C_8H_{20}NO_6P$	-6.6	Glycerophosphocholine	127789	25270	160769	42072	123163	58312	133968	52803
Glycine*	HMDB0000123	C00037	76.040	75.033	12.4	$C_2H_5NO_2$	-16.0	Amino acid	6603418	216961	6580973	296395	6639584	430728	6760226	275980
L-Arginine*	HMDB0000517	C00062	175.119	174.112	11.02	$C_6H_{14}N_4O_2$	-0.6	Amino acid	29124920	435728	30051342	1349877	31304706	1701226	31485846	708786
L-Histidine*	HMDB0000177	C00135	156.077	155.070	11.27	$C_6H_9N_3O_2$	-1.9	Amino acid	10173982	341559	9958571	718051	10818801	841431	10411978	780617
L-Kynurenine*	HMDB0000684	C00328	209.092	208.084	14.45	$C_{10}H_{12}N_2O_3$	1.9	Amino acid	153802	1561	156136	5041	170801	15390	161431	6106
L-Lysine*	HMDB0000182	C00047	147.113	146.106	10.67	$C_6H_{14}N_2O_2$	-0.7	Amino acid	37594167	958324	41313443	1110984	42439641	2851323	41526525	2692841
L-Phenylalanine*	HMDB0000159	C00079	166.085	165.078	15.45	$C_9H_{11}NO_2$	7.9	Amino acid	38361311	1170934	40351140	1909566	42228595	3296824	41847726	1725396
L-Threonine*	HMDB0000167	C00188	120.064	119.057	14.83	$C_4H_9NO_3$	13.4	Amino acid	24521281	806946	21934092	1837672	25783750	2241904	26468313	722985
L-Tyrosine*	HMDB0000158	C00082	182.081	181.074	15.76	$C_9H_{11}NO_3$	0.0	Amino acid	21623335	782120	22399941	1267744	23634704	2162819	23700241	1465384
L-Valine*	HMDB0000883	C00183	118.086	117.079	14.23	$C_5H_{11}NO_2$	0.0	Amino acid	39987304	1198734	38923623	134566	42176016	3828891	42898550	1707313
Methylnicotinamide	HMDB0000699	C02918	137.071	136.064	11.12	$C_7H_{10}N_4O$	1.5	Pyridines derivatives	283568	14083	293532	18838	271691	14687	248311	15958
N-Formyl-4-amino… (FAMP)	N/A	C19872	167.092	166.085	12.6	$C_7H_{10}N_4O$	1.8	Thiamine metabolism	403660	7047	403963	14663	420454	8499	414002	29786
Pantothenic acid*	HMDB0000210	C00864	220.118	219.111	25.59	$C_9H_{17}NO_5$	0.5	Vitamin	1378393	14292	1455757	27309	1442995	97213	1470808	49963
Prolylphenylalanine	HMDB0011179	N/A	263.138	262.131	12.45	$C_{14}H_{18}N_2O_3$	4.6	Peptide	159841	30363	129177	6290	161130	15754	117431	47202
Pryroglutamic acid*	HMDB0000267	C01879	130.050	129.043	26.69	$C_5H_7NO_3$	-1.5	Amino acid	14929862	297510	15371695	53545	15350674	1273146	15562434	563234

*SDM confirmed with commercial standard.

[1]Human Metabolome Database Number (HMDN) or Kyoto Encyclopedia of Genes and Genomes (KEGG) Accesion Number. N/A, Not available.

[2]MM, molecular mass in dalton (Da).

[3]MT, migration time in min.

[4]ppm, MM tolerance.

[A]Data are represented as area of the peak (abundance), and the mean ± standard deviation (SD) ($n = 3$). C, non-exposed cells; D, cells exposed to Der p1; O, cells exposed to Ole e 1; OD, cells exposed to Der p 1 and Ole e 1.

Table 16. Significantly different metabolites identified in the basolateral media of ALI-cultured Calu-3 cells exposed to Der p 1 and/or Ole e 1, on day 7 of culture

Metabolite	HMDB[1]	KEGG[1]	m/z	MM[2]	MT[3]	Formula	ppm[4]	Biochemical Class	Abundance[A]							
									C		O		D		OD	
									Mean ± SD		Mean ± SD		Mean ± SD		Mean ± SD	
Acetylgalactosamine	HMDB0000212	C01074	222.097	221.090	26.64	$C_8H_{15}NO_6$	0.0	Hexose	552789	147644	422627	84160	591253	286152	506050	99174
Folic acid*	HMDB0000121	C00504	442.148	441.140	18.76	$C_{19}H_{19}N_7O_6$	-1.6	Vitamin	383735	17012	388583	9584	390565	25476	383077	36473
L-Glutamine*	HMDB0000641	C00064	147.074	146.067	15.08	$C_5H_{10}N_2O_3$	13.7	Amino acid	7498419	227508	7311405	79273	7678528	316254	7249465	327852
Glutaminylglutamic acid	HMDB0029147	N/A	276.119	275.112	17.48	$C_{10}H_{17}N_3O_6$	0.4	Dipeptide	225741	19568	267996	17474	239134	25174	272703	59587
Glycerophosphocholine	HMDB0000086	C00670	258.112	257.105	25.19	$C_8H_{20}NO_6P$	-6.6	Glycerophosphocholine	152690	33036	202707	26803	175668	13091	204899	32140
Glycine*	HMDB0000123	C00037	76.040	75.033	12.4	$C_2H_5NO_2$	-16.0	Amino acid	7619587	232682	7340969	1133471	7688418	662440	6941506	389517
L-Arginine*	HMDB0000517	C00062	175.119	174.112	11.02	$C_6H_{14}N_4O_2$	-0.6	Amino acid	35428083	3608764	35179197	3373799	36020762	1592896	34058067	3220753
L-Histidine*	HMDB0000177	C00135	156.077	155.070	11.27	$C_6H_9N_3O_2$	-1.9	Amino acid	12784368	613651	12516626	1006266	13040348	259362	11626475	141833
L-Kynurenine*	HMDB0000684	C00328	209.092	208.084	14.45	$C_{10}H_{12}N_2O_3$	1.9	Amino acid	83425	58910	81979	68459	83282	61690	80977	62997
L-Lysine*	HMDB0000182	C00047	147.113	146.106	10.67	$C_6H_{14}N_2O_2$	-0.7	Amino acid	45161952	1102022	45158573	2697420	45511347	829493	44203305	392265
L-Phenylalanine*	HMDB0000159	C00079	166.085	165.078	15.45	$C_9H_{11}NO_2$	7.9	Amino acid	43529699	969972	43332227	1652412	44954689	86732	42783492	833120
L-Threonine*	HMDB0000167	C00188	120.064	119.057	14.83	$C_4H_9NO_3$	13.4	Amino acid	27824193	656615	26353513	1605084	27048409	2289371	27070685	486291
L-Tyrosine*	HMDB0000158	C00082	182.081	181.074	15.76	$C_9H_{11}NO_3$	0.0	Amino acid	25070113	414139	24697102	735085	25899425	128205	24801945	661209
L-Valine*	HMDB0000883	C00183	118.086	117.079	14.23	$C_5H_{11}NO_2$	0.0	Amino acid	45495610	1482586	43776693	2671990	45852863	1788394	44006419	499560
Methylnicotinamide	HMDB0000699	C02918	137.071	136.064	11.12	$C_7H_{10}N_4O$	1.5	Pyridines derivatives	284780	78353	298862	89972	289058	95060	292859	55140
N-Formyl-4-amino… (FAMP)	N/A	C19872	167.092	166.085	12.6	$C_7H_{10}N_4O$	1.8	Thiamine metabolism	346096	33353	331504	80870	352208	13867	340677	32846
Pantothenic acid*	HMDB0000210	C00864	220.118	219.111	25.59	$C_9H_{17}NO_5$	0.5	Vitamin	1567016	68082	1554632	72957	1628923	60212	1605452	65951
Prolylphenylalanine	HMDB0011179	N/A	263.138	262.131	12.45	$C_{14}H_{18}N_2O_3$	4.6	Peptide	204881	66643	152967	47646	198475	86063	157635	22037
Pryroglutamic acid*	HMDB0000267	C01879	130.050	129.043	26.69	$C_5H_7NO_3$	-1.5	Amino acid	10943816	5099719	10028294	5079599	11074363	5274431	10908316	4038925

*SDM confirmed with commercial standard.

[1]Human Metabolome Database Number (HMDN) or Kyoto Encyclopedia of Genes and Genomes (KEGG) Accesion Number. N/A, Not available.

[2]MM, molecular mass in dalton (Da).

[3]MT, migration time in min.

[4]ppm, MM tolerance.

[A]Data are represented as area of the peak (abundance), and the mean ± standard deviation (SD) (*n = 3*). C, non-exposed cells; D, cells exposed to Der p1; O, cells exposed to Ole e 1; OD, cells exposed to Der p 1 and Ole e 1.

Interestingly, among the large number of SDMs, we focused on L-Arg, kynurenine (Kyn) and L-Trp as potential biomarkers associated to Der p 1 exposure, since these 3 metabolites have been reported to contribute to the control of inflammatory response, including allergies.

On day 2 of culture, exposure to Der p 1 induced high Trp levels on the apical media of ALI-cultured Calu-3 cells, compared to control cells, but not in day 7 (Figure 45). Co-exposure to Ole e 1 did not further modified the Trp levels. In contrast, cells exposed to Ole e 1 exhibited Trp levels comparable to those of control cells. No significant changes on Trp levels were observed in the basolateral media on day 2 or 7 at ALI. Kyn levels were also significantly increased on the apical media of Calu-3 cells by Der p 1 exposure on day 2 at ALI but not on day 7, compared to control cells. Again, Kyn levels were not altered in the basolateral media, neither day 2 nor day 7 at ALI.

Finally, similar behaviour was found for L-Arg levels. Only, Der p 1 exposure lead to an increased on the L-Arg levels in the apical media, in comparison to control cells, on day 2 at ALI, but neither in the basolateral media nor on day 7 of culture.

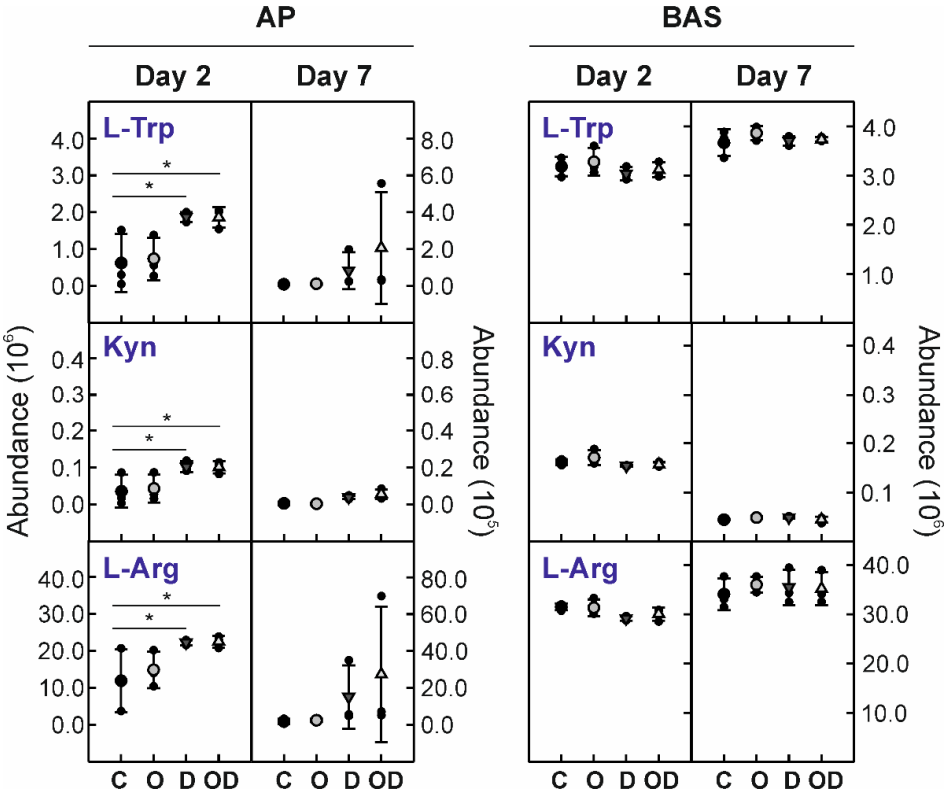

Figure 45. Relative abundance of L-Trp, Kyn and L-Arg in the media of ALI-cultured Calu-3 cells exposed to Der p 1 and/or Ole e 1 for 24 h, in comparison to control cells, on days 2 and 7 of culture. AP, apical medium; BAS, basolateral medium; C, non-exposed cells; D, cells exposed to Der p 1; O, cells exposed to Ole e 1; OD, cells exposed to Der p 1 and Ole e 1. Data are showed as means ± SD of 3 independent experiments. Significant differences are indicated by: *p < 0.05.

DISCUSSION

Bronchial epithelium constitutes a key orchestrator of the lung immune response to some environmental substances by releasing a wide range of mediators, including cytokines chemokines and lipids antimicrobial peptides, among them [103]. During the last years, the development of inflammatory diseases such as respiratory allergies has been correlated with changes in particular metabolites, either generated by the oxidative metabolism or in response to environmental substances, such as aeroallergens [319-322].

In this work, the comparative metabolite profiling was obtained after the exposure of ALI-cultured Calu-3 cells to Der p 1 and/or Ole e 1 for 24 h, on days 2 and 7 of culture. To our knowledge, this is the first comparative metabolomics' study reported on the response of human bronchial epithelium cells to aeroallergen co-exposure. Overall, our data showed the strong dependence of the metabolic response to aeroallergen exposure on the epithelium state at the time of contact, as indicate by the day of culture at ALI (day 2 *versus* day 7). In addition, we also described the metabolic pathways of particular SDM that could be involved in the allergic response: L-Arg, Kyn and L-Trp.

It has been shown that ALI-cultured Calu-3 cells release a wide range of soluble metabolites in both steady-state and after aeroallergen exposure. Significant differences were found in the metabolite profiling of the cells according to the time of exposure, mainly in the apical medium. These can be due to a combination of factors. The high barrier permeability on day 2 at ALI may facilitate the paracellular transport of small metabolites. In addition, the apices of epithelial cells may be developing high activity, since it is the first site of contact with environmental substances, defencing the organism to them with three main mechanisms: (i) the mucociliary escalator, (ii) AJC, in particular TJ; and (iii) the release of a wide range of chemical mediators.

Moreover, the multivariate analysis of the metabolic footprinting revealed differences between the epithelial cell metabolic response to Ole e 1 and Der p 1 exposure. The metabolic profile of Ole e 1-exposed cells resembled to that of non-exposed cells, while Der p 1 exposure induced significant changes in the metabolic profile. The cysteine-protease activity of Der p 1 could be responsible, in part, of these changes, since it has been previously reported that the protease activity contributes to the allergic response by different mechanisms. In this sense, Der p 1 is able to alter the bronchial epithelial barrier permeability by the disruption of TJ, cleaving occludins, claudins, and ZO-1 [201]. Der p 1 degrades the lung surfactant collectins SP-A and SP-D [59], and cleaves the

human protease inhibitors α1-antitrypsin, elafin and SLPI [204, 205], and the low-affinity IgE receptor (CD23) on the surface of activated human B lymphocytes. Moreover, Der p 1 induces the secretion of pro-inflammatory mediators, including IL-6, IL-8, eotaxins and GM-CSF by pulmonary epithelial cells. Der p 1 causes *in vitro* IgE-independent release of IL-4 and IL-13 from mast cells and basophils [206, 209, 211, 292, 293].

Among the large number of SDMs, L-Trp, L-Arg and Kyn have been associated to allergy [323, 324]. Levels of these three metabolites were only significantly increased on the apical media of Calu-3 cells by Der p 1 exposure on day 2 at ALI but not on day 7, compared to control cells. No significant changes on the levels of these metabolites were observed in the basolateral media, neither day 2 nor day 7 at ALI.

L-Trp is one of the nine essential amino acid, which participates in the protein synthesis and as a precursor of important biologically compounds, such as serotonin, melatonin, tryptamine, niacin and auxins. In mammals, Trp is breakdown via the Kyn pathway into several bioactive metabolites [325] (Figure 46). The indoleamine 2,3-dioxygenase (IDO) enzyme is responsible for catalysing the degradation of Trp in N-formyl-Kyn, which is then transformed into Kyn and Kyn-derivatives by the Kyn-aminotransferase (Kyn-AT) and Kyn-monooxygenase (Kyn-MO) enzymes [325-327]. In the lung and other tissues, IDO exhibits several enzymatic activities. Two isoforms have been described so far, IDO-1 or IDO-2, which exhibit similar structures but differed in signalling pathways and expression patterns. IDO-1 is the predominant isoform and is expressed on a broad variety of cell types, including APCs and epithelial cells, among others [328, 329]. Apart from their role in infection, pregnancy, transplantation, autoimmunity and cancer, in the last years, IDO has been involved in the control of allergic inflammation [330, 331].

IDO-1 exerts its immunomodulatory effect by controlling the local concentration of Trp. It has been reported that the induction of Trp degradation occurs during systemic allergen immunotherapy by IDO activation [332, 333]. In particular, 3-OH-Kyn, xanturenic acid and Kyn contribute to tolerance induction against allergens [332, 334-337]. In this sense, the high Trp levels in the apical media of cells exposed to Der p 1 can be associated to an accumulation of this amino acid by IDO downregulation. An impaired IDO-1 activity has been reported in patients with allergic rhinitis [338]. Finally, Adajani *et al*. [339] have shown that airway epithelial primary cultures as well as cell lines, including Calu-3, downregulate IDO-1 activity after exposure to LPS and HDM. Moreover, asthmatic patients exhibit lower ratio Kyn/L-Trp than non-asthmatic individuals [340, 341]. Finally, increased plasma levels of Trp have been found in patients with pollinosis [342].

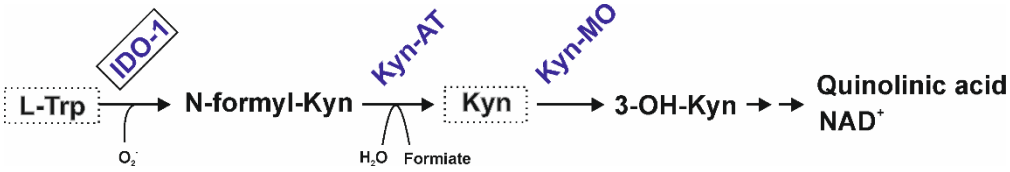

Figure 46. L-Tryptophan (L-Trp) degradation via Kynurenine (Kyn) pathway, involving indoleamine 2,3-dioxygenase (IDO-1), Kyn-aminotransferase (Kyn-AT) and Kyn-monooxygenase (Kyn-MO) enzymes. Trp and Kyn metabolites (3-hidroxy-Kyn, 3-OH-Kyn, among others) exhibit immunological, protective and toxic functions.

L-Arg is considered a semi-essential or conditionally essential amino acid, which acts as a precursor in protein synthesis and a substrate for several enzymes, including nitric oxide synthase (NOS) [343]. L-Arg is hydrolysed by NOS into NO and L-citrulline (Figure 47). L-Arg is also the substrate of the arginase (ARG), yielding, L-Ornithine (L-Orn) and urea [344-346]. L-Arg homeostasis is involved in the regulation of airway function via NOS, which determines the production of the endogenous bronchodilator NO [347], and thus being linked to allergic asthma [324]. However, controversy exists about the role of NO in the development of airway responsiveness [348, 349].

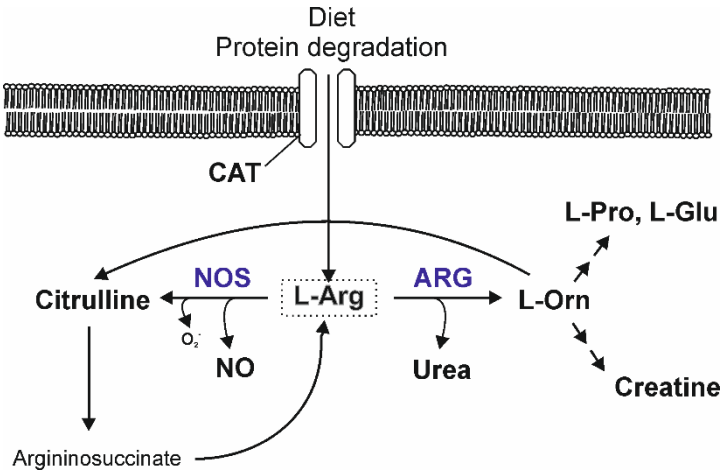

Figure 47. L-Arginine metabolism. In airways, L-Arg uptake occurs by membrane cationic amino acid transporters (CATs). Once at the cytosol, L-Arg is degraded by nitric oxide synthase (NOS) into nitric oxide (NO) and L-citrulline, or alternatively by arginase (ARG), yielding, L-Ornithine (L-Orn) and urea. L-citrulline can be incorporated in the urea cycle to be transformed into L-Arg. L-Orn is a precursor of L-Pro, L-Glu, creatine and other polyamines.

Two of the three NOS isoenzymes are expressed in the airway epithelial cells: the constitutive NOS (cNOS), which is involved in the controlled production of NO in healthy subjects, and the inducible NOS (iNOS), which is highly expressed in asthmatics and in the airways after allergen exposure [350]. iNOS is also induced by pro-inflammatory cytokines, altering the cytosolic levels of both NO and O_2^-, and inducing the formation of $ONOO^-$, and thus, contributing to airway inflammation and remodelling [351-354].

Endogenous levels of L-Arg are mainly controlled by a membrane specific cationic amino acid transporter (CAT) [355]. CAT is tightly regulated in response to either exogenous stimulus such as LPS or inflammatory cytokines [356], which in turn reduced the cytosolic levels of L-Arg and the production of NO by NOS. In this sense, NO levels can also be compromised in the airway epithelium by upregulation of ARG activity by either Th2 cytokines [357, 358], LPS [359] or cigarette smoke [360].

Collectively, our data shown the strong dependence of metabolic response to aeroallergen exposure on epithelium state at the time of contact, as indicate by the comparative metabolite profiling obtained after the exposure of ALI-cultured Calu-3 cells to Der p 1 and/or Ole e 1 for 24 h, on days 2 and 7 of culture.

***Part III*. Human Glutathione-S-transferase pi, a cysteine-protease elicitor of Der p 1 allergen from house dust mite**

Environmental proteases have been widely associated with the pathogenesis of allergic disorders. Der p 1, a cysteine-protease from HDM *Dermatophagoides pteronyssinus*, constitutes one of the most clinically relevant indoor aeroallergens worldwide. Der p 1-protease activity depends on the redox state of its catalytic cysteine residue, which has to be in the reduced state to be active. So far, it is unknown whether Der p 1-protease activity could be regulated by the host redox microenvironment once it reaches the lung epithelial lining fluid. In this sense, GSTpi, an enzyme traditionally linked to phase II detoxification, is highly expressed in human lung epithelial cells, which represent the first line of defence against aeroallergens. Moreover, GSTpi is a generalist catalyst of protein S-glutathionylation reactions, and some polymorphic variants of this enzyme has been associated to the development of allergic asthma. Here, we showed that human GSTpi increased the cysteine-protease activity of Der p 1, while GSTmu (the isoenzyme from mite) did not alter it. GSTpi induced the reduction of Cys residues in Der p 1, probably by rearranging its disulphide bridges. Furthermore, GSTpi was detected in the apical medium collected from human bronchial epithelial cell cultures, and more interestingly, it increased cysteine-protease activity of Der p 1. Our findings support the role of human GSTpi from airways in modulating of Der p 1 cysteine-protease activity, which may have important clinical implications in the immune response to this aeroallergen in genetically susceptible individuals.

Human GSTpi upregulates the cysteine-protease activity of Der p 1

To analyse whether GST affected the cysteine-protease activity of Der p 1, the proteolysis of the fluorogenic peptide Boc-QAR-AMC by Der p 1 was performed in the presence of human GSTpi or mite GSTmu, with or without one of the reducing agents indicated (GSH or L-Cys, from 0.1 to 2 mM). Control was merely carried out with the cysteine-protease (Figure 48). The cysteine-protease activity of Der p 1 was upregulated by GSTpi in a dose-dependent manner, after its pre-activation with the reducing agent GSH. However, no activity was observed without pre-treatment with the reducing agent, required to regenerate the catalytic thiol group of this cysteine-protease. The highest increase on Der p 1-protease activity was observed with 2.5 µM GSTpi in the presence of 0.5 mM GSH. Saturating concentrations of GSH (1 and 2 mM) largely reduced GSTpi-upregulatory effect. Interestingly, the same effect was found when L-Cys was used as reducing agent. Thus, this suggests that upregulation of Der p 1-protease activity by GSTpi does not depend on its glutathione transferase or S-glutathionylation activity, and thus other mechanism may be involved. In contrast, GSTmu had not effect on the cysteine-protease activity of Der p 1. This experiment shows that GSTpi, but not GSTmu, increases Der p 1 protease activity by GSTpi in the presence of reduced thiols.

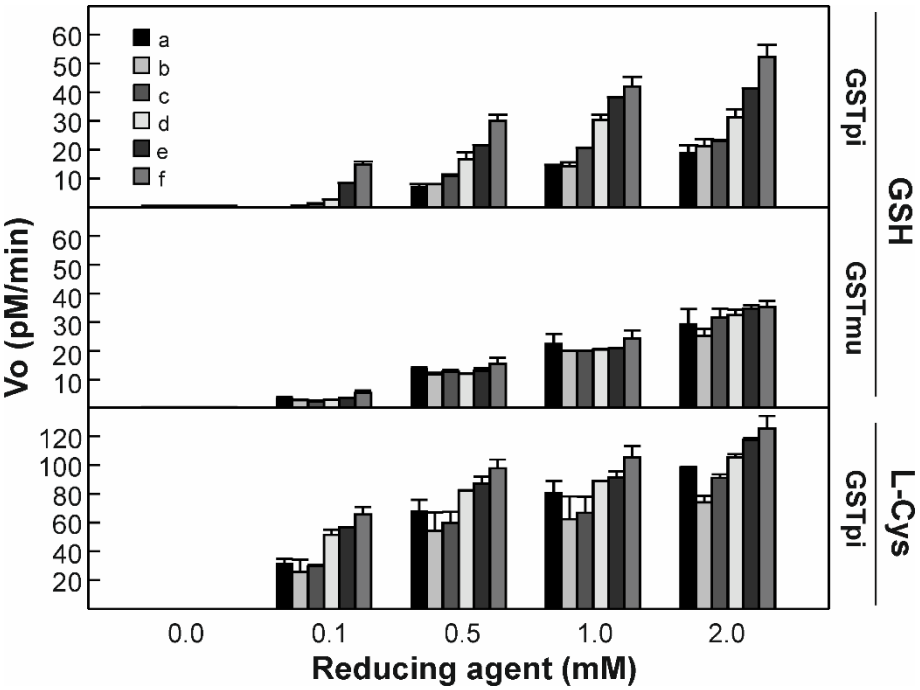

Figure 48. Human GSTpi, but not mite GSTmu, increased the cysteine-protease activity of Der p 1 allergen. The proteolysis of the fluorogenic peptide (Boc-QAR-AMC, 75 µM) by Der p 1 was measured in the presence of different concentration of GSTpi or GSTmu, after pre-activation with GSH or L-Cys (range from 0.1 mM to 2 mM), for 90 min. Data are expressed as initial rate of hydrolysis (pM/min) and showed as means ± SD of duplicate measurements. A representative experiment of 2 is shown. GST concentrations (µM): a, 0; b, 0.15; c, 0.3; d, 0.6; e, 1.3; f, 2.5.

Identification of the modified-Cys residues of Der p 1

To identify which Cys residues were modified by GSH, Der p 1 was digested alternatively with trypsin or chymotrypsin after incubation with GSTpi in the absence or presence of the reducing agent. Peptide analysis was carried out by RP-LC-MS/MS. Cys modification assignment was done considering the absolute number of peptide spectra containing Cys residues (Figure 49A) (Tables 18 and 19).

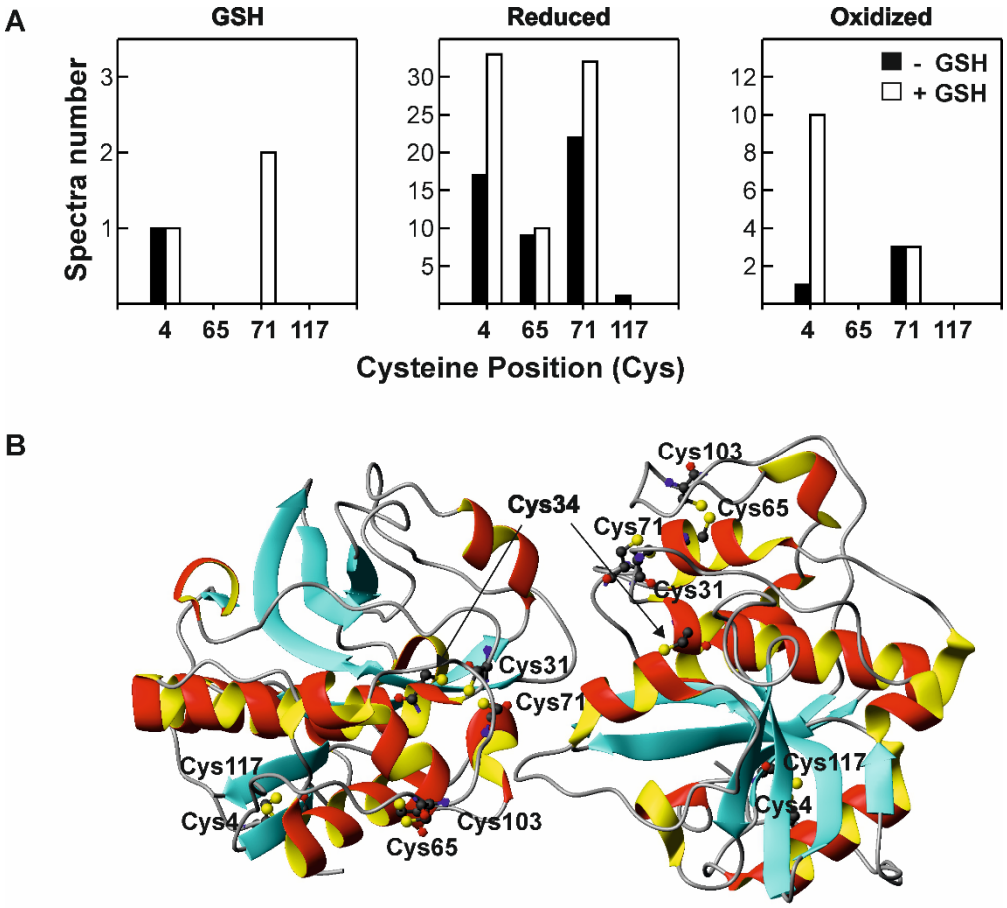

Figure 49. Analysis of modified-Cys residues of Der p 1 by in-gel digestion, followed by RP-LC-MS/MS, after incubation with GSTpi in the absence or presence of GSH. A) Summary of peptide spectra number containing GSH conjugated, reduced (including free and NEM conjugated) and oxidized (including sulfonic, sulfenic and sulfinic-modified) Cys residues. B) 3D-structure of Der p 1 dimer. Ribbon representation was generated using PyMOL by using the known structure as template (PDB Ref. 3F5V). Cys residues are indicated in the structure. Mature enzyme has three disulphide bridges: Cys4-Cys117, Cys31-Cys71, and Cys65-Cys103. The catalytic cysteine residue (Cys34) is indicated.

The highest number of modifications was displayed by Cys4, followed by Cys71 (Tables 18 and 19). The lowest number of modifications were displayed by Cys65 and Cys117. These modifications took place either without or with GSH, and included GSH conjugation, free residues (including NEM conjugation) and Cys oxidation (including sulfonic, sulfenic and sulfinic-modified residues), among others. Neither Cys31, Cys34 nor Cys103 were detected in any of the peptides, and Cys117 was found in only one

spectrum, so we could not draw conclusions regarding their redox state. Both Cys4 and Cys71 increased the number of spectra in the free form after treatment with GSH and GSTpi (Tables 17 and 18). Figure 49B shows the reported 3D-structure of Der p 1 dimer, where monomers face each other covering the catalytic Cys residue (Cys34) [194, 361]. The three-disulphide bridges formed between Cys residues (Cys4- Cys117, Cys31-Cys71, and Cys65-Cys103) that stabilized the protein folding are indicated. Although we have not obtained a detailed map of the redox state of all the Cys residues, our data and the model suggest that addition of GSH with GSTpi produces a disulphide-bridge rearrangement in Der p1, which may involve at least Cys4 and Cys71.

Table 17. Sequence of Der p 1-derived peptides containing cysteine residues analysed by in-gel digestion and LC-MS, after incubation with GSTpi in the absence of GSH.

Peptide sequence	MM[1]	ppm[2]	m/z	To[3]	QT[4]	T[5]	Cys modification[6]	Pos[7]
T.NW(sub A)C(+57.02)SID(sub N)GNAPAEIDLR.Q	1829.837	14.3	915.939	1	0	1	Carbamidomethylation	4
A.C(+25.00)SINGNAPAEIDLR.Q	1496.704	6.9	749.365	3	1	2	Cyano	4
A.C(+25.00)SINGNAPAEIDLRQM.R	1755.803	5.1	878.913	2	1	1	Cyano	4
E.TNAC(+25.00)SINGNAPAEIDLR.Q	1782.832	4.8	892.428	2	2	0	Cyano	4
A.C(+25.00)SINGNAPAEIDL.R	1340.603	9.6	671.315	1	1	0	Cyano	4
E.TNAC(-33.99)SINGNAPAEIDLR.Q	1723.849	7.5	862.938	2	1	1	Dehydroalanine	4
E.TNACSIN(+.98)GNAPAEIDLR.Q	1758.821	-3.1	880.415	2	1	1	Free	4
A.ETN(+15.00)ACSINGNAPAEIDLR.Q	1901.879	6.6	951.953	2	0	2	Free	4
E.T(+79.97)NACSINGNAPAEIDLR.Q	1837.803	5.6	919.914	1	0	1	Free	4
T.N(+68.06)ACSINGNAPAEIDLR.Q	1724.852	-3.7	575.956	3	0	3	Free	4
N.R(sub A)CN(sub S)INGNAPAEIDLR.Q	1654.821	-0.8	828.417	1	0	1	Free	4
A.C(+305.07)SIN(+.98)GNAPAEIDLR.Q	1777.761	-1.3	593.594	1	0	1	Glutathione disulfide	4
A.ETNAC(+14.02)SINGNAPAEIDLR.Q	1900.895	6.1	951.461	6	3	3	Methylation	4
T.N(+.98)AC(+125.05)SINGNAPAEIDLR.Q	1782.821	11.1	892.428	2	0	2	NEM	4
E.TNAC(+125.05)SINGNAPAEIDL.R	1726.783	7.5	864.405	2	1	1	NEM	4
E.TNAC(+125.05)SINGNAPAEIDLR.Q	1882.884	9.1	942.458	2	1	1	NEM	4
E.TNAC(+125.05)SID(sub N)GNAPAEIDLR.Q	1883.868	3.7	942.945	1	1	0	NEM	4
E.TNAC(+125.05)SIN(+.98)GNAPAEIDLR.Q	1883.868	3.7	942.945	1	0	1	NEM	4
E.TNAC(+47.98)SINGNAPAEIDLR.Q	1805.821	8.4	903.926	1	0	1	Sulfonic	4
A.SQHGC(+125.05)HGDTIPR.G	1431.631	9.5	716.83	8	4	4	NEM	71
H.GC(+125.05)HGDTIPR.G	1079.482	8.5	540.753	2	1	1	NEM	71
Q.HGC(+125.05)HGDTIPR.G	1216.541	8	406.524	2	1	1	NEM	71
A.SQHGC(+125.05)HGDTIPRGIEY.I	1893.843	7.4	632.293	2	1	1	NEM	71
C.ASQHGC(+31.99)HGDTIPR.G	1409.611	0.4	470.878	2	0	2	Sulfinic	71
A.SQHGC(+31.99)HGDTIPR.G	1338.574	8.2	447.202	1	0	1	Sulfinic	71
Y.C(+25.00)QIYPPNVNK.I	1199.576	5.8	600.799	6	3	3	Cyano	65;71
R.FGISNYC(-33.99)QIYPPNVNK.I	1821.905	6.2	911.965	2	1	1	Dehydroalanine	65;71
R.FGISNYC(+125.05)QIYPPNA(sub V)NK.I	1952.909	7.8	977.469	1	0	1	NEM	65;71
V.DC(+57.02)ASQHGCHGDTIPR.G	1652.678	7.9	551.904	1	0	1	Carbamidomethylation; Free	65;71
D.C(+25.00)ASQHGCHGDTIPR.G	1505.625	9.1	502.887	1	0	1	Cyano; Free	65;71
L.VDCASQHGC(-20.03)HGDTIPR.G	1674.699	8.7	559.245	2	1	1	Free; Aromatic heterocycle	65;71
L.VDCAS(-2.02)QHGCHGDTIPR.G	1692.710	2.7	847.364	4	2	2	Free; Free	117
L.VDCAS(-20.03)QHGCHGDTIPR.G	1674.699	8.1	559.245	2	1	1	Free; Free	117
L.VDCASQHGC(-1.01)HGDTIPR.G	1693.718	-8.1	847.859	1	0	1	Free; Half of a disulfide bridge	117

[1] MM, Molecular mass in dalton (Da).

[2] Mass tolerance (ppm).

[3] To, Total peptide spectra.

[4] QT, peptide derived from in-gel chymotrypsin digestion.

[5] T, peptide derived from in-gel trypsin digestion.

[6] PTM, Cys postranslation modification assignment.

[7] Pos, position of the Cys residue in the amino acid sequence of Der p 1.

Table 18. Sequence of Der p 1-derived peptides containing cysteine residues analysed by in-gel digestion and LC-MS, after incubation with GSTpi in the presence of GSH.

Peptide sequence	MM[1]	ppm[2]	m/z	To[3]	QT[4]	T[5]	Cys modification[6]	Pos[7]
E.TNAC(+57.02)T(sub S)ID(sub N)GNAPAEIDLR.Q	1829.858	3.2	915.939	2	1	1	Carbamidomethylation	4
A.C(+25.00)SINGNAPAEIDLR.Q	1496.704	7.6	749.365	2	1	1	Cyano	4
E.TNAC(+25.00)SINGNAPAEIDLR.Q	1782.832	7.6	892.430	1	1	0	Cyano	4
E.TNACSIN(+.98)GNAPAEIDLR.Q	1758.821	-5.7	880.413	2	1	1	Free	4
A.ETNACSIN(+15.00)GNAPAEIDLR.Q	1901.879	3.8	951.950	5	2	3	Free	4
A.ETN(+15.00)ACSINGNAPAEIDLR.Q	1901.879	1.7	951.948	5	1	4	Free	4
A.ETNACS(-2.02)INGNAPAEIDLR.Q	1884.864	-7.8	943.432	1	0	1	Free	4
A.E(+14.02)TNACSINGNAPAEIDLR.Q	1900.895	2	951.457	3	1	2	Free	4
A.ET(+14.02)NACSINGNAPAEIDLR.Q	1900.895	3	951.458	3	2	1	Free	4
T.N(+127.06)ACSINGNAPAEIDLR.Q	1783.852	-13.8	892.921	1	0	1	Free	4
T.NACS(+87.05)INGNAPAEIDLR.Q	1743.840	8.8	872.935	1	0	1	Free	4
T.N(+68.06)ACSINGNAPAEIDLR.Q	1724.852	-7.2	863.427	2	0	2	Free	4
E.T(+79.96)NACSINGNAPAEIDLR.Q	1837.794	4.9	919.909	2	1	1	Free	4
A.ETG(sub N)ACSINGNAPAEIDLR.Q	1829.858	0.3	915.937	2	1	1	Free	4
A.ETNACT(sub S)ID(sub N)GNAPAEIDLR.Q	1901.879	2.3	951.949	1	1	0	Free	4
N.AC(+305.07)SIP(sub N)GNAPAEIDLR.Q	1830.824	16.1	916.434	1	0	1	Glutathione disulfide	4
T.N(+.98)AC(+125.05)SINGNAPAEIDLR.Q	1782.821	13.9	892.430	1	0	1	NEM	4
E.TNAC(+125.05)SINGNAPAEIDLR.Q	1882.884	0.6	942.450	2	1	1	NEM	4
E.TNAC(+125.05)SIN(+.98)GNAPAEIDLR.Q	1883.868	-0.9	942.941	2	0	2	NEM	4
A.ETNAC(+15.99)SINGNAPAEIDLR.Q	1902.874	1.3	952.446	5	2	3	Sulfenic	4
E.TNAC(+31.99)SINGNAPAEIDLR.Q	1789.826	4.4	895.924	1	0	1	Sulfinic	4
E.TNAC(+47.98)SINGNAPAEIDLR.Q	1805.821	3.8	903.921	4	2	2	Sulfonic	4
Q.SLDLAEQELVDC(+362.14)A.S	1766.781	6.3	589.938	1	0	1	Nucleophilic addition to cytopiloyne	65
D.LAEQELVDC(+362.14)A.S	1451.638	2.1	726.828	1	0	1	Nucleophilic addition to cytopiloyne	65
A.SQHGC(+149.03)HGDTIPR.G	1455.614	-5.6	728.810	1	0	1	Benzyl isothiocyanate	71
G.C(+25.00)HGDTIPR.G	922.408	6.4	462.214	1	0	1	Cyano	71
C.AS(+77.99)QHGCHGDTIPR.G	1455.608	1.5	728.812	2	0	2	Free	71
A.SQHGCHGDTIPR.G	1306.584	4.1	436.537	4	1	3	Free	71
H.GCHGDTIPR.G	954.434	0.7	478.225	1	0	1	Free	71
C.ASQHE(sub G)CHGDTIPR.G	1449.642	9.2	484.226	1	0	1	Free	71
H.GC(+305.07)HGDTIPR.G	1259.502	5.2	420.844	1	0	1	Glutathione disulfide	71
A.SQHP(sub G)C(+305.07)HGDTIPR.G	1651.683	5.4	826.853	1	0	1	Glutathione disulfide	71
H.GC(+125.05)HGDTIPR.G	1079.482	4.6	540.751	2	1	1	NEM	71
A.SQHGC(+125.05)HGDTIPR.G	1431.631	5.5	716.827	6	3	3	NEM	71
Q.HGC(+125.05)HGDTIPR.G	1216.541	5.8	406.523	2	1	1	NEM	71
H.GC(+125.05)N(sub H)GDTIPR.G	1056.466	4.4	529.243	1	0	1	NEM	71
A.SQHGC(+125.05)HGDTIPRGIEY.I	1893.843	3.8	632.291	1	1	0	NEM	71
Q.HGC(+125.05)N(sub H)GDTIPR.G	1193.525	0.8	597.770	1	0	1	NEM	71
A.SQHGC(+31.99)HGDTIPR.G	1338.574	5.9	447.201	1	0	1	Sulfinic	71
A.SQHGC(+47.98)HGDTIPR.G	1354.568	4.2	452.532	1	0	1	Sulfonic	71
Y.C(+25.00)QIYPPNVNK.I	1199.576	1.9	600.796	3	0	3	Cyano	117
L.VDCASQHGC(+15.99)HGDTIPR.G	1710.720	8	571.252	1	0	1	Free; Sulfenic	65; 71
Q.ELVDC(-1.01)ASQHGCHGDTIPR.G	1935.844	-7.8	968.922	1	0	1	Half of a disulfide bridge; Free	65; 71
V.DC(+57.02)ASQHGCHGDTIPR.G	1652.678	7.9	551.904	1	0	1	Carbamidomethylation; Free	65;71
L.VDCAS(-2.02)QHGCHGDTIPR.G	1692.710	0.6	847.363	3	1	2	Free; Free	65;71
Q.ELVDCAS(-2.02)QHGCHGDTIPR.G	1934.836	-1	968.425	1	0	1	Free; Free	65;71
D.CAS(-2.02)QHGCHGDTIPR.G	1478.614	4.3	493.881	1	0	1	Free; Free	65;71
L.VDCASQH(+15.99)GCHGDTIPR.G	1710.720	8	571.252	4	2	2	Free; Free	65;71

[1] MM, Molecular mass in dalton (Da).

[2] ppm, Mass tolerance.

[3] To, Total peptide spectra.

[4] QT, peptide derived from in-gel chymotrypsin digestion.

[5] T, peptide derived from in-gel trypsin digestion.

[6] Cys postranslation modification assignment.

[7] Pos, position of the Cys residue in the amino acid sequence of Der p 1.

GSH induces a change on the global folding of Der p 1

The effect of the reducing agents (GSH or L-Cys) on the secondary structure of Der p 1 was determined by obtaining its far-UV CD spectra (Figure 50A). GSH altered the shape of Der p 1 spectrum, indicating a change in the secondary structure of the protein. Deconvolution of the ellipticity data allowed quantifying the changes in the secondary structure composition. In absence of the reducing agent, the determined secondary structure of Der p 1 showed 20.1% for α-helix, 34.0% for β-strand, 15.8% for β-turn and 30.1% for random coil, in agreement to previously published [362]. GSH induced a reduction in the α-helix component, and an increase in both β-strand and random coil components. In contrast, L-Cys did not induce significant changes in the CD spectrum of Der p 1.

GSH modifies the redox state of Cys residues in Der p 1

We analysed whether GSTpi and GSH could induce a change in the redox state of the Cys residues of Der p 1. SDS-PAGE and Coomasie blue staining showed that GSH caused a retardation in the relative migration distance of Der p 1 by comparing to both controls, untreated- and DTT-treated Der p 1; thus, suggesting a change in the protein global folding (Figure 50B).

Finally, we used a modification of the RFS assay to determine the relative number of reduced and oxidized Cys residues in Der p 1 without or with GSH (Figure 50C) There was a faint labelling of reduced Cys residues (without the addition or NEM or DTT), which clearly increased with GSH addition. There was a higher signal of reversibly oxidized Cys residues (after addition of NEM and DTT), in corresponding to the high proportion of Cys residues involved in disulphide bonds, which was slightly decreased with GSH treatment. Thus, GSH treatment is altering the redox state of some of the Cys residues, increasing the proportion of Cys in the free thiol form.

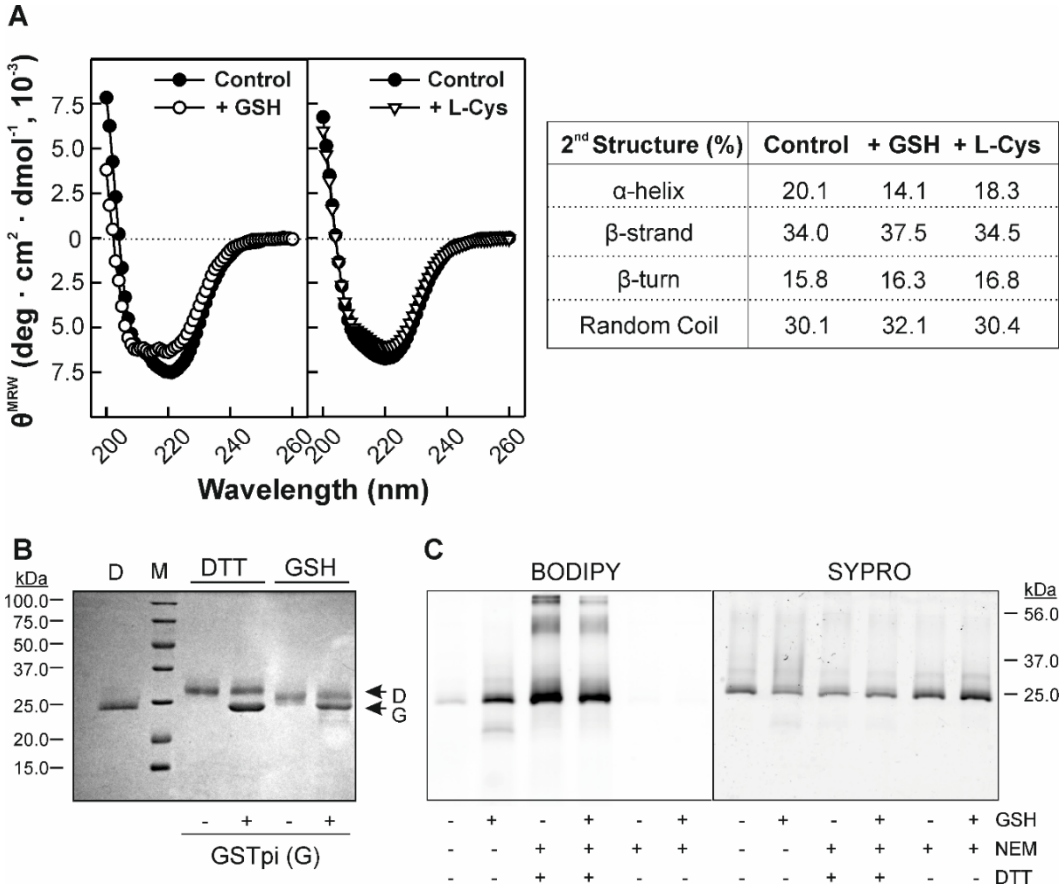

2nd Structure (%)	Control	+ GSH	+ L-Cys
α-helix	20.1	14.1	18.3
β-strand	34.0	37.5	34.5
β-turn	15.8	16.3	16.8
Random Coil	30.1	32.1	30.4

Figure 50. Effects of GSH on the global folding of Der p 1. A) Far-UV circular dichroism (CD) spectra of Der p 1 in absence or presence of a reducing agent: GSH or L-Cys. Secondary structure composition of Der p 1 determined from CD spectra by CDNN. B) SDS-PAGE analysis of the effect of 1 mM GSH on the relative migration distance of Der p 1. Untreated- and DTT-treated proteins were used as controls. The positions of Der p 1 (D) and the GSTpi (G) are indicated by the arrows. C) RFS assay of Der p 1. The protein was incubated with 1 mM GSH for 30 min and then with BODIPY FL N-maleimide. If indicated, Der p 1 was pre-treated with NEM (50 mM) and reduced with 2.5 mM DTT, before the fluorescence labelling. The loaded-protein was analysed with SYPRO staining. Molecular mass marker in kDa are indicated. A representative experiment out of 3 is shown.

GSH increases the catalytic efficiency of Der p 1

Since GSH induced a change on the global folding of Der p 1, catalytic efficiency (K_{cat}/Km) with Boc-QAR-AMC in the presence of either GSH or L-Cys as alternative reducing agents was determined. The kinetic parameters Km and V_{max} were calculated using both Hanes-Woolf and Eadie-Hofstee equations, and the data are presented in Table 19. GSH produced a significant increase on the affinity of the cysteine-protease enzyme for Boc-QAR-AMC in a dose-dependent manner, as indicated by a decrease on the Km values (up to 2.7-folds).

By contrast, the effect of L-Cys on Km was much lower. In addition, GSH increased the V_{max} values of Der p 1 about 4.5-folds, and again the effect of L-Cys was lower (about 2-folds). Thus, resulting in a higher catalytic efficiency of Der p 1 in the presence of GSH. The increment in this kinetic parameter with GSH was overall higher than with L-Cys,

being up to 11-fold and 3-fold for L-Cys, respectively, with 2 mM concentration of the reduction agent.

Table 19. Kinetic parameters for the Der p 1 proteolysis in the presence of GSH or L-Cys.

Reducing agent		GSH (mM)				L-Cys (mM)			
		0.1	**0.5**	**1.0**	**2.0**	**0.1**	**0.5**	**1.0**	**2.0**
Hanes-Woolf	V_{max} (nM/min)	109.6	265.3	387	466.2	726	1233	1495	1421
	Km (μM)	128.9	62.14	59.98	47.45	179.2	116.2	131.4	111.8
	K_{cat}/Km (min^{-1})	$8.5 \cdot 10^{-4}$	$4.3 \cdot 10^{-3}$	$6.5 \cdot 10^{-3}$	$9.8 \cdot 10^{-3}$	$4.1 \cdot 10^{-3}$	$1.1 \cdot 10^{-2}$	$1.1 \cdot 10^{-2}$	$1.3 \cdot 10^{-2}$
Eadie-Hofstee	V_{max} (nM/min)	107.3	272.4	397.2	485.5	625.2	1208	1406	1429
	Km (μM)	124.3	65.44	63.13	51.88	144.9	112.3	119.4	112.5
	K_{cat}/Km (min^{-1})	$8.6 \cdot 10^{-4}$	$4.2 \cdot 10^{-3}$	$6.3 \cdot 10^{-3}$	$9.4 \cdot 10^{-3}$	$4.3 \cdot 10^{-3}$	$1.1 \cdot 10^{-2}$	$1.2 \cdot 10^{-2}$	$1.3 \cdot 10^{-2}$

V_{max}, Km and K_{cat}/Km values were determined using both Hanes-Woolf and Eadie-Hofstee plots.
Different concentrations of fluorogenic substrate Boc-AMC (17.5-150 μM) were used.

Human bronchial epithelial cells secrete GSTpi into the apical medium

To determine whether human bronchial epithelial cells secreted GSTpi, the apical medium from Calu-3 cells cultured at ALI was used for the proteolytic assay of the fluorogenic peptide by Der p 1. The apical medium showed the capacity to increase the proteolytic activity of the cysteine-protease compared to PBS as control (Figure 51A). When the assay was performed in the presence of the specific inhibitor of GSTpi TLK199, the upregulatory effect of the apical medium was partially inhibited, whereas heat-treatment of the medium carried out at 95ºC completely abolished its upregulatory effect.

Moreover, the presence of GSTpi in the apical medium was demonstrated by means of immunoblotting with an anti-human GSTpi antibody (Figure 51B). Our data indicated that GSTpi is one of the components secreted into the medium by cells that could be involved in the upregulation of the cysteine-protease activity of Der p 1.

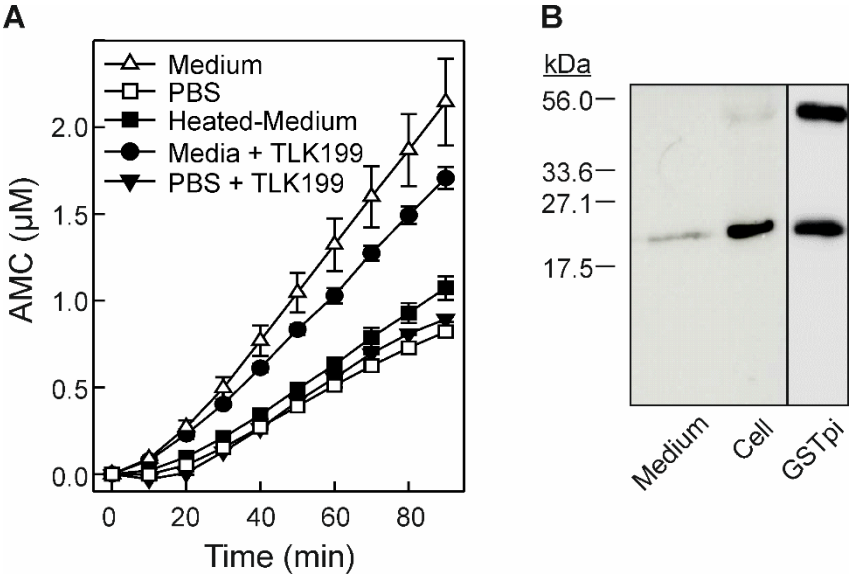

Figure 51. GSTpi is secreted by human bronchial epithelial cells into the apical medium. A) Effect of apical medium secreted by Calu-3 cells on the proteolysis of the fluorogenic peptide by Der p 1. Data are expressed as the µM of 7-amino-4-methylcoumarin (AMC) released by Der p 1, and showed as means ± SD of duplicate measurements. Medium, apical medium added to Der p 1 before reaction with the substrate; PBS, assay performed in the presence of the buffer alone; Heated-medium, medium heated at 95ºC for 5 min before the assay; Medium + TLK199; medium treated with the inhibitor of GSTpi before the assay; PBS + TLK199; PBS treated with the inhibitor before the assay. B) Detection of human GSTpi on apical medium by immunoblotting using an anti-GSTpi pAb. Medium, apical medium from Calu-3 cells cultured at ALI; Cell, Lysate from Calu-3 cells; GSTpi, human GSTpi from placenta as control. Marker of molecular masses in kDa are indicated.

DISCUSSION

Der p 1 from HDM, one of the most clinically relevant indoor aeroallergens worldwide, is a cysteine-protease which catalytic activity has been linked to its allergenicity [10, 14-17, 19]. However, it is unknown whether Der p 1-protease activity could be regulated by host redox microenvironment once it reaches ELF. In this study, we described a novel mechanism by which Der p 1 cysteine-protease activity is upregulated.

Our data showed that GSTpi, but not GSTmu from mite, upregulated the cysteine-protease activity of Der p 1 in a dose-dependent manner, in the presence of either GSH or L-Cys, as reducing agent. This fact suggested that upregulation of Der p 1 protease activity by GSTpi may involve a mechanism different of S-glutathionylation and glutathione transferase activity. In support, several reports have demonstrated that GSTpi acts as a regulator of protein function through its direct interaction with certain proteins [152]. GSTpi binds to NFκB, c-JNK or p53, thus regulating processes of inflammation, apoptosis or cell proliferation [155, 363, 364]. In addition, GSTpi modulates NF-κB activation in lung epithelial cells [151]. Physical interaction of GSTpi with Der p 1 could be further analysed by using different spectroscopic techniques, including fluorescence, raman scattering or surface plasmon resonance.

Moreover, GSH was shown to produce a significant increase on the catalytic efficiency of the Der p 1 for the substrate Boc-QAR-AMC in a dose-dependent manner. Despite of a direct reducing action over the catalytic site, GSH induced a conformational change in the global folding of Der p 1, as indicated by CD, SDS-PAGE and RFS assays, that could be explained in part by the increase observed in the kinetic constants (Km, V_{max} and K_{cat}/Km). Mass spectrometry data supported that GSH could induce a disulphide-bridge rearrangement, accounting for the increase in protease activity of Der p 1 by GSTpi. Cys4 and Cys71 could be involved in this rearrangement, since they are the Cys residues that display the highest number of modifications. A disulphide-bridge rearrangement has been previously described for regulations of enzymes, including GAPDH, protein tyrosine phosphatase α (PTPα), PTP1B, and other papain-like thiol proteases such as cathepsin B and calpain [365-367].

Finally, our data have shown that GSTpi is secreted into the apical medium by human bronchial epithelial Calu-3 cells. Although GSTpi has been widely described as a cytosolic protein, it has been detected in (and purified from) bronchoalveolar lavage fluid of patients with neoplastic and non-neoplastic lung diseases [368]. Moreover, our results suggest that secreted GSTpi might be involved in the upregulation of the cysteine-protease activity of Der p 1, since the upregulation effect of the apical medium was

reduced by TLK199, a specific inhibitor of GSTpi. In this sense, cystatin A and divalent metal ions (i.e., Ca^{2+}, Mg^{2+}) have already been described as regulators of papain and other papain-like proteases activity such as cathepsin B and Der p 1 [367, 369, 370]. Moreover, Herbert *et al*. have shown that the protease activity from several allergenic sources were increased by cell lysates as well by cell-secreted medium [202]. The fact that human GSTpi and GSH are present in the lung epithelial lining fluid supported the proposed mechanism by which cysteine-protease activity of Der p 1 could be upregulated once it reaches airway mucosa, and thus increasing its allergenicity and contributing to the patient sensitization.

In conclusion, human GSTpi was shown to be an elicitor of the cysteine-protease activity of Der p 1, the main allergen from HDM, upon addition of a reducing agent such as GSH or L-Cys. GSH induced a significant increase in the catalytic efficiency of Der p 1. Our results supported that GSH could induce a disulphide-bridge rearrangement, accounting for the increase in the activity of Der p 1 by GSTpi. The potential clinical implication for these findings in allergy is supported by the fact that GSTpi occurs in the apical secretion of human bronchial epithelial Calu-3 cells cultured at ALI. Further studies are needed to determine the contribution of human GSTpi on the allergenicity of Der p 1.

Capítulo III

Estudio del efecto de la co-exposición al humo del tabaco en la respuesta inmune del epitelio bronquial a Ole e 1

Chapter III

Study of the effect of co-exposure to cigarette smoke on the immune response of the bronchial epithelium to Ole e 1

Bronchial epithelium represents the first defence line against inhaled substances including aeroallergens and environmental pollutants. The maintenance of their physiological functions is pivotal for the clearance of airborne substances. It is well documented that exogenous oxidants play a significant role in the impairment of the bronchial epithelium. In this context, CSE, which contains a mixture of more than 7000 toxic and carcinogenic components, is reported to be an important risk factor in the development of lung diseases such as asthma, cancer and COPD. In addition, CSE exposure has been linked to an increased prevalence of allergic diseases, however its contribution in the development and exacerbation of these clinical disorders remains completely understood.

In this chapter **we evaluated the effects of the co-exposure to CSE in the response of human bronchial epithelial cells to Ole e 1 aeroallergen**. Calu-3 cells were exposed to 10% CSE, Ole e 1 or the combination of CSE and Ole e 1 for 24 h, on days 2 and 7 at ALI. Exposure of Calu-3 cells to 10% CSE on day 2 at ALI impaired the integrity of epithelial barrier, as indicated by a decrease on both TEER values and *TJP1* mRNA levels. This effect was not further observed by the presence of Ole e 1. In addition, co-exposure to CSE led to increase the permeability of Calu-3 cells to Ole e 1 on day 2 at ALI, but not on day 7. Moreover, co-exposure to CSE and Ole e 1 significantly increased IL-6 secretion by cells into the apical medium compared to CSE or the aeroallergen alone, being the levels higher on day 2 than on day 7 at ALI. Finally, *IDO-1* mRNA levels were over 2-folds decreased by CSE exposure of ALI-cultured cells, while the presence of the aeroallergen did not significantly increase the effects of CSE alone.

Our results have demonstrated that CSE exposure impaired bronchial epithelial function, probably by downregulation of *TJP1* and *IDO-1* genes. These effects together may increase the individual susceptibility to an aeroallergen, contributing to the development and/or exacerbation of respiratory allergies. These findings highlighted the importance of bronchial epithelial cell state in response to aeroallergens and other environmental substances.

CSE preparation and analytical determination of components by GC-MS/MS

To date, a standard method for CSE has not been established, thus we first aimed to set one by using a continuous smoking protocol. For this purpose, one Marlboro® cigarette was combusted during 5 min and the resultant smoke was bubbled into 15 mL of PBS using a constant flow rate, and then filtered. Marlboro® was chosen because it is a top-selling international brand. The filtered solution was considered as 100% CSE. To normalize CSE, the content of nicotine (3- (1-methyl-2-pyrrolidinyl- (S) -pyridine) in the extract was estimated by recording the absorption at 260 nm in comparison to a commercial standard [240]. The nicotine concentration were similar in the 3 independent extractions tested, ranging from 0.75 to 0.96 mg/cigarette; thus indicating the feasibility of this method to normalize CSE samples. 100% CSE had approximately 0.06 mg/mL (351 μM) nicotine.

In addition, the identification of CSE compounds from the 3 independent preparations were performed by GC-MS/MS. Up to a total of 55 compounds were detected in all CSE preparations (Table 20). Equivalent peak areas of most of the chemical compounds were detected in all CSE preparations. As expected, CSE presented a high number of volatile components with oxidant properties, such as phenol and its derivatives (i.e., 3,4-dimethylpehenol and 4-ethylphenol). Numerous nitrogenous compounds were also detected in CSE samples, including pyridine and its derivatives (i.e., nicotine). Tar derivatives were also detected, including styrene, indoles and pyrazines, as well as numerous polycyclic aromatic hydrocarbons (PAH). Finally, ketones, terpenes and even fatty acids were also detected in CSE preparations, for whose cytotoxic and inflammatory effects have been reported.

Table 20. Tentative composition of the CSE obtained from a Marlboro® cigarette determined by GC-MS/MS.

Compound name	CAS[1]	Formula[1]	RT[2]
Pyridine, 3-methyl	108-99-6	C_6H_7N	4.533
Cyclohexane nitro-	1122-60-7	$C_6H_{11}NO_2$	5.005
Styrene	100-42-5	C_8H_8	6.083
Pyridine, 2-ethyl	100-71-0	C_7H_9N	6.363
Pyrazine, 2,6-dimethyl-	108-50-9	$C_6H_8N_2$	6.595
Pyrazine, 2,5-dimethyl-	123-32-0	$C_6H_8N_2$	6.612
Benzeneacetic acid, 4-amino	1197-55-3	$C_8H_9NO_2$	7.05
3-Octyne	15232-76-5	C_8H_{14}	7.158
Pyridine, 2,3-dimethyl-	533-61-9	C_7H_9N	7.316
2-Furancarboxialdehyde, 5-methyl	620-02-0	$C_6H_6O_2$	7.752
Pyridine, 3-ethenyl-	1121-55-8	C_7H_7N	7.925
Phenol	108-95-2	C_6H_6O	8.457
2-Cyclopenten-1-one, 2,3-dimethyl	1121-05-7	$C_7H_{10}O$	9.606
Indene	95-13-6	C_9H_8	9.841
Phenol, 2-methyl-	95-48-7	C_7H_8O	10.14
Benzoyl bromide	618-32-6	C_6H_5COBr	10.391
Mequinol	150-76-5	$C_7H_8O_2$	10.895
cis-1,4-dimethyl-2-methylenecyclohexane	No Ref.	C_9H_{16}	11.178
Phenol, 2,4-dimethyl-	105-67-9	$C_8H_{10}O$	11.43
Benzene, heptyl-	1078-71-3	$C_{13}H_2O$	11.634
3-Heptyne, 2,2-dimethyl-	29022-29-5	C_9H_{16}	11.904
Phenol, 3-ethyl-	620-17-7	$C_8H_{10}O$	12.175
Phthalan	496-14-0	C_8H_8O	12.634
Phenol, 4-ethyl-	123-079	$C_8H_{10}O$	12.918
Phenol,3,4-dimethyl-	95-65-8	$C_8H_{10}O$	13.15
1,5,5-trimethyl-6-methylene-cyclohexene	514-95-4	$C_{10}H_{16}$	13.32
2-Methoxy-5-methylphenol	1195-09-1	$C_8H_{10}O_2$	13.431
Phenol, 2,4,6-trimethyl-	527-60-6	$C_9H_{12}O$	13.827
3-Cyclopenten-1-one, 2-hydroxy-3-(3-methyl-2-butenyl)-	69745-70-6	$C_{10}H_{14}O_2$	14.095
2-Propenoic acid, 3-(2-hydroxyphenyl)-	614-60-8	$C_9H_8O_3$	14.22
Phenol, 2-ethyl-6-methyl	1687-64-5	$C_9H_{12}O$	14.333
Phenol, 2,3,6-trimethyl-	2416-94-6	$C_9H_{12}O$	14.455
Phenol, 2-ethyl-6-methyl-	1687-64-5	$C_9H_{12}O$	14.58
Phenol-ethyl-4-methyl	3855-26-3	$C_9H_{12}O$	14.703
10,12-Octadecadiynoic acid	7333-25-7	$C_{18}H_{28}O_2$	14.898
3-Carene	13466-78-9	$C_{10}H_{16}$	14.945
Benzenemethanol, 4-(1-methylethyl)-	536-60-7	$C_{10}H_{14}O$	15.007
Phenol, 3-propyl-	621-27-2	$C_9H_{12}O$	15.084
Cyclopental[1,3]cyclopropa[1,2]cyclohepten-3(3ah)-one,1,2,3b,6,7,8-hexahydr..	No Ref.	No Ref.	15.678

[1]CAS, *Chemical Abstract Service* number and a simplified formula are indicated.

[2]RT, Retention time (min).

Table 20. (*continuation*) Tentative composition of the CSE obtained from a Marlboro® cigarette determined by GC-MS/MS.

Compound name	CAS[1]	Formula[1]	RT[2]
Bicyclo[4,1,0]heptane,-3-cyclopropyl,-7-hydroxymethyl,(-E)	No Ref.	$C_{11}H_{18}O$	15.758
Indole	120-72-9	C_8H_7N	15.9
Phenol,3,4,5-trimethyl-	527-54-8	$C_9H_{12}O$	16.066
1H-Inden-1-one,2,3-dihydro-2methyl-	17496-14-9	$C_{10}H10O$	16.175
2-Methoxy-4-vinylphenol	7786-61-0	$C_9H_{10}O_2$	16.273
2,5-Octadecadiynoic acid, methyl ester	57156-91-9	$C_{19}H_{30}O_2$	16.442
2H-Inden-2-one, 1,4,5,6,7,7 a-hexadydro-7a-methyl, (S)-	No Ref.	No Ref.	16.538
2-Methyl-6-propylphenol	3520-52-3	$C_{10}H_{14}O$	16.63
1,2,3-Propanetriol, diacetate	25395-31-7	$C_7H_{12}O_5$	16.943
Pyridine, 3-(1-methyl-2-pyrrolidinyl)-, (S)- (*Nicotine*)	54-11-5	$C_{10}H_{14}N_2$	17.09
Phenol, 2-methoxy-5-(1-propenyl)-,(E)-	19784-98-6	$C_{10}H_{12}O_2$	17.212
1H-Indene,1-ethylideneoctahydro-7a-methyl-, cis-	No Ref.	$C_{12}H_{20}$	17.337
1H-indole, 3-methyl-	83-34-1	C_9H_9N	17.971
1,2,4-Metheno-1H-cyclobuta(cd)pentalene-3,5-diol, octahydro-	No Ref.	$C_{10}H_{12}O_2$	18.097
Phenol, 2-methoxy-4-(1-propenyl)-	97-54-1	$C_{10}H_{12}O_2$	19.275
syn-Tricyclo[5,1,0(2,4)]oct-5-ene,3,3,5,6,8,8-hexamethyl-	No Ref.	No Ref.	21.918

[1]CAS, *Chemical Abstract Service* number and a simplified formula are indicated.

[2]RT, Retention time (min).

CSE impairs bronchial epithelial barrier integrity

First, Calu-3 cells were treated with different doses of CSE (0-25%) for 24 h and 48 h, on days 2 and 7 at ALI, and TEER was monitored (Figure 52). CSE caused a decrease in TEER values in a dose-dependent manner, either at 24 h or 48 h of treatment. This effect was more pronounced on day 2 at ALI, which corresponded to an undifferentiated state of bronchial epithelial barrier.

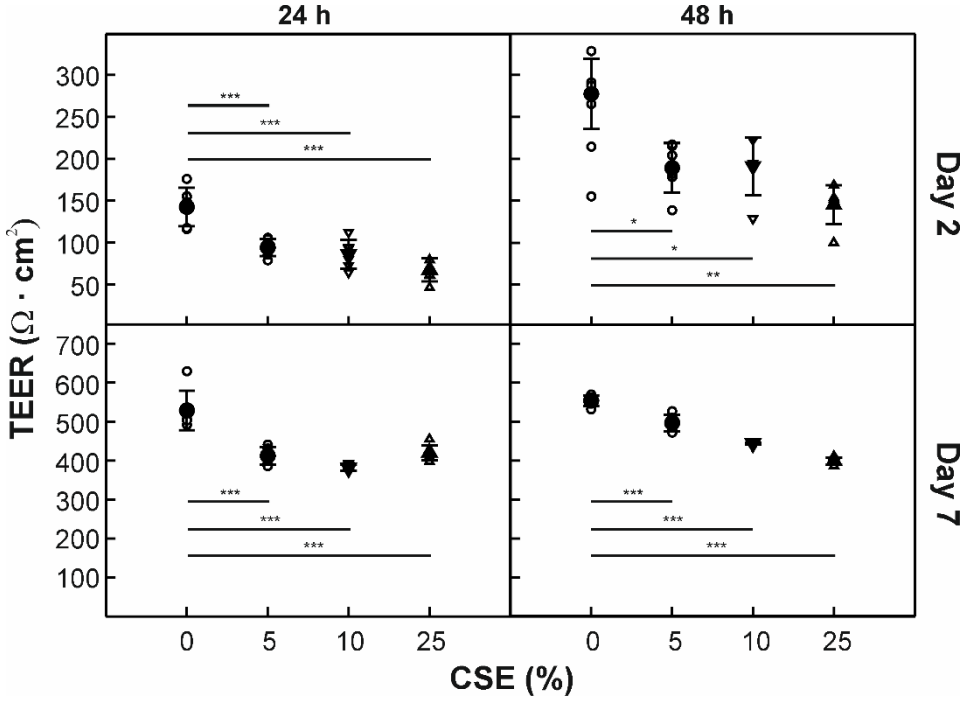

Figure 52. Effect of CSE on the TEER of Calu-3 cells on days 2 and 7 at ALI. TEER values represents the mean ± SD of triplicate determinations from a representative experiment out of two. Significant differences are indicated by: *p < 0.05, **p < 0.01, *** p < 0.001. White symbol, individual value; and black symbol, mean value.

To get an additional insight into the effect of CSE exposure on epithelial barrier integrity, the localization and expression of E-cadherin and ZO-1 -which play critical roles in the establishment of the AJ and TJ, respectively- were analysed. ALI-cultured Calu-3 cells were exposed to 10% CSE for 48 h and the expression of E-cadherin and ZO-1 proteins analysed by CSLM, on days 2 and 7 at ALI (Figure 53). CSE exposure did not alter significantly the expression pattern of E-cadherin and ZO-1 over Calu-3 differentiation compared to untreated cells.

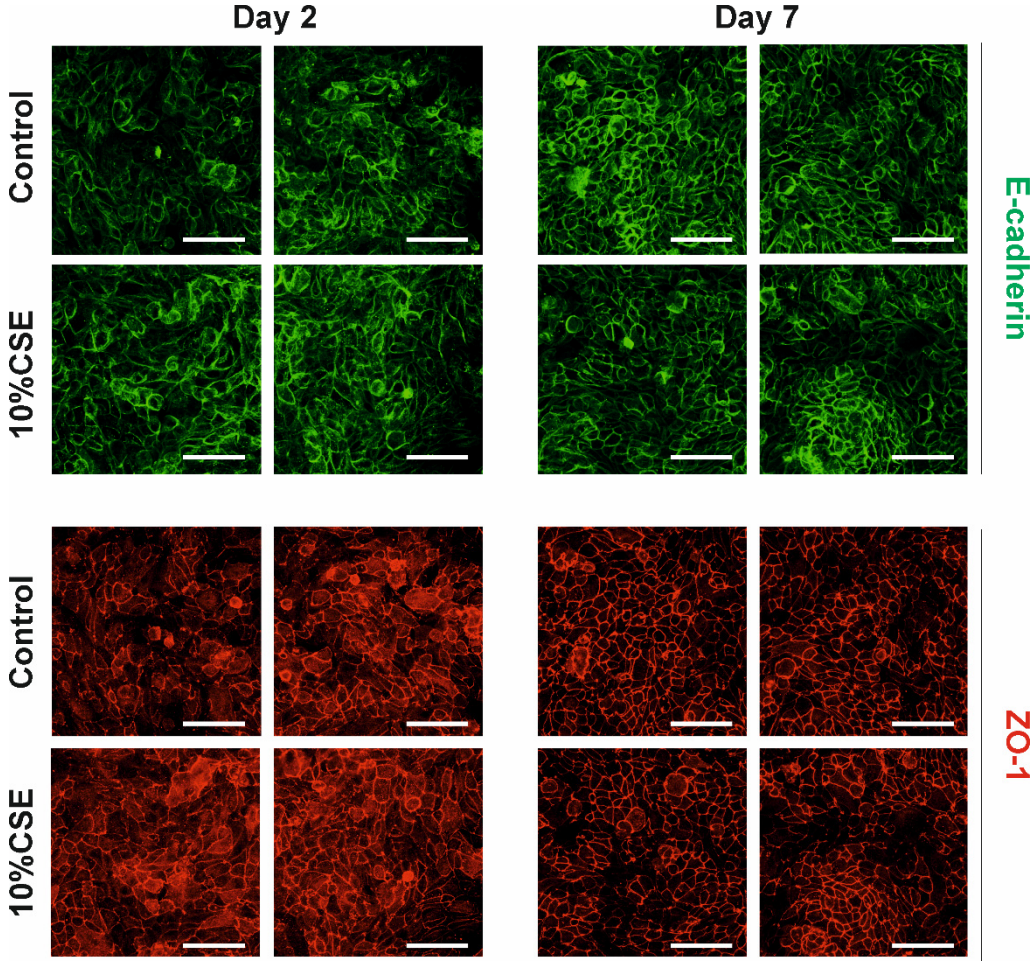

Figure 53. Effect of 10% CSE on apical junctional complex structures in Calu-3 cells on ALI culture (for days 2 and 7). CLSM analysis for E-cadherin (green) and ZO-1 (red) proteins. Representative Z-stacks are shown. Scale bar = 25 µm.

In contrast, *TJP1* mRNA levels determined by RT-PCR, using *GAPDH* as housekeeping control, were decreased on day 2 at ALI, compared to control cells, suggesting a post-transcriptional regulation of this TJ protein in response to CSE (Figure 54). In contrast, the *CDH1* mRNA levels did not change after 48 h of CSE exposure. Furthermore, no effect on mRNA levels of the AJC proteins were observed on day 7 at ALI. Taken together, these results suggested that the bronchial epithelial integrity was impaired by CSE exposure via down-regulation of *TJP1* mRNA.

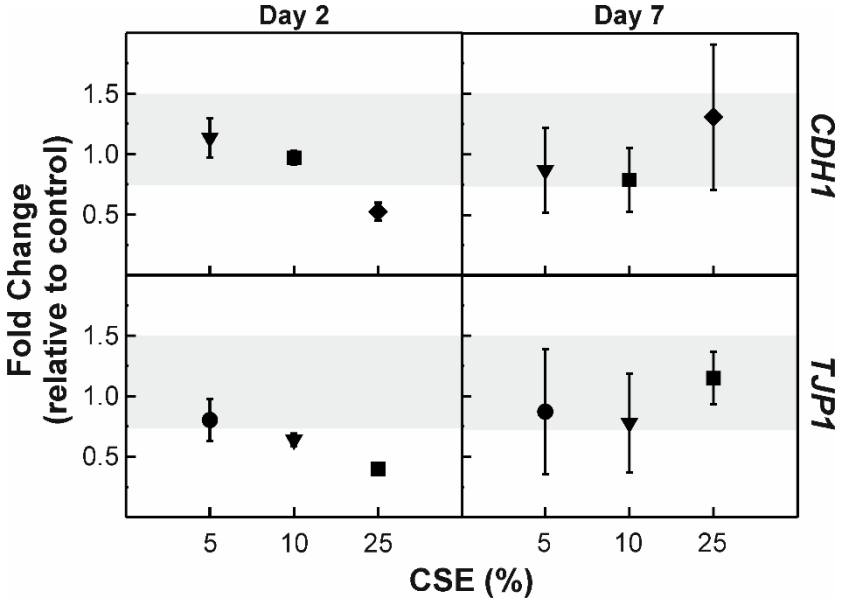

Figure 54. Effect of CSE (0-25%) on *CDH1* and *TJP1* gene expression of bronchial epithelial cells. Following treatment with CSE (0-25%) on days 2 and 7 at ALI, gene expression was analysed by RT-PCR. Relative mRNA expression of a gene is expressed as a fold-change of control values defined as 1, after normalizing to *GADPH*. Fold-changes ≤0.65 and ≥1.5 were considered significant (shaded area). Data represents the mean ± SD of 2 replicates. Genes: *CDH1*, cadherin 1; *TJP1,* tight junction protein 1.

CSE affects the cell viability of Calu-3 cells in a dose- and time-dependent manner

To clarify whether the impairment on bronchial epithelial barrier integrity is caused by a cytotoxic action of CSE, we analysed the effect of CSE on Calu-3 cell viability by using MTT assay. Cells were exposed to CSE (0-50%) for 24 h or 48 h, and as shown in Figure 55, CSE reduced cell viability in a dose- and time-dependence manner. After 24 h, the highest concentration of CSE (50%, equivalent to a theoretical nicotine concentration of 0.03 mg/mL) resulted in a marked reduction (over 40%) of cell viability, being even more pronounced after 48 h of treatment (about 70%). Cells exposed to 10% CSE showed a viability higher than 80% for both 24 h and 48 h of treatment. Therefore, a 48 h exposure with 10% CSE was selected to be used in the subsequent co-exposure studies.

pH values of PBS containing CSE were measured to exclude the possibility that the cytotoxicity was caused by a pH change in culture medium following addition of CSE. The pH values ranged from 7.2 to 7.5, indicating that addition of CSE to culture medium had no effect on its pH value.

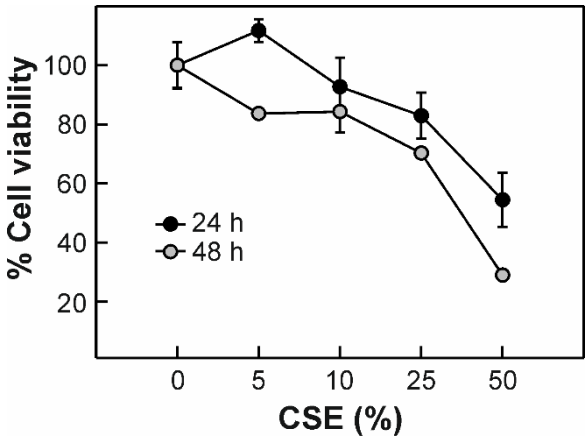

Figure 55. Effect of CSE on the viability of Calu-3 cells after 24 h and 48 h of exposure. Cell viability was determined by using MTT assay. Data are expressed as a percentage of the viability of untreated cell and are means ± SD from four replicates from a representative experiment out of 3.

CSE does not affect the structural and immunological properties of Ole e 1

To determine whether oxidant molecules containing on CSE altered the structure and immunological properties of the aeroallergen, Ole e 1 was incubated with different concentrations of CSE and the effect on the secondary structure was analysed by obtaining its far-UV CD spectra (Figure 56A). Neither 10% nor 50% CSE treatment altered significantly the secondary structure of Ole e 1. The secondary structure contribution calculated for Ole e 1 showed 17.2 ± 1.7% for α-helix, 32.4 ± 0.7% for β-strand, 17.0 ± 0.9% for β-turn and 33.3 ± 0.1% for random coil, in accordance to previously data published for this aeroallergen [175].

Moreover, the effect of CSE treatment on IgG binding of Ole e 1 was analysed by inhibition ELISA using a specific anti-Ole e 1 (Figure 56B). None of the CSE-treatments affected the Ole e 1-specific IgG-binding ability in comparison with the untreated protein. Similarly, no significant differences were observed on IgE reactivity of Ole e 1 after CSE-treatment as determined by inhibition ELISA using sera from 2 allergic patients with specific IgE to this aeroallergen (Figure 56B).

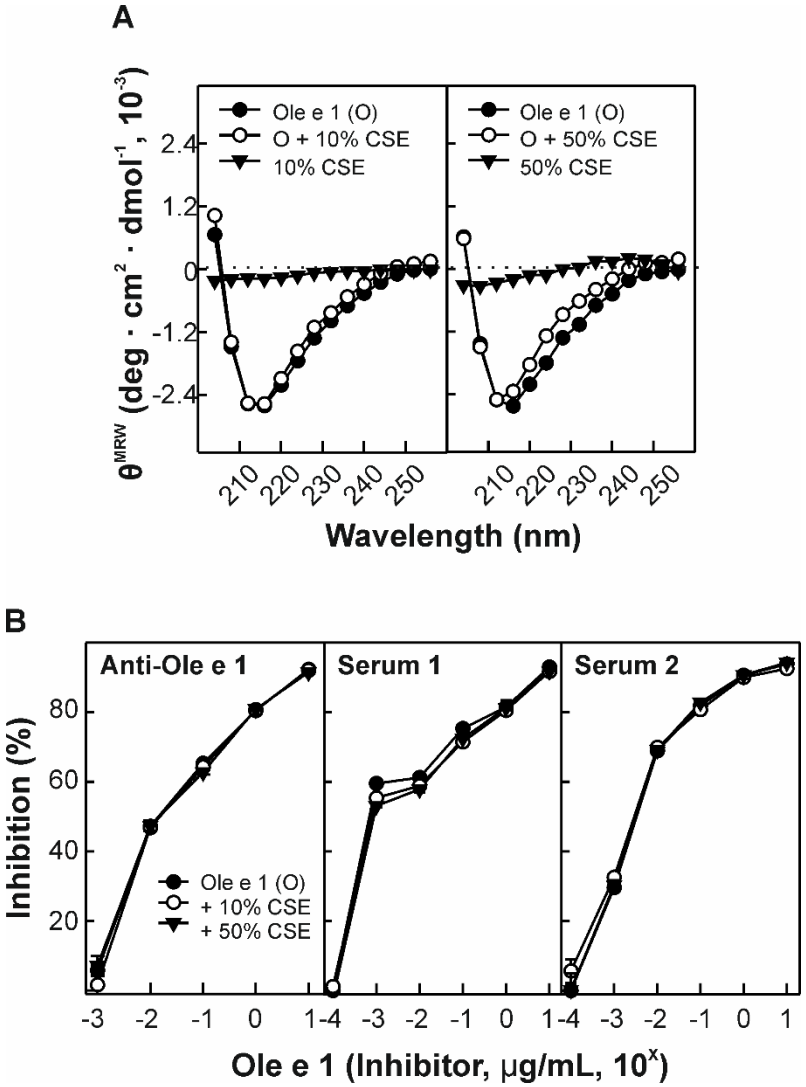

Figure 56. Effect of CSE exposure on the structure and immunological properties of Ole e 1. A) Far-UV CD spectra of Ole e 1 in absence or presence of CSE (10% and 50%). CSE contribution to the CD spectra is shown. B) IgG- and IgE-binding capacity of Ole e 1 after CSE exposure analysed by inhibition ELISA using a specific pAb and 2 individual patients' sera, respectively. Data are shown as percentage (%) of inhibition and are means ± SD of duplicate determinations.

Effect of co-exposure to CSE on the bronchial epithelial permeability to Ole e 1

To determine the effect of co-exposure to CSE on the permeability of bronchial epithelium to Ole e 1, ALI-cultured Calu-3 cells were exposed to 10% CSE for 24 h, on days 2 and 7, and then co-exposed to Ole e 1 for another 24 h. Changes in TEER values were then determined (Figure 57). As shown before, under the presence of 10% CSE, TEER values decreased after 48 h exposure both on days 2 and 7 at ALI. This effect was similar to those exposed to a combination of Ole e 1 and CSE. In contrast, exposure

to Ole e 1 alone did not result in significant changes on TEER values, compared to control cells.

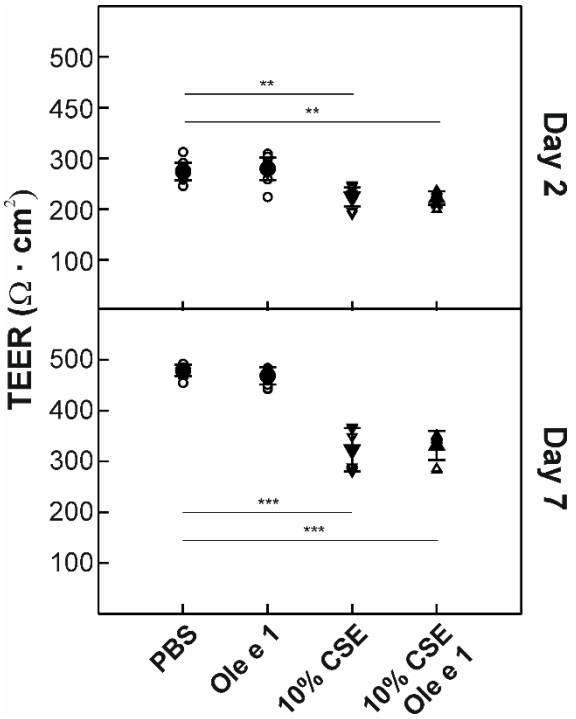

Figure 57. TEER values of Calu-3 cells exposure to Ole e 1 in presence of 10% CSE for 48 h, in comparison to non-treated cells (PBS), at the indicated days during differentiation at ALI. Data are the mean ± SD of triplicate determinations. Significant differences are indicated by: **, $p < 0.01$; ***, $p < 0.001$.

Figure 58 shows the results of Ole e 1 detection in culture media by Western blot, using a specific pAb. On day 2 at ALI, the aeroallergen was detected on the basolateral medium after 1 h of culture and Ole e 1 levels were increased over the time of incubation. Interestingly, CSE exposure significantly increased Ole e 1 levels in the basolateral medium, reaching values 4-fold higher after 24 h of exposure. Surprisingly, and despite of the decrease in TEER values, no additional effect of CSE exposure on the cell permeability of Calu-3 cells to Ole e 1 was observed on day 7 at ALI. Thus, our results supported that co-exposure to CSE led to an increase in the permeability to Ole e 1 aeroallergen dependent on the bronchial epithelium state.

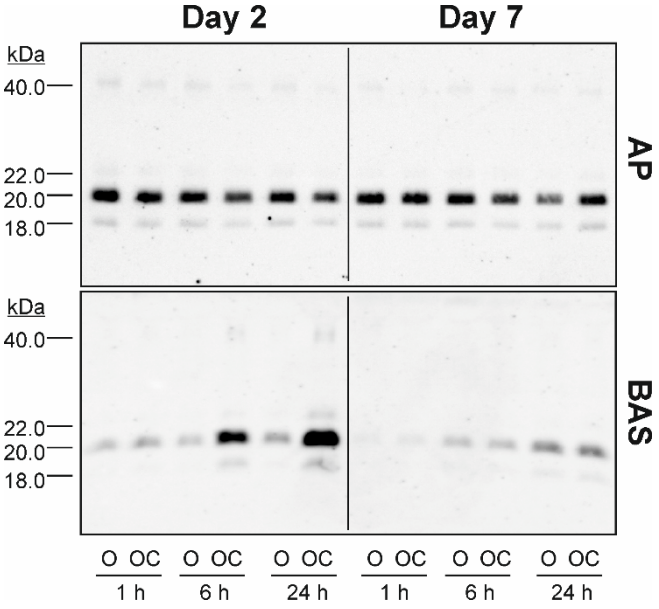

Figure 58. Effect of co-exposure to CSE on the bronchial epithelial permeability to Ole e 1. Following treatment with CSE, ALI-cultured Calu-3 cells were co-exposed to 10% CSE and Ole e 1 on days 2 and 7, and the presence of the aeroallergen was determined in medium at different time points (1 h, 6 h and 24 h). AP, apical medium; BAS, basolateral medium; O, exposure to Ole e 1; and OC, exposure to Ole e 1 in combination with CSE. Molecular masses of Ole e 1 forms in kDa are indicated.

CSE increases the secretion of IL-6 by bronchial epithelial cells induced by co-exposure to Ole e 1

The secretion of the pro-inflammatory cytokine IL-6 by Calu-3 cells was analysed in both the apical and the basolateral media, on days 2 and 7 at ALI (Figure 59). Cells secreted IL-6 spontaneously into both apical and the basolateral media, being the levels significantly higher on day 2 in comparison to day 7 at ALI, and into the apical medium respect to the basolateral medium. Spontaneous IL-6 secretion by cells into both media were significantly increased after exposure to 10% CSE, on day 2 at ALI. No effect on IL-6 production was observed after aeroallergen exposure. The co-exposure to CSE and Ole e 1 significantly increased IL-6 secretion by cells into the apical medium compared to either CSE or Ole e 1 alone, on day 2 at ALI. Whereas neither Ole e 1 nor CSE significantly modified the production of IL-6 by cells on day 7 at ALI, again co-exposure to both significantly elevated IL-6 secretion into the apical medium, but not to the basolateral.

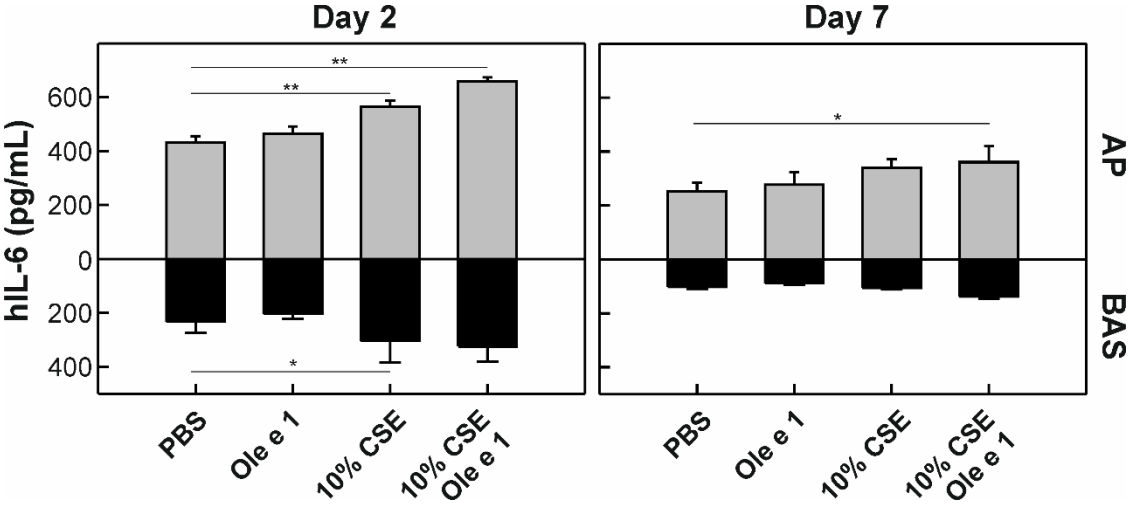

Figure 59. Effect of the co-exposure to Ole e 1 and CSE on the secretion of human IL-6 (hIL-6) by bronchial epithelial cells. Following treatment with CSE, ALI-cultured Calu-3 cells were co-exposure to 10% CSE and Ole e 1 on days 2 and 7, and the levels of IL-6 in medium analysed by sandwich ELISA. AP, apical medium; BAS, basolateral medium; PBS, untreated cells. Data are the mean ± SD of duplicate determinations. Significant differences are indicated by: *, $p < 0.05$; **, $p < 0.01$.

Effect of co-exposure to CSE and Ole e 1 on the gene expression of bronchial epithelial cells

Finally, we analysed the expression of different genes by ALI-cultured Calu-3 cells after co-exposure to 10% CSE and Ole e 1 on days 2 and 7, using RT-PCR: *CDH1*, *GSTP1* *IDO-1*, *JUN*, *NFKB*, *NRF2*, *TJP1* and *XOR* (Figure 60). As reported before, 10% CSE exposure decreased *TJP1* mRNA expression levels by Calu-3 cells on day 2 at ALI, but not those of *CDH1* mRNA. The co-exposure to CSE and Ole e 1 did not induce a greater decrease on *TJP1* mRNA levels. Similarly, *IDO-1* mRNA levels were decreased by CSE exposure (over 2-folds), while the aeroallergen did not significantly alter the effects of CSE alone. No changes were observed on mRNA levels of the transcription factors *JUN, NFKB* and *NRF2*, by the exposure to CSE or Ole e 1 alone, or the combination. In addition, no effects were detected on the mRNA levels of *XOR* and *GSTP1* by either CSE or Ole e 1 alone, or the combination of them. *IDO-1* enzyme mRNA was the only mRNA modified by CSE exposure for 48 h on day 7 at ALI. Our data showed a decreased in *IDO-1* mRNA levels (over 2-folds) compared to control cells, which were not further modified by the co-exposure to Ole e 1.

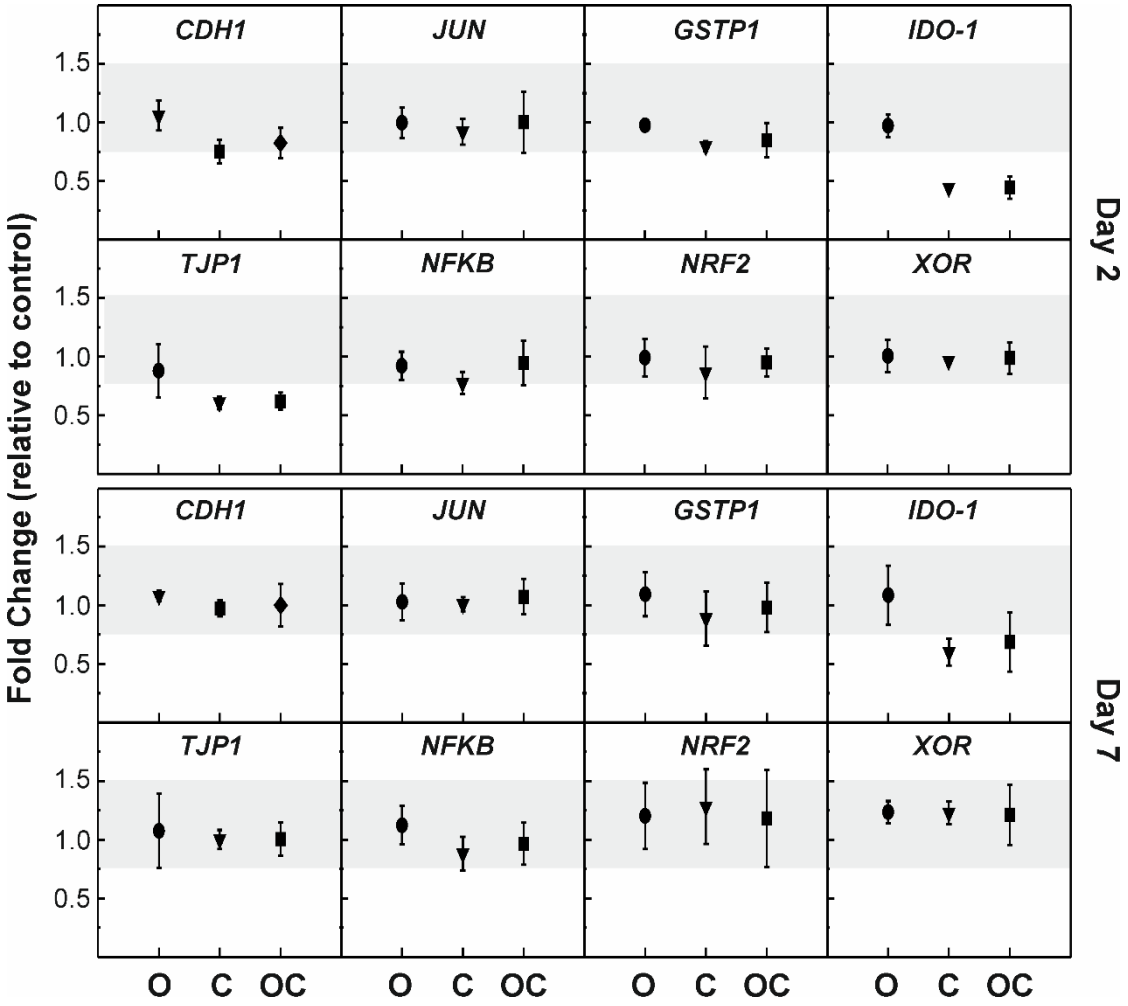

Figure 60. Effect of the co-exposure to Ole e 1 and CSE on gene expression of bronchial epithelial cells. Following treatment with CSE, ALI-cultured Calu-3 cells were co-exposed to 10% CSE and Ole e 1 on days 2 and 7, and gene expression analysed by RT-PCR. Relative mRNA expression of a gene is expressed as a fold-change of control values defined as 1, after normalizing to GADPH. Fold-changes ≤ 0.65 and ≥ 1.5 were considered significant (shaded area). Data represents the mean ± SD of 2 independent experiments. O, cells exposed to Ole e 1; C, cells exposed to 10% CSE; and OC, cells exposed to Ole e 1 in combination with 10% CSE. Genes: *CDH1*, cadherin 1; *GSTP1*, glutathione S-transferase pi 1; *IDO-1*, indoleamine-pyrrole 2,3-dioxygenase-1; *JUN, Jun proto-oncogene; NFKB,* nuclear factor kappa B subunit*; NRF2,* nuclear factor (erythroid 2)-like 2*; TJP1,* tight junction protein 1; *XOR*, xanthine oxidoreductase.

DISCUSSION

CSE, one of the most clinically relevant pollutant, contains a complex mixture of over 7000 components, some of them with toxic and carcinogenic confirmed effects. Moreover, CSE exposure has been largely associated with an increased prevalence and exacerbation of allergic diseases. In this study, we analysed the contribution of CSE exposure to the response of bronchial Calu-3 cells to the Ole e 1 aeroallergen.

Although CSE is widely used in cell culture research, its inherent complexity makes quite difficult to work with, being criticised because of an absence of both CSE standardization and normalization protocols. In this study, we have standardized a method for CSE preparation following a continuous smoking protocol described by Higashi *et al.* [239], with some modifications. CSE was prepared by bubbling into PBS the smoke of one cigarette combusted during 5 min. CSE was normalized in terms nicotine concentration determined by UV-absorption at 260 nm [240]. The alkaloid nicotine is an abundant constituent of CSE, which besides to its strong relation to addiction also contributes to the damage of airway induced by CSE [371-373]. Among CSE preparations, nicotine concentrations were not significantly different from each other. Indeed, Higashi *et al.* [239] used tar concentrations to normalize CSE preparations, and they found that it can be used irrespective of the number of combusted cigarettes, cigarette brands and the protocol. We provided a list of 55 volatile components by using GS-MS/MS, including: phenol and its derivatives (i.e., 3,4-dimethylpehenol and 4-ethylphenol); pyridine and its derivatives (i.e., nicotine); and tar derivatives (styrene, indoles, pyrazines, and PAH). Some of them are reported in the revised Hoffman's list, which include 98 hazardous components of CSE [218]. The list of CSE compounds includes carcinogens derived from tar combustion (nitrosamines and PAH), toxic substances that may trigger inflammation (metals, aromatic ketones, polyphenols, terpenes) and even proteins, such as the immunogenic p-glycoprotein [218, 374-376]. Most of them have been reported to affect lung epithelial cell responses, involving both innate and adaptive immune defences [227]. However, many components of CSE were not detected in the analysed sample such as acrolein, the most abundant volatile thiol-reactive component. Acrolein, together with nicotine, are largely responsible for strong cytotoxic effects of CSE [372]. In this sense, acrolein and nicotine concentrations in ELF of smokers are around 80 μM and 30 μM, respectively [377, 378]. This nicotine concentration is comparable to the 31.5 μM nicotine dose (10% CSE) used in this study.

We showed that the permeability of ALI-cultured Calu-3 cells to Ole e 1 increased progressively with the time and was markedly enhanced by exposure to 10% CSE.

Moreover, the analysis of the permeability to Ole e 1 showed that CSE-specific effect on aeroallergen-passage is dependent on epithelium state, since no effect was observed on day 7 at ALI. These findings support that co-exposure to CSE significantly increase the permeability of Calu-3 cells to Ole e 1 in an epithelium state-dependent manner. These results are in agreement with those reported by Rusznak *et al.* [379], who showed that passage of Der p 1 aeroallergen was increased by the exposure of primary human bronchial epithelial cell cultures to CSE in a dose- and time-dependent manner. In addition, we found that exposure to CSE alone impaired epithelial barrier integrity, as indicated by a decrease of TEER and *TJP1* gene expression. This effect was not augmented when cells were further exposed to the aeroallergen. It is likely that the decrease on TJ protein expression of Calu-3 cells by CSE could increase the passage of Ole e 1 through the cell barrier, thus potentially facilitating aeroallergen sensitization in susceptible individuals. In this sense, it has been described that CSE induced dose- and time-dependent TJ (ZO-1) disassembly, via EGFR-ERK1/2 signalling pathway [380, 381]. These effects seem to be mediated by the lipophilic compounds of CSE such as aldehydes, PAH or polyphenols, which can easily cross the plasma membrane [382]. Recently Gerloff *et al.* [383] reported that nicotine and some flavouring agents compromised the integrity of TJ both dose and time dependently, with impaired of epithelial barrier function. Moreover, other TJ proteins can be affected such as occludins and claudins. CSE-induced tyrosine phosphorylation of occludins impaired barrier integrity of Calu-3 cells [384, 385]. Jiménez *et al.* [386] demonstrated that CSE exposure induced downregulation of claudin-6 expression in AEC-II. We did not observe a significant effect on the localization of AJC proteins after CSE exposure of Calu-3 cells, entailing a molecular mechanism that may require a chronic exposure to CSE as reported with other epithelial models. In this sense, chronic exposure to CSE caused alterations in actin cytoskeleton and thereby in the correct establishment of AJC in lung epithelial cells [387, 388].

Following CSE exposure, it was observed an increase in the secretion of the pro-inflammatory IL-6 by ALI-cultured Calu-3 cells mainly into the apical medium on days 2 and 7 of culture, which was further enhanced by the exposure of the cultures to Ole e 1. IL-6 secretion by Calu-3 cells was higher on day 2 at ALI than those achieved on day 7, which supports the hypothesis that the bronchial epithelial response to an aeroallergen is dependent of the epithelium state. IL-6 production is mainly controlled by the oxidative stress-sensitive transcription factors NFκB and AP-1 [389, 390]. In our study, we found that CSE exposure did not alter neither *NFKB* nor *AP-1 (JUN)* mRNA levels in Calu-3 cells. In this sense, there are some contradictory data about the effect of CSE on NFκB

in the airways. Manzel *et al.* [391] reported that CSE exposure inhibited NFκB signalling pathway and the consequent expression of genes that are involved in airway defence to *H. influenza*, using both human tracheo-bronchial epithelial cells and mouse models. This inhibitory effect of CSE was suppressed by antioxidants. Moreover, the immunosuppressive effect of nicotine is mediated by *NFKB* repression [373]. In contrast, styrene induced ROS-mediated NFκB activation in human airway epithelial cells [392]. It is shown that CSE effect on NFκB is strictly dependent on the cell line, CSE doses, exposure time and cigarette brand [391, 393-396]. On the other hand, IL-6 secretion can be controlled by alternative signalling pathway. Thus, CSE exposure increases the release of IL-6 in BEAS-2B cells through phospholipase D1 activation via the PKC/p38MAPK signalling pathway [397]. Further studies are required to determine the signalling pathway involved in the secretion of IL-6 by ALI-cultured Calu-3 cells.

CSE exposure induces the release of a set of pro-inflammatory mediators that promote the recruitment and/or activation of immune cells such as DCs, macrophages, neutrophils, among others, thus contributing to ROS generation and reinforced epithelial damage. In this sense, CSE exposure promotes the secretion of IL-8 [219, 398, 399], IL-1β [221], IL-33 [400], MCP-1 [222], and TSLP and GM-CSF [223, 401] by human bronchial epithelial cells. Overall, CSE exposure may generate a local airway environment, which is increasingly recognized as an important contributor to respiratory allergy.

Exposure of ALI-cultured cells to 10% CSE did not alter the mRNA levels of the transcription factor Nrf2, which regulates the synthesis of several lung antioxidant enzymes, such as those involved in GSH metabolism, such as GSTpi [120, 144]. In contrast, some studies have reported that Nrf2 is inhibited by CSE oxidants [402, 403]. Moreover, CSE oxidation altered the modulatory properties of both KEAP1 and DJ-1, an inhibitor and a stabilizer of Nrf2, respectively [404]. Once again, these contradictory results could be explained in terms of exposure conditions and CSE preparation (cigarette number, cigarette brand, combustion condition, etc.). Overall, our data supported the hypothesis proposed by Schamberger *et al*. that the response of bronchial epithelial cells to CSE is affected by the epithelium state [405].

CSE exposure induced a significantly decrease in the *IDO-1* mRNA levels of ALI-cultured Calu-3 cells on both 2 and 7 days of culture, regardless of the presence of Ole e 1 aeroallergen. In agreement, Pertovaara *et al.* [406] reported that IDO-1 is downregulated in DCs from smokers in comparison to non-smokers. In addition, it has been shown that NO –one of the CSE components- is a potent inhibitor of IDO-1 [337, 407]. NO levels are

enhanced in patients with asthma [408]. Several studies have shown that the Kyn pathway (involving IDO-1 enzyme) plays a critical role in allergic diseases [334]. IDO-1 catabolizes L-Trp degradation, leading to the accumulation of L-Trp metabolites, which exhibit immunomodulatory properties [409]. Moreover, patients with pollinosis exhibit low IDO-1 activity [338, 342].

Finally, in our study, cytotoxicity is unlikely to have a major contribution to the CSE effects on ALI-cultured Calu-3 cells, since the viability of cells following exposure to 10% dose is over 80%. In agreement with this data, Schamberger *et al.* demonstrated that epithelial barrier integrity was impaired due to TJ disassembly following exposure to a non-toxic dose of CSE [405]. Apart from its cytotoxicity, dose- and time- dependence on CSE effects have been described by several authors on cytokine secretion, transcription factor modulation, gene expression and epithelial barrier damage [380, 410-414].

During the last decades increasing evidences have supported the crucial role of ROS and free radical on the CSE cytotoxicity [372, 415, 416]. Thus, nicotine was shown to induce apoptosis and senescence in bronchial epithelial cells via ROS-mediated autophagy-impairment [371]. Moreover, sesaminol protects against the induction of apoptosis by CSE via ROS-dependent mechanism [416]. Also, PAH induce apoptosis via p53-dependent mitochondrial pathway [417, 418]. In addition, others products derived from cigarette combustion such as metals (i.e., iron) can contribute to the generation of radicals following interaction with ELF, thus perpetuating epithelial cell damage [419].

In conclusion, our data demonstrate that 10% CSE exposure impaired bronchial epithelial function, probably by downregulation of *TJP1* and *IDO-1* genes. A better knowledge of how cigarette smoke impairs the host immune response to an aeroallergen will require future studies. As a further consequence, it is likely that these effects may increase the individual susceptibility to an aeroallergen, contributing to the development and/or exacerbation of respiratory allergies. These findings highlight the importance of the airway epithelial cell state in response to aeroallergens and other environmental substances.

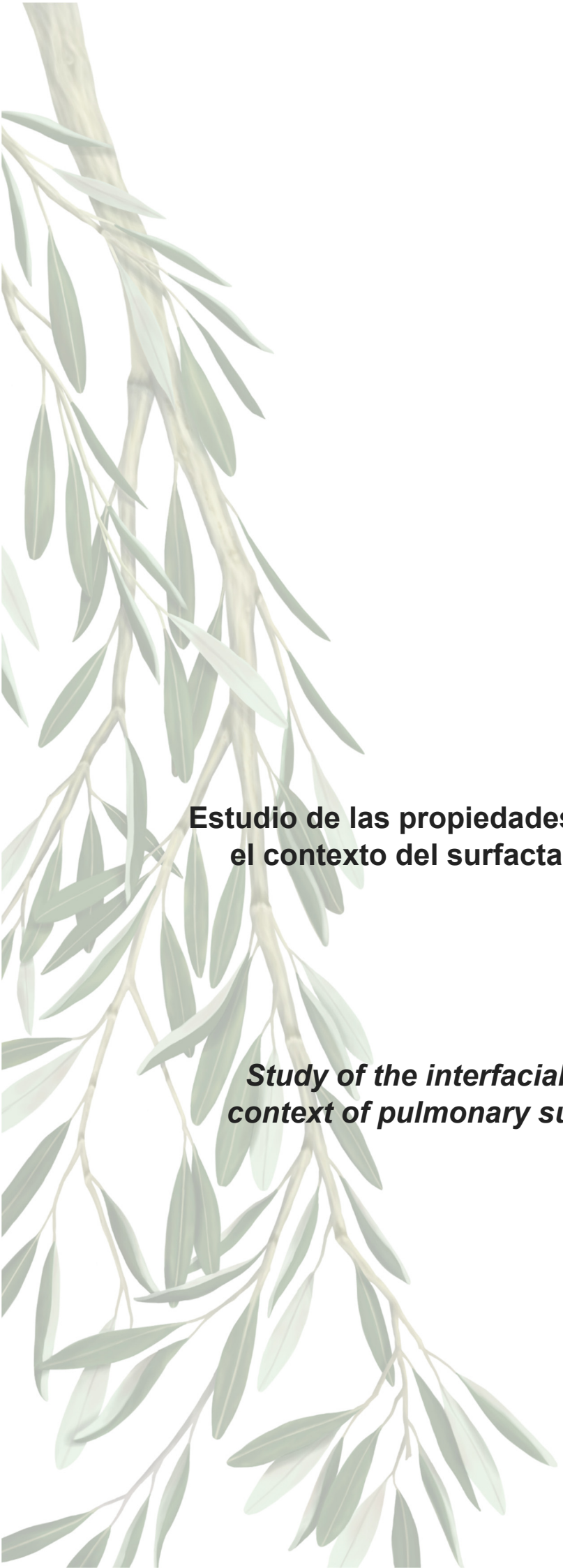

Capítulo IV

Estudio de las propiedades interfaciales de Ole e 1 en el contexto del surfactante pulmonar y modelos de membranas celulares

Chapter IV

Study of the interfacial properties of Ole e 1 in the context of pulmonary surfactant and models of cell membranes

Aeroallergens are airborne substances –mainly proteins- capable of triggering Th2-immune responses in respiratory allergies. They enter into the body through the upper airways, then reaching the mucosae afterwards. Mucosae lining at the luminal side consists of an epithelial barrier completely covered by mucus and pulmonary surfactant. Both, pulmonary surfactant and plasma membrane of the epithelial cells represent two physiological phospholipid-based barriers where aeroallergens first impact before triggering their biological effects. The interaction of aeroallergens with lipids at relevant physiological surfaces could promote structural changes on the molecule, resulting on a potential modification of its allergenic properties.

In this chapter, we have firstly described the surface and phospholipid interaction capabilities of the clinically relevant aeroallergen Ole e 1 by using Langmuir devices. Langmuir-derived methods allow to evaluate efficiently the surface activity of proteins and protein-lipid interactions by indirect measurements of surface tension. Epifluorescence microscopy of Langmuir transferred films allowed us to observe that lipid-packed ordered domains may function as a preferential location for aeroallergen to accumulate at the ALI, an effect that is abolished in the presence of cholestenone. The possible implications of phospholipid-interfacial effects in the modification of aeroallergen structural and functional properties will be discussed.

Characterization of Ole e 1 allergen adsorption at ALI

Ole e 1 adsorbs at ALI, forming a stable protein film as monitored by the increase in surface pressure (Figure 61). Its interfacial adsorption is highly dependent on protein concentration, fitting to a rectangular hyperbola as defined by equation (a):

$$(a) \qquad \Pi = \frac{\Pi_{max} \cdot C}{K + C}$$

where Π is the surface pressure value achieved at time = 20 min for each concentration, C is the aeroallergen concentration (μM), Π_{max} depicts the theoretical maximum value of surface pressure that would be achieved at very high protein concentrations and K represents a constant value for the protein concentration that yields half of the Π_{max} value.

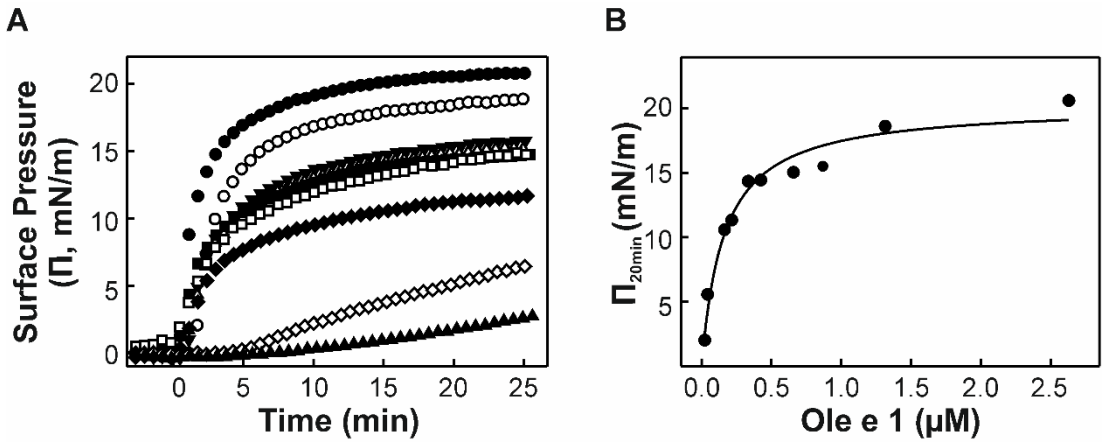

Figure 61. Interfacial adsorption kinetics of Ole e 1. A) Π-t isotherms (25 ± 1ºC) of different amounts of Ole e 1 injected at time = 0 (minutes) in a subphase composed of Tris 5 mM, pH 7, 150 mM NaCl. Protein concentration in the subphase was 2.78 (●), 1.36 (○), 0.89 (▼), 0.68 (Δ), 0.42 (■), 0.37 (□), 0.21 (♦), 0.16 (◊), 0.05 (▲) μM. B) Maximum surface pressure achieved at 20 min after injection (Π_{20min}, mN/m) *versus* Ole e 1 (μM). Solid line shows the hyperbolic trend that best fits protein interfacial behaviour (r^2 = 0.97).

The values obtained after data fitting were K = 0.16 ± 0.03 μM and Π_{max} = 20.3 ± 0.9 mN/m, with an R-squared correlation value of 0.97. For the following experiments, an aeroallergen concentration of 0.55 μM was fixed, because it allowed us to detect an acceptable protein interfacial activity, while avoiding the complete saturation of the liquid surface. Gibbs adsorption equations (b and c) were also used to calculate the protein surface excess concentration (Γ) and surface molecular area (A), respectively.

$$(b) \qquad \Delta\Pi = LnC \cdot R \cdot T \cdot \Gamma$$

$$(c) \qquad A = 1/(\Gamma_{max} \cdot N)$$

where ΔΠ is the maximum increment in surface pressure reached for each protein concentration, R is the gas constant (8.314 J/K/mol), T is the temperature of the assay (298 K), A is the surface molecular area ($Å^2$), Γ_{max} is the surface excess concentration at saturation and N is Avogadro's constant number ($6.022 \cdot 10^{23}$ mol^{-1}). Data obtained for Ole e 1 interfacial activity was $\Gamma_{max} = 6.94 \pm 0.31 \cdot 10^{20}$ residues/m^2 and A = 0.144 ± 0.01 $Å^2$/residue.

Interaction of Ole e 1 with POPC:SM:CHO (2:1:1) and DPPC lipid surfaces

Next, the interfacial adsorption of Ole e 1 to interfaces that have been previously occupied by DPPC or POPC:SM:CHO (2:1:1, molar ratio) spread monolayers was monitored at different initial pressures (Π_i). These mixtures were chosen due to the different nature of the lipid packaging structures that they produce in the interphase. DPPC is a saturated lipid that organizes in liquid-condensed (LC) phases above its phase transition pressure; on the other hand, the POPC:SM:CHO mixture produces segregation of immiscible liquid-ordered (Lo) and liquid-disordered (Ld) regions because of the presence of cholesterol, even at low surface pressures [420]. Figure 62 shows that Ole e 1 injection into the aqueous subphase causes an increase in surface pressure in films made of both type of films, which never exceeded the maximum pressure value reached for the protein, 20 mN/m.

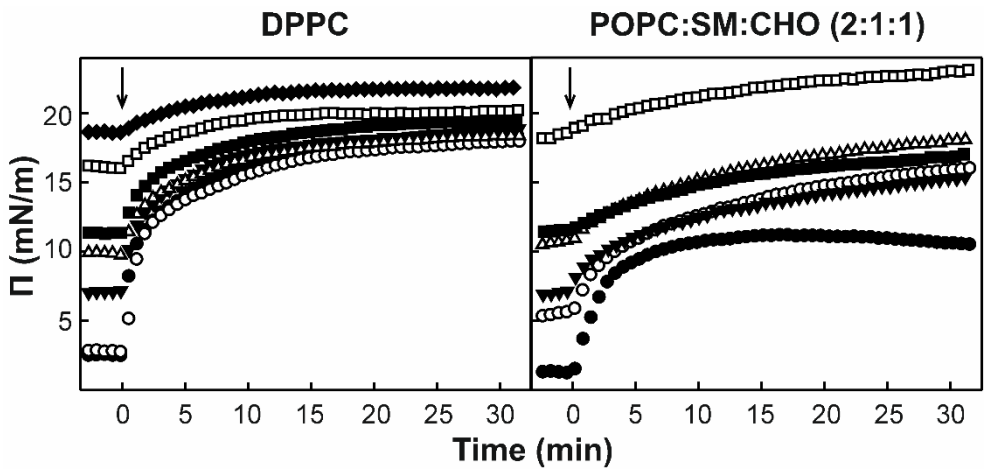

Figure 62. Insertion/adsorption kinetics of Ole e 1 into preformed phospholipid monolayers. Insertion/adsorption kinetics of Ole e 1 in DPPC (left) or POPC:SM:CHO (2:1:1 molar ratio, right) monolayers preformed at different initial surface pressures (symbol lines). Arrows indicate aeroallergen injection (0.55 μM) into the subphase. All the assays were carried out at 25 ± 1 ºC. The subphase was composed of Tris 5 mM, pH 7, 150 mM NaCl.

Kinetics plots showed that the protein exhibits a similar behaviour on both films compressed to pressures higher than 10 mN/m, but not for films preformed at low pressures. The protein was unable to cause a pressure change higher than 10 mN/m

when injected underneath POPC:SM:CHO monolayers, while it reached much higher values of surface pressure on DPPC experiments.

We estimated the critical pressure of insertion (Π_c) by plotting the pressure changes caused by the aeroallergen as a function of initial pressure values (Figure 63). This value represents the theoretical maximum initial pressure that allows the insertion of the protein within preformed monolayers. The Π_c values calculated for Ole e 1 insertion in both types of monolayers was the same, 21.0 ± 0.5 mN/m, according to the maximum adsorption values. A linear trend was obtained for the insertion of the aeroallergen into layers of both lipid mixtures compressed to most surface pressures. However, as noticed above, the insertion of the protein into POPC:SM:CHO films exhibits an inflection point at pressures below 5 mN/m, suggesting a potential reorientation of Ole e 1 upon interaction with compositional or structural motifs generated within this monolayer at those lower surface pressures.

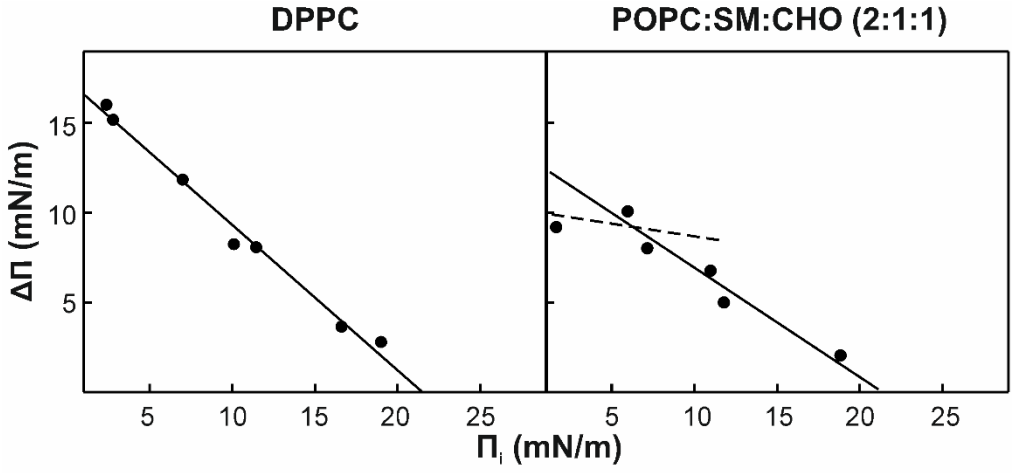

Figure 63. Critical insertion pressure of Ole e 1 into phospholipid monolayers. Increase in surface pressure (ΔΠ) versus initial pressure (Π_i) of DPPC or POPC:SM:CHO (2:1:1, molar ratio) preformed lipid monolayers upon injection of Ole e 1 at 25 ± 1 ºC. The subphase and Ole e 1 solution (0.55 µM) was composed of Tris 5 mM, pH 7, 150 mM NaCl. In the left plot, the line represents the linear regression that best fits the experimental data ($r^2 \rangle 0.97$). Each plot shows 1 out of 2 independent experiments. The intersection with the horizontal axis allows estimation of the critical insertion pressure (Π_c) in each of the films. The right panel shows the trends observed when the aeroallergen was injected under POPC:SM:CHO films at low (dashed) and high (solid line) pressure regimes.

Organization of lipid and lipid/Ole e 1 films: compression isotherms and epifluorescence analysis

The interaction of Ole e 1 protein with lipid monolayers at ALI and its effect on lipid packing are analysed in Figures 64 and 65. Figure 64A shows the Π-A isotherm of a POPC:SM:CHO (2:1:1) film in the absence (Control) and in the presence of 15 or 30 μg of Ole e 1. Protein injection (30 μg) expanded the isotherm up to 20 $Å^2$/molecule, which indicates that Ole e 1 molecules are able to insert into the monolayer to occupy an area of the interface, by themselves or upon interaction with the surrounding lipids. All the films, including the ones containing protein, collapse at pressures around 50 mN/m without a clear indication of partial squeeze-out plateaus, indicating that Ole e 1 is able to remain associated with the interface under lateral compression at pressures much higher than its Π_c.

Epifluorescence images of POPC:SM:CHO films transferred at different pressures during compression are illustrated in the Figure 64B. For all the epifluorescence experiments 15 μg of Alexa488-labeled Ole e 1 (green fluorescent dots) were used. This amount of protein was judged to be optimal in order to obtain defined and high-resolution images showing the aeroallergen effect and its localization within the lipid film. To reveal the occurrence of lateral phase separation in the chosen lipid system, Rho-PE -a fluorescent lipid probe preferentially partitioning into “Ld” phases- was added to the organic lipid solution (red). Compression of POPC:SM:CHO films up to 7 mN/m generated dark regions, likely corresponding to “Lo” domains enriched in SM and CHO but depleted in Rho-PE probe. These condensed areas were less numerous, and they had diffuse edges in lipid/protein films compared to the morphology of domains in protein-free control films. Protein was observed to mainly co-localize within these dark areas, suggesting a relative affinity of the protein for these ordered structures. At pressures higher than 7 mN/m, these dark areas seemed to disappear, at least at the microscopic scale observable by epifluorescence, and the protein reordered as large green clusters, coexisting with the remaining lipids at the interface until its apparent complete exclusion at pressures higher than 23 mN/m. These observations supported the change of the trend in protein insertion detected at low initial pressures in the adsorption experiments towards POPC:SM:CHO films.

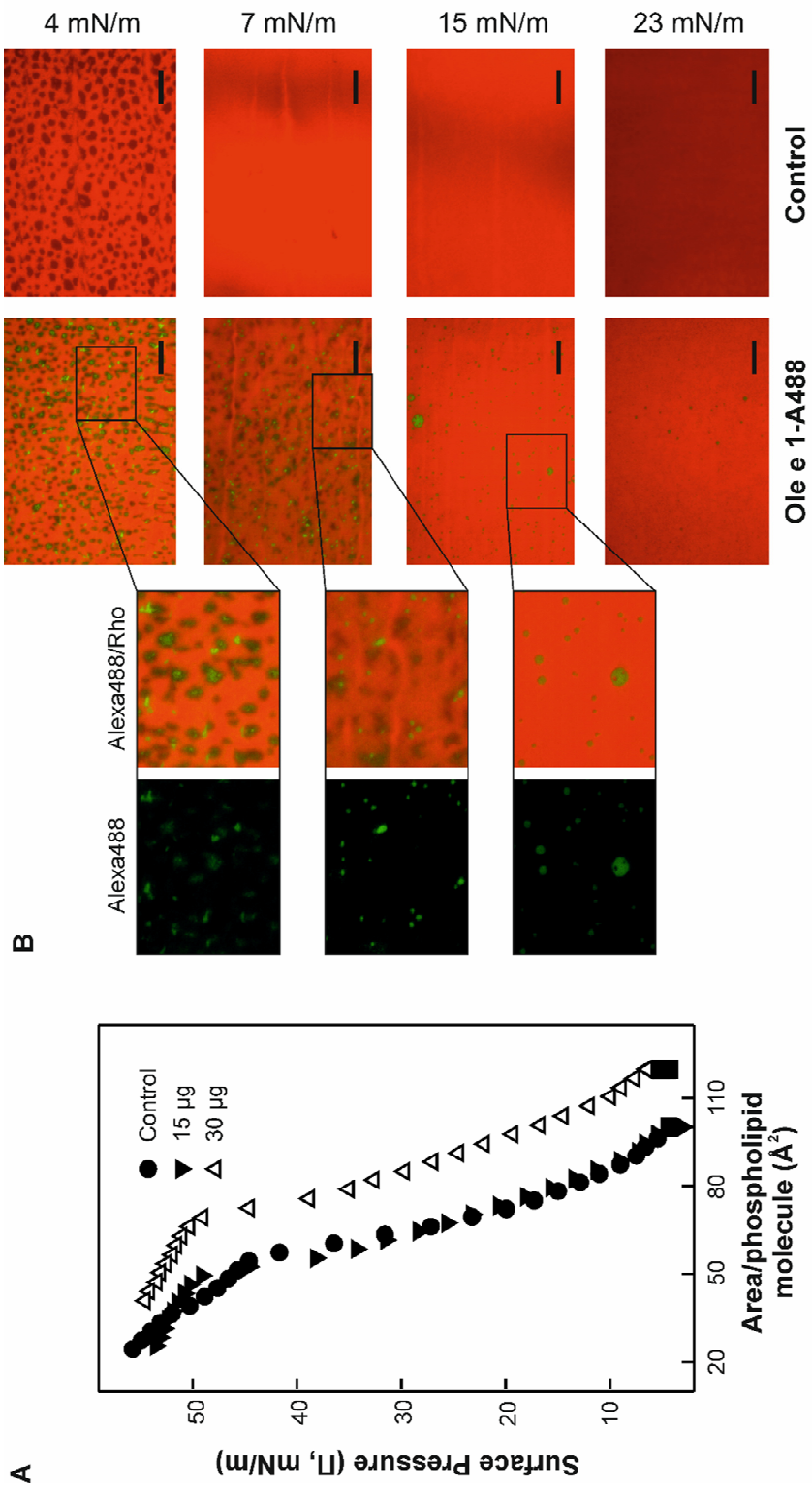

Figure 64. Interaction of Ole e 1 with POPC:SM:CHO (2:1:1, molar ratio) films. A) Π-A compression isotherms obtained upon injection of different protein amounts (µg) and B) effects on the organization of POPC:SM:CHO monolayers in the absence (Control) or in the presence of Ole e 1-Alexa488 (green spots). B) Epifluorescence images taken from transferred films compressed to the indicated pressures. The films contained Rho-PE (red) to allow for observation of the phospholipid distribution at the interface at 25 ± 1ºC. Images with Ole e 1-Alexa488 represent the merge of both channels where a magnification (x3) of the details is represented (left, Alexa488 channel; right, Alexa488 and Rho channel). Scale bar at the bottom of all the pictures represents 25 µm. Figure shows representative images taken from 1 out of 3 independent experiments.

As stated before, the effect of Ole e 1 in DPPC isotherms relied on an expansion of 20 $Å^2$/molecule to larger areas, suggesting the interfacial occupation of the protein (Figure 65A). This effect was more pronounced when injecting 30 µg in the subphase than upon injection of 15 µg of protein. The presence of the protein at the DPPC interface caused a delay in the onset of the liquid-expanded (LE) to LC transition plateau, without apparently causing its alteration or disappearance. Control and lipid/protein curves converged at a surface pressure around 50 mN/m, suggesting that at this pressure, the protein was totally excluded from the interface and lipids remained in a highly condensed state. Epifluorescence analysis showed that the interaction of the protein with DPPC films was very different than observed in POPC:SM:CHO experiments (Figure 65B). At surface pressures below the LE-LC transition plateau (< 10 mN/m), the protein appeared as numerous and homogenously distributed clusters, evenly coexisting with the LE lipid phase. At pressures above 10 mN/m dark LC domains that exclude the Rhodamine-PE probe emerge, as it was previously observed by Perez-Gil *et al*. [421] These presumably condensed lipid domains were slightly more numerous and smaller in the presence of the protein, which tends to be located at the boundaries as green aggregates. At the highest pressures tested, rosette-shaped domains occupied almost the entire interface and the protein appeared as smaller aggregates at their edges. Even at these pressures with the aeroallergen almost excluded, Ole e 1 caused a slight alteration in the shape of the lipid domains, generating greater number of pits and more abrupt edges with respect to the domains nucleated in protein-free control films.

Finally, the interaction of Ole e 1 with other lipid systems was tested by using lipid mixtures in which one of the POPC:SM:CHO components were depleted: SM:CHO (2:1), and POPC:CHO (2:1). As an additional reference we tested a system, POPC:SM:CNE (2:1:1, molar ratio), in which CHO was substituted by CNE, an sterol that inhibits the formation of “Lo” domains [422]. Figure 66A shows the determination of both the maximum change in surface pressure ($\Delta\Pi_{max}$) and the critical pressure value (Π_c) for these additional mixtures. The values of $\Delta\Pi_{max}$ were very similar in these systems, being the highest the one obtained for SM:CHO (12.7 mN/m), followed by the insertion in POPC:SM:CNE (11.3 mN/m) and that in POPC:CHO (10.3 mN/m). POPC:CHO achieved the highest value of Π_c (22.1 mN/m), not far followed by POPC:SM:CNE (19.8 mN/m) and SM:CHO (18.1 mN/m) films.

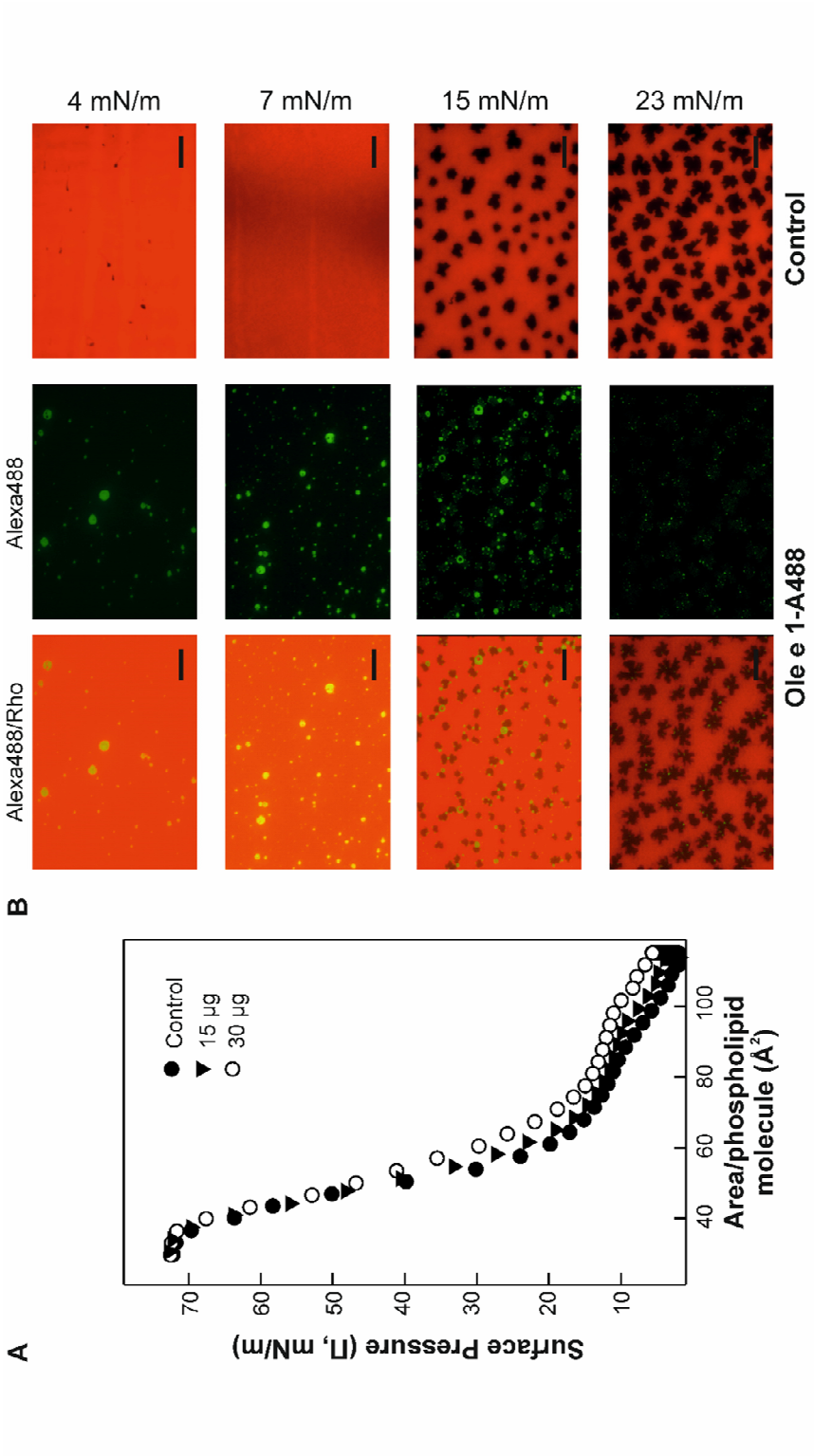

Figure 65. Interaction of Ole e 1 with DPPC films. Π-A compression isotherms obtained upon injection of different protein amounts (µg) A) and effects on the organization of DPPC monolayers B) in the absence (Control) or in the presence of Ole e 1-Alexa488 (green spots). B) Epifluorescence images were taken from transferred films compressed to the indicated pressures. The films contained Rho-PE (red) to allow for observation of the phospholipid distribution at the interface at 25 ± 1 ºC. Images from films containing the aeroallergen compare fluorescence from the protein (dark, right) and on the left, the merge of both, lipid (red) and protein (green), channels. Scale bar at the bottom of each picture represents 25 µm. Figure shows representative images taken from 1 out of 3 independent experiments.

Epifluorescence images illustrated in Figure 66B supported interfacial adsorption results. At 4 mN/m, only POPC:CHO films exhibited segregation of dark regions corresponding to cholesterol-enriched “Lo” domains. However, the fluorescent-labelled protein seemed not to be located in these domains and its presence therein was much less conspicuous than observed in POPC:SM:CHO films.

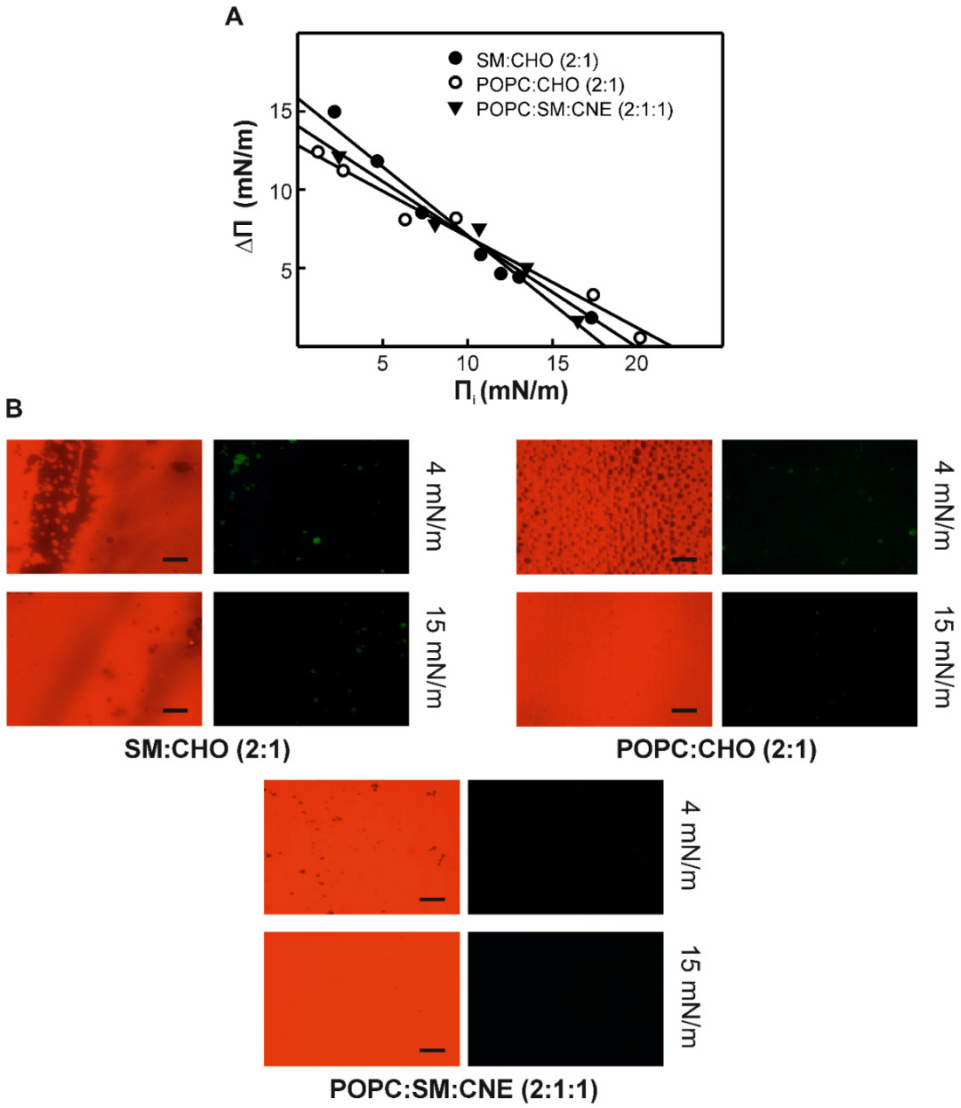

Figure 66. Interaction of Ole e 1 with SM:CHO (2:1), POPC:CHO (2:1) and POPC:SPM:CNE (2:1:1) films. A) Increase in surface pressure (ΔΠ) versus initial pressure (Π_i) of SM:CHO (2:1), POPC:CHO (2:1) and POPC:SM:CNE (2:1:1) preformed lipid monolayers upon injection of Ole e 1 at 25 ± 1ºC. The subphase and Ole e 1 solution (0.55 µM) was composed of Tris 5 mM, pH 7, 150 mM NaCl. Lines represent the linear regression that best fits the experimental data ($r^2 > 0.97$) for each of the lipid systems. Figure shows representative data of 1 out of 2 independent experiments. B) Epifluorescence images of transferred films compressed to the indicated pressures. The films contained Rho-PE (red, 1% mol/mol) to allow for observation of the phospholipid distribution at the interface at 25 ± 1 ºC. 15 µg of Ole e 1 labelled with Alexa-Fluor488 (green) were used in all the cases. Left picture of each condition represents the merge of both channels. Scale bar at the bottom of each picture represents 25 µm. Figure shows representative images taken from 1 out of 3 independent experiments.

Noteworthy, cholestenone (CNE) fully prevented the presence of liquid-ordered domains, and that was associated with a clearly lower interfacial presence of Ole e 1. At high pressures (15 mN/m), the protein appeared again as green clusters, coexisting with lipid films characterized by having a total absence of ordered regions, at least at a microscopic length-scale. In general terms, values, trends and images obtained for these partially-depleted systems seemed to be very different from to those obtained for POPC:SM:CHO films, suggesting a crucial requirement of the three components -POPC, SM and CHO- to define maximal affinity in the interaction between Ole e 1 and lipid domains.

Ole e 1 inhibits the interfacial adsorption of pulmonary surfactant

Adsorption assays were carried out to analyse the effect of the interfacial activity of Ole e 1 on the biophysical properties of the native surfactant from swine. For this purpose, fluorescence emission measurements were performed with the presence of the fluorescence quencher, *Brilliant Black* (Figure 67).

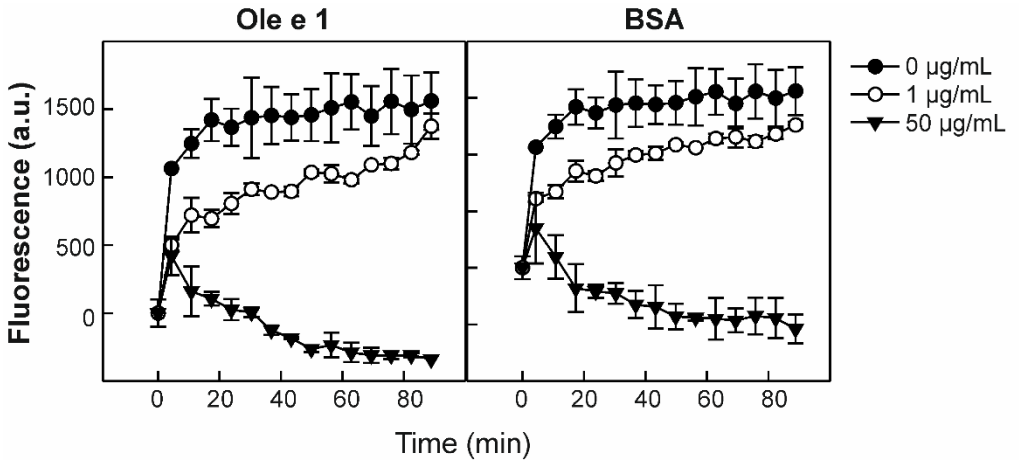

Figure 67. Effect of Ole e 1 aeroallergen on the interfacial adsorption kinetics of surfactant compared to bovine serum albumin (BSA). Data are expressed as fluorescence intensity in arbitrary units (a.u.) and represent the mean ± SD of 1 out of 2 independent experiments.

Surfactant displayed a rapid adsorption to the interface, as indicated by the *plateau* reached few minutes after injection. Ole e 1 inhibited the interfacial adsorption of surfactant in a dose-dependent manner as compared to BSA. At the highest concentration (50 µg/mL), Ole e 1 completely inhibited the adsorption of surfactant, suggesting an effective occupation of the interface by the aeroallergen, which forms a stable film that prevents the adsorption of the surfactant. These results strongly supported the interfacial activity observed for Ole e 1.

DISCUSSION

In this chapter we have demonstrated that, underneath air-aqueous interfaces, Ole e 1 aeroallergen showed an interfacial adsorption capability comparable to those of technologically important surface-active proteins such as BSA, lysozyme, β-lactoglobulin or β-casein in the same conditions [423-427].

Ole e 1 aeroallergen is an N-glycosylated protein, showing a high-content (40%) in aperiodic conformation determined by CD [175]. Moreover, predictive analysis of Ole e 1 showed that it is a highly flexible and hydrophobic protein [175]. All these properties support the high surface activity here demonstrated for Ole e 1 at the interface. This is in agreement with the features of other proteins reported to adsorb to air-water interfaces, such as β-casein where a combination of a flexible non-globular structure and a hydrophilic and charged N-terminal region governs the interfacial adsorption [428]. In this sense, Ole e 1 polar regions may keep the exposure to the liquid subphase while hydrophobic ones may be transferred to the airspace, potentially promoting aeroallergen diffusion from the bulk solution towards the interface.

Interfacial activity is associated to conformational changes of the protein, which might induce process of oligomerization and aggregation, as it has been previously shown for β-lactoglobulin [429], latherin [430], BSA, fibrinogen and IgG [431]. In this sense, protein allergenicity is highly influenced by structural rearrangements, such as oligomerization and aggregation, as it has been reported for the major birch pollen allergen, Bet v 1 [432]. Ole e 1 is a protein with a high tendency to form oligomers, which exhibit higher allergenicity [175]. Thus, the relation between Ole e 1 allergenicity and the potential conformational changes induced upon its interfacial adsorption could be critical once the aeroallergen enters the respiratory tract and impacts its wet surface. Potential structural rearrangement of Ole e 1 during its interaction with lipid films could be further explored by using a combination of techniques such as Raman and FTIR spectroscopy.

Considering the marked interfacial activity revealed by Ole e 1 aeroallergen, we proceeded to describe its behaviour in a lipid film context by using Langmuir-Wilhelmy and Blodgett monolayers. Two physiologically relevant lipid mixtures were used as a model: POPC:SM:CHO (2:1:1, molar ratio), a mixture previously described as potentially mimicking segregation of raft-like domains thought to exist in cellular membranes [433-435] and DPPC, which constitutes the most abundant and surface-active component in pulmonary surfactant.

Ole e 1 adsorption/insertion plot described a linear tendency with DPPC films, achieving a Π_c value (21 mN/m) comparable to those obtained for the rest of lipid systems assessed. Although this Π_c value did not exceed the threshold of surface pressure value of 30 mN/m, which is commonly considered as indicative of the potential ability of a protein to insert into lipid bilayers [436], the Π-A isotherm exhibited an expansion of 20 $Å^2$/molecule that was sustained up to 50 mN/m after Ole e 1 injection into the subphase, confirming aeroallergen coexistence within the lipid film. Epifluorescence images of DPPC Langmuir films at surface pressures higher than 15 mN/m showed LC or bean-shaped domains of DPPC, where the fluorescent-labelled aeroallergen was localized as protein clusters where the lipids seem to be excluded. This observation suggests that lipid domains can act as nucleation sites for the aeroallergen, in which new non-covalent interactions could be established between neighbouring molecules, due to the interfacial exposition of hydrophobic residues that are normally hidden in the protein structure [437].

The coexistence of protein and DPPC at the interface suggests the existence of several mechanisms that could take place *in vivo* during the first stages of allergen sensitization. On the one hand, Ole e 1 adsorption could impair or abolish the normal surface activity of pulmonary surfactant, which is crucial particularly during expiration. This surfactant inhibition process could be explained because of a steric competition, as it has been previously reported for the surface-active plasma proteins BSA or haemoglobin [438-440]. On the other hand, surfactant interfacial spreading properties has been recently proposed as a promising tool for transporting several drugs along the airways and into the body [441, 442]. In this context, it is conceivable that pulmonary surfactant could act as a potential carrier or shuttle for a wide variety of airborne compounds and aeroallergens, including Ole e 1, as our results are pointing out. Ole e 1 diffusion along the entire conducting airways (from bronchial to alveolar region) might contribute to the development of allergic responses.

The examination of the ΔΠ versus Π_i plot for POPC:SM:CHO (2:1:1) revealed a biphasic trend not observed in the linear tendency obtained with DPPC films (Figure 63), suggesting a different mode of lipid-protein interaction with those monolayers at low surface pressures. It could be confirmed afterwards by epifluorescence analysis, whose fluorescent images (Figure 64B) showed the existence of “Lo” lipid domains (dark areas) at pressures lower than 7 mN/m, where fluorescent-labelled Ole e 1 (green dots) is mainly localized. At pressures higher than 7 mN/m, lateral segregation completely disappeared, and the aeroallergen appeared as homogenously distributed clusters. The absence of “Lo” domains at the interface seemed to correspond to the linear behaviour obtained at the highest pressures of films made of POPC:SM:CHO, DPPC or other lipid

mixtures in which the generation of cholesterol-rich domains was prevented (SM:CHO or POPC:SM:CNE). In addition, the presence of all lipid components in the POPC:SM:CHO mixture seems to be required for Ole e 1-domain interaction (Figure 66), as it is shown with the presence of ordered domains of different nature (POPC:CHO).

In spite of Ole e 1 showed critical interfacial insertion pressures not exceeding 30 mN/m, the aeroallergen was able to remain in the interface under high lateral compression states. Taken together, these results could indicate a mechanism of interaction of Ole e 1 with “Lo” domains of the epithelial cell membrane at the time of contact. Thus, it has been reported that other allergens interact with structures localized in “Lo” domains involved in signalling pathways related to the immune response such as Th2-type inflammation. In this sense, Bet v 1 co-localizes with caveolar markers [443], and house dust mite group-2 allergens interact with the Toll-like receptor 4 (TLR4) [444].

In summary, our study has demonstrated the interfacial adsorption capabilities of the aeroallergen Ole e 1. Moreover, Ole e 1 displayed a particular behaviour on lipid layers generated at ALI, which show lateral phase separation. The aeroallergen tended to localize associated with liquid-condensed and ordered domains. Collectively, these results support the concept that the interfacial activity of certain allergens -such as Ole e 1- is related to their association with surface lipid films, accumulating preferentially in the coexisting lipid phases. Thus, aeroallergen clustering at surface could be a key feature to define their stable presence at the epithelial barrier, triggering the allergic response.

Conclusiones

Conclusions

CAPÍTULO I. *Estudio de la influencia del estado de diferenciación del epitelio bronquial en la respuesta inmune a Ole e 1*

CHAPTER I. *Study of the influence of the state of differentiation of the bronchial epithelium on the immune response to Ole e 1*

I. Se ha establecido y caracterizado un modelo *in vitro* de epitelio bronquial humano basado en cultivos primarios de células epiteliales bronquiales humanas (NHBE) crecidas en ALI. Este modelo se ha utilizado para analizar la influencia del estado de diferenciación -días 7 y 21 en ALI- del epitelio bronquial en la respuesta inmune a Ole e 1.

It has been established and characterized an in vitro model of human bronchial epithelium based on primary cultures of human bronchial epithelial cells (NHBE) cultured at ALI. This model has been used to analyse the influence of the bronchial epithelial state of differentiation - days 7 and 21 on ALI- on the immune response to Ole e 1.

II. Las medidas de TEER y los estudios ultraestructurales han demostrado que la exposición a Ole e 1 no afecta a la formación de la barrera epitelial *in vitro*.

TEER measurements and ultrastructural studies have shown that Ole e 1 does not affect to the in vitro establishment of the epithelial barrier.

III. Se ha demostrado que la exposición a Ole e 1 no alteraba la formación de los AJC durante la diferenciación de las células NHBE, según los análisis mediante *Western blot* y CLSM. Esta exposición tampoco alteraba significativamente la diferenciación de las células NHBE, como indica el análisis mediante PCR semicuantitativa de los niveles de expresión de marcadores específicos de las distintas poblaciones celulares: CC-10 (células Club), FOXJ1 (ciliadas), MUC5AC (mucosas), NKX2.1 (progenitoras), y P63 (basales).

It has been shown that Ole e 1 exposure did not alter the AJC formation during NHBE cell differentiation, according to Western blot and CLSM analyses. This exposure did not significantly alter the differentiation of NHBE cells, as assessed by the semiquantitative PCR analysis of the expression levels of specific markers of the different cell populations: CC-10 (Club cells), FOXJ1 (ciliated cells), MUC5AC (globet cells), NKX2.1 (progenitor cells), and P63 (basal cells).

IV. Se ha estudiado la secreción de citoquinas por las células NHBE utilizando *microarrays* de anticuerpos. Este estudio ha demostrado que la exposición a Ole e 1 alteraba el patrón de citoquinas secretadas por las células NHBE de manera dependiente del estado de diferenciación celular y de las características del donante.

It has been studied the cytokine secretion by NHBE cells using antibody microarray. This study has shown that Ole e 1 exposure altered the cytokine profile secreted by NHBE cells in a both state- and donor feature-dependent manner.

CAPÍTULO II. ***Análisis del papel de las proteasas ambientales en la respuesta inmune del epitelio bronquial a Ole e 1***

CHAPTER II. Analysis of the role of environmental proteases on the immune response of the bronchial epithelium to Ole e 1

I. Se ha establecido y caracterizado un modelo *in vitro* de epitelio bronquial basado en la línea celular Calu-3 de células epiteliales bronquiales humanas inmortalizadas, crecidas en ALI. Este modelo se ha utilizado para analizar el papel de la co-exposición a proteasas y al humo del tabaco en la respuesta inmune a Ole e 1.

It has been established and characterized an in vitro model of bronchial epithelium based on the Calu-3 cell line of immortalized human bronchial epithelial cells, cultured at ALI. This model has been used to analyse the role of the co-exposure to proteases and cigarette smoke in the immune response to Ole e 1.

II. Se ha demostrado que la exposición a la cisteín-proteasa Der p 1 de HDM disminuye los valores de TEER y altera las TJ de manera dependiente del estado de diferenciación del epitelio bronquial.

It has been shown that exposure to Der p 1 cysteine-protease from HDM caused a decrease in TEER values and altered TJ in a bronchial epithelial state-dependent manner.

III. Se ha demostrado que la permeabilidad epitelial de Ole e 1 depende del estado funcional del epitelio bronquial y no tanto de la actividad proteasa de Der p 1. Sin embargo, la exposición crónica a Der p 1 sí alteraba la integridad del epitelio bronquial y, en consecuencia, la permeabilidad epitelial de Ole e 1.

It has been shown that epithelial permeability to Ole e 1 depends on the functional state of the bronchial epithelium but not on Der p 1 protease activity. However, chronic exposure to Der p 1 altered the integrity of the bronchial epithelium and, consequently, the epithelial permeability to Ole e 1.

IV. Se ha demostrado que Ole e 1 es una nueva diana proteolítica de Der p 1, y que los péptidos resultantes mantienen la capacidad de unir IgG y de activar basófilos derivados de pacientes alérgicos al polen de olivo.

It has been shown that Ole e 1 aeroallergen is a novel proteolytic target of Der p 1, and the derived peptides keep the capability to bind IgG and activate basophils derived from olive pollen allergic patients.

V. Se ha llevado a cabo un estudio comparativo del metaboloma de las células Calu-3 expuestas a Ole e 1 y/o Der p 1, los días 2 y 7 de cultivo en ALI. Este estudio ha demostrado que el perfil de metabolitos apicales obtenido exhibe gran dependencia del día de exposición al alérgeno en ALI y de la presencia de Der p 1. Además, este estudio ha permitido proponer varios metabolitos candidatos que podrían estar implicados en la reacción alérgica: L-Arg, kinurenina y L-Trp.

It has been carried out a comparative metabolomic's study of Calu-3 cells exposed to Ole e 1 and/or Der p 1 on days 2 and 7 of culture at ALI. This study has shown that apical metabolite profile shows great dependence on both the day of exposure to the allergen at ALI and the presence of Der p 1. In addition, this study has allowed to propose several candidate metabolites that could be involved in the allergic reaction: L- Arg, kynurenine and L-Trp.

VI. Se ha demostrado que la GSTpi humana incrementa la actividad cisteín-proteasa de Der p 1, pero no la isoforma GSTmu de ácaro. Este efecto parece estar mediado por un mecanismo redox que implica la reorganización de puentes disulfuro en presencia de GSH.

It has been shown that human GSTpi increases the cysteine-protease activity of Der p 1, but not mite GSTmu isoform. This effect seems to be mediated by a redox mechanism involving a disulphide-bridge rearrangement in the presence of GSH.

VII. Se ha demostrado que GSTpi es secretada en el medio apical por las células Calu-3 cultivadas en ALI, modulando la actividad proteolítica de Der p 1.

It has been shown that GSTpi is secreted in the apical medium by Calu-3 cells cultured at ALI, modulating the proteolytic activity of Der p 1.

CAPÍTULO III. *Estudio del Efecto de la co-exposición al humo del tabaco en la respuesta inmune del epitelio bronquial a Ole e 1*

CHAPTER III. *Study of the effect of co-exposure to cigarette smoke on the immune response of the bronchial epithelium to Ole e 1*

I. Se ha optimizado la preparación y la estandarización del CSE, y se han identificado un total de 55 componentes mediante GS-MS.

It has been optimized the preparation and standardization of CSE, being identified a total of 55 components by GS-MS.

II. Se ha demostrado que la exposición a CSE altera la función de la barrera epitelial formada por las células epiteliales Calu-3 cultivadas en ALI, al reducir los valores de TEER y los niveles de expresión de los mRNAs *TJP1* e *IDO-1*. Además, la exposición a CSE afectaba a la viabilidad de las células epiteliales de manera dependiente de la dosis y del tiempo de exposición.

It has been shown that CSE exposure alters the function of ALI-cultured Calu-3 epithelial barrier by decreasing both TEER values and mRNAs expression levels of TJP1 and IDO-1. In addition, CSE exposure affected epithelial cell viability in a dose- and time-dependent manner.

III. Se ha demostrado que la co-exposición a CSE incrementa la permeabilidad epitelial de Ole e 1 de manera dependiente del estado funcional del epitelio bronquial en el momento de contacto con el aeroalérgeno. Juntos todos estos efectos podrían incrementar la susceptibilidad de un individuo a un aeroalérgeno, contribuyendo así al desarrollo y /o exacerbación de la alergia respiratoria.

It has been shown that CSE co-exposure increases the epithelial permeability to Ole e 1 depending on the functional state of the bronchial epithelium at the time of contact with the aeroallergen. Together all these effects could increase the individual susceptibility to an aeroallergen, thus contributing to the development and/or exacerbation of respiratory allergy.

CAPÍTULO IV. ***Estudio de las propiedades interfaciales de Ole e 1 en el contexto del surfactante pulmonar y de membranas celulares modelo***

CHAPTER IV. ***Study of the interfacial properties of Ole e 1 in the context of pulmonary surfactant and models of cell membranes***

I. Se ha descrito, por primera vez, la capacidad interfacial del aeroalérgeno Ole e 1, así como su interacción con dominios líquido-condensados y líquido-ordenados generados en el contexto de monocapas lipídicas como modelo de surfactante pulmonar y membrana celular eucariota, utilizando balanzas de Langmuir y derivadas. El aeroalérgeno tiende a localizarse en dominios líquido-condensados de DPPC y líquido-ordenados de POPC:SM:CHO. Además, la presencia de POPC, SM y CHO parece ser crucial para la interacción de Ole e 1.

   For the first time, it has been described the interfacial activity of the Ole e 1 aeroallergen, as well as its interfacial interaction with liquid-condensed and liquid-ordered domains, generated in the context of lipid monolayers as models of pulmonary surfactant and eukaryotic cell membrane, using Langmuir-derived balances. The aeroallergen tends to localize associated to liquid-condensed domains of DPPC and liquid-ordered POPC:SM:CHO. Moreover, the presence of POPC, SM and CHO seems to be crucial for the Ole e 1 interaction.

II. Se ha demostrado que Ole e 1 inhibe la adsorción interfacial del surfactante pulmonar nativo.

   It has been shown that Ole e 1 inhibits the interfacial adsorption of native pulmonary surfactant.

Bibliografía
References

1. Molfino, NA. *Lung function evolution and respiratory symptoms.* Arch Bronconeumol, 2004. 40: 429.
2. Herriges, M and Morrisey, EE. *Lung development: orchestrating the generation and regeneration of a complex organ.* Development, 2014. 141: 502.
3. Schittny, JC. *Development of the lung.* Cell Tissue Res, 2017. 367: 427.
4. Ganesan, S, Comstock, AT, and Sajjan, US. *Barrier function of airway tract epithelium.* Tissue Barriers, 2013. 1: e24997.
5. Georas, SN and Rezaee, F. *Epithelial barrier function: at the front line of asthma immunology and allergic airway inflammation.* J Allergy Clin Immunol, 2014. 134: 509.
6. Rock, JR, Randell, SH, and Hogan, BLM. *Airway basal stem cells: a perspective on their roles in epithelial homeostasis and remodeling.* Disease Models & Amp; Mechanisms, 2010. 3: 545.
7. Gomez-Galvez, P, Vicente-Munuera, P, Bermudez-Gallardo, M, Serrano-Perez-Higueras, O, Cavodeassi, F, Sotillos, S, Buceta, J, Escudero, LM, and Grima, C. *Scutoids are a geometrical solution to three-dimensional packing of epithelia.* Nat Commun, 2018. 9: 2960.
8. Reynolds, SD and Malkinson, AM. *Clara cell: progenitor for the bronchiolar epithelium.* Int J Biochem Cell Biol, 2010. 42: 1.
9. Guillot, L, Nathan, N, Tabary, O, Thouvenin, G, Le Rouzic, P, Corvol, H, Amselem, S, and Clement, A. *Alveolar epithelial cells: master regulators of lung homeostasis.* Int J Biochem Cell Biol, 2013. 45: 2568.
10. Pérez B, F, Méndez G, A, Lagos R, A, and Vargas M, SL. *Dinámica y patología del barrido mucociliar como mecanismo defensivo del pulmón y alternativas farmacológicas de tratamiento.* Revista médica de Chile, 2014. 142: 606.
11. Thomas, J, Morle, L, Soulavie, F, Laurencon, A, Sagnol, S, and Durand, B. *Transcriptional control of genes involved in ciliogenesis: a first step in making cilia.* Biol Cell, 2010. 102: 499.
12. Choksi, SP, Babu, D, Lau, D, Yu, X, and Roy, S. *Systematic discovery of novel ciliary genes through functional genomics in the zebrafish.* Development, 2014. 141: 3410.
13. Jain, R, Pan, J, Driscoll, JA, Wisner, JW, Huang, T, Gunsten, SP, You, Y, and Brody, SL. *Temporal relationship between primary and motile ciliogenesis in airway epithelial cells.* Am J Respir Cell Mol Biol, 2010. 43: 731.
14. You, Y, Huang, T, Richer, EJ, Schmidt, JE, Zabner, J, Borok, Z, and Brody, SL. *Role of f-box factor foxj1 in differentiation of ciliated airway epithelial cells.* Am J Physiol Lung Cell Mol Physiol, 2004. 286: L650.

15. Lin, L, Spoor, MS, Gerth, AJ, Brody, SL, and Peng, SL. *Modulation of Th1 activation and inflammation by the NF-kappaB repressor Foxj1.* Science, 2004. 303: 1017.
16. Tilley, AE, Walters, MS, Shaykhiev, R, and Crystal, RG. *Cilia dysfunction in lung disease.* Annu Rev Physiol, 2015. 77: 379.
17. Thomas, B, Rutman, A, Hirst, RA, Haldar, P, Wardlaw, AJ, Bankart, J, Brightling, CE, and O'Callaghan, C. *Ciliary dysfunction and ultrastructural abnormalities are features of severe asthma.* J Allergy Clin Immunol, 2010. 126: 722.
18. Smith, CM, Kulkarni, H, Radhakrishnan, P, Rutman, A, Bankart, MJ, Williams, G, Hirst, RA, Easton, AJ, Andrew, PW, and O'Callaghan, C. *Ciliary dyskinesia is an early feature of respiratory syncytial virus infection.* Eur Respir J, 2014. 43: 485.
19. Leopold, PL, O'Mahony, MJ, Lian, XJ, Tilley, AE, Harvey, BG, and Crystal, RG. *Smoking is associated with shortened airway cilia.* PLoS One, 2009. 4: e8157.
20. Rogers, DF. *The airway goblet cell.* Int J Biochem Cell Biol, 2003. 35: 1.
21. Thornton, DJ, Rousseau, K, and McGuckin, MA. *Structure and function of the polymeric mucins in airways mucus.* Annu Rev Physiol, 2008. 70: 459.
22. Hovenberg, HW, Davies, JR, and Carlstedt, I. *Different mucins are produced by the surface epithelium and the submucosa in human trachea: identification of MUC5AC as a major mucin from the goblet cells.* Biochem J, 1996. 318 319.
23. Turner, J and Jones, CE. *Regulation of mucin expression in respiratory diseases.* Biochem Soc Trans, 2009. 37: 877.
24. Vareille, M, Kieninger, E, Edwards, MR, and Regamey, N. *The airway epithelium: soldier in the fight against respiratory viruses.* Clin Microbiol Rev, 2011. 24: 210.
25. Lumsden, AB, McLean, A, and Lamb, D. *Goblet and Clara cells of human distal airways: evidence for smoking induced changes in their numbers.* Thorax, 1984. 39: 844.
26. Turner, J, Roger, J, Fitau, J, Combe, D, Giddings, J, Heeke, GV, and Jones, CE. *Goblet cells are derived from a FOXJ1-expressing progenitor in a human airway epithelium.* Am J Respir Cell Mol Biol, 2011. 44: 276.
27. Li, F, He, J, Wei, J, Cho, WC, and Liu, X. *Diversity of epithelial stem cell types in adult lung.* Stem Cells Int, 2015. 2015: 728307.
28. Irwin, RS, Hogarth, DK, and Barnes, PJ. *Introducing a new series: Giants in chest medicine.* Chest, 2013. 144: 1087.
29. Phelps, DS and Floros, J. *Localization of pulmonary surfactant proteins using immunohistochemistry and tissue in situ hybridization.* Exp Lung Res, 1991. 17: 985.

30. De Water, R, Willems, LN, Van Muijen, GN, Franken, C, Fransen, JA, Dijkman, JH, and Kramps, JA. *Ultrastructural localization of bronchial antileukoprotease in central and peripheral human airways by a gold-labeling technique using monoclonal antibodies.* Am Rev Respir Dis, 1986. 133: 882.
31. Widdicombe, JG and Pack, RJ. *The Clara cell.* Eur J Respir Dis, 1982. 63: 202.
32. Fanucchi, MV, Murphy, ME, Buckpitt, AR, Philpot, RM, and Plopper, CG. *Pulmonary cytochrome P450 monooxygenase and Clara cell differentiation in mice.* Am J Respir Cell Mol Biol, 1997. 17: 302.
33. Evans, MJ and Plopper, CG. *The role of basal cells in adhesion of columnar epithelium to airway basement membrane.* Am Rev Respir Dis, 1988. 138: 481.
34. Evans, MJ, Van Winkle, LS, Fanucchi, MV, and Plopper, CG. *Cellular and molecular characteristics of basal cells in airway epithelium.* Exp Lung Res, 2001. 27: 401.
35. Tadokoro, T, Wang, Y, Barak, LS, Bai, Y, Randell, SH, and Hogan, BL. *IL-6/STAT3 promotes regeneration of airway ciliated cells from basal stem cells.* Proc Natl Acad Sci U S A, 2014. 111: E3641.
36. Puchelle, E, Zahm, JM, Tournier, JM, and Coraux, C. *Airway epithelial repair, regeneration, and remodeling after injury in chronic obstructive pulmonary disease.* Proc Am Thorac Soc, 2006. 3: 726.
37. Shaykhiev, R and Crystal, RG. *Basal cell origins of smoking-induced airway epithelial disorders.* Cell Cycle, 2014. 13: 341.
38. Walters, MS, Gomi, K, Ashbridge, B, Moore, MA, Arbelaez, V, Heldrich, J, Ding, BS, Rafii, S, Staudt, MR, and Crystal, RG. *Generation of a human airway epithelium derived basal cell line with multipotent differentiation capacity.* Respir Res, 2013. 14: 135.
39. Goerke, J. *Pulmonary surfactant: functions and molecular composition.* Biochim Biophys Acta, 1998. 1408: 79.
40. Zuo, YY, Veldhuizen, RA, Neumann, AW, Petersen, NO, and Possmayer, F. *Current perspectives in pulmonary surfactant--inhibition, enhancement and evaluation.* Biochim Biophys Acta, 2008. 1778: 1947.
41. Lopez-Rodriguez, E and Perez-Gil, J. *Structure-function relationships in pulmonary surfactant membranes: from biophysics to therapy.* Biochim Biophys Acta, 2014. 1838: 1568.
42. Roldan, N, Perez-Gil, J, Morrow, MR, and Garcia-Alvarez, B. *Divide & Conquer: Surfactant Protein SP-C and Cholesterol Modulate Phase Segregation in Lung Surfactant.* Biophys J, 2017. 113: 847.

43. Orgeig, S, Morrison, JL, and Daniels, CB. *Evolution, Development, and Function of the Pulmonary Surfactant System in Normal and Perturbed Environments.* Compr Physiol, 2015. 6: 363.
44. Baoukina, S and Tieleman, DP. *Computer simulations of lung surfactant.* Biochim Biophys Acta, 2016. 1858: 2431.
45. Perez-Gil, J. *Structure of pulmonary surfactant membranes and films: the role of proteins and lipid-protein interactions.* Biochim Biophys Acta, 2008. 1778: 1676.
46. Orgeig, S, Bernhard, W, Biswas, SC, Daniels, CB, Hall, SB, Hetz, SK, Lang, CJ, Maina, JN, Panda, AK, Perez-Gil, J*, et al. The anatomy, physics, and physiology of gas exchange surfaces: is there a universal function for pulmonary surfactant in animal respiratory structures?* Integr Comp Biol, 2007. 47: 610.
47. Winkler, C and Hohlfeld, JM. *Surfactant and allergic airway inflammation.* Swiss Med Wkly, 2013. 143: w13818.
48. Voorhout, WF, Veenendaal, T, Kuroki, Y, Ogasawara, Y, van Golde, LM, and Geuze, HJ. *Immunocytochemical localization of surfactant protein D (SP-D) in type II cells, Clara cells, and alveolar macrophages of rat lung.* J Histochem Cytochem, 1992. 40: 1589.
49. Arroyo, R, Martin-Gonzalez, A, Echaide, M, Jain, A, Brondyk, WH, Rosenbaum, J, Moreno-Herrero, F, and Perez-Gil, J. *Supramolecular Assembly of Human Pulmonary Surfactant Protein SP-D.* J Mol Biol, 2018. 430: 1495.
50. Glasser, JR and Mallampalli, RK. *Surfactant and its role in the pathobiology of pulmonary infection.* Microbes Infect, 2012. 14: 17.
51. Malherbe, DC, Erpenbeck, VJ, Abraham, SN, Crouch, EC, Hohlfeld, JM, and Wright, JR. *Surfactant protein D decreases pollen-induced IgE-dependent mast cell degranulation.* Am J Physiol Lung Cell Mol Physiol, 2005. 289: L856.
52. Madan, T, Kishore, U, Shah, A, Eggleton, P, Strong, P, Wang, JY, Aggrawal, SS, Sarma, PU, and Reid, KB. *Lung surfactant proteins A and D can inhibit specific IgE binding to the allergens of Aspergillus fumigatus and block allergen-induced histamine release from human basophils.* Clin Exp Immunol, 1997. 110: 241.
53. Hortobagyi, L, Kierstein, S, Krytska, K, Zhu, X, Das, AM, Poulain, F, and Haczku, A. *Surfactant protein D inhibits TNF-alpha production by macrophages and dendritic cells in mice.* J Allergy Clin Immunol, 2008. 122: 521.
54. Sano, H, Chiba, H, Iwaki, D, Sohma, H, Voelker, DR, and Kuroki, Y. *Surfactant proteins A and D bind CD14 by different mechanisms.* J Biol Chem, 2000. 275: 22442.
55. Borron, P, Veldhuizen, RA, Lewis, JF, Possmayer, F, Caveney, A, Inchley, K, McFadden, RG, and Fraher, LJ. *Surfactant associated protein-A inhibits human*

lymphocyte proliferation and IL-2 production. Am J Respir Cell Mol Biol, 1996. 15: 115.

56. Borron, PJ, Crouch, EC, Lewis, JF, Wright, JR, Possmayer, F, and Fraher, LJ. *Recombinant rat surfactant-associated protein D inhibits human T lymphocyte proliferation and IL-2 production.* J Immunol, 1998. 161: 4599.
57. Erpenbeck, VJ, Schmidt, R, Gunther, A, Krug, N, and Hohlfeld, JM. *Surfactant protein levels in bronchoalveolar lavage after segmental allergen challenge in patients with asthma.* Allergy, 2006. 61: 598.
58. Wang, JY, Kishore, U, Lim, BL, Strong, P, and Reid, KB. *Interaction of human lung surfactant proteins A and D with mite (Dermatophagoides pteronyssinus) allergens.* Clin Exp Immunol, 1996. 106: 367.
59. Deb, R, Shakib, F, Reid, K, and Clark, H. *Major house dust mite allergens Dermatophagoides pteronyssinus 1 and Dermatophagoides farinae 1 degrade and inactivate lung surfactant proteins A and D.* J Biol Chem, 2007. 282: 36808.
60. Nogee, LM. *Alterations in SP-B and SP-C expression in neonatal lung disease.* Annu Rev Physiol, 2004. 66: 601.
61. Mulugeta, S and Beers, MF. *Surfactant protein C: its unique properties and emerging immunomodulatory role in the lung.* Microbes Infect, 2006. 8: 2317.
62. Hallstrand, TS, Hackett, TL, Altemeier, WA, Matute-Bello, G, Hansbro, PM, and Knight, DA. *Airway epithelial regulation of pulmonary immune homeostasis and inflammation.* Clin Immunol, 2014. 151: 1.
63. Davies, JA and Garrod, DR. *Molecular aspects of the epithelial phenotype.* Bioessays, 1997. 19: 699.
64. Kojima, T, Go, M, Takano, K, Kurose, M, Ohkuni, T, Koizumi, J, Kamekura, R, Ogasawara, N, Masaki, T, Fuchimoto, J*, et al. Regulation of tight junctions in upper airway epithelium.* Biomed Res Int, 2013. 2013: 947072.
65. Kaarteenaho, R, Merikallio, H, Lehtonen, S, Harju, T, and Soini, Y. *Divergent expression of claudin -1, -3, -4, -5 and -7 in developing human lung.* Respir Res, 2010. 11: 59.
66. Amasheh, S, Meiri, N, Gitter, AH, Schoneberg, T, Mankertz, J, Schulzke, JD, and Fromm, M. *Claudin-2 expression induces cation-selective channels in tight junctions of epithelial cells.* J Cell Sci, 2002. 115: 4969.
67. Cong, X, Zhang, Y, Li, J, Mei, M, Ding, C, Xiang, RL, Zhang, LW, Wang, Y, Wu, LL, and Yu, GY. *Claudin-4 is required for modulation of paracellular permeability by muscarinic acetylcholine receptor in epithelial cells.* J Cell Sci, 2015. 128: 2271.

68. Heijink, IH, Nawijn, MC, and Hackett, TL. *Airway epithelial barrier function regulates the pathogenesis of allergic asthma.* Clin Exp Allergy, 2014. 44: 620.
69. Wittekindt, OH. *Tight junctions in pulmonary epithelia during lung inflammation.* Pflugers Arch, 2017. 469: 135.
70. Gon, Y and Hashimoto, S. *Role of airway epithelial barrier dysfunction in pathogenesis of asthma.* Allergol Int, 2018. 67: 12.
71. Tawar, RG, Colpitts, CC, Lupberger, J, El-Saghire, H, Zeisel, MB, and Baumert, TF. *Claudins and pathogenesis of viral infection.* Semin Cell Dev Biol, 2015. 42: 39.
72. Wan, H, Winton, HL, Soeller, C, Tovey, ER, Gruenert, DC, Thompson, PJ, Stewart, GA, Taylor, GW, Garrod, DR, Cannell, MB*, et al. Der p 1 facilitates transepithelial allergen delivery by disruption of tight junctions.* J Clin Invest, 1999. 104: 123.
73. Vinhas, R, Cortes, L, Cardoso, I, Mendes, VM, Manadas, B, Todo-Bom, A, Pires, E, and Verissimo, P. *Pollen proteases compromise the airway epithelial barrier through degradation of transmembrane adhesion proteins and lung bioactive peptides.* Allergy, 2011. 66: 1088.
74. van Roy, F and Berx, G. *The cell-cell adhesion molecule E-cadherin.* Cell Mol Life Sci, 2008. 65: 3756.
75. Lilien, J and Balsamo, J. *The regulation of cadherin-mediated adhesion by tyrosine phosphorylation/dephosphorylation of beta-catenin.* Curr Opin Cell Biol, 2005. 17: 459.
76. Braga, V. *Spatial integration of E-cadherin adhesion, signalling and the epithelial cytoskeleton.* Curr Opin Cell Biol, 2016. 42: 138.
77. de Boer, WI, Sharma, HS, Baelemans, SM, Hoogsteden, HC, Lambrecht, BN, and Braunstahl, GJ. *Altered expression of epithelial junctional proteins in atopic asthma: possible role in inflammation.* Can J Physiol Pharmacol, 2008. 86: 105.
78. Nawijn, MC, Hackett, TL, Postma, DS, van Oosterhout, AJ, and Heijink, IH. *E-cadherin: gatekeeper of airway mucosa and allergic sensitization.* Trends Immunol, 2011. 32: 248.
79. Coyne, CB, Vanhook, MK, Gambling, TM, Carson, JL, Boucher, RC, and Johnson, LG. *Regulation of airway tight junctions by proinflammatory cytokines.* Mol Biol Cell, 2002. 13: 3218.
80. Whitsett, JA and Alenghat, T. *Respiratory epithelial cells orchestrate pulmonary innate immunity.* Nat Immunol, 2015. 16: 27.
81. Lambrecht, BN and Hammad, H. *Allergens and the airway epithelium response: gateway to allergic sensitization.* J Allergy Clin Immunol, 2014. 134: 499.

82. Hammad, H and Lambrecht, BN. *Dendritic cells and epithelial cells: linking innate and adaptive immunity in asthma.* Nat Rev Immunol, 2008. 8: 193.

83. Cherry, WB, Yoon, J, Bartemes, KR, Iijima, K, and Kita, H. *A novel IL-1 family cytokine, IL-33, potently activates human eosinophils.* J Allergy Clin Immunol, 2008. 121: 1484.

84. Lloyd, CM and Saglani, S. *Epithelial cytokines and pulmonary allergic inflammation.* Curr Opin Immunol, 2015. 34: 52.

85. Pawankar, R, Hayashi, M, Yamanishi, S, and Igarashi, T. *The paradigm of cytokine networks in allergic airway inflammation.* Curr Opin Allergy Clin Immunol, 2015. 15: 41.

86. Mitchell, PD and O'Byrne, PM. *Epithelial-Derived Cytokines in Asthma.* Chest, 2017. 151: 1338.

87. Willart, MA, Deswarte, K, Pouliot, P, Braun, H, Beyaert, R, Lambrecht, BN, and Hammad, H. *Interleukin-1alpha controls allergic sensitization to inhaled house dust mite via the epithelial release of GM-CSF and IL-33.* J Exp Med, 2012. 209: 1505.

88. Carriere, V, Roussel, L, Ortega, N, Lacorre, DA, Americh, L, Aguilar, L, Bouche, G, and Girard, JP. *IL-33, the IL-1-like cytokine ligand for ST2 receptor, is a chromatin-associated nuclear factor in vivo.* Proc Natl Acad Sci U S A, 2007. 104: 282.

89. Luthi, AU, Cullen, SP, McNeela, EA, Duriez, PJ, Afonina, IS, Sheridan, C, Brumatti, G, Taylor, RC, Kersse, K, Vandenabeele, P*, et al. Suppression of interleukin-33 bioactivity through proteolysis by apoptotic caspases.* Immunity, 2009. 31: 84.

90. Cohen, ES, Scott, IC, Majithiya, JB, Rapley, L, Kemp, BP, England, E, Rees, DG, Overed-Sayer, CL, Woods, J, Bond, NJ*, et al. Oxidation of the alarmin IL-33 regulates ST2-dependent inflammation.* Nat Commun, 2015. 6: 8327.

91. Gour, N and Lajoie, S. *Epithelial Cell Regulation of Allergic Diseases.* Curr Allergy Asthma Rep, 2016. 16: 65.

92. Iwakura, Y, Ishigame, H, Saijo, S, and Nakae, S. *Functional specialization of interleukin-17 family members.* Immunity, 2011. 34: 149.

93. Yagami, A, Orihara, K, Morita, H, Futamura, K, Hashimoto, N, Matsumoto, K, Saito, H, and Matsuda, A. *IL-33 mediates inflammatory responses in human lung tissue cells.* J Immunol, 2010. 185: 5743.

94. Besnard, AG, Togbe, D, Guillou, N, Erard, F, Quesniaux, V, and Ryffel, B. *IL-33-activated dendritic cells are critical for allergic airway inflammation.* Eur J Immunol, 2011. 41: 1675.

95. Toy, D, Kugler, D, Wolfson, M, Vanden Bos, T, Gurgel, J, Derry, J, Tocker, J, and Peschon, J. *Cutting edge: interleukin 17 signals through a heteromeric receptor complex.* J Immunol, 2006. 177: 36.

96. Chang, J, Xia, YF, Zhang, MZ, and Zhang, LM. *IL-33 Signaling in Lung Injury.* Transl Perioper Pain Med, 2016. 1: 24.

97. Andrade, MV, Iwaki, S, Ropert, C, Gazzinelli, RT, Cunha-Melo, JR, and Beaven, MA. *Amplification of cytokine production through synergistic activation of NFAT and AP-1 following stimulation of mast cells with antigen and IL-33.* Eur J Immunol, 2011. 41: 760.

98. Sabatino, G, Nicoletti, M, Neri, G, Saggini, A, Rosati, M, Conti, F, Cianchetti, E, Toniato, E, Fulcheri, M, Caraffa, A*, et al. Impact of IL -9 and IL-33 in mast cells.* J Biol Regul Homeost Agents, 2012. 26: 577.

99. Iikura, M, Suto, H, Kajiwara, N, Oboki, K, Ohno, T, Okayama, Y, Saito, H, Galli, SJ, and Nakae, S. *IL-33 can promote survival, adhesion and cytokine production in human mast cells.* Lab Invest, 2007. 87: 971.

100. Blom, L, Poulsen, BC, Jensen, BM, Hansen, A, and Poulsen, LK. *IL-33 induces IL-9 production in human CD4+ T cells and basophils.* PLoS One, 2011. 6: e21695.

101. Hongjia, L, Caiqing, Z, Degan, L, Fen, L, Chao, W, Jinxiang, W, and Liang, D. *IL-25 promotes Th2 immunity responses in airway inflammation of asthmatic mice via activation of dendritic cells.* Inflammation, 2014. 37: 1070.

102. Huang, Y and Paul, WE. *Inflammatory group 2 innate lymphoid cells.* Int Immunol, 2016. 28: 23.

103. Mitchell, PD and O'Byrne, PM. *Biologics and the lung: TSLP and other epithelial cell-derived cytokines in asthma.* Pharmacol Ther, 2017. 169: 104.

104. Allakhverdi, Z, Comeau, MR, Jessup, HK, Yoon, BR, Brewer, A, Chartier, S, Paquette, N, Ziegler, SF, Sarfati, M, and Delespesse, G. *Thymic stromal lymphopoietin is released by human epithelial cells in response to microbes, trauma, or inflammation and potently activates mast cells.* J Exp Med, 2007. 204: 253.

105. Kato, A, Favoreto, S, Jr., Avila, PC, and Schleimer, RP. *TLR3- and Th2 cytokine-dependent production of thymic stromal lymphopoietin in human airway epithelial cells.* J Immunol, 2007. 179: 1080.

106. Pan, G, Liang, Y, Lu, L, Chen, X, Wang, M, Wang, L, Yan, C, and Zhang, W. *Blockage of thymic stromal lymphopoietin signaling improves acute lung injury in mice by regulating pulmonary dendritic cells.* Int J Clin Exp Pathol, 2015. 8: 10698.

107. Levin, SD, Koelling, RM, Friend, SL, Isaksen, DE, Ziegler, SF, Perlmutter, RM, and Farr, AG. *Thymic stromal lymphopoietin: a cytokine that promotes the development of IgM+ B cells in vitro and signals via a novel mechanism.* J Immunol, 1999. 162: 677.

108. Park, LS, Martin, U, Garka, K, Gliniak, B, Di Santo, JP, Muller, W, Largaespada, DA, Copeland, NG, Jenkins, NA, Farr, AG*, et al. Cloning of the murine thymic stromal lymphopoietin (TSLP) receptor: Formation of a functional heteromeric complex requires interleukin 7 receptor.* J Exp Med, 2000. 192: 659.

109. Moon, TC, St Laurent, CD, Morris, KE, Marcet, C, Yoshimura, T, Sekar, Y, and Befus, AD. *Advances in mast cell biology: new understanding of heterogeneity and function.* Mucosal Immunol, 2010. 3: 111.

110. Gohy, ST, Hupin, C, Pilette, C, and Ladjemi, MZ. *Chronic inflammatory airway diseases: the central role of the epithelium revisited.* Clin Exp Allergy, 2016. 46: 529.

111. Reibman, J, Hsu, Y, Chen, LC, Bleck, B, and Gordon, T. *Airway epithelial cells release MIP-3alpha/CCL20 in response to cytokines and ambient particulate matter.* Am J Respir Cell Mol Biol, 2003. 28: 648.

112. Xue, L, Salimi, M, Panse, I, Mjosberg, JM, McKenzie, AN, Spits, H, Klenerman, P, and Ogg, G. *Prostaglandin D2 activates group 2 innate lymphoid cells through chemoattractant receptor-homologous molecule expressed on TH2 cells.* J Allergy Clin Immunol, 2014. 133: 1184.

113. Ito, T, Wang, YH, Duramad, O, Hori, T, Delespesse, GJ, Watanabe, N, Qin, FX, Yao, Z, Cao, W, and Liu, YJ. *TSLP-activated dendritic cells induce an inflammatory T helper type 2 cell response through OX40 ligand.* J Exp Med, 2005. 202: 1213.

114. Coleman, JM, Naik, C, Holguin, F, Ray, A, Ray, P, Trudeau, JB, and Wenzel, SE. *Epithelial eotaxin-2 and eotaxin-3 expression: relation to asthma severity, luminal eosinophilia and age at onset.* Thorax, 2012. 67: 1061.

115. Kono, H and Rock, KL. *How dying cells alert the immune system to danger.* Nat Rev Immunol, 2008. 8: 279.

116. Willart, MA and Lambrecht, BN. *The danger within: endogenous danger signals, atopy and asthma.* Clin Exp Allergy, 2009. 39: 12.

117. Lopez-Rodriguez, JC, Benede, S, Barderas, R, Villalba, M, and Batanero, E. *Airway Epithelium Plays a Leading Role in the Complex Framework Underlying Respiratory Allergy.* J Investig Allergol Clin Immunol, 2017. 27: 346.

118. Iyer, D, Mishra, N, and Agrawal, A. *Mitochondrial Function in Allergic Disease.* Curr Allergy Asthma Rep, 2017. 17: 29.

119. Akimoto, H. *Global air quality and pollution.* Science, 2003. 302: 1716.
120. Biswas, SK and Rahman, I. *Environmental toxicity, redox signaling and lung inflammation: the role of glutathione.* Mol Aspects Med, 2009. 30: 60.
121. Boldogh, I, Bacsi, A, Choudhury, BK, Dharajiya, N, Alam, R, Hazra, TK, Mitra, S, Goldblum, RM, and Sur, S. *ROS generated by pollen NADPH oxidase provide a signal that augments antigen-induced allergic airway inflammation.* J Clin Invest, 2005. 115: 2169.
122. Comhair, SA and Erzurum, SC. *Redox control of asthma: molecular mechanisms and therapeutic opportunities.* Antioxid Redox Signal, 2010. 12: 93.
123. Radi, R. *Peroxynitrite, a stealthy biological oxidant.* J Biol Chem, 2013. 288: 26464.
124. Jones, DP. *Redefining oxidative stress.* Antioxid Redox Signal, 2006. 8: 1865.
125. Hoffman, S, Nolin, J, McMillan, D, Wouters, E, Janssen-Heininger, Y, and Reynaert, N. *Thiol redox chemistry: role of protein cysteine oxidation and altered redox homeostasis in allergic inflammation and asthma.* J Cell Biochem, 2015. 116: 884.
126. Brandt, EB, Myers, JM, Ryan, PH, and Hershey, GK. *Air pollution and allergic diseases.* Curr Opin Pediatr, 2015. 27: 724.
127. Hristova, M, Habibovic, A, Veith, C, Janssen-Heininger, YM, Dixon, AE, Geiszt, M, and van der Vliet, A. *Airway epithelial dual oxidase 1 mediates allergen-induced IL-33 secretion and activation of type 2 immune responses.* J Allergy Clin Immunol, 2016. 137: 1545.
128. Erzurum, SC. *New Insights in Oxidant Biology in Asthma.* Ann Am Thorac Soc, 2016. 13 S35.
129. Yang, SN, Hsieh, CC, Kuo, HF, Lee, MS, Huang, MY, Kuo, CH, and Hung, CH. *The effects of environmental toxins on allergic inflammation.* Allergy Asthma Immunol Res, 2014. 6: 478.
130. Levetin, E and Van de Water, P. *Environmental contributions to allergic disease.* Curr Allergy Asthma Rep, 2001. 1: 506.
131. Kelly, FJ and Fussell, JC. *Air pollution and airway disease.* Clin Exp Allergy, 2011. 41: 1059.
132. Provost, EB, Chaumont, A, Kicinski, M, Cox, B, Fierens, F, Bernard, A, and Nawrot, TS. *Serum levels of club cell secretory protein (Clara) and short- and long-term exposure to particulate air pollution in adolescents.* Environ Int, 2014. 68: 66.

133. Dietert, RR, DeWitt, JC, Germolec, DR, and Zelikoff, JT. *Breaking patterns of environmentally influenced disease for health risk reduction: immune perspectives.* Environ Health Perspect, 2010. 118: 1091.

134. Ormstad, H, Johansen, BV, and Gaarder, PI. *Airborne house dust particles and diesel exhaust particles as allergen carriers.* Clin Exp Allergy, 1998. 28: 702.

135. Senechal, H, Visez, N, Charpin, D, Shahali, Y, Peltre, G, Biolley, JP, Lhuissier, F, Couderc, R, Yamada, O, Malrat-Domenge, A*, et al. A Review of the Effects of Major Atmospheric Pollutants on Pollen Grains, Pollen Content, and Allergenicity.* ScientificWorldJournal, 2015. 2015: 940243.

136. Schiavoni, G, D'Amato, G, and Afferni, C. *The dangerous liaison between pollens and pollution in respiratory allergy.* Ann Allergy Asthma Immunol, 2017. 118: 269.

137. Bartra, J, Mullol, J, del Cuvillo, A, Davila, I, Ferrer, M, Jauregui, I, Montoro, J, Sastre, J, and Valero, A. *Air pollution and allergens.* J Investig Allergol Clin Immunol, 2007. 17 3.

138. Chehregani, A, Majde, A, Moin, M, Gholami, M, Ali Shariatzadeh, M, and Nassiri, H. *Increasing allergy potency of Zinnia pollen grains in polluted areas.* Ecotoxicol Environ Saf, 2004. 58: 267.

139. Janssen-Heininger, YM, Mossman, BT, Heintz, NH, Forman, HJ, Kalyanaraman, B, Finkel, T, Stamler, JS, Rhee, SG, and van der Vliet, A. *Redox-based regulation of signal transduction: principles, pitfalls, and promises.* Free Radic Biol Med, 2008. 45: 1.

140. Fitzpatrick, AM, Jones, DP, and Brown, LA. *Glutathione redox control of asthma: from molecular mechanisms to therapeutic opportunities.* Antioxid Redox Signal, 2012. 17: 375.

141. Moss, M, Guidot, DM, Wong-Lambertina, M, Ten Hoor, T, Perez, RL, and Brown, LA. *The effects of chronic alcohol abuse on pulmonary glutathione homeostasis.* Am J Respir Crit Care Med, 2000. 161: 414.

142. Mudway, IS, Stenfors, N, Blomberg, A, Helleday, R, Dunster, C, Marklund, SL, Frew, AJ, Sandstrom, T, and Kelly, FJ. *Differences in basal airway antioxidant concentrations are not predictive of individual responsiveness to ozone: a comparison of healthy and mild asthmatic subjects.* Free Radic Biol Med, 2001. 31: 962.

143. Allocati, N, Masulli, M, Di Ilio, C, and Federici, L. *Glutathione transferases: substrates, inihibitors and pro-drugs in cancer and neurodegenerative diseases.* Oncogenesis, 2018. 7: 8.

144. Sahiner, UM, Birben, E, Erzurum, S, Sackesen, C, and Kalayci, O. *Oxidative stress in asthma.* World Allergy Organ J, 2011. 4: 151.

145. Nadeem, A, Masood, A, and Siddiqui, N. *Oxidant--antioxidant imbalance in asthma: scientific evidence, epidemiological data and possible therapeutic options.* Ther Adv Respir Dis, 2008. 2: 215.

146. Janssen-Heininger, Y, Ckless, K, Reynaert, N, and van der Vliet, A. *SOD inactivation in asthma: bad or no news?* Am J Pathol, 2005. 166: 649.

147. Dalle-Donne, I, Rossi, R, Giustarini, D, Colombo, R, and Milzani, A. *S-glutathionylation in protein redox regulation.* Free Radic Biol Med, 2007. 43: 883.

148. Mallis, RJ, Hamann, MJ, Zhao, W, Zhang, T, Hendrich, S, and Thomas, JA. *Irreversible thiol oxidation in carbonic anhydrase III: protection by S-glutathiolation and detection in aging rats.* Biol Chem, 2002. 383: 649.

149. Pineda-Molina, E, Klatt, P, Vazquez, J, Marina, A, Garcia de Lacoba, M, Perez-Sala, D, and Lamas, S. *Glutathionylation of the p50 subunit of NF-kappaB: a mechanism for redox-induced inhibition of DNA binding.* Biochemistry, 2001. 40: 14134.

150. Qanungo, S, Starke, DW, Pai, HV, Mieyal, JJ, and Nieminen, AL. *Glutathione supplementation potentiates hypoxic apoptosis by S-glutathionylation of p65-NFkappaB.* J Biol Chem, 2007. 282: 18427.

151. Reynaert, NL, van der Vliet, A, Guala, AS, McGovern, T, Hristova, M, Pantano, C, Heintz, NH, Heim, J, Ho, YS, Matthews, DE*, et al. Dynamic redox control of NF-kappaB through glutaredoxin-regulated S-glutathionylation of inhibitory kappaB kinase beta.* Proc Natl Acad Sci U S A, 2006. 103: 13086.

152. Zhang, J, Grek, C, Ye, ZW, Manevich, Y, Tew, KD, and Townsend, DM. *Pleiotropic functions of glutathione S-transferase P.* Adv Cancer Res, 2014. 122: 143.

153. Wilce, MC and Parker, MW. *Structure and function of glutathione S-transferases.* Biochim Biophys Acta, 1994. 1205: 1.

154. Fletcher, ME, Boshier, PR, Wakabayashi, K, Keun, HC, Smolenski, RT, Kirkham, PA, Adcock, IM, Barton, PJ, Takata, M, and Marczin, N. *Influence of glutathione-S-transferase (GST) inhibition on lung epithelial cell injury: role of oxidative stress and metabolism.* Am J Physiol Lung Cell Mol Physiol, 2015. 308: L1274.

155. Vasieva, O. *The many faces of glutathione transferase pi.* Curr Mol Med, 2011. 11: 129.

156. Jones, JT, Qian, X, van der Velden, JL, Chia, SB, McMillan, DH, Flemer, S, Hoffman, SM, Lahue, KG, Schneider, RW, Nolin, JD*, et al. Glutathione S-transferase pi modulates NF-kappaB activation and pro-inflammatory responses in lung epithelial cells.* Redox Biol, 2016. 8: 375.

157. Lo, HW and Ali-Osman, F. *Structure of the human allelic glutathione S-transferase-pi gene variant, hGSTP1 C, cloned from a glioblastoma multiforme cell line.* Chem Biol Interact, 1998. 111-112: 91.

158. Schroer, KT, Gibson, AM, Sivaprasad, U, Bass, SA, Ericksen, MB, Wills-Karp, M, Lecras, T, Fitzpatrick, AM, Brown, LA, Stringer, KF*, et al. Downregulation of glutathione S-transferase pi in asthma contributes to enhanced oxidative stress.* J Allergy Clin Immunol, 2011. 128: 539.

159. Bowatte, G, Lodge, CJ, Perret, JL, Matheson, MC, and Dharmage, SC. *Interactions of GST Polymorphisms in Air Pollution Exposure and Respiratory Diseases and Allergies.* Curr Allergy Asthma Rep, 2016. 16: 85.

160. Dai, X, Bowatte, G, Lowe, AJ, Matheson, MC, Gurrin, LC, Burgess, JA, Dharmage, SC, and Lodge, CJ. *Do Glutathione S-Transferase Genes Modify the Link between Indoor Air Pollution and Asthma, Allergies, and Lung Function? A Systematic Review.* Curr Allergy Asthma Rep, 2018. 18: 20.

161. Fryer, AA, Bianco, A, Hepple, M, Jones, PW, Strange, RC, and Spiteri, MA. *Polymorphism at the glutathione S-transferase GSTP1 locus. A new marker for bronchial hyperresponsiveness and asthma.* Am J Respir Crit Care Med, 2000. 161: 1437.

162. Gandhi, VD and Vliagoftis, H. *Airway epithelium interactions with aeroallergens: role of secreted cytokines and chemokines in innate immunity.* Front Immunol, 2015. 6: 147.

163. Petersen, KD, Kronborg, C, Gyrd-Hansen, D, Dahl, R, Larsen, JN, and Linneberg, A. *Characteristics of patients receiving allergy vaccination: to which extent do socio-economic factors play a role?* Eur J Public Health, 2011. 21: 323.

164. Dullaers, M, De Bruyne, R, Ramadani, F, Gould, HJ, Gevaert, P, and Lambrecht, BN. *The who, where, and when of IgE in allergic airway disease.* J Allergy Clin Immunol, 2012. 129: 635.

165. Akkoc, T, Akdis, M, and Akdis, CA. *Update in the mechanisms of allergen-specific immunotheraphy.* Allergy Asthma Immunol Res, 2011. 3: 11.

166. Holgate, ST. *A brief history of asthma and its mechanisms to modern concepts of disease pathogenesis.* Allergy Asthma Immunol Res, 2010. 2: 165.

167. Branzk, N, Gronke, K, and Diefenbach, A. *Innate lymphoid cells, mediators of tissue homeostasis, adaptation and disease tolerance.* 2018. 286: 86.

168. Akdis, CA and Akdis, M. *Mechanisms of allergen-specific immunotherapy.* J Allergy Clin Immunol, 2011. 127: 18.

169. Scheurer, S, Toda, M, and Vieths, S. *What makes an allergen?* Clin Exp Allergy, 2015. 45: 1150.

170. Villalba, M, Rodriguez, R, and Batanero, E. *The spectrum of olive pollen allergens. From structures to diagnosis and treatment.* Methods, 2014. 66: 44.

171. Esteve, C, Montealegre, C, Marina, ML, and Garcia, MC. *Analysis of olive allergens.* Talanta, 2012. 92: 1.

172. Palomares, O, Swoboda, I, Villalba, M, Balic, N, Spitzauer, S, Rodriguez, R, and Valenta, R. *The major allergen of olive pollen Ole e 1 is a diagnostic marker for sensitization to Oleaceae.* Int Arch Allergy Immunol, 2006. 141: 110.

173. Batanero, E, Crespo, JF, Monsalve, RI, Martin-Esteban, M, Villalba, M, and Rodriguez, R. *IgE-binding and histamine-release capabilities of the main carbohydrate component isolated from the major allergen of olive tree pollen, Ole e 1.* J Allergy Clin Immunol, 1999. 103: 147.

174. Hamman-Khalifa, A, Castro, AJ, Jimenez-Lopez, JC, Rodriguez-Garcia, MI, and Alche Jde, D. *Olive cultivar origin is a major cause of polymorphism for Ole e 1 pollen allergen.* BMC Plant Biol, 2008. 8: 10.

175. Villalba, M, Batanero, E, Lopez-Otin, C, Sanchez, LM, Monsalve, RI, Gonzalez de la Pena, MA, Lahoz, C, and Rodriguez, R. *The amino acid sequence of Ole e I, the major allergen from olive tree (Olea europaea) pollen.* Eur J Biochem, 1993. 216: 863.

176. Batanero, E, Villalba, M, and Rodriguez, R. *Glycosylation site of the major allergen from olive tree pollen. Allergenic implications of the carbohydrate moiety.* Mol Immunol, 1994. 31: 31.

177. Twell, D, Wing, R, Yamaguchi, J, and McCormick, S. *Isolation and expression of an anther-specific gene from tomato.* Mol Gen Genet, 1989. 217: 240.

178. Batanero, E, Villalba, M, Lopez-Otin, C, and Rodriguez, R. *Isolation and characterization of an olive allergen-like protein from lilac pollen. Sequence analysis of three cDNA encoding protein isoforms.* Eur J Biochem, 1994. 221: 187.

179. Tang, W, Ezcurra, I, Muschietti, J, and McCormick, S. *A cysteine-rich extracellular protein, LAT52, interacts with the extracellular domain of the pollen receptor kinase LePRK2.* Plant Cell, 2002. 14: 2277.

180. Johnson, MA and Preuss, D. *On your mark, get set, GROW! LePRK2-LAT52 interactions regulate pollen tube growth.* Trends Plant Sci, 2003. 8: 97.

181. Muschietti, J, Dircks, L, Vancanneyt, G, and McCormick, S. *LAT52 protein is essential for tomato pollen development: pollen expressing antisense LAT52 RNA hydrates and germinates abnormally and cannot achieve fertilization.* Plant J, 1994. 6: 321.

182. Rodriguez, R, Villalba, M, Batanero, E, Palomares, O, Quiralte, J, Salamanca, G, Sirvent, S, Castro, L, and Prado, N. *Olive pollen recombinant allergens: value in diagnosis and immunotherapy.* J Investig Allergol Clin Immunol, 2007. 17 4.

183. Castro, AJ, Alche, JD, Calabozo, B, Rodriguez-Garcia, MI, and Polo, F. *Pla 1 1 and Ole e 1 pollen allergens share common epitopes and similar ultrastructural localization.* J Investig Allergol Clin Immunol, 2007. 17 41.

184. Castro, L, Mas, S, Barderas, R, Colas, C, Garcia-Selles, J, Barber, D, Rodriguez, R, and Villalba, M. *Sal k 5, a member of the widespread Ole e 1-like protein family, is a new allergen of Russian thistle (Salsola kali) pollen.* Int Arch Allergy Immunol, 2014. 163: 142.

185. Cardaba, B, Del Pozo, V, Jurado, A, Gallardo, S, Cortegano, I, Arrieta, I, Del Amo, A, Tramon, P, Florido, F, Sastre, J*, et al. Olive pollen allergy: searching for immunodominant T-cell epitopes on the Ole e 1 molecule.* Clin Exp Allergy, 1998. 28: 413.

186. Gonzalez, EM, Villalba, M, Quiralte, J, Batanero, E, Roncal, F, Albar, JP, and Rodriguez, R. *Analysis of IgE and IgG B-cell immunodominant regions of Ole e 1, the main allergen from olive pollen.* Mol Immunol, 2006. 43: 570.

187. Reithofer, M and Jahn-Schmid, B. *Allergens with Protease Activity from House Dust Mites.* Int J Mol Sci, 2017. 18.

188. Kale, SL, Agrawal, K, Gaur, SN, and Arora, N. *Cockroach protease allergen induces allergic airway inflammation via epithelial cell activation.* Scientific Reports, 2017. 7: 42341.

189. Leino, MS, Loxham, M, Blume, C, Swindle, EJ, Jayasekera, NP, Dennison, PW, Shamji, BW, Edwards, MJ, Holgate, ST, Howarth, PH*, et al. Barrier disrupting effects of alternaria alternata extract on bronchial epithelium from asthmatic donors.* PLoS One, 2013. 8: e71278.

190. Jacquet, A. *Interactions of airway epithelium with protease allergens in the allergic response.* Clinical & Experimental Allergy, 2011. 41: 305.

191. Arlian, LG, Morgan, MS, and Neal, JS. *Dust mite allergens: ecology and distribution.* Curr Allergy Asthma Rep, 2002. 2: 401.

192. Calderon, MA, Linneberg, A, Kleine-Tebbe, J, De Blay, F, Hernandez Fernandez de Rojas, D, Virchow, JC, and Demoly, P. *Respiratory allergy caused by house dust mites: What do we really know?* J Allergy Clin Immunol, 2015. 136: 38.

193. Thomas, WR, Hales, BJ, and Smith, WA. *House dust mite allergens in asthma and allergy.* Trends Mol Med, 2010. 16: 321.

194. Chruszcz, M, Chapman, MD, Vailes, LD, Stura, EA, Saint-Remy, JM, Minor, W, and Pomes, A. *Crystal structures of mite allergens Der f 1 and Der p 1 reveal*

differences in surface-exposed residues that may influence antibody binding. J Mol Biol, 2009. 386: 520.

195. Thomas, WR. *Hierarchy and molecular properties of house dust mite allergens.* Allergol Int, 2015. 64: 304.
196. Bessot, JC and Pauli, G. *Mite allergens: an overview.* Eur Ann Allergy Clin Immunol, 2011. 43: 141.
197. Gregory, LG and Lloyd, CM. *Orchestrating house dust mite-associated allergy in the lung.* Trends Immunol, 2011. 32: 402.
198. Dumez, ME, Herman, J, Campizi, V, Galleni, M, Jacquet, A, and Chevigne, A. *Orchestration of an uncommon maturation cascade of the house dust mite protease allergen quartet.* Front Immunol, 2014. 5: 138.
199. Chevigne, A, Barumandzadeh, R, Groslambert, S, Cloes, B, Dehareng, D, Filee, P, Marx, JC, Frere, JM, Matagne, A, Jacquet, A*, et al. Relationship between propeptide pH unfolding and inhibitory ability during ProDer p 1 activation mechanism.* J Mol Biol, 2007. 374: 170.
200. Herman, J, Thelen, N, Smargiasso, N, Mailleux, AC, Luxen, A, Cloes, M, De Pauw, E, Chevigne, A, Galleni, M, and Dumez, ME. *Der p 1 is the primary activator of Der p 3, Der p 6 and Der p 9 the proteolytic allergens produced by the house dust mite Dermatophagoides pteronyssinus.* Biochim Biophys Acta, 2014. 1840: 1117.
201. Wan, H, Winton, HL, Soeller, C, Taylor, GW, Gruenert, DC, Thompson, PJ, Cannell, MB, Stewart, GA, Garrod, DR, and Robinson, C. *The transmembrane protein occludin of epithelial tight junctions is a functional target for serine peptidases from faecal pellets of Dermatophagoides pteronyssinus.* Clin Exp Allergy, 2001. 31: 279.
202. Herbert, CA, King, CM, Ring, PC, Holgate, ST, Stewart, GA, Thompson, PJ, and Robinson, C. *Augmentation of permeability in the bronchial epithelium by the house dust mite allergen Der p1.* Am J Respir Cell Mol Biol, 1995. 12: 369.
203. Henriquez, OA, Den Beste, K, Hoddeson, EK, Parkos, CA, Nusrat, A, and Wise, SK. *House dust mite allergen Der p 1 effects on sinonasal epithelial tight junctions.* Int Forum Allergy Rhinol, 2013. 3: 630.
204. Kalsheker, NA, Deam, S, Chambers, L, Sreedharan, S, Brocklehurst, K, and Lomas, DA. *The house dust mite allergen Der p1 catalytically inactivates alpha 1-antitrypsin by specific reactive centre loop cleavage: a mechanism that promotes airway inflammation and asthma.* Biochem Biophys Res Commun, 1996. 221: 59.

205. Brown, A, Farmer, K, MacDonald, L, Kalsheker, N, Pritchard, D, Haslett, C, Lamb, J, and Sallenave, JM. *House dust mite Der p 1 downregulates defenses of the lung by inactivating elastase inhibitors.* Am J Respir Cell Mol Biol, 2003. 29: 381.

206. Hammad, H, Charbonnier, AS, Duez, C, Jacquet, A, Stewart, GA, Tonnel, AB, and Pestel, J. *Th2 polarization by Der p 1--pulsed monocyte-derived dendritic cells is due to the allergic status of the donors.* Blood, 2001. 98: 1135.

207. Schulz, O, Sewell, HF, and Shakib, F. *Proteolytic cleavage of CD25, the alpha subunit of the human T cell interleukin 2 receptor, by Der p 1, a major mite allergen with cysteine protease activity.* J Exp Med, 1998. 187: 271.

208. Asokananthan, N, Graham, PT, Stewart, DJ, Bakker, AJ, Eidne, KA, Thompson, PJ, and Stewart, GA. *House dust mite allergens induce proinflammatory cytokines from respiratory epithelial cells: the cysteine protease allergen, Der p 1, activates protease-activated receptor (PAR)-2 and inactivates PAR-1.* J Immunol, 2002. 169: 4572.

209. King, C, Brennan, S, Thompson, PJ, and Stewart, GA. *Dust mite proteolytic allergens induce cytokine release from cultured airway epithelium.* J Immunol, 1998. 161: 3645.

210. Zhang, J, Chen, J, Allen-Philbey, K, Perera Baruhupolage, C, Tachie-Menson, T, Mangat, SC, Garrod, DR, and Robinson, C. *Innate generation of thrombin and intracellular oxidants in airway epithelium by allergen Der p 1.* J Allergy Clin Immunol, 2016. 138: 1224.

211. Machado, DC, Horton, D, Harrop, R, Peachell, PT, and Helm, BA. *Potential allergens stimulate the release of mediators of the allergic response from cells of mast cell lineage in the absence of sensitization with antigen-specific IgE.* Eur J Immunol, 1996. 26: 2972.

212. Cayrol, C, Duval, A, Schmitt, P, Roga, S, Camus, M, Stella, A, Burlet-Schiltz, O, Gonzalez-de-Peredo, A, and Girard, JP. *Environmental allergens induce allergic inflammation through proteolytic maturation of IL-33.* Nat Immunol, 2018. 19: 375.

213. Sopori, M. *Effects of cigarette smoke on the immune system.* Nat Rev Immunol, 2002. 2: 372.

214. Stampfli, MR and Anderson, GP. *How cigarette smoke skews immune responses to promote infection, lung disease and cancer.* Nat Rev Immunol, 2009. 9: 377.

215. Hoffmann, D and Hoffmann, I. *The changing cigarette, 1950-1995.* J Toxicol Environ Health, 1997. 50: 307.

216. Smith, CJ, Perfetti, TA, Mullens, MA, Rodgman, A, and Doolittle, DJ. *"IARC group 2B Carcinogens" reported in cigarette mainstream smoke.* Food Chem Toxicol, 2000. 38: 825.

217. Proulx, LI, Castonguay, A, and Bissonnette, EY. *Cytokine production by alveolar macrophages is down regulated by the alpha-methylhydroxylation pathway of 4-(methylnitrosamino)-1-(3-pyridyl)-1-butanone (NNK).* Carcinogenesis, 2004. 25: 997.

218. Talhout, R, Schulz, T, Florek, E, van Benthem, J, Wester, P, and Opperhuizen, A. *Hazardous compounds in tobacco smoke.* Int J Environ Res Public Health, 2011. 8: 613.

219. Mio, T, Romberger, DJ, Thompson, AB, Robbins, RA, Heires, A, and Rennard, SI. *Cigarette smoke induces interleukin-8 release from human bronchial epithelial cells.* Am J Respir Crit Care Med, 1997. 155: 1770.

220. Yang, SR, Chida, AS, Bauter, MR, Shafiq, N, Seweryniak, K, Maggirwar, SB, Kilty, I, and Rahman, I. *Cigarette smoke induces proinflammatory cytokine release by activation of NF-kappaB and posttranslational modifications of histone deacetylase in macrophages.* Am J Physiol Lung Cell Mol Physiol, 2006. 291: L46.

221. Hellermann, GR, Nagy, SB, Kong, X, Lockey, RF, and Mohapatra, SS. *Mechanism of cigarette smoke condensate-induced acute inflammatory response in human bronchial epithelial cells.* Respir Res, 2002. 3: 22.

222. de Boer, WI, Sont, JK, van Schadewijk, A, Stolk, J, van Krieken, JH, and Hiemstra, PS. *Monocyte chemoattractant protein 1, interleukin 8, and chronic airways inflammation in COPD.* J Pathol, 2000. 190: 619.

223. Damia Ade, D, Gimeno, JC, Ferrer, MJ, Fabregas, ML, Folch, PA, and Paya, JM. *A study of the effect of proinflammatory cytokines on the epithelial cells of smokers, with or without COPD.* Arch Bronconeumol, 2011. 47: 447.

224. Nakamura, Y, Miyata, M, Ohba, T, Ando, T, Hatsushika, K, Suenaga, F, Shimokawa, N, Ohnuma, Y, Katoh, R, Ogawa, H*, et al. Cigarette smoke extract induces thymic stromal lymphopoietin expression, leading to T(H)2-type immune responses and airway inflammation.* J Allergy Clin Immunol, 2008. 122: 1208.

225. Mahanonda, R, Sa-Ard-Iam, N, Eksomtramate, M, Rerkyen, P, Phairat, B, Schaecher, KE, Fukuda, MM, and Pichyangkul, S. *Cigarette smoke extract modulates human beta-defensin-2 and interleukin-8 expression in human gingival epithelial cells.* J Periodontal Res, 2009. 44: 557.

226. Jukosky, J, Gosselin, BJ, Foley, L, Dechen, T, Fiering, S, and Crane-Godreau, MA. *In vivo Cigarette Smoke Exposure Decreases CCL20, SLPI, and BD-1 Secretion by Human Primary Nasal Epithelial Cells.* Front Psychiatry, 2015. 6: 185.

227. Strzelak, A, Ratajczak, A, Adamiec, A, and Feleszko, W. *Tobacco Smoke Induces and Alters Immune Responses in the Lung Triggering Inflammation, Allergy, Asthma and Other Lung Diseases: A Mechanistic Review.* Int J Environ Res Public Health, 2018. 15.

228. Armentia, A, Bartolome, B, Puyo, M, Paredes, C, Calderon, S, Asensio, T, and del Villar, V. *Tobacco as an allergen in bronchial disease.* Ann Allergy Asthma Immunol, 2007. 98: 329.

229. Armentia, A, Castrodeza, J, Ruiz-Munoz, P, Martinez-Quesada, J, Postigo, I, Herrero, M, Gonzalez-Sagrado, M, de Luis, D, Martin-Armentia, B, and Guisantes, JA. *Allergic hypersensitivity to cannabis in patients with allergy and illicit drug users.* Allergol Immunopathol (Madr), 2011. 39: 271.

230. Aun, MV, Bonamichi-Santos, R, Arantes-Costa, FM, Kalil, J, and Giavina-Bianchi, P. *Animal models of asthma: utility and limitations.* J Asthma Allergy, 2017. 10: 293.

231. Bastarache, JA and Blackwell, TS. *Development of animal models for the acute respiratory distress syndrome.* Dis Model Mech, 2009. 2: 218.

232. Hasan, S, Sebo, P, and Osicka, R. *A guide to polarized airway epithelial models for studies of host-pathogen interactions.* Febs j, 2018.

233. Yamaya, M, Finkbeiner, WE, Chun, SY, and Widdicombe, JH. *Differentiated structure and function of cultures from human tracheal epithelium.* Am J Physiol, 1992. 262: L713.

234. Min, KA, Rosania, GR, and Shin, MC. *Human Airway Primary Epithelial Cells Show Distinct Architectures on Membrane Supports Under Different Culture Conditions.* Cell Biochem Biophys, 2016. 74: 191.

235. Hermanns, MI, Unger, RE, Kehe, K, Peters, K, and Kirkpatrick, CJ. *Lung epithelial cell lines in coculture with human pulmonary microvascular endothelial cells: development of an alveolo-capillary barrier in vitro.* Lab Invest, 2004. 84: 736.

236. Huh, D, Matthews, BD, Mammoto, A, Montoya-Zavala, M, Hsin, HY, and Ingber, DE. *Reconstituting organ-level lung functions on a chip.* Science, 2010. 328: 1662.

237. Sellgren, KL, Butala, EJ, Gilmour, BP, Randell, SH, and Grego, S. *A biomimetic multicellular model of the airways using primary human cells.* Lab Chip, 2014. 14: 3349.

238. Simons, PC and Vander Jagt, DL. *Purification of glutathione S-transferases from human liver by glutathione-affinity chromatography.* Anal Biochem, 1977. 82: 334.

239. Higashi, T, Mai, Y, Noya, Y, Horinouchi, T, Terada, K, Hoshi, A, Nepal, P, Harada, T, Horiguchi, M, Hatate, C*, et al. A simple and rapid method for standard preparation of gas phase extract of cigarette smoke.* PLoS One, 2014. 9: e107856.

240. Clayton, PM, Vas, CA, Bui, TT, Drake, AF, and McAdam, K. *Spectroscopic studies on nicotine and nornicotine in the UV region.* Chirality, 2013. 25: 288.

241. Taeusch, HW, Bernardino de la Serna, J, Perez-Gil, J, Alonso, C, and Zasadzinski, JA. *Inactivation of pulmonary surfactant due to serum-inhibited adsorption and reversal by hydrophilic polymers: experimental.* Biophys J, 2005. 89: 1769.

242. Rouser, G, Siakotos, AN, and Fleischer, S. *Quantitative analysis of phospholipids by thin-layer chromatography and phosphorus analysis of spots.* Lipids, 1966. 1: 85.

243. Srinivasan, B, Kolli, AR, Esch, MB, Abaci, HE, Shuler, ML, and Hickman, JJ. *TEER measurement techniques for in vitro barrier model systems.* J Lab Autom, 2015. 20: 107.

244. Denizot, F and Lang, R. *Rapid colorimetric assay for cell growth and survival. Modifications to the tetrazolium dye procedure giving improved sensitivity and reliability.* J Immunol Methods, 1986. 89: 271.

245. Laemmli, UK. *Cleavage of structural proteins during the assembly of the head of bacteriophage T4.* Nature, 1970. 227: 680.

246. Towbin, H, Staehelin, T, and Gordon, J. *Electrophoretic transfer of proteins from polyacrylamide gels to nitrocellulose sheets: procedure and some applications.* Proc Natl Acad Sci U S A, 1979. 76: 4350.

247. Schmittgen, TD and Livak, KJ. *Analyzing real-time PCR data by the comparative C(T) method.* Nat Protoc, 2008. 3: 1101.

248. Schulz, O, Sewell, HF, and Shakib, F. *A sensitive fluorescent assay for measuring the cysteine protease activity of Der p 1, a major allergen from the dust mite Dermatophagoides pteronyssinus.* Mol Pathol, 1998. 51: 222.

249. Izquierdo-Alvarez, A, Tello, D, Cabrera-Garcia, JD, and Martinez-Ruiz, A. *Identification of S-Nitrosylated and Reversibly Oxidized Proteins by Fluorescence Switch and Complementary Techniques.* Methods Mol Biol, 2018. 1747: 73.

250. Canuto, GA, Castilho-Martins, EA, Tavares, MF, Rivas, L, Barbas, C, and Lopez-Gonzalvez, A. *Multi-analytical platform metabolomic approach to study miltefosine mechanism of action and resistance in Leishmania.* Anal Bioanal Chem, 2014. 406: 3459.

251. Smith, PF. *On the Application of Multivariate Statistical and Data Mining Analyses to Data in Neuroscience.* J Undergrad Neurosci Educ, 2018. 16: R20.

252. LeGendre, N and Matsudaira, P. *Direct protein microsequencing from Immobilon-P Transfer Membrane.* Biotechniques, 1988. 6: 154.

253. Perez, M, Garcia-Limones, C, Zapico, I, Marina, A, Schmitz, ML, Munoz, E, and Calzado, MA. *Mutual regulation between SIAH2 and DYRK2 controls hypoxic and genotoxic signaling pathways.* J Mol Cell Biol, 2012. 4: 316.

254. Alonso, R, Pisa, D, Marina, AI, Morato, E, Rabano, A, Rodal, I, and Carrasco, L. *Evidence for fungal infection in cerebrospinal fluid and brain tissue from patients with amyotrophic lateral sclerosis.* Int J Biol Sci, 2015. 11: 546.

255. Clements, JA. *Surface tension of lung extracts.* Proc Soc Exp Biol Med, 1957. 95: 170.

256. Blodgett, KB. *Films Built by Depositing Successive Monomolecular Layers on a Solid Surface.* Journal of the American Chemical Society, 1935. 57: 1007.

257. Takamoto, DY, Lipp, MM, von Nahmen, A, Lee, KY, Waring, AJ, and Zasadzinski, JA. *Interaction of lung surfactant proteins with anionic phospholipids.* Biophys J, 2001. 81: 153.

258. Wustneck, R, Perez-Gil, J, Wustneck, N, Cruz, A, Fainerman, VB, and Pison, U. *Interfacial properties of pulmonary surfactant layers.* Adv Colloid Interface Sci, 2005. 117: 33.

259. Ravasio, A, Cruz, A, Perez-Gil, J, and Haller, T. *High-throughput evaluation of pulmonary surfactant adsorption and surface film formation.* J Lipid Res, 2008. 49: 2479.

260. Medoff, BD, Sauty, A, Tager, AM, Maclean, JA, Smith, RN, Mathew, A, Dufour, JH, and Luster, AD. *IFN-gamma-inducible protein 10 (CXCL10) contributes to airway hyperreactivity and airway inflammation in a mouse model of asthma.* J Immunol, 2002. 168: 5278.

261. Hung, JY, Chiang, SR, Tsai, MJ, Tsai, YM, Chong, IW, Shieh, JM, and Hsu, YL. *LIGHT is a crucial mediator of airway remodeling.* J Cell Physiol, 2015. 230: 1042.

262. Lamkhioued, B, Garcia-Zepeda, EA, Abi-Younes, S, Nakamura, H, Jedrzkiewicz, S, Wagner, L, Renzi, PM, Allakhverdi, Z, Lilly, C, Hamid, Q*, et al. Monocyte chemoattractant protein (MCP)-4 expression in the airways of patients with asthma. Induction in epithelial cells and mononuclear cells by proinflammatory cytokines.* Am J Respir Crit Care Med, 2000. 162: 723.

263. Samitas, K, Zervas, E, Vittorakis, S, Semitekolou, M, Alissafi, T, Bossios, A, Gogos, H, Economidou, E, Lotvall, J, Xanthou, G*, et al. Osteopontin expression and relation to disease severity in human asthma.* Eur Respir J, 2011. 37: 331.

264. Chihara, J, Yasuba, H, Tsuda, A, Urayama, O, Saito, N, Honda, K, Kayaba, H, Yamashita, T, Kurimoto, F, and Yamada, H. *Elevation of the plasma level of RANTES during asthma attacks.* Journal of Allergy and Clinical Immunology, 1997. 100: S52.

265. Powell, N, Humbert, M, Durham, SR, Assoufi, B, Kay, AB, and Corrigan, CJ. *Increased expression of mRNA encoding RANTES and MCP-3 in the bronchial mucosa in atopic asthma.* Eur Respir J, 1996. 9: 2454.

266. Shore, SA, Schwartzman, IN, Mellema, MS, Flynt, L, Imrich, A, and Johnston, RA. *Effect of leptin on allergic airway responses in mice.* J Allergy Clin Immunol, 2005. 115: 103.

267. Ciprandi, G, Filaci, G, Negrini, S, De Amici, M, Fenoglio, D, and Marseglia, G. *Serum leptin levels in patients with pollen-induced allergic rhinitis.* Int Arch Allergy Immunol, 2009. 148: 211.

268. Kohan, M, Breuer, R, and Berkman, N. *Osteopontin induces airway remodeling and lung fibroblast activation in a murine model of asthma.* Am J Respir Cell Mol Biol, 2009. 41: 290.

269. Elshal, MF and McCoy, JP. *Multiplex bead array assays: performance evaluation and comparison of sensitivity to ELISA.* Methods, 2006. 38: 317.

270. Knight, PR, Sreekumar, A, Siddiqui, J, Laxman, B, Copeland, S, Chinnaiyan, A, and Remick, DG. *Development of a sensitive microarray immunoassay and comparison with standard enzyme-linked immunoassay for cytokine analysis.* Shock, 2004. 21: 26.

271. Ross, AJ, Dailey, LA, Brighton, LE, and Devlin, RB. *Transcriptional profiling of mucociliary differentiation in human airway epithelial cells.* Am J Respir Cell Mol Biol, 2007. 37: 169.

272. Martinez-Anton, A, Sokolowska, M, Kern, S, Davis, AS, Alsaaty, S, Taubenberger, JK, Sun, J, Cai, R, Danner, RL, Eberlein, M*, et al. Changes in microRNA and mRNA expression with differentiation of human bronchial epithelial cells.* Am J Respir Cell Mol Biol, 2013. 49: 384.

273. Klein, SG, Hennen, J, Serchi, T, Blomeke, B, and Gutleb, AC. *Potential of coculture in vitro models to study inflammatory and sensitizing effects of particles on the lung.* Toxicol In Vitro, 2011. 25: 1516.

274. Blume, C and Davies, DE. *In vitro and ex vivo models of human asthma.* Eur J Pharm Biopharm, 2013. 84: 394.

275. Chan, RW, Yuen, KM, Yu, WC, Ho, CC, Nicholls, JM, Peiris, JS, and Chan, MC. *Influenza H5N1 and H1N1 virus replication and innate immune responses in*

bronchial epithelial cells are influenced by the state of differentiation. PLoS One, 2010. 5: e8713.

276. Krunkosky, TM, Jordan, JL, Chambers, E, and Krause, DC. *Mycoplasma pneumoniae host-pathogen studies in an air-liquid culture of differentiated human airway epithelial cells.* Microb Pathog, 2007. 42: 98.
277. Takai, T and Ikeda, S. *Barrier dysfunction caused by environmental proteases in the pathogenesis of allergic diseases.* Allergol Int, 2011. 60: 25.
278. Antony, AB, Tepper, RS, and Mohammed, KA. *Cockroach extract antigen increases bronchial airway epithelial permeability.* J Allergy Clin Immunol, 2002. 110: 589.
279. Tai, HY, Tam, MF, Chou, H, Peng, HJ, Su, SN, Perng, DW, and Shen, HD. *Pen ch 13 allergen induces secretion of mediators and degradation of occludin protein of human lung epithelial cells.* Allergy, 2006. 61: 382.
280. Steelant, B, Farre, R, Wawrzyniak, P, Belmans, J, Dekimpe, E, Vanheel, H, Van Gerven, L, Kortekaas Krohn, I, Bullens, DMA, Ceuppens, JL*, et al. Impaired barrier function in patients with house dust mite-induced allergic rhinitis is accompanied by decreased occludin and zonula occludens-1 expression.* J Allergy Clin Immunol, 2016. 137: 1043.
281. Heijink, IH, van Oosterhout, A, and Kapus, A. *Epidermal growth factor receptor signalling contributes to house dust mite-induced epithelial barrier dysfunction.* Eur Respir J, 2010. 36: 1016.
282. Kauffman, HF, Tamm, M, Timmerman, JA, and Borger, P. *House dust mite major allergens Der p 1 and Der p 5 activate human airway-derived epithelial cells by protease-dependent and protease-independent mechanisms.* Clin Mol Allergy, 2006. 4: 5.
283. Trompette, A, Divanovic, S, Visintin, A, Blanchard, C, Hegde, RS, Madan, R, Thorne, PS, Wills-Karp, M, Gioannini, TL, Weiss, JP*, et al. Allergenicity resulting from functional mimicry of a Toll-like receptor complex protein.* Nature, 2009. 457: 585.
284. Tomee, JF, van Weissenbruch, R, de Monchy, JG, and Kauffman, HF. *Interactions between inhalant allergen extracts and airway epithelial cells: effect on cytokine production and cell detachment.* J Allergy Clin Immunol, 1998. 102: 75.
285. Bhowmick, R and Gappa-Fahlenkamp, H. *Cells and Culture Systems Used to Model the Small Airway Epithelium.* Lung, 2016. 194: 419.
286. Marshall, LJ, Oguejiofor, W, Willetts, RS, Griffiths, HR, and Devitt, A. *Developing accurate models of the human airways.* J Pharm Pharmacol, 2015. 67: 464.

287. Berube, K, Prytherch, Z, Job, C, and Hughes, T. *Human primary bronchial lung cell constructs: the new respiratory models.* Toxicology, 2010. 278: 311.

288. Kreft, ME, Jerman, UD, Lasic, E, Hevir-Kene, N, Rizner, TL, Peternel, L, and Kristan, K. *The characterization of the human cell line Calu-3 under different culture conditions and its use as an optimized in vitro model to investigate bronchial epithelial function.* Eur J Pharm Sci, 2015. 69: 1.

289. Forbes, B, Shah, A, Martin, GP, and Lansley, AB. *The human bronchial epithelial cell line 16HBE14o- as a model system of the airways for studying drug transport.* Int J Pharm, 2003. 257: 161.

290. Papazian, D, Wurtzen, PA, and Hansen, SW. *Polarized Airway Epithelial Models for Immunological Co-Culture Studies.* Int Arch Allergy Immunol, 2016. 170: 1.

291. de Souza Carvalho, C, Daum, N, and Lehr, CM. *Carrier interactions with the biological barriers of the lung: advanced in vitro models and challenges for pulmonary drug delivery.* Adv Drug Deliv Rev, 2014. 75: 129.

292. Asokananthan, N, Graham, PT, Fink, J, Knight, DA, Bakker, AJ, McWilliam, AS, Thompson, PJ, and Stewart, GA. *Activation of protease-activated receptor (PAR)-1, PAR-2, and PAR-4 stimulates IL-6, IL-8, and prostaglandin E2 release from human respiratory epithelial cells.* J Immunol, 2002. 168: 3577.

293. Adam, E, Hansen, KK, Astudillo Fernandez, O, Coulon, L, Bex, F, Duhant, X, Jaumotte, E, Hollenberg, MD, and Jacquet, A. *The house dust mite allergen Der p 1, unlike Der p 3, stimulates the expression of interleukin-8 in human airway epithelial cells via a proteinase-activated receptor-2-independent mechanism.* J Biol Chem, 2006. 281: 6910.

294. Jeong, SK, Kim, HJ, Youm, JK, Ahn, SK, Choi, EH, Sohn, MH, Kim, KE, Hong, JH, Shin, DM, and Lee, SH. *Mite and cockroach allergens activate protease-activated receptor 2 and delay epidermal permeability barrier recovery.* J Invest Dermatol, 2008. 128: 1930.

295. Chevigne, A and Jacquet, A. *Emerging roles of the protease allergen Der p 1 in house dust mite-induced airway inflammation.* J Allergy Clin Immunol, 2018. 142: 398.

296. Anderson, JM and Van Itallie, CM. *Tight junctions and the molecular basis for regulation of paracellular permeability.* Am J Physiol, 1995. 269: G467.

297. Denker, BM and Nigam, SK. *Molecular structure and assembly of the tight junction.* Am J Physiol, 1998. 274: F1.

298. Kesic, MJ, Hernandez, M, and Jaspers, I. *Airway protease/antiprotease imbalance in atopic asthmatics contributes to increased influenza A virus cleavage and replication.* Respir Res, 2012. 13: 82.

299. Hohlfeld, JM, Erpenbeck, VJ, and Krug, N. *Surfactant proteins SP-A and SP-D as modulators of the allergic inflammation in asthma.* Pathobiology, 2002. 70: 287.

300. Vignola, AM, Chanez, P, Bonsignore, G, Godard, P, and Bousquet, J. *Structural consequences of airway inflammation in asthma.* Journal of Allergy and Clinical Immunology, 2000. 105: S514.

301. Bonser, LR and Erle, DJ. *Airway Mucus and Asthma: The Role of MUC5AC and MUC5B.* J Clin Med, 2017. 6.

302. Xiao, C, Puddicombe, SM, Field, S, Haywood, J, Broughton-Head, V, Puxeddu, I, Haitchi, HM, Vernon-Wilson, E, Sammut, D, Bedke, N*, et al. Defective epithelial barrier function in asthma.* J Allergy Clin Immunol, 2011. 128: 549.

303. Johnson, JR, Roos, A, Berg, T, Nord, M, and Fuxe, J. *Chronic respiratory aeroallergen exposure in mice induces epithelial-mesenchymal transition in the large airways.* PLoS One, 2011. 6: e16175.

304. Johnson, JR, Wiley, RE, Fattouh, R, Swirski, FK, Gajewska, BU, Coyle, AJ, Gutierrez-Ramos, JC, Ellis, R, Inman, MD, and Jordana, M. *Continuous exposure to house dust mite elicits chronic airway inflammation and structural remodeling.* Am J Respir Crit Care Med, 2004. 169: 378.

305. Jacquet, A, Campisi, V, Szpakowska, M, Dumez, ME, Galleni, M, and Chevigne, A. *Profiling the Extended Cleavage Specificity of the House Dust Mite Protease Allergens Der p 1, Der p 3 and Der p 6 for the Prediction of New Cell Surface Protein Substrates.* Int J Mol Sci, 2017. 18.

306. Gallwitz, M, Enoksson, M, Thorpe, M, and Hellman, L. *The extended cleavage specificity of human thrombin.* PLoS One, 2012. 7: e31756.

307. Deu, E, Verdoes, M, and Bogyo, M. *New approaches for dissecting protease functions to improve probe development and drug discovery.* Nat Struct Mol Biol, 2012. 19: 9.

308. Furmonaviciene, R, Ghaemmaghami, AM, Boyd, SE, Jones, NS, Bailey, K, Willis, AC, Sewell, HF, Mitchell, DA, and Shakib, F. *The protease allergen Der p 1 cleaves cell surface DC-SIGN and DC-SIGNR: experimental analysis of in silico substrate identification and implications in allergic responses.* Clin Exp Allergy, 2007. 37: 231.

309. Lopez-Rodriguez, JC, Solis-Fernandez, G, Barderas, R, Villalba, M, and Batanero, E. *Effects of Ole e 1 on Human Bronchial Epithelial Cells Cultured at the Air-Liquid Interface.* J Investig Allergol Clin Immunol, 2018. 28: 186.

310. Phillips, C, Coward, WR, Pritchard, DI, and Hewitt, CR. *Basophils express a type 2 cytokine profile on exposure to proteases from helminths and house dust mites.* J Leukoc Biol, 2003. 73: 165.

311. Bieneman, AP, Chichester, KL, Chen, YH, and Schroeder, JT. *Toll-like receptor 2 ligands activate human basophils for both IgE-dependent and IgE-independent secretion.* J Allergy Clin Immunol, 2005. 115: 295.

312. Siracusa, MC, Saenz, SA, Hill, DA, Kim, BS, Headley, MB, Doering, TA, Wherry, EJ, Jessup, HK, Siegel, LA, Kambayashi, T*, et al. TSLP promotes interleukin-3-independent basophil haematopoiesis and type 2 inflammation.* Nature, 2011. 477: 229.

313. Noti, M, Wojno, ED, Kim, BS, Siracusa, MC, Giacomin, PR, Nair, MG, Benitez, AJ, Ruymann, KR, Muir, AB, Hill, DA*, et al. Thymic stromal lymphopoietin-elicited basophil responses promote eosinophilic esophagitis.* Nat Med, 2013. 19: 1005.

314. Wildner, S, Elsasser, B, Stemeseder, T, Briza, P, Soh, WT, Villalba, M, Lidholm, J, Brandstetter, H, and Gadermaier, G. *Endolysosomal Degradation of Allergenic Ole e 1-Like Proteins: Analysis of Proteolytic Cleavage Sites Revealing T Cell Epitope-Containing Peptides.* Int J Mol Sci, 2017. 18.

315. Gika, HG, Theodoridis, GA, and Wilson, ID. *Metabolic Profiling: Status, Challenges, and Perspective.* Methods Mol Biol, 2018. 1738: 3.

316. Ramautar, R, Somsen, GW, and de Jong, GJ. *CE-MS for metabolomics: Developments and applications in the period 2016-2018.* Electrophoresis, 2019. 40: 165.

317. Kuehnbaum, NL and Britz-McKibbin, P. *New advances in separation science for metabolomics: resolving chemical diversity in a post-genomic era.* Chem Rev, 2013. 113: 2437.

318. Worley, B and Powers, R. *Multivariate Analysis in Metabolomics.* Curr Metabolomics, 2013. 1: 92.

319. Galli, SJ, Tsai, M, and Piliponsky, AM. *The development of allergic inflammation.* Nature, 2008. 454: 445.

320. Caldeira, M, Barros, AS, Bilelo, MJ, Parada, A, Camara, JS, and Rocha, SM. *Profiling allergic asthma volatile metabolic patterns using a headspace-solid phase microextraction/gas chromatography based methodology.* J Chromatogr A, 2011. 1218: 3771.

321. Villasenor, A, Rosace, D, Obeso, D, Perez-Gordo, M, Chivato, T, Barbas, C, Barber, D, and Escribese, MM. *Allergic asthma: an overview of metabolomic strategies leading to the identification of biomarkers in the field.* Clin Exp Allergy, 2017. 47: 442.

322. Scrivo, R, Casadei, L, Valerio, M, Priori, R, Valesini, G, and Manetti, C. *Metabolomics approach in allergic and rheumatic diseases.* Curr Allergy Asthma Rep, 2014. 14: 445.

323. Gostner, JM, Becker, K, Kofler, H, Strasser, B, and Fuchs, D. *Tryptophan Metabolism in Allergic Disorders.* Int Arch Allergy Immunol, 2016. 169: 203.

324. Maarsingh, H, Zaagsma, J, and Meurs, H. *Arginine homeostasis in allergic asthma.* Eur J Pharmacol, 2008. 585: 375.

325. Van der Leek, AP, Yanishevsky, Y, and Kozyrskyj, AL. *The Kynurenine Pathway As a Novel Link between Allergy and the Gut Microbiome.* Front Immunol, 2017. 8: 1374.

326. Schmidt, SK, Muller, A, Heseler, K, Woite, C, Spekker, K, MacKenzie, CR, and Daubener, W. *Antimicrobial and immunoregulatory properties of human tryptophan 2,3-dioxygenase.* Eur J Immunol, 2009. 39: 2755.

327. Badawy, AA. *Kynurenine Pathway of Tryptophan Metabolism: Regulatory and Functional Aspects.* Int J Tryptophan Res, 2017. 10: 1178646917691938.

328. Allegri, G, Bertazzo, A, Biasiolo, M, Costa, CV, and Ragazzi, E. *Kynurenine pathway enzymes in different species of animals.* Adv Exp Med Biol, 2003. 527: 455.

329. Jia, S, Guo, P, Ge, X, Wu, H, Lu, J, and Fan, X. *Overexpression of indoleamine 2, 3-dioxygenase contributes to the repair of human airway epithelial cells inhibited by dexamethasone via affecting the MAPK/ERK signaling pathway.* Exp Ther Med, 2018. 16: 282.

330. Munn, DH and Mellor, AL. *Indoleamine 2,3 dioxygenase and metabolic control of immune responses.* Trends Immunol, 2013. 34: 137.

331. Orabona, C, Pallotta, MT, and Grohmann, U. *Different partners, opposite outcomes: a new perspective of the immunobiology of indoleamine 2,3-dioxygenase.* Mol Med, 2012. 18: 834.

332. Taher, YA, Piavaux, BJ, Gras, R, van Esch, BC, Hofman, GA, Bloksma, N, Henricks, PA, and van Oosterhout, AJ. *Indoleamine 2,3-dioxygenase-dependent tryptophan metabolites contribute to tolerance induction during allergen immunotherapy in a mouse model.* J Allergy Clin Immunol, 2008. 121: 983.

333. Wu, H, Gong, J, and Liu, Y. *Indoleamine 2, 3-dioxygenase regulation of immune response (Review).* Mol Med Rep, 2018. 17: 4867.

334. von Bubnoff, D and Bieber, T. *The indoleamine 2,3-dioxygenase (IDO) pathway controls allergy.* Allergy, 2012. 67: 718.

335. Moingeon, P, Batard, T, Fadel, R, Frati, F, Sieber, J, and Van Overtvelt, L. *Immune mechanisms of allergen-specific sublingual immunotherapy.* Allergy, 2006. 61: 151.

336. Fallarino, F and Grohmann, U. *Using an ancient tool for igniting and propagating immune tolerance: IDO as an inducer and amplifier of regulatory T cell functions.* Curr Med Chem, 2011. 18: 2215.

337. Fallarino, F, Grohmann, U, and Puccetti, P. *Indoleamine 2,3-dioxygenase: from catalyst to signaling function.* Eur J Immunol, 2012. 42: 1932.

338. Ciprandi, G, De Amici, M, Tosca, M, and Fuchs, D. *Tryptophan metabolism in allergic rhinitis: the effect of pollen allergen exposure.* Hum Immunol, 2010. 71: 911.

339. Aldajani, WA, Salazar, F, Sewell, HF, Knox, A, and Ghaemmaghami, AM. *Expression and regulation of immune-modulatory enzyme indoleamine 2,3-dioxygenase (IDO) by human airway epithelial cells and its effect on T cell activation.* Oncotarget, 2016. 7: 57606.

340. Raitala, A, Karjalainen, J, Oja, SS, Kosunen, TU, and Hurme, M. *Indoleamine 2,3-dioxygenase (IDO) activity is lower in atopic than in non-atopic individuals and is enhanced by environmental factors protecting from atopy.* Mol Immunol, 2006. 43: 1054.

341. Luukkainen, A, Karjalainen, J, Hurme, M, Paavonen, T, Huhtala, H, and Toppila-Salmi, S. *Relationships of indoleamine 2,3-dioxygenase activity and cofactors with asthma and nasal polyps.* Am J Rhinol Allergy, 2014. 28: e5.

342. Kositz, C, Schroecksnadel, K, Grander, G, Schennach, H, Kofler, H, and Fuchs, D. *High serum tryptophan concentration in pollinosis patients is associated with unresponsiveness to pollen extract therapy.* Int Arch Allergy Immunol, 2008. 147: 35.

343. Scott, JA and Grasemann, H. *Arginine metabolism in asthma.* Immunol Allergy Clin North Am, 2014. 34: 767.

344. Morris, SM, Jr. *Regulation of enzymes of the urea cycle and arginine metabolism.* Annu Rev Nutr, 2002. 22: 87.

345. Morris, SM, Jr. *Arginine metabolism: boundaries of our knowledge.* J Nutr, 2007. 137: 1602s.

346. Wu, G and Morris, SM, Jr. *Arginine metabolism: nitric oxide and beyond.* Biochem J, 1998. 336 1.

347. Ricciardolo, FL, Sterk, PJ, Gaston, B, and Folkerts, G. *Nitric oxide in health and disease of the respiratory system.* Physiol Rev, 2004. 84: 731.

348. Kenyon, NJ, Last, M, Bratt, JM, Kwan, VW, O'Roark, E, and Linderholm, A. *l-Arginine Supplementation and Metabolism in Asthma.* Pharmaceuticals, 2011. 4: 187.

349. Mabalirajan, U, Ahmad, T, Leishangthem, GD, Joseph, DA, Dinda, AK, Agrawal, A, and Ghosh, B. *Beneficial effects of high dose of L-arginine on airway hyperresponsiveness and airway inflammation in a murine model of asthma.* J Allergy Clin Immunol, 2010. 125: 626.

350. Roos, AB, Mori, M, Gronneberg, R, Osterlund, C, Claesson, HE, Wahlstrom, J, Grunewald, J, Eklund, A, Erjefalt, JS, Lundberg, JO*, et al. Elevated exhaled nitric oxide in allergen-provoked asthma is associated with airway epithelial iNOS.* PLoS One, 2014. 9: e90018.

351. Saleh, D, Ernst, P, Lim, S, Barnes, PJ, and Giaid, A. *Increased formation of the potent oxidant peroxynitrite in the airways of asthmatic patients is associated with induction of nitric oxide synthase: effect of inhaled glucocorticoid.* Faseb j, 1998. 12: 929.

352. van der Vliet, A, Eiserich, JP, and Cross, CE. *Nitric oxide: a pro-inflammatory mediator in lung disease?* Respir Res, 2000. 1: 67.

353. Sadeghi-Hashjin, G, Folkerts, G, Henricks, PA, Verheyen, AK, van der Linde, HJ, van Ark, I, Coene, A, and Nijkamp, FP. *Peroxynitrite induces airway hyperresponsiveness in guinea pigs in vitro and in vivo.* Am J Respir Crit Care Med, 1996. 153: 1697.

354. Hanazawa, T, Kharitonov, SA, and Barnes, PJ. *Increased nitrotyrosine in exhaled breath condensate of patients with asthma.* Am J Respir Crit Care Med, 2000. 162: 1273.

355. Closs, EI, Simon, A, Vekony, N, and Rotmann, A. *Plasma membrane transporters for arginine.* J Nutr, 2004. 134: 2752S.

356. Durante, W. *Regulation of L-arginine transport and metabolism in vascular smooth muscle cells.* Cell Biochem Biophys, 2001. 35: 19.

357. Corraliza, IM, Soler, G, Eichmann, K, and Modolell, M. *Arginase induction by suppressors of nitric oxide synthesis (IL-4, IL-10 and PGE2) in murine bone-marrow-derived macrophages.* Biochem Biophys Res Commun, 1995. 206: 667.

358. Modolell, M, Corraliza, IM, Link, F, Soler, G, and Eichmann, K. *Reciprocal regulation of the nitric oxide synthase/arginase balance in mouse bone marrow-derived macrophages by TH1 and TH2 cytokines.* Eur J Immunol, 1995. 25: 1101.

359. Klasen, S, Hammermann, R, Fuhrmann, M, Lindemann, D, Beck, KF, Pfeilschifter, J, and Racke, K. *Glucocorticoids inhibit lipopolysaccharide-induced*

up-regulation of arginase in rat alveolar macrophages. Br J Pharmacol, 2001. 132: 1349.

360. Bergeron, C, Boulet, LP, Page, N, Laviolette, M, Zimmermann, N, Rothenberg, ME, and Hamid, Q. *Influence of cigarette smoke on the arginine pathway in asthmatic airways: increased expression of arginase I.* J Allergy Clin Immunol, 2007. 119: 391.
361. de Halleux, S, Stura, E, VanderElst, L, Carlier, V, Jacquemin, M, and Saint-Remy, JM. *Three-dimensional structure and IgE-binding properties of mature fully active Der p 1, a clinically relevant major allergen.* J Allergy Clin Immunol, 2006. 117: 571.
362. Stewart, GA, Simpson, RJ, Thomas, WR, and Turner, KJ. *Physicochemical characterization of a major protein allergen, Der p I, from the house dust mite, Dermatophagoides pteronyssinus. Amino acid analysis and circular dichroism studies.* Int Arch Allergy Appl Immunol, 1987. 82: 444.
363. Tew, KD and Townsend, DM. *Regulatory functions of glutathione S-transferase P1-1 unrelated to detoxification.* Drug Metab Rev, 2011. 43: 179.
364. Bartolini, D and Galli, F. *The functional interactome of GSTP: A regulatory biomolecular network at the interface with the Nrf2 adaption response to oxidative stress.* J Chromatogr B Analyt Technol Biomed Life Sci, 2016. 1019: 29.
365. Klomsiri, C, Karplus, PA, and Poole, LB. *Cysteine-based redox switches in enzymes.* Antioxid Redox Signal, 2011. 14: 1065.
366. Burgoyne, JR, Madhani, M, Cuello, F, Charles, RL, Brennan, JP, Schroder, E, Browning, DD, and Eaton, P. *Cysteine redox sensor in PKGIa enables oxidant-induced activation.* Science, 2007. 317: 1393.
367. Giles, NM, Watts, AB, Giles, GI, Fry, FH, Littlechild, JA, and Jacob, C. *Metal and redox modulation of cysteine protein function.* Chem Biol, 2003. 10: 677.
368. Howie, AF, Bell, D, Hayes, PC, Hayes, JD, and Beckett, GJ. *Glutathione S-transferase isoenzymes in human bronchoalveolar lavage: a possible early marker for the detection of lung cancer.* Carcinogenesis, 1990. 11: 295.
369. Kaul, P, Sathish, HA, and Prakash, V. *Effect of metal ions on structure and activity of papain from Carica papaya.* Nahrung, 2002. 46: 2.
370. Takai, T, Kato, T, Hatanaka, H, Inui, K, Nakazawa, T, Ichikawa, S, Mitsuishi, K, Ogawa, H, and Okumura, K. *Modulation of allergenicity of major house dust mite allergens Der f 1 and Der p 1 by interaction with an endogenous ligand.* J Immunol, 2009. 183: 7958.

371. Bodas, M, Van Westphal, C, Carpenter-Thompson, R, D, KM, and Vij, N. *Nicotine exposure induces bronchial epithelial cell apoptosis and senescence via ROS mediated autophagy-impairment.* Free Radic Biol Med, 2016. 97: 441.

372. Comer, DM, Elborn, JS, and Ennis, M. *Inflammatory and cytotoxic effects of acrolein, nicotine, acetylaldehyde and cigarette smoke extract on human nasal epithelial cells.* BMC Pulm Med, 2014. 14: 32.

373. Li, Q, Zhou, X, Kolosov, VP, and Perelman, JM. *Nicotine suppresses inflammatory factors in HBE16 airway epithelial cells after exposure to cigarette smoke extract and lipopolysaccharide.* Transl Res, 2010. 156: 326.

374. Wright, HE, Jr., Burton, WW, and Berry, RC, Jr. *Soluble browning reaction pigments of aged Burleytobacco. I. The non-dialyzable fraction.* Arch Biochem Biophys, 1960. 86: 94.

375. Becker, CG and Dubin, T. *Activation of factor XII by tobacco glycoprotein.* J Exp Med, 1977. 146: 457.

376. Koethe, SM, Nelson, KE, and Becker, CG. *Activation of the classical pathway of complement by tobacco glycoprotein (TGP).* J Immunol, 1995. 155: 826.

377. Eiserich, JP, van der Vliet, A, Handelman, GJ, Halliwell, B, and Cross, CE. *Dietary antioxidants and cigarette smoke-induced biomolecular damage: a complex interaction.* Am J Clin Nutr, 1995. 62: 1490s.

378. Clunes, LA, Bridges, A, Alexis, N, and Tarran, R. *In vivo versus in vitro airway surface liquid nicotine levels following cigarette smoke exposure.* J Anal Toxicol, 2008. 32: 201.

379. Rusznak, C, Sapsford, RJ, Devalia, JL, Justin John, R, Hewitt, EL, Lamont, AG, Wood, AJ, Shah, SS, Davies, RJ, and Lozewicz, S. *Cigarette smoke potentiates house dust mite allergen-induced increase in the permeability of human bronchial epithelial cells in vitro.* Am J Respir Cell Mol Biol, 1999. 20: 1238.

380. Petecchia, L, Sabatini, F, Varesio, L, Camoirano, A, Usai, C, Pezzolo, A, and Rossi, GA. *Bronchial airway epithelial cell damage following exposure to cigarette smoke includes disassembly of tight junction components mediated by the extracellular signal-regulated kinase 1/2 pathway.* Chest, 2009. 135: 1502.

381. Heijink, IH, Brandenburg, SM, Postma, DS, and van Oosterhout, AJ. *Cigarette smoke impairs airway epithelial barrier function and cell-cell contact recovery.* Eur Respir J, 2012. 39: 419.

382. van der Toorn, M, Rezayat, D, Kauffman, HF, Bakker, SJ, Gans, RO, Koeter, GH, Choi, AM, van Oosterhout, AJ, and Slebos, DJ. *Lipid-soluble components in cigarette smoke induce mitochondrial production of reactive oxygen species in lung epithelial cells.* Am J Physiol Lung Cell Mol Physiol, 2009. 297: L109.

383. Gerloff, J, Sundar, IK, Freter, R, Sekera, ER, Friedman, AE, Robinson, R, Pagano, T, and Rahman, I. *Inflammatory Response and Barrier Dysfunction by Different e-Cigarette Flavoring Chemicals Identified by Gas Chromatography-Mass Spectrometry in e-Liquids and e-Vapors on Human Lung Epithelial Cells and Fibroblasts.* Appl In Vitro Toxicol, 2017. 3: 28.

384. Olivera, DS, Boggs, SE, Beenhouwer, C, Aden, J, and Knall, C. *Cellular mechanisms of mainstream cigarette smoke-induced lung epithelial tight junction permeability changes in vitro.* Inhal Toxicol, 2007. 19: 13.

385. Olivera, D, Knall, C, Boggs, S, and Seagrave, J. *Cytoskeletal modulation and tyrosine phosphorylation of tight junction proteins are associated with mainstream cigarette smoke-induced permeability of airway epithelium.* Exp Toxicol Pathol, 2010. 62: 133.

386. Jimenez, FR, Lewis, JB, Belgique, ST, Milner, DC, Lewis, AL, Dunaway, TM, Egbert, KM, Winden, DR, Arroyo, JA, and Reynolds, PR. *Cigarette smoke and decreased oxygen tension inhibit pulmonary claudin-6 expression.* Exp Lung Res, 2016. 42: 440.

387. Shaykhiev, R, Otaki, F, Bonsu, P, Dang, DT, Teater, M, Strulovici-Barel, Y, Salit, J, Harvey, BG, and Crystal, RG. *Cigarette smoking reprograms apical junctional complex molecular architecture in the human airway epithelium in vivo.* Cell Mol Life Sci, 2011. 68: 877.

388. Gangl, K, Reininger, R, Bernhard, D, Campana, R, Pree, I, Reisinger, J, Kneidinger, M, Kundi, M, Dolznig, H, Thurnher, D*, et al. Cigarette smoke facilitates allergen penetration across respiratory epithelium.* Allergy, 2009. 64: 398.

389. Schuliga, M. *NF-kappaB Signaling in Chronic Inflammatory Airway Disease.* Biomolecules, 2015. 5: 1266.

390. Xiao, W, Hodge, DR, Wang, L, Yang, X, Zhang, X, and Farrar, WL. *NF-kappaB activates IL-6 expression through cooperation with c-Jun and IL6-AP1 site, but is independent of its IL6-NFkappaB regulatory site in autocrine human multiple myeloma cells.* Cancer Biol Ther, 2004. 3: 1007.

391. Manzel, LJ, Shi, L, O'Shaughnessy, PT, Thorne, PS, and Look, DC. *Inhibition by cigarette smoke of nuclear factor-kappaB-dependent response to bacteria in the airway.* Am J Respir Cell Mol Biol, 2011. 44: 155.

392. Roder-Stolinski, C, Fischader, G, Oostingh, GJ, Feltens, R, Kohse, F, von Bergen, M, Morbt, N, Eder, K, Duschl, A, and Lehmann, I. *Styrene induces an inflammatory response in human lung epithelial cells via oxidative stress and NF-kappaB activation.* Toxicol Appl Pharmacol, 2008. 231: 241.

393. Liu, X, Togo, S, Al-Mugotir, M, Kim, H, Fang, Q, Kobayashi, T, Wang, X, Mao, L, Bitterman, P, and Rennard, S. *NF-kappaB mediates the survival of human bronchial epithelial cells exposed to cigarette smoke extract.* Respir Res, 2008. 9: 66.

394. Moodie, FM, Marwick, JA, Anderson, CS, Szulakowski, P, Biswas, SK, Bauter, MR, Kilty, I, and Rahman, I. *Oxidative stress and cigarette smoke alter chromatin remodeling but differentially regulate NF-kappaB activation and proinflammatory cytokine release in alveolar epithelial cells.* Faseb j, 2004. 18: 1897.

395. Lennon, SV, Martin, SJ, and Cotter, TG. *Dose-dependent induction of apoptosis in human tumour cell lines by widely diverging stimuli.* Cell Prolif, 1991. 24: 203.

396. Rastrick, JM, Stevenson, CS, Eltom, S, Grace, M, Davies, M, Kilty, I, Evans, SM, Pasparakis, M, Catley, MC, Lawrence, T*, et al. Cigarette smoke induced airway inflammation is independent of NF-kappaB signalling.* PLoS One, 2013. 8: e54128.

397. Koo, JB and Han, JS. *Cigarette smoke extract-induced interleukin-6 expression is regulated by phospholipase D1 in human bronchial epithelial cells.* J Toxicol Sci, 2016. 41: 77.

398. Mortaz, E, Henricks, PA, Kraneveld, AD, Givi, ME, Garssen, J, and Folkerts, G. *Cigarette smoke induces the release of CXCL-8 from human bronchial epithelial cells via TLRs and induction of the inflammasome.* Biochim Biophys Acta, 2011. 1812: 1104.

399. Zhou, G, Xiao, W, Xu, C, Hu, Y, Wu, X, Huang, F, Lu, X, Shi, C, and Wu, X. *Chemical constituents of tobacco smoke induce the production of interleukin-8 in human bronchial epithelium, 16HBE cells.* Tob Induc Dis, 2016. 14: 24.

400. Pace, E, Di Sano, C, Sciarrino, S, Scafidi, V, Ferraro, M, Chiappara, G, Siena, L, Gangemi, S, Vitulo, P, Giarratano, A*, et al. Cigarette smoke alters IL-33 expression and release in airway epithelial cells.* Biochim Biophys Acta, 2014. 1842: 1630.

401. Pace, E, Ferraro, M, Siena, L, Melis, M, Montalbano, AM, Johnson, M, Bonsignore, MR, Bonsignore, G, and Gjomarkaj, M. *Cigarette smoke increases Toll-like receptor 4 and modifies lipopolysaccharide-mediated responses in airway epithelial cells.* Immunology, 2008. 124: 401.

402. Cantin, AM. *Cellular response to cigarette smoke and oxidants: adapting to survive.* Proc Am Thorac Soc, 2010. 7: 368.

403. Rangasamy, T, Cho, CY, Thimmulappa, RK, Zhen, L, Srisuma, SS, Kensler, TW, Yamamoto, M, Petrache, I, Tuder, RM, and Biswal, S. *Genetic ablation of Nrf2*

enhances susceptibility to cigarette smoke-induced emphysema in mice. J Clin Invest, 2004. 114: 1248.

404. Kobayashi, M and Yamamoto, M. *Molecular mechanisms activating the Nrf2-Keap1 pathway of antioxidant gene regulation.* Antioxid Redox Signal, 2005. 7: 385.
405. Schamberger, AC, Mise, N, Jia, J, Genoyer, E, Yildirim, AO, Meiners, S, and Eickelberg, O. *Cigarette smoke-induced disruption of bronchial epithelial tight junctions is prevented by transforming growth factor-beta.* Am J Respir Cell Mol Biol, 2014. 50: 1040.
406. Pertovaara, M, Heliovaara, M, Raitala, A, Oja, SS, Knekt, P, and Hurme, M. *The activity of the immunoregulatory enzyme indoleamine 2,3-dioxygenase is decreased in smokers.* Clin Exp Immunol, 2006. 145: 469.
407. Hucke, C, MacKenzie, CR, Adjogble, KD, Takikawa, O, and Daubener, W. *Nitric oxide-mediated regulation of gamma interferon-induced bacteriostasis: inhibition and degradation of human indoleamine 2,3-dioxygenase.* Infect Immun, 2004. 72: 2723.
408. Samelson-Jones, BJ and Yeh, SR. *Interactions between nitric oxide and indoleamine 2,3-dioxygenase.* Biochemistry, 2006. 45: 8527.
409. Chen, W, Liang, X, Peterson, AJ, Munn, DH, and Blazar, BR. *The indoleamine 2,3-dioxygenase pathway is essential for human plasmacytoid dendritic cell-induced adaptive T regulatory cell generation.* J Immunol, 2008. 181: 5396.
410. Buro-Auriemma, LJ, Salit, J, Hackett, NR, Walters, MS, Strulovici-Barel, Y, Staudt, MR, Fuller, J, Mahmoud, M, Stevenson, CS, Hilton, H*, et al. Cigarette smoking induces small airway epithelial epigenetic changes with corresponding modulation of gene expression.* Hum Mol Genet, 2013. 22: 4726.
411. Kode, A, Yang, SR, and Rahman, I. *Differential effects of cigarette smoke on oxidative stress and proinflammatory cytokine release in primary human airway epithelial cells and in a variety of transformed alveolar epithelial cells.* Respir Res, 2006. 7: 132.
412. Mathis, C, Poussin, C, Weisensee, D, Gebel, S, Hengstermann, A, Sewer, A, Belcastro, V, Xiang, Y, Ansari, S, Wagner, S*, et al. Human bronchial epithelial cells exposed in vitro to cigarette smoke at the air-liquid interface resemble bronchial epithelium from human smokers.* Am J Physiol Lung Cell Mol Physiol, 2013. 304: L489.
413. Beisswenger, C, Platz, J, Seifart, C, Vogelmeier, C, and Bals, R. *Exposure of differentiated airway epithelial cells to volatile smoke in vitro.* Respiration, 2004. 71: 402.

414. Rusznak, C, Sapsford, RJ, Devalia, JL, Shah, SS, Hewitt, EL, Lamont, AG, Davies, RJ, and Lozewicz, S. *Interaction of cigarette smoke and house dust mite allergens on inflammatory mediator release from primary cultures of human bronchial epithelial cells.* Clin Exp Allergy, 2001. 31: 226.

415. Vanella, L, Li Volti, G, Distefano, A, Raffaele, M, Zingales, V, Avola, R, Tibullo, D, and Barbagallo, I. *A new antioxidant formulation reduces the apoptotic and damaging effect of cigarette smoke extract on human bronchial epithelial cells.* Eur Rev Med Pharmacol Sci, 2017. 21: 5478.

416. Dong, P, Fu, X, Wang, X, Wang, WM, Cao, WM, and Zhang, WY. *Protective effects of sesaminol on BEAS-2B cells impaired by cigarette smoke extract.* Cell Biochem Biophys, 2015. 71: 1207.

417. Vu, AT, Taylor, KM, Holman, MR, Ding, YS, Hearn, B, and Watson, CH. *Polycyclic Aromatic Hydrocarbons in the Mainstream Smoke of Popular U.S. Cigarettes.* Chem Res Toxicol, 2015. 28: 1616.

418. Franco, R, Sanchez-Olea, R, Reyes-Reyes, EM, and Panayiotidis, MI. *Environmental toxicity, oxidative stress and apoptosis: menage a trois.* Mutat Res, 2009. 674: 3.

419. Macnee, W and Rahman, I. *Oxidants and antioxidants as therapeutic targets in chronic obstructive pulmonary disease.* Am J Respir Crit Care Med, 1999. 160: S58.

420. Saez-Cirion, A, Nir, S, Lorizate, M, Agirre, A, Cruz, A, Perez-Gil, J, and Nieva, JL. *Sphingomyelin and cholesterol promote HIV-1 gp41 pretransmembrane sequence surface aggregation and membrane restructuring.* J Biol Chem, 2002. 277: 21776.

421. Perez-Gil, J, Nag, K, Taneva, S, and Keough, KM. *Pulmonary surfactant protein SP-C causes packing rearrangements of dipalmitoylphosphatidylcholine in spread monolayers.* Biophys J, 1992. 63: 197.

422. Xu, X and London, E. *The effect of sterol structure on membrane lipid domains reveals how cholesterol can induce lipid domain formation.* Biochemistry, 2000. 39: 843.

423. Vaidya, SV and Narvaez, AR. *Understanding interactions between immunoassay excipient proteins and surfactants at air-aqueous interface.* Colloids Surf B Biointerfaces, 2014. 113: 285.

424. Sunde, M, Pham, CLL, and Kwan, AH. *Molecular Characteristics and Biological Functions of Surface-Active and Surfactant Proteins.* Annu Rev Biochem, 2017. 86: 585.

425. Damodaran, S. *Protein Stabilization of Emulsions and Foams.* Journal of Food Science, 2005. 70: R54.

426. Bos, MA and van Vliet, T. *Interfacial rheological properties of adsorbed protein layers and surfactants: a review.* Adv Colloid Interface Sci, 2001. 91: 437.

427. Mitropoulos, V, Mutze, A, and Fischer, P. *Mechanical properties of protein adsorption layers at the air/water and oil/water interface: a comparison in light of the thermodynamical stability of proteins.* Adv Colloid Interface Sci, 2014. 206: 195.

428. Gangnard, S, Zuev, Y, Gaudin, J-C, Fedotov, V, Choiset, Y, Axelos, MAV, Chobert, J-M, and Haertlé, T. *Modifications of the charges at the N-terminus of bovine β-casein: Consequences on its structure and its micellisation.* Food Hydrocolloids, 2007. 21: 180.

429. Husband, FA, Garrood, MJ, Mackie, AR, Burnett, GR, and Wilde, PJ. *Adsorbed protein secondary and tertiary structures by circular dichroism and infrared spectroscopy with refractive index matched emulsions.* J Agric Food Chem, 2001. 49: 859.

430. Vance, SJ, McDonald, RE, Cooper, A, Smith, BO, and Kennedy, MW. *The structure of latherin, a surfactant allergen protein from horse sweat and saliva.* J R Soc Interface, 2013. 10: 20130453.

431. Sahin, NO and Burgess, DJ. *Competitive interfacial adsorption of blood proteins.* Farmaco, 2003. 58: 1017.

432. Scholl, I, Kalkura, N, Shedziankova, Y, Bergmann, A, Verdino, P, Knittelfelder, R, Kopp, T, Hantusch, B, Betzel, C, Dierks, K*, et al. Dimerization of the major birch pollen allergen Bet v 1 is important for its in vivo IgE-cross-linking potential in mice.* J Immunol, 2005. 175: 6645.

433. Dietrich, C, Bagatolli, LA, Volovyk, ZN, Thompson, NL, Levi, M, Jacobson, K, and Gratton, E. *Lipid rafts reconstituted in model membranes.* Biophys J, 2001. 80: 1417.

434. Simons, K and Toomre, D. *Lipid rafts and signal transduction.* Nat Rev Mol Cell Biol, 2000. 1: 31.

435. Dufourc, EJ. *Sterols and membrane dynamics.* J Chem Biol, 2008. 1: 63.

436. Marsh, D. *Lateral pressure in membranes.* Biochim Biophys Acta, 1996. 1286: 183.

437. Moskovitz, Y and Srebnik, S. *Conformational changes of globular proteins upon adsorption on a hydrophobic surface.* Phys Chem Chem Phys, 2014. 16: 11698.

438. Taeusch, HW and Keough, KM. *Inactivation of pulmonary surfactant and the treatment of acute lung injuries.* Pediatr Pathol Mol Med, 2001. 20: 519.

439. Holm, BA, Wang, Z, and Notter, RH. *Multiple mechanisms of lung surfactant inhibition.* Pediatr Res, 1999. 46: 85.

440. Warriner, HE, Ding, J, Waring, AJ, and Zasadzinski, JA. *A concentration-dependent mechanism by which serum albumin inactivates replacement lung surfactants.* Biophys J, 2002. 82: 835.

441. Hidalgo, A, Cruz, A, and Perez-Gil, J. *Barrier or carrier? Pulmonary surfactant and drug delivery.* Eur J Pharm Biopharm, 2015. 95: 117.

442. Hidalgo, A, Salomone, F, Fresno, N, Orellana, G, Cruz, A, and Pérez-Gil, J. *Efficient Interfacially Driven Vehiculization of Corticosteroids by Pulmonary Surfactant.* Langmuir, 2017. 33: 7929.

443. Mogensen, JE, Wimmer, R, Larsen, JN, Spangfort, MD, and Otzen, DE. *The major birch allergen, Bet v 1, shows affinity for a broad spectrum of physiological ligands.* J Biol Chem, 2002. 277: 23684.

444. Ichikawa, S, Takai, T, Yashiki, T, Takahashi, S, Okumura, K, Ogawa, H, Kohda, D, and Hatanaka, H. *Lipopolysaccharide binding of the mite allergen Der f 2.* Genes Cells, 2009. 14: 1055.

Lista de abreviaturas
List of abreviations

LISTA DE ABREVIATURAS / *LIST OF ABREVIATIONS*

a.u.	Arbitrary Units
AEC-I	Alveolar Epithelial Cell-type I
AEC-II	Alveolar Epithelial Cell-type II
AJ	Adherens Junctions
AJC	Apical Junction Complexes
ALI	Air Liquid Interface
B-ALI-D	B-ALI-Differentiation
B-ALI-G	B-ALI-Growth
BCA	Bicinchoninic Acid
Boc-QAR-AMC	N-tert-butoxycarbonyl-Gln-Ala-Arg-[AMC = 7-Amino-4-methylcoumarin]
BODIPY-PC	Boron-Dipyrromethene-PC
BSA	Bovine Serum Albumin
CC-10	Club-Cell-specific 10 kD Protein
CCL-22	C-C motif ligand 22
CD-4/-8	Cluster Domain-4 / -8
CDNB	2,4-Dinitrochlorobenzene
CE	Capillary Electrophoresis
CF	Correction Factor
CHO	Cholesterol
CNE	Cholestenone
COPD	Chronic Obstructive Pulmonary Disease
CSE	Cigarette Smoke Extract
CSLM	Confocal Scanning Laser Microscopy
DC	Dendritic Cells
DMEM	Dulbecco's Modified Eagle Medium
DNA	Deoxyribonucleic Acid
DPPC	Dipalmitoylphosphatidylcholine
EDTA	EthyleneDiamineTetraacetic Acid
ELF	Epithelial Lining Fluid
ELISA	Enzyme-linked immunosorbent assay
FBS	Fetal bovine serum
FOXJ1	Forkhead Box Protein J1
GAPDH	Glyceraldehyde 3-Phosphate Dehydrogenase
GC-MS	Gas Cromatography coupled to Mass Spectrometry
GM-CSF	Granulocyte/Macrophage Colony-Stimulating Factor
Grx	Glutaredoxin
GSH	Glutathione (Reduced)
GSSG	Glutathione (Oxidized)
GST	Glutathione-S-transferase

HDM	House Dust Mite
HMDN	Human Metabolome Data Number
HRP	Horse Radish Peroxidase
IDO-1	Indoleamine-pyrrole 2,3-dioxygenase Isoform 1
IFN-γ	Interferon Gamma
IgE	Immunoglobulin E
IgG	Immunoglobulin G
IKK	IκB Kinase
IL	Interleukine
ILC2	Innate Lymphoid Cells Type 2
iNOS	Inducible Nitric Oxide Synthase
IκB-β	Inhibitor of kappa B-beta
JAM-A	Junctional Adhesion Molecule-A
JUN	C-jun gene
KEGG	Kyoto Encyclopaedia of Genes and Genomes
LC-MS	Liquid Chromatography coupled to Mass Spectrometry
LC	Liquid-Condensed phase
LE	Liquid-Expanded phase
LPS	Lipopolysaccharide (endotoxin)
MALDI-TOF	Matrix-Assisted Laser Desorption/Ionization-Time Of Flight
MCP-3/4	Monocyte Chemotactic Protein-3/-4
MIG	Monokine Induced by Gamma interferon
MIP-3α	Macrophage Inflammatory Protein 3 Alpha
mRNA	Messenger RNA
MS	Mass spectrometry
MTT	3-(4,5-dimethylthiazol-2-yl)-2,5-Diphenyltetrazolium Bromide
MUC5AC	Mucin-5AC
NADPH	Nicotinamide Adenine Dinucleotide Phosphate
NEM	N-Ethylmaleimide
NFκB	Nuclear Factor kappa-light-chain-enhancer of Activated B Cells
NHBE	Normal Human Bronchial Epithelial cells
NRF2	Nuclear Factor (Erythroid-derived 2)-Related Factor-2
OPN	Osteopontin
PAH	Polycyclic Aromatic Hydrocarbons
PBS	Phosphate Buffer Saline
PC	Phosphatidylcholine
PCA	Principal Components Analysis
PCR	Polymerase Chain Reaction
PE	Phosphatidylethanolamine
PFA	Paraformaldehyde

PG	Phosphatidylglycerol
PI	Phosphatidylinositol
POPC	1-Palmitoyl-2-oleoyl-sn-glycero-3-phosphocholine
PRR	Pattern Recognition Receptor
PS	Phosphatidylserine
PTP	Protein Tyrosin Phosphatase
RANTES	Regulated on Activation, Normal T Cell Expressed and Secreted
RFS	Redox Fluorescence Switch assay
Rho-PE	Rhodamine-PE
RIPA	Radioimmunoprecipitation Assay Buffer
RNA	Ribonucleic Acid
RNS	Reactive Nitrogen Species
ROS	Reactive Oxygen Species
RT-PCR	Real-time PCR
SD	Standard Deviation
SDM	Significantly Different Metabolite
SDS-PAGE	Sodium Dodecyl Sulfate–PolyAcrylamide Gel Electrophoresis
SEM	Scanning Electron Microscopy
SLPI	Secretory Leukoprotease Inhibitor
SM	Sphingomyelin
SOD	SuperOxide Dismutase
SP	Surfactant Protein
sqPCR	Semi-quantitative PCR
TAE	Tris-Acetic-EDTA buffer
TBS	Tris Buffer Saline
TCR	T-Cell Receptor
TEER	Transepithelial Electrical Resistance
TEM	Transmission Electron Microscopy
Th2	T-helper type 2
TJ	Tight Junctions
TLR	Toll-Like Receptor
TNF	Tumor Necrosis Factor
Trx	Thioredoxin
TSLP	Thymic Stromal Lymphopoietin
XOR	Xanthine Oxidase Reductase
ZO-1	Zonula Occludens-1
$\Delta\Pi$	Change in Surface Pressure
Π_c	Critical Surface Pressure
Π_i	Initial Surface Pressure
Π_{max}	Maximum Surface Pressure

Artículos publicados
Published articles

LANGMUIR

Article

pubs.acs.org/Langmuir

Surface Activity as a Crucial Factor of the Biological Actions of Ole e 1, the Main Aeroallergen of Olive Tree (*Olea europaea*) Pollen

Juan C. López-Rodríguez,[†] Rodrigo Barderas,[†] Mercedes Echaide,[‡,§] Jesús Pérez-Gil,[‡,§] Mayte Villalba,[†] Eva Batanero,[*,†,#] and Antonio Cruz[*,‡,§,#]

[†]Departamento de Bioquímica y Biología Molecular I, Facultad de Ciencias Químicas and [‡]Departamento de Bioquímica y Biología Molecular I, Facultad de Ciencias Biológicas, Universidad Complutense de Madrid, 28040 Madrid, Spain

[§]Instituto de Investigación "Hospital 12 de Octubre", 28041 Madrid, Spain

ABSTRACT: Aeroallergens are airborne substances—mainly proteins—capable of triggering Th2-immune responses in respiratory allergies. They enter into the body through the upper airways, reaching the mucosa afterward. Mucosae lining at the luminal side consists of an epithelial barrier completely covered by mucus and pulmonary surfactant. Both pulmonary surfactant and plasma membrane of the epithelial cells represent two physiological phospholipid-based barriers where allergens first impact before triggering their biological effects. The interaction of allergens with lipids at relevant physiological surfaces could promote structural changes on the molecule, resulting on a potential modification of its allergenic properties. In this work, we have first described the surface and phospholipid interaction capabilities of the clinically relevant aeroallergen Ole e 1, the main allergen of olive tree pollen. By using epifluorescence microscopy of Langmuir transferred films, we observed that lipid-packed ordered domains may function as a preferential location for allergen to accumulate at the air−liquid interface, an effect that is abolished in the presence of cholestenone. The possible implications of phospholipid-interfacial effects in the modification of allergen structural and functional properties will be discussed.

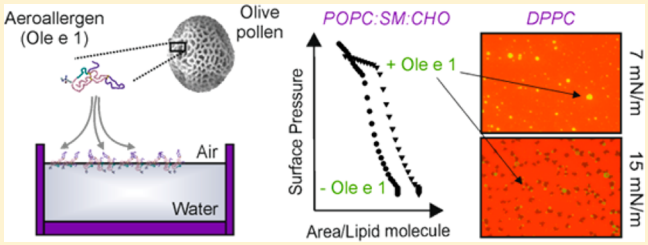

INTRODUCTION

Respiratory allergies constitute a growing health problem that affects approximately 25% of the world population.[1] These inflammatory disorders of the airways involve an exacerbated T helper 2 (Th2)-type immune response against environmental substances, usually harmless to most people, called aeroallergens or airborne allergens.[2] Aeroallergens—mainly proteins or glycoproteins—enter into the body through the upper airways, generally associated with inhaled particles that are deposited along the airway surface during breathing.[3]

Upon reaching the mucosal surface, aeroallergens make contact with two anatomical, physiological, and immunological barriers of lipid nature, in addition to the mucus layer: the pulmonary surfactant on the outer side of the mucus and the luminal plasma membrane of the airway epithelial cells.

Pulmonary surfactant is an interfacial lipoprotein complex synthesized by type II pneumocytes, which lines the entire respiratory epithelium. It is composed of approximately 90% of lipid—mainly dipalmitoyl-phosphatidylcholine (DPPC), which accounts for 40−50% of total surfactant mass—and 10% of surfactant proteins (SP): SP-A, SP-B, SP-C, and SP-D. Surfactant is primarily known for its surface-active properties at the alveolar air−liquid interface.[4] In addition to its biophysical properties, an immunomodulatory character has been shown by the hydrophilic collectins SP-A and SP-D that bind to various glycosylated ligands such as aeroallergens, thus playing a role in the control of airway inflammation including allergy.[5−7] However, the role of the hydrophobic proteins SP-B and SP-C in the pulmonary immune system has not yet been well-established.[8,9]

The airway epithelium consists of a continuous layer composed of different cell types with specific functions. It forms a physical barrier that prevents the invasion of various inhaled particles—including aeroallergens—through the establishment of intercellular junctions, and an active mucociliary clearance.[10] Therefore, there is increasing evidence for an important role played by the airway epithelial cells in orchestrating and influencing the immune responses.[11]

Surface activity of proteins is a fundamental property that strongly determines its interaction with biological lipid barriers. Protein surface activity is a thermodynamic process influenced by not only its molecular properties such as molecular size, amphipathicity, net charge, conformational flexibility, and stability, but also external factors including temperature and pH.[12] Rheological features of surface-active proteins—such as bovine serum albumin (BSA), β-lactoglobulin, lysozyme, and β-casein—have been widely studied for food industry applications in the formation and stability of food emulsions and foams.[13,14] However, so far the interfacial behavior of clinically relevant proteins, including allergens, has been poorly characterized.[15]

Received: July 29, 2016
Revised: October 10, 2016
Published: October 10, 2016

© 2016 American Chemical Society

DOI: 10.1021/acs.langmuir.6b02831
Langmuir 2016, 32, 11055−11062

Our study characterizes in detail, for the first time, the surface activity of the airborne allergen Ole e 1, and its interfacial behavior in the context of phospholipid layers, by using Langmuir devices. Langmuir-derived methods give us the chance to evaluate efficiently the surface activity of proteins and protein−lipid interactions by indirect measurements of surface tension. Due to its abundance and high prevalence, Ole e 1 is considered the main allergen of olive tree (*Olea europaea*) pollen, one of the most important causes of seasonal respiratory allergy in Mediterranean countries and large areas of America, South Africa, and Australia.[16]

EXPERIMENTAL SECTION

Materials. 1,2-Dihexadecanoyl-*sn*-glycero-3-phosphocholine (DPPC), 1-hexadecanoyl-2-(9*Z*-octadecenoyl)-*sn*-glycero-3-phosphocholine (POPC), sphingomyelin (SM, porcine brain), cholesterol (CHO), and 1,2-dioleoyl-*sn*-glycero-3-phosphoethanolamine-*N*-(lissamine rhodamine B sulfonyl) (Rho-PE), were provided by Avanti Polar Lipids (Alabaster, AL, USA). 4-Cholesten-3-one (CNE) was supplied by Sigma-Aldrich (St. Louis, MO, USA).

Methanol and chloroform were from Scharlab (Barcelona, Spain). Experiments were performed in 5 mM Tris-HCl, pH 7.4, containing 0.15 M NaCl, prepared in double-distilled water.

Methods. *Preparation of Lipid Mixtures.* Lipid mixtures were obtained by dissolving the appropriate amounts of lipids in chloroform:methanol (2:1, v/v): DPPC, POPC:SM:CHO (2:1:1, molar ratio), POPC:CHO (2:1, molar ratio), SM:CHO (2:1, molar ratio), and POPC:SM:CNE (2:1:1, molar ratio).

Allergen Purification and Fluorescent Labeling. Ole e 1 protein was isolated and purified from olive pollen (IBERPOLEN SL, Jaén, Spain) as previously described.[17] For epifluorescence experiments, Ole e 1 was labeled with Alexa 488 Fluor Succinimidyl Ester (Thermo Fisher Scientific, MA, USA), following manufacturer instructions. Labeled protein concentration and the degree of labeling were determinated.

Measurements of Surface Pressure and Interaction with Preformed Monolayers. Ole e 1 adsorption into an air−water interface was determinated by means of surface pressure changes ($\Delta\Pi$) over a time interval (Π-t isotherms), after injection of the protein into the buffer subphase (1.8 mL), at a final concentration ranging from 0.05 to 2.78 μM. Studies were carried out using a Langmuir-Wilhemy Teflon trough from NIMA Technologies (Coventry, UK) at 25 ± 1 °C, with constant stirring.

Changes in surface pressure were also monitored after injection of 10 μL Ole e 1 (0.55 μM) underneath preformed lipid monolayers at different initial pressures (Π_i), as described above. Lipid monolayers were formed by depositing small volumes of the different lipid solutions (0.1 mg/mL) on the surface until the required pressure was achieved. After 10 min to allow for solvent evaporation, protein solution was injected into the subphase and $\Delta\Pi$ were monitored. Maximum increase in pressure ($\Delta\Pi_{max}$) and critical insertion surface (Π_c) pressures were estimated from $\Delta\Pi$ versus Π_i plots for each phospholipid mixture assayed.

Compression Isotherms and Epifluorescence Microscopy Experiments. Lipid monolayers were formed on the top of the subphase using a thermostated Langmuir−Blodgett ribbon trough (NIMA Technologies), as described above. For epifluorescence experiments, Rho-PE (1:100, probe:lipid molar ratio) was included in each lipid mixture, and Alexa 488-labeled Ole e 1 (15 μg) was used. After 10 min to allow for solvent evaporation, monolayers were compressed to 2 mN/m surface pressure. After 5 min of equilibration, the allergen was injected into the subphase and the films were transferred onto a glass slide that was previously immersed in the subphase, to form Langmuir−Blodgett films. Monolayer−protein interaction was monitored as $\Delta\Pi$ for 10 min. For the epifluorescence microscopy experiments, all the monolayers were compressed at the transfer rate of 25 cm^2/min, thus allowing the correct transference without altering its structure.[18] Epifluorescence microscopy observation of the supported films was performed in a Leica DM4000B microscope (Leica Microsystems, Wetzlar, Germany) by using a Hamamatsu camera (C10600−10B ORCA-R2, Herrsching am Ammersee, Germany). Images were obtained at different positions from the transferred films, and subsequently assigned to the surface pressures obtained during film transfer. Equivalent compression isotherms were subsequently registered by compressing lipid monolayers at 65 cm^2/min until reaching their collapse pressure.

RESULTS

Characterization of Ole e 1 Allergen Adsorption at the Air−Liquid Interface. Ole e 1 adsorbs at the air−liquid interface, forming a stable protein film as monitored by the increase in surface pressure (Figure 1). Its interfacial adsorption

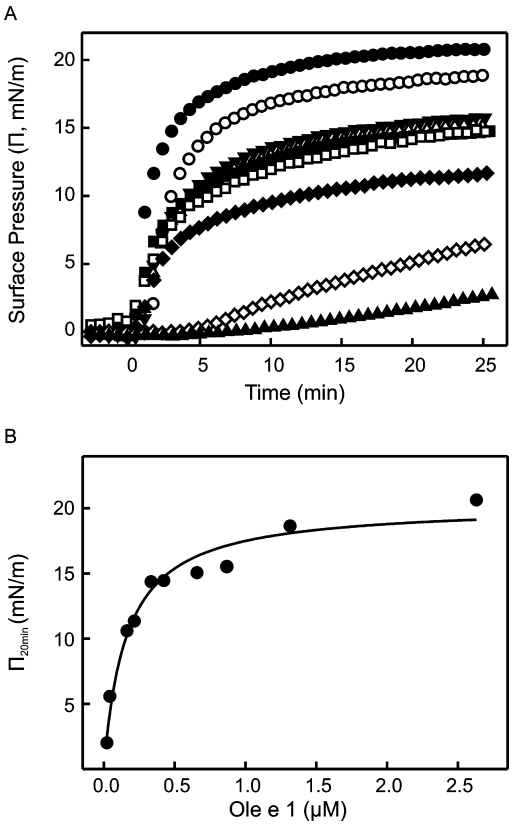

Figure 1. Interfacial adsorption kinetics of Ole e 1, the major olive pollen allergenic protein. (A) Π−*t* isotherms (25 ± 1 °C) of different amounts of Ole e 1 injected at time = 0 (minutes) in a subphase composed of 5 mM Tris buffer, pH 7, 150 mM NaCl. Protein concentration in the subphase was 2.78 (●), 1.36 (○), 0.89 (▼), 0.68 (△), 0.42 (■), 0.37 (□), 0.21 (♦), 0.16 (◊), 0.05 (▲) μM, respectively. (B) Maximum surface pressure achieved at 20 min after injection ($\Pi_{20\ min}$, mN/m) versus Ole e 1 (μM). Solid line shows the hyperbolic trend that best fits protein interfacial behavior (r^2 = 0.97).

is highly dependent on protein concentration, fitting to a rectangular hyperbola as defined by eq 1

$$\Pi = \frac{\Pi_{max} \cdot C}{K + C} \quad (1)$$

where Π is the surface pressure value achieved at time = 20 min for each concentration, C is the allergen concentration (μM), Π_{max} depicts the theoretical maximum value of surface pressure that would be achieved at very high protein concentrations, and K represents an invariable value for the protein concentration

DOI: 10.1021/acs.langmuir.6b02831
Langmuir 2016, 32, 11055−11062

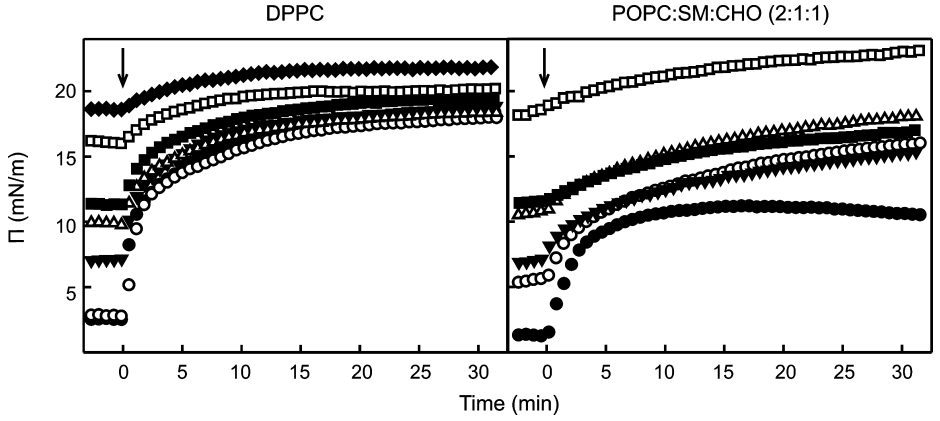

Figure 2. Insertion/adsorption kinetics of Ole e 1 into preformed phospholipid monolayers. Insertion/adsorption kinetics of Ole e 1 in DPPC (left) or POPC:SM:CHO (2:1:1 molar ratio, right) monolayers preformed at different initial surface pressures (symbol lines). Arrows indicate allergen injection (0.55 μM) into the subphase. All the assays were carried out at 25 ± 1 °C. The subphase was composed of 5 mM Tris buffer, pH 7, 150 mM NaCl.

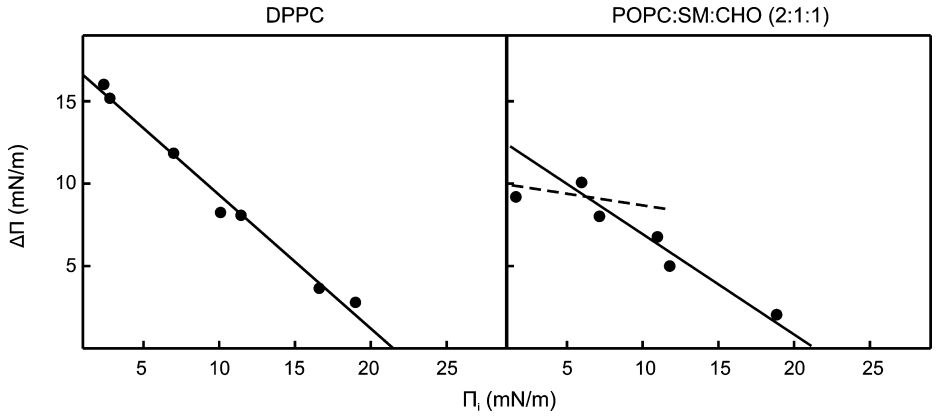

Figure 3. Critical insertion pressure of Ole e 1 into phospholipid monolayers. Increase in surface pressure (ΔΠ) versus initial pressure (Π_i) of DPPC or POPC:SM:CHO (2:1:1, molar ratio) preformed lipid monolayers upon injection of Ole e 1 at 25 ± 1 °C. The subphase and Ole e 1 solution (0.55 μM) was composed of a 5 mM Tris buffer, pH 7, 150 mM NaCl. In the left plot, the line represents the linear regression that best fits the experimental data ($r^2 > 0.97$). Each plot shows 1 out of 2 independent experiments. The intersection with the horizontal axis allows estimation of the critical insertion pressure (Π_c) in each of the films. The right panel shows the trends observed when the allergen was injected under POPC:SM:CHO films at low (dashed) and high (solid line) pressure regimes.

that yields half of the Π_{max} value. The values obtained after data fitting were $K = 0.16 \pm 0.03$ μM and $\Pi_{max} = 20.3 \pm 0.9$ mN/m, with an R^2 correlation value of 0.97. For the following experiments, an allergen concentration of 0.55 μM was fixed, because it allowed us to detect an acceptable protein interfacial activity, while avoiding the complete saturation of the liquid surface. Gibbs adsorption eqs 2 and 3 were also used to calculate the protein surface excess concentration (Γ) and surface molecular area (A), respectively

$$\Delta\Pi = \mathrm{Ln}C \cdot R \cdot T \cdot \Gamma \tag{2}$$

$$A = \frac{1}{\Gamma_{max} \cdot N}(\text{Å}^2) \tag{3}$$

where ΔΠ is the maximum increment in surface pressure reached for each protein concentration, R is the gas constant (8.314 J·K^{-1}·mol^{-1}), T is the temperature of the assay (298 K), A is the surface molecular area (Å^2), Γ_{max} is the surface excess concentration at saturation, and N is Avogadro's constant number (6.022×10^{23} mol^{-1}). Data obtained for Ole e 1 interfacial activity was $\Gamma_{max} = (6.94 \pm 0.31) \times 10^{20}$ residues/m^2 and $A = 0.144 \pm 0.01$ Å^2/residue.

Interaction of Ole e 1 with POPC:SM:CHO (2:1:1) and DPPC Lipid Surfaces. Next, the interfacial adsorption of Ole e 1 to interfaces that have been previously occupied by DPPC or POPC:SM:CHO (2:1:1, molar ratio) spread monolayers was monitored at different initial pressures (Π_i). These mixtures were chosen due to the different nature of the lipid packaging structures that they produce in the interphase. DPPC is a saturated lipid that organizes in liquid-condensed (LC) phases above its phase transition pressure; on the other hand, the POPC:SM:CHO mixture produces segregation of immiscible liquid-ordered (Lo) and liquid-disordered (Ld) regions because of the presence of cholesterol, even at low surface pressures.[19] Figure 2 shows that Ole e 1 injection into the aqueous subphase causes an increase in surface pressure in both type of films, which never exceed the maximum pressure value reached for the protein, 20 mN/m. Kinetics plots showed that the protein exhibits similar behavior on both films compressed to pressures higher than 10 mN/m, but not for films preformed at low pressures. The protein was unable to cause a pressure change higher than 10 mN/m when injected underneath POPC:SM:CHO monolayers, while it reached much higher values of surface pressure on DPPC experiments.

DOI: 10.1021/acs.langmuir.6b02831
Langmuir 2016, 32, 11055−11062

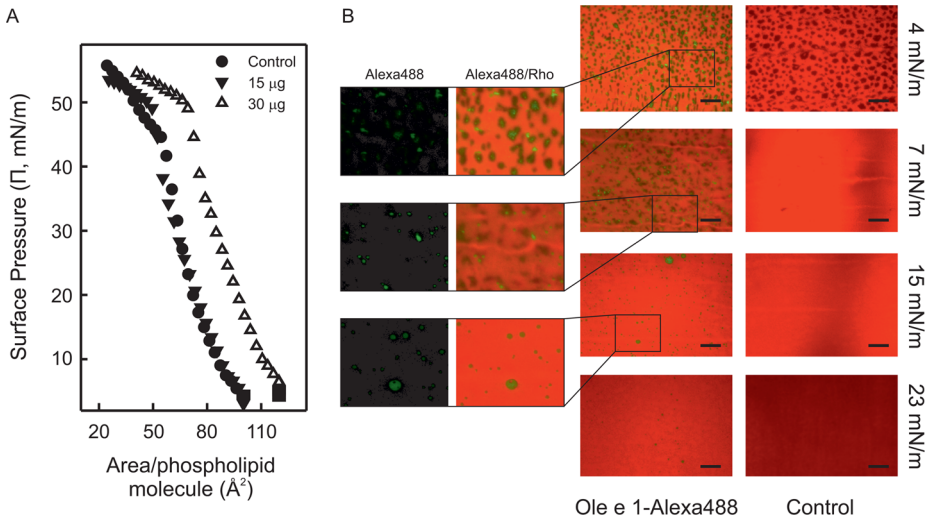

Figure 4. Interaction of Ole e 1 with POPC:SM:CHO (2:1:1 molar ratio) films. Π–*A* compression isotherms obtained upon injection of different protein amounts (μg) (A) and effects on the organization of POPC:SM:CHO monolayers (B) in the absence (Control) or in the presence of Ole e 1-Alexa488 (green spots). In B, epifluorescence images were taken from transferred films compressed to the indicated pressures. The films contained Rho-PE (red) to allow for observation of the phospholipid distribution at the interface at 25 ± 1 °C. Images with Ole e 1-Alexa488 represent the merge of both channels where a magnification (×3) of the details is represented (left, Alexa488 channel; right, Alexa488 and Rho channel). Scale bar at the bottom of all the pictures represents 25 μm. Figure shows representative images taken from 1 out of 3 independent experiments.

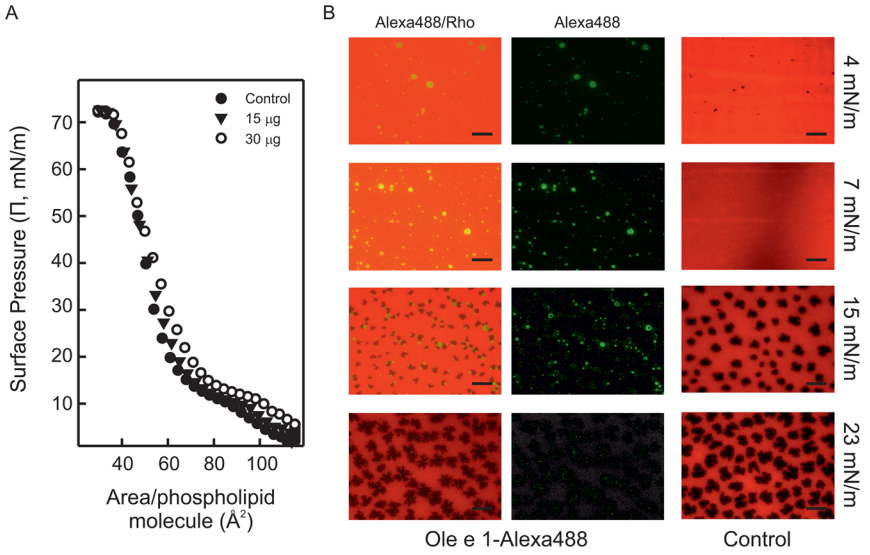

Figure 5. Interaction of Ole e 1 with DPPC films. Π–*A* compression isotherms obtained upon injection of different protein amounts (μg) (A) and effects on the organization of DPPC monolayers (B) in the absence (Control) or in the presence of Ole e 1-Alexa488 (green spots). In B, epifluorescence images were taken from transferred films compressed to the indicated pressures. The films contained Rho-PE (red) to allow for observation of the phospholipid distribution at the interface at 25 ± 1 °C. Images from films containing the allergen compare fluorescence from the protein (dark, right) and, on the left, the merger of both lipid (red) and protein (green) channels. Scale bar at the bottom of each picture represents 25 μm. Figure shows representative images taken from 1 out of 3 independent experiments.

We estimated the critical pressure of insertion (Π_c) by plotting the pressure changes caused by the allergen as a function of initial pressure values (Figure 3). This value represents the theoretical maximum initial pressure that allows the insertion of the protein within preformed monolayers. The Π_c values calculated for Ole e 1 insertion in both types of monolayers was the same, 21.0 ± 0.5 mN/m, according to the maximum adsorption values. A linear trend was obtained for the insertion of the allergen into layers of both lipid mixtures compressed to most surface pressures. However, as noticed above, the insertion of the protein into POPC:SM:CHO films exhibits an inflection point at pressures below 5 mN/m, suggesting a potential reorientation of Ole e 1 upon interaction with compositional or structural motifs generated within this monolayer at those lower surface pressures.

Organization of Lipid and Lipid/Ole e 1 Films: Compression Isotherms and Epifluorescence Analysis. The interaction of Ole e 1 protein with lipid monolayers at the air–liquid interface and its effect on lipid packing are analyzed in Figures 4 and 5. Figure 4A shows the π–*A* isotherm of a POPC:SM:CHO (2:1:1) film in the absence (Control) and in the presence of 15 or 30 μg of Ole e 1. Protein injection (30 μg) expanded the isotherm up to 20 Å^2/molecule, which indicates that Ole e 1 molecules are able to insert into the

DOI: 10.1021/acs.langmuir.6b02831
Langmuir 2016, 32, 11055–11062

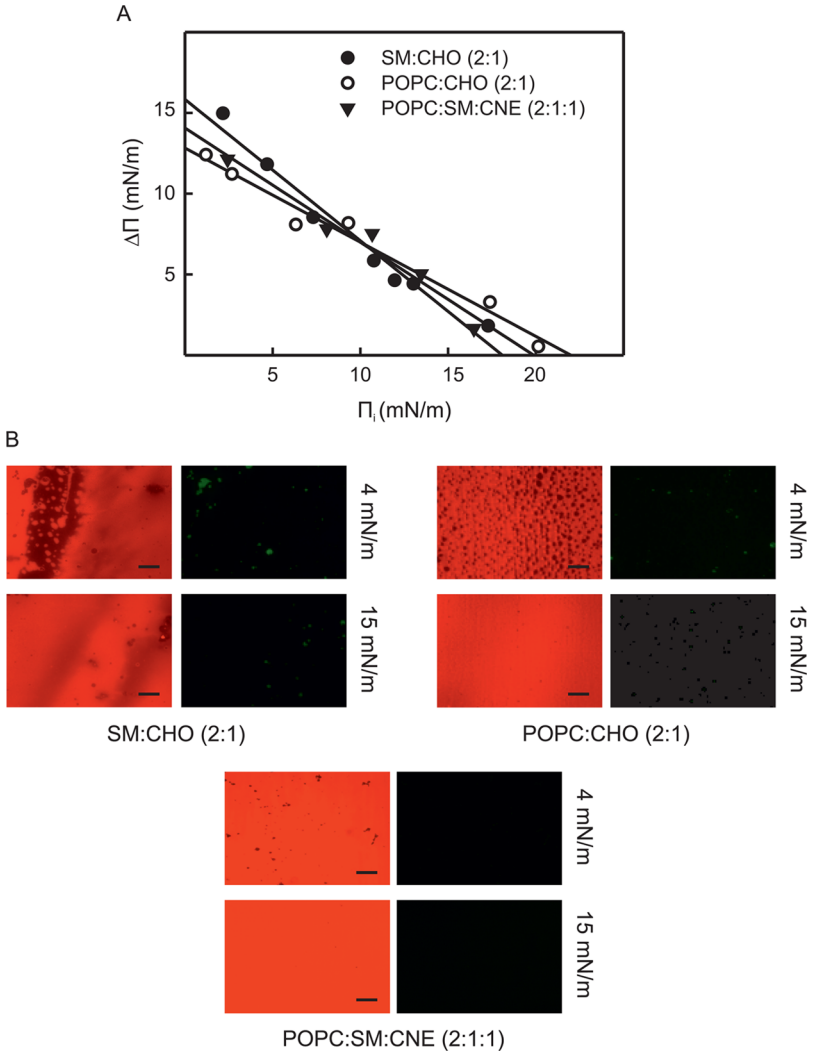

Figure 6. Interaction of Ole e 1 with SM:CHO (2:1), POPC:CHO (2:1), and POPC:SPM:CNE (2:1:1) films. (A) Increase in surface pressure ($\Delta\Pi$) versus initial pressure (Π_i) of SM:CHO (2:1), POPC:CHO (2:1), and POPC:SM:CNE (2:1:1) preformed lipid monolayers upon injection of Ole e 1 at 25 ± 1 °C. The subphase and Ole e 1 solution (0.55 μM) was composed of a 5 mM Tris buffer, pH 7, 150 mM NaCl. Lines represent the linear regression that best fits the experimental data (r^2 > 0.97) for each of the lipid systems. Figure shows representative data of 1 out of 2 independent experiments. (B) Epifluorescence images of transferred films compressed to the indicated pressures. The films contained Rho-PE (red, 1% mol/mol) to allow for observation of the phospholipid distribution at the interface at 25 ± 1 °C. 15 μg of Ole e 1 labeled with Alexa-Fluor488 (green) were used in all the cases. The left image of each condition represents the merger of both channels. Scale bar at the bottom of each picture represents 25 μm. Figure shows representative images taken from 1 out of 3 independent experiments.

monolayer to occupy an area of the interface, by themselves or upon interaction with the surrounding lipids. All the films, including the ones containing protein, collapse at pressures around 50 mN/m without a clear indication of partial squeeze-out plateaus, indicating that Ole e 1 is able to remain associated with the interface under lateral compression at pressures much higher than its Π_c.

Epifluorescence images of POPC:SM:CHO films transferred at different pressures during compression are illustrated in the Figure 4B. For all the epifluorescence experiments 15 μg of Alexa488-labeled Ole e 1 (green fluorescent dots) were used. This amount of protein was judged to be optimal to obtain defined and high-resolution images showing the allergen effect and its localization within the lipid film. To reveal the occurrence of lateral phase separation in the chosen lipid system, Rho-PE—a fluorescent lipid probe preferentially partitioning into Ld phases—was added to the organic lipid solution (red). Compression of POPC:SM:CHO films up to 7 mN/m generated dark regions, likely corresponding to Lo domains enriched in SM and CHO but depleted in Rho-PE probe. These condensed areas were less numerous and they had diffuse edges in lipid/protein films compared to the morphology of domains in protein-free control films. Protein was observed to mainly colocalize within these dark areas, suggesting a relative affinity of the protein for these ordered structures. At pressures higher than 7 mN/m, these dark areas seem to disappear, at least at the microscopic scale observable by epifluorescence, and the protein reordered as large green clusters, coexisting with the remaining lipids at the interface until its apparent complete exclusion at pressures higher than 23 mN/m. These observations support the change of the trend in protein insertion detected at low initial pressures in the adsorption experiments toward POPC:SM:CHO films.

As stated before, the effect of Ole e 1 in DPPC isotherms (Figure 5A) relies on an expansion of 20 Å^2/molecule to larger areas, suggesting the interfacial occupation of the protein. This

DOI: 10.1021/acs.langmuir.6b02831
Langmuir 2016, 32, 11055−11062

effect was more pronounced when injecting 30 μg in the subphase than upon injection of 15 μg of protein. The presence of the protein at the DPPC interface caused a delay in the onset of the liquid-expanded (LE) to LC transition plateau, without apparently causing its alteration or disappearance. Control and lipid/protein curves converge at a surface pressure around 50 mN/m, suggesting that, at this pressure, the protein was totally excluded from the interface and the lipids remained in a highly condensed state. Epifluorescence analysis show that the interaction of the protein with DPPC films (Figure 5B) was very different than observed in POPC:SM:CHO experiments. At surface pressures below the LE−LC transition plateau (<10 mN/m), the protein appeared as numerous and homogeneously distributed clusters, evenly coexisting with the LE lipid phase. At pressures above 10 mN/m dark LC domains that exclude the Rhodamine-PE probe emerge, as previously observed by Perez-Gil et al.[20] These presumably condensed lipid domains were slightly more numerous and smaller in the presence of the protein, which tends to be located at the boundaries as green aggregates. At the highest pressures tested, rosette-shaped domains occupied almost the entire interface and the protein appears as smaller aggregates at their edges. Even at these pressures with the allergen almost excluded, Ole e 1 causes a slight alteration in the shape of the lipid domains, generating greater number of pits and more abrupt edges with respect to the domains nucleated in protein-free control films.

Finally, the interaction of Ole e 1 with other lipid systems was tested by using lipid mixtures in which one of the POPC:SM:CHO components were depleted: SM:CHO (2:1) and POPC:CHO (2:1). As an additional reference, we tested a system, POPC:SM:CNE (2:1:1, molar ratio), in which CHO was substituted by CNE, an sterol that inhibits the formation of Lo domains.[21] Figure 6A shows the determination of both the maximum change in surface pressure ($\Delta\Pi_{max}$) and the critical pressure value (Π_c) for these additional mixtures. The values of $\Delta\Pi_{max}$ were very similar in these systems, being the highest the one obtained for SM:CHO (12.7 mN/m), followed by the insertion in POPC:SM:CNE (11.3 mN/m) and that in POPC:CHO (10.3 mN/m). POPC:CHO achieved the highest value of Π_c (22.1 mN/m), followed not far behind by POPC:SM:CNE (19.8 mN/m) and SM:CHO (18.1 mN/m) films. Epifluorescence images illustrated in Figure 6B support interfacial adsorption results. At 4 mN/m, only POPC:CHO films exhibited segregation of dark regions corresponding to cholesterol-enriched Lo domains. However, the fluorescent-labeled protein seemed not to be located in these domains and its presence therein was much less conspicuous than observed in POPC:SM:CHO films. Noteworthy, cholestenone (CNE) fully prevented the presence of Lo domains, and that was associated with a clearly lower interfacial presence of Ole e 1. At high pressures (15 mN/m), the protein appeared again as green clusters, coexisting with lipid films characterized by having a total absence of ordered regions, at least at a microscopic length scale. In general terms, values, trends, and images obtained for these partially depleted systems seem to be very different from to those obtained for POPC:SM:CHO films, suggesting a crucial requirement of the three components—POPC, SM, and CHO—to define maximal affinity in the interaction between Ole e 1 and lipid domains.

DISCUSSION

Ole e 1 Aeroallergen Is Able to Interact Efficiently with Air−Liquid Interfaces. Underneath air−aqueous interfaces, Ole e 1 allergen has shown an interfacial adsorption capability comparable to those of technologically important surface-active proteins such as BSA, lysozyme, β-lactoglobulin, or β-casein in the same conditions.[22]

Ole e 1 allergen is an N-glycosylated protein, showing a high content (40%) in aperiodic conformation determined by circular dichroism.[17] Moreover, predictive analysis of Ole e 1 showed that it is a highly flexible and hydrophobic protein.[17] All these properties support the high surface activity demonstrated here for Ole e 1 at the interface. This is in agreement with the features of other proteins reported to adsorb to air−water interfaces, such as β-casein where a combination of a flexible nonglobular structure and a hydrophilic and charged N-terminal region governs the interfacial adsorption.[23] In this sense, Ole e 1 polar regions may keep exposure to the liquid subphase while hydrophobic ones may be transferred to the airspace, potentially promoting allergen diffusion from the bulk solution toward the interface.

Interfacial activity is associated with conformational changes of the protein, which might induce process of oligomerization and aggregation, as it has been previously shown for β-lactoglobulin,[24] latherin,[15] BSA, fibrinogen, and immunoglobulin G.[25] In this sense, protein allergenicity is highly influenced by structural rearrangements, oligomerization and aggregation, as it has been reported for the major birch pollen allergen, Bet v 1,[26] and other relevant allergenic proteins.[26,27] Ole e 1 is a protein with a high trend to form oligomers, exhibiting a higher allergenicity.[17] Thus, the relation between Ole e 1 allergenicity and the potential conformational changes induced upon its interfacial adsorption could be key features once the aeroallergen enters the respiratory tract and impacts its wet surface. Potential structural rearrangement of Ole e 1 during its interaction with lipid films could be further explored by using a combination of techniques such as Raman and FTIR spectroscopy.

Ole e 1 Aeroallergen Interacts with Lipid Films Generated at the Air−Liquid Interface. Considering the marked interfacial activity revealed by Ole e 1 aeroallergen, we proceeded to describe its behavior in a lipid film context by using Langmuir-Wilhelmy and Blodgett monolayers. Two physiologically relevant lipid mixtures were used as a model, POPC:SM:CHO (2:1:1, molar ratio), a mixture previously described as potentially mimicking segregation of raft-like domains thought to exist in cellular membranes[27] and DPPC, which constitutes the most abundant and surface-active component in pulmonary surfactant.

Ole e 1 adsorption/insertion plot describes a linear tendency with DPPC films, achieving a Π_c value (21 mN/m) comparable to those obtained for the rest of lipid systems assessed. Although this Π_c value did not exceed the threshold of surface pressure value of 30 mN/m, which is commonly considered as indicative of potential ability of a protein to insert into lipid bilayers,[28] the Π−A isotherm exhibited an expansion of 20 Å^2/molecule that was sustained up to 50 mN/m after Ole e 1 injection into the subphase, confirming allergen coexistence within the lipid film. Epifluorescence images of DPPC Langmuir films at surface pressures higher than 15 mN/m showed LC or bean-shaped domains of DPPC, where the fluorescent-labeled allergen was localized as protein clusters that seem to exclude the lipid. This observation suggests that lipid domains can act as nucleation sites for the allergen, in which new noncovalent interactions could be established between neighboring molecules, due to the interfacial

DOI: 10.1021/acs.langmuir.6b02831
Langmuir 2016, 32, 11055−11062

exposition of hydrophobic residues that are normally hidden in the protein structure.[29] The coexistence of protein and DPPC at the interface suggests the existence of several mechanisms that could take place in vivo during the first stages of allergen sensitization. On one hand, Ole e 1 adsorption could impair or abolish normal surface activity of pulmonary surfactant, which is crucial particularly during expiration. This surfactant inhibition process could be explained because of a steric competition, as has been previously reported for the surface-active plasma proteins BSA or hemoglobin.[30,31] On the other hand, surfactant interfacial spreading properties has been recently proposed as a promising tool for transporting several drugs along the airways and into the body.[32] In this context, it is conceivable that pulmonary surfactant could act as a potential carrier or shuttle for a wide variety of airborne compounds and aeroallergens, including Ole e 1, as our results are pointing out. Ole e 1 diffusion along the entire conducting airways (from bronchial to alveolar region) might contribute to the development of allergic responses.

The examination of the $\Delta\Pi$ versus Π_i plot for POPC:SM:-CHO (2:1:1) revealed a biphasic trend not observed in the linear tendency obtained with DPPC films (Figure 3), suggesting a different mode of lipid−protein interaction with those monolayers at low surface pressures. It could be confirmed afterward by epifluorescence analysis, whose fluorescent images (Figure 4B) showed the existence of Lo lipid domains (dark areas) at pressures lower than 7 mN/m, where fluorescent-labeled Ole e 1 (green dots) is mainly localized. At pressures higher than 7 mN/m, lateral segregation completely disappeared, and the allergen appeared as homogeneously distributed clusters. The absence of Lo domains at the interface seems to correspond to the linear behavior obtained at the highest pressures of films made of POPC:SM:CHO, DPPC or other lipid mixtures in which the generation of cholesterol-rich domains was prevented (SM:CHO or POPC:SM:CNE). In addition, the presence of all lipid components in the POPC:SM:CHO mixture seems to be required for Ole e 1−domain interaction (Figure 6), as shown with the presence of ordered domains of different nature (POPC:CHO).

In spite of Ole e 1 showing critical interfacial insertion pressures not exceeding 30 mN/m, the allergen was able to remain in the interface under high lateral compression states. Taken together, these results could indicate a mechanism of interaction of Ole e 1 with Lo domains of the epithelial cell membrane at the time of contact. Thus, it has been reported that other allergens interact with structures localized in Lo domains involved in signaling pathways related to the immune response such as Th2-type inflammation. In this sense, Bet v 1 colocalizes with caveolar markers,[33] and house dust mite group-2 allergens interact with the Toll-like receptor 4 (TLR4).[34]

CONCLUSIONS

In summary, our study has demonstrated the interfacial adsorption capabilities of the aeroallergen Ole e 1. Moreover, Ole e 1 displayed a particular behavior on lipid layers generated at air−liquid interfaces, which show lateral phase separation. The allergen tended to localize associated with liquid-condensed and ordered domains. Collectively, these results support the concept that the interfacial activity of certain allergens—such as Ole e 1—are related to their association with surface lipid films, accumulating preferentially in the coexisting lipid phases. Thus, surface clustering could be a key feature to define their stable presence at the epithelial barrier, triggering the allergic response.

AUTHOR INFORMATION

Corresponding Authors

*E-mail: ebataner@ucm.es.

*E-mail: acruz@quim.ucm.es.

Author Contributions

#The last two authors act as equivalent co-senior authors and corresponding authors.

Notes

The authors declare no competing financial interest.

ACKNOWLEDGMENTS

This work was supported by grants from the Spanish Ministry of Economy and Competitivity (SAF2011-26716, SAF2014-53209-R, BIO2012-30733, BIO2015-67930-R), the Regional Government of Madrid (S2013/MIT-2807), and RIRAAF Network RD12/0013/0015 from the ISCIII. R.B. is a fellow of the Ramón y Cajal program of the Spanish Ministry of Economy and Competitivity. J.C.L.-R. is supported by a FPU fellowship from the Spanish Ministry of Education, Culture and Sport.

REFERENCES

(1) Petersen, K. D.; Kronborg, C.; Gyrd-Hansen, D.; Dahl, R.; Larsen, J. N.; Linneberg, A. Characteristics of patients receiving allergy vaccination: to which extent do socio-economic factors play a role? *Eur. J. Public Health* **2011**, *21* (3), 323−328.

(2) Akdis, M.; Akdis, C. A. Mechanisms of allergen-specific immunotherapy. *J. Allergy Clin. Immunol.* **2007**, *119* (4), 780−791.

(3) Craig, T. J. Aeroallergen sensitization in asthma: prevalence and correlation with severity. *Allergy Asthma Proc.* **2010**, *31* (2), 96−102.

(4) Lopez-Rodriguez, E.; Perez-Gil, J. Structure-function relationships in pulmonary surfactant membranes: from biophysics to therapy. *Biochim. Biophys. Acta, Biomembr.* **2014**, *1838* (6), 1568−1585.

(5) Madan, T.; Kishore, U.; Shah, A.; Eggleton, P.; Strong, P.; Wang, J. Y.; Aggrawal, S. S.; Sarma, P. U.; Reid, K. B. Lung surfactant proteins A and D can inhibit specific IgE binding to the allergens of Aspergillus fumigatus and block allergen-induced histamine release from human basophils. *Clin. Exp. Immunol.* **1997**, *110* (2), 241−249.

(6) Malhotra, R.; Haurum, J.; Thiel, S.; Jensenius, J. C.; Sim, R. B. Pollen grains bind to lung alveolar type II cells (A549) via lung surfactant protein A (SP-A). *Biosci. Rep.* **1993**, *13* (2), 79−90.

(7) Wang, J. Y.; Kishore, U.; Lim, B. L.; Strong, P.; Reid, K. B. Interaction of human lung surfactant proteins A and D with mite (Dermatophagoides pteronyssinus) allergens. *Clin. Exp. Immunol.* **1996**, *106* (2), 367−373.

(8) Mulugeta, S.; Beers, M. F. Surfactant protein C: its unique properties and emerging immunomodulatory role in the lung. *Microbes Infect.* **2006**, *8* (8), 2317−2323.

(9) Kaser, M. R.; Skouteris, G. G. Inhibition of bacterial growth by synthetic SP-B1−78 peptides. *Peptides* **1997**, *18* (9), 1441−1444.

(10) Lambrecht, B. N.; Hammad, H. Allergens and the airway epithelium response: gateway to allergic sensitization. *J. Allergy Clin. Immunol.* **2014**, *134* (3), 499−507.

(11) Hallstrand, T. S.; Hackett, T. L.; Altemeier, W. A.; Matute-Bello, G.; Hansbro, P. M.; Knight, D. A. Airway epithelial regulation of pulmonary immune homeostasis and inflammation. *Clin. Immunol.* **2014**, *151* (1), 1−15.

(12) Mitropoulos, V.; Mutze, A.; Fischer, P. Mechanical properties of protein adsorption layers at the air/water and oil/water interface: a comparison in light of the thermodynamical stability of proteins. *Adv. Colloid Interface Sci.* **2014**, *206*, 195−206.

DOI: 10.1021/acs.langmuir.6b02831
Langmuir 2016, 32, 11055−11062

(13) Bos, M. A.; van Vliet, T. Interfacial rheological properties of adsorbed protein layers and surfactants: a review. *Adv. Colloid Interface Sci.* **2001**, *91* (3), 437−471.
(14) Damodaran, S. Protein Stabilization of Emulsions and Foams. *J. Food Sci.* **2005**, *70* (3), R54−R66.
(15) Vance, S. J.; McDonald, R. E.; Cooper, A.; Smith, B. O.; Kennedy, M. W. The structure of latherin, a surfactant allergen protein from horse sweat and saliva. *J. R. Soc., Interface* **2013**, *10* (85), 20130453.
(16) Liccardi, G.; D'Amato, M.; D'Amato, G. Oleaceae pollinosis: a review. *Int. Arch. Allergy Immunol.* **1996**, *111* (3), 210−217.
(17) Villalba, M.; Batanero, E.; Lopez-Otin, C.; Sanchez, L. M.; Monsalve, R. I.; Gonzalez de la Pena, M. A.; Lahoz, C.; Rodriguez, R. The amino acid sequence of Ole e I, the major allergen from olive tree (Olea europaea) pollen. *Eur. J. Biochem.* **1993**, *216* (3), 863−869.
(18) Wang, L.; Cruz, A.; Flach, C. R.; Perez-Gil, J.; Mendelsohn, R. Langmuir-Blodgett films formed by continuously varying surface pressure. Characterization by IR spectroscopy and epifluorescence microscopy. *Langmuir* **2007**, *23* (9), 4950−4958.
(19) Saez-Cirion, A.; Nir, S.; Lorizate, M.; Agirre, A.; Cruz, A.; Perez-Gil, J.; Nieva, J. L. Sphingomyelin and cholesterol promote HIV-1 gp41 pretransmembrane sequence surface aggregation and membrane restructuring. *J. Biol. Chem.* **2002**, *277* (24), 21776−21785.
(20) Perez-Gil, J.; Nag, K.; Taneva, S.; Keough, K. M. Pulmonary surfactant protein SP-C causes packing rearrangements of dipalmitoylphosphatidylcholine in spread monolayers. *Biophys. J.* **1992**, *63* (1), 197−204.
(21) Xu, X.; London, E. The effect of sterol structure on membrane lipid domains reveals how cholesterol can induce lipid domain formation. *Biochemistry* **2000**, *39* (5), 843−849.
(22) Niño, M. R. R.; Patino, J. M. R. Surface tension of protein and insoluble lipids at the air-aqueous phase interface. *J. Am. Oil Chem. Soc.* **1998**, *75* (10), 1233−1239.
(23) Gangnard, S.; Zuev, Y.; Gaudin, J.-C.; Fedotov, V.; Choiset, Y.; Axelos, M. A. V.; Chobert, J.-M.; Haertlé, T. Modifications of the charges at the N-terminus of bovine β-casein: Consequences on its structure and its micellisation. *Food Hydrocolloids* **2007**, *21* (2), 180−190.
(24) Husband, F. A.; Garrood, M. J.; Mackie, A. R.; Burnett, G. R.; Wilde, P. J. Adsorbed protein secondary and tertiary structures by circular dichroism and infrared spectroscopy with refractive index matched emulsions. *J. Agric. Food Chem.* **2001**, *49* (2), 859−866.
(25) Sahin, N. O.; Burgess, D. J. Competitive interfacial adsorption of blood proteins. *Farmaco* **2003**, *58* (10), 1017−1021.
(26) Scholl, I.; Kalkura, N.; Shedziankova, Y.; Bergmann, A.; Verdino, P.; Knittelfelder, R.; Kopp, T.; Hantusch, B.; Betzel, C.; Dierks, K.; Scheiner, O.; Boltz-Nitulescu, G.; Keller, W.; Jensen-Jarolim, E. Dimerization of the major birch pollen allergen Bet v 1 is important for its in vivo IgE-cross-linking potential in mice. *J. Immunol.* **2005**, *175* (10), 6645−6650.
(27) Simons, K.; Toomre, D. Lipid rafts and signal transduction. *Nat. Rev. Mol. Cell Biol.* **2000**, *1* (1), 31−39.
(28) Marsh, D. Lateral pressure in membranes. *Biochim. Biophys. Acta, Rev. Biomembr.* **1996**, *1286* (3), 183−223.
(29) Moskovitz, Y.; Srebnik, S. Conformational changes of globular proteins upon adsorption on a hydrophobic surface. *Phys. Chem. Chem. Phys.* **2014**, *16* (23), 11698−11707.
(30) Holm, B. A.; Wang, Z.; Notter, R. H. Multiple mechanisms of lung surfactant inhibition. *Pediatr. Res.* **1999**, *46* (1), 85−93.
(31) Warriner, H. E.; Ding, J.; Waring, A. J.; Zasadzinski, J. A. A concentration-dependent mechanism by which serum albumin inactivates replacement lung surfactants. *Biophys. J.* **2002**, *82* (2), 835−842.
(32) Hidalgo, A.; Cruz, A.; Perez-Gil, J. Barrier or carrier? Pulmonary surfactant and drug delivery. *Eur. J. Pharm. Biopharm.* **2015**, *95*, 117−127.
(33) Mogensen, J. E.; Wimmer, R.; Larsen, J. N.; Spangfort, M. D.; Otzen, D. E. The major birch allergen, Bet v 1, shows affinity for a broad spectrum of physiological ligands. *J. Biol. Chem.* **2002**, *277* (26), 23684−23692.
(34) Ichikawa, S.; Takai, T.; Yashiki, T.; Takahashi, S.; Okumura, K.; Ogawa, H.; Kohda, D.; Hatanaka, H. Lipopolysaccharide binding of the mite allergen Der f 2. *Genes Cells* **2009**, *14* (9), 1055−1065.

DOI: 10.1021/acs.langmuir.6b02831
Langmuir 2016, 32, 11055−11062

Airway Epithelium Plays a Leading Role in the Complex Framework Underlying Respiratory Allergy

López-Rodríguez JC[1], Benedé S[1], Barderas R[1,2], Villalba M[1], Batanero E[1]

[1]Departamento de Bioquímica y Biología Molecular I, Facultad de Ciencias Químicas, Universidad Complutense, Madrid, Spain
[2]UFIEC, National Institute of Health Carlos III, Majadahonda, Spain

J Investig Allergol Clin Immunol 2017; Vol. 27(6): 346-355
doi: 10.18176/jiaci.0201

Abstract

Airway epithelium is the cellular structure with the greatest surface exposed to a plethora of environmental airborne substances, including microorganisms, respiratory viruses, air pollutants, and allergens. In addition to being a protective physical barrier at the air–liquid interface, the airway epithelium acts as an effective chemical and immunological barrier that plays a crucial role in orchestrating the immune response in the lungs, by supporting the activation, recruitment, and mobilization of immune cells. Airway epithelium dysfunction has been clearly associated with various airway inflammatory diseases, such as allergic asthma. Although it is not fully understood why a person develops respiratory allergy, a growing body of evidence shows that the nature of the host's immune response is strongly determined by the state of the airway epithelium at the time of contact with the inhaled allergen. Our review highlights the physiological state of airway epithelium as a key element in the development of allergy and, particularly, in exacerbation of asthma. We review the role of physiological oxidants as signaling molecules in lung biology and allergic diseases and examine how high exposure to air pollutants (eg, cigarette smoke and diesel particles) can contribute to the increased incidence of respiratory allergy and exacerbation of the disease.

Key words: Airway epithelium. Barrier dysfunction. Respiratory allergy. Redox biology. Air pollutants.

Resumen

El epitelio pulmonar constituye la barrera celular más susceptible a la acción deletérea de la multitud de agentes que se encuentran en el ambiente, incluidos los alérgenos. Además de prevenir su acceso al organismo, la barrera epitelial de las vías respiratorias juega un papel inmunomodulador crucial, regulando de forma local la acción de las células del sistema inmune subyacentes. Una disfunción epitelial, provocada tanto directa como indirectamente por la acción de los aeroalérgenos, parece ser una de las causas principales de desregulación de la homeostasis pulmonar, causando una respuesta proinflamatoria descontrolada que cada vez más autores atribuyen al origen de las reacciones alérgicas. En esta revisión se quiere destacar el papel de la barrera epitelial pulmonar como regulador de la respuesta inmune en el contexto de la alergia. Las enfermedades crónicas que afectan a las vías respiratorias, tales como el asma alérgica, muestran frecuentemente una función epitelial defectuosa, apoyando así la hipótesis antes mencionada que subyace al origen de la alergia. El impacto de otros contaminantes ambientales -como virus respiratorios, bacterias, humo del tabaco y partículas diésel- sobre la integridad epitelial, así como su influencia en la biología redox pulmonar relacionada con el desarrollo de la respuesta alérgica, también se abordarán en la presente revisión.

Palabras clave: Epitelio pulmonar. Disfunción epitelial. Alergia respiratoria. Biología redox. Contaminantes ambientales.

© 2017 Esmon Publicidad

Introduction

The lung is a complex internal organ that is widely exposed to airborne substances (eg, microorganisms, respiratory viruses, air pollutants, and allergens), which are frequently expelled without inducing lung inflammatory responses because of the crucial role of the airway epithelium in the regulation of immune homeostasis and the development of defense mechanisms.

Over the last few decades, increasing evidence has indicated an association between a dysfunctional epithelium and airway inflammatory diseases [1], of which respiratory allergy is considered a key inflammatory disorder of the conducting airways. Respiratory allergy is characterized by a dominant $CD4^+$ T-helper 2 (T_H2)–type immune response and by the production of high levels of specific IgE against antigens called aeroallergens (Figure 1). Pollen from trees, weeds and grasses, mold spores, house dust mite fecal particles, and animal dander are common sources of aeroallergens. These particles use the upper airways as the main portal of entry into the body, with the airway epithelium being not only the protective physical barrier that they have to overcome, but also an active immunochemical capable of orchestrating allergen-associated immune responses [2]. It is not fully understood why a person develops respiratory allergy, although a growing number of studies suggest that this clinical disorder is the result of a complex interplay between genetics and the environment [3].

Although the debate about whether an impaired airway epithelium can be the cause of allergy—as opposed to the consequence—remains unresolved, a growing body of evidence indicates that the nature of the host immune response is strongly determined by the developmental state of the epithelium at the time of contact with the inhaled allergen [4].

Moreover, several studies have addressed the role of oxidative stress in allergic inflammation (Figure 2) [5]. The lung epithelium is continuously exposed to oxidants generated during normal metabolism or present in the environment (eg, ozone, nitrogen dioxide, car exhaust emissions, and cigarette smoke). Besides the deleterious effects of these molecules, physiologic oxidants have been shown to be signaling molecules and key regulators of allergic responses in the lung [6,7].

Our review focuses on the airway epithelium as the key orchestrator in the complex framework underlying respiratory allergy. We examine the role of the airway epithelium as a key

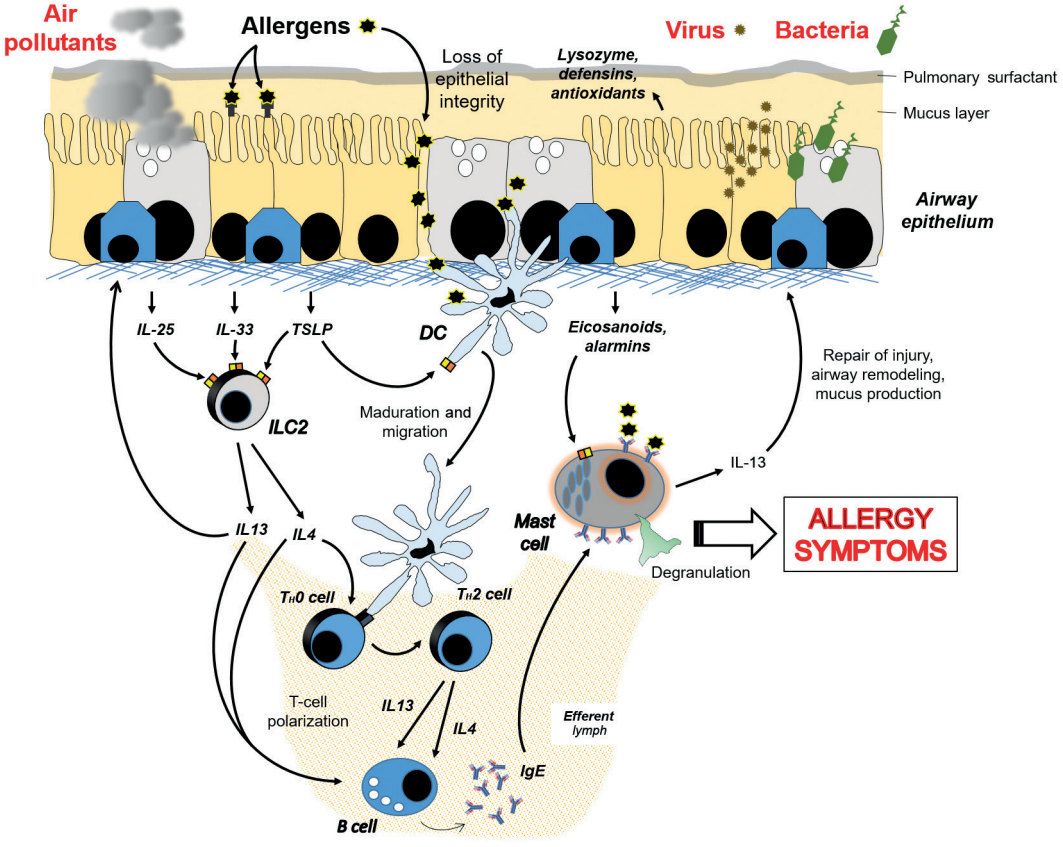

Figure 1. Schematic representation of the role of airway epithelial cells in promoting a T_H2-type immune response to aeroallergens. Airway epithelial cells are able to sense inhaled substances (including air pollutants, allergens, viruses, and bacteria) that are constantly threatening epithelial integrity and homeostasis. They can promote the release of a vast set of molecules, including interleukins (IL), chemokines, and inflammatory mediators. This in turn contributes to the characteristic T_H2-mediated response of allergic reactions through activation of dendritic cells (DC), type-2 innate lymphoid cells (ILC2), and mast cells.

© 2017 Esmon Publicidad

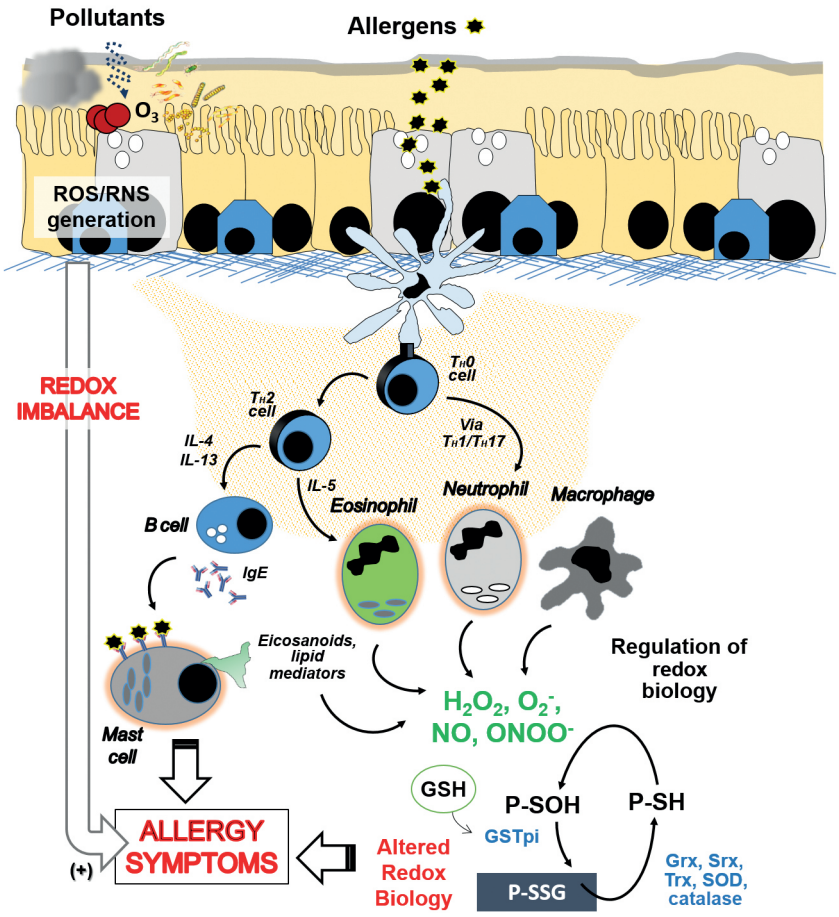

Figure 2. Overview of the molecular mechanisms involved in allergen-triggered immune responses in the context of the lung epithelial redox homeostasis. Reactive oxygen species (ROS) and reactive nitrogen species (RNS) are produced endogenously by eosinophils, neutrophils, and airway macrophages, resulting in S-glutathionylation of reactive cysteine residues within a protein, thus further controlling its activity. Air pollutant interaction with the airway epithelial barrier constitutes an alternate source of oxidants that finally lead to a tissue redox imbalance, enhancing allergic symptoms as stated above. Endogenous and exogenous oxidant species are constantly controlling redox biology in the lung; their levels may act in favor of or against the development of allergic disease. GSH indicates reduced glutathione; Grx, glutaredoxin, GSTpi, glutathione-S-transferase pi; H_2O_2, hydrogen peroxide; NO, nitric oxide; O_2, superoxide; ONOO-, peroxynitrite; P-SH, protein thiol; P-SOH, protein sulfonic acid; P-SSG, protein S-glutathionylation; SOD, superoxide dismutase; Srx, sulfiredoxin; Trx, thioredoxin.

player in orchestrating the allergen immune response, the role of lung "redox biology" in respiratory allergic inflammation, and the effect of air pollutants on the airway epithelium and respiratory allergies.

Airway Epithelium as a Key Player in Orchestrating the Allergic Immune Response

Besides its role as a selective and highly regulated physical barrier through the establishment of the intercellular apical junctional complexes between neighbouring airway epithelial cells (AECs) [8-11], airway epithelium also acts as a critical orchestrator of the airway immune response through the secretion of a wide repertoire of molecules, including antimicrobial peptides and proteins (eg, lysozyme, defensins, and protease inhibitors), antioxidants (eg, superoxide dismutase and glutathione), chemokines, and cytokines, in response to environmental stimuli [2,12-14].

AECs have been identified as the main source of interleukin 25 (IL-25), IL-33, and thymic stromal lymphopoietin (TSLP), the so-called triad of AEC-derived cytokines. These molecules operate upstream of the canonical T_H2 cytokines, primarily IL-4, IL-5, and IL-13, which play a pivotal role in allergy (Figure 1) [15]. At the mucosal surface, the triad of AEC-derived cytokines are important regulators of maintenance of immune homeostasis and induction of both a protective and an inflammatory T_H2-type immune response [16-18]. Dysregulation of these cytokines can lead to exacerbated recruitment and activation of specific immune cells, such as dendritic cells (DCs), type-2 innate lymphoid cells (ILC2s), mast cells (MCs), eosinophils, neutrophils, and basophils, and thus promote a long-term T_H2-type airway hyper-responsiveness spiral. Increased levels of these cytokines have been widely detected in asthma patients [19].

© 2017 Esmon Publicidad

Expression and secretion of IL-33 (IL1F11) and IL-25 (IL-17E) are highly regulated in AECs [20–22]. Both cytokines act as amplifiers of the allergic inflammatory immune response [23,24] via the membrane receptors IL-33R and IL-17RA/IL-17RB, respectively, which are highly expressed in various immune cells, including ILC2s, MCs, basophils, DCs and macrophages [25–29]. In particular, IL-33 can stimulate MC degranulation [30] and release of IL-8 [31], IL-1B, IL-6, tumor necrosis factor-alpha (TNF-α), and chemokine (C-C motif) ligand (CCL) 2 [32], which lead to formation of leukotrienes and prostaglandins and can enhance the inflammatory environment in the lungs [33]. In addition, IL-33 also induces expression of IL-9 in freshly isolated basophils and $CD4^+$ T cells [34]. IL-25 is able to induce promotion of the T_H2 lineage via activation of DCs [35] and is involved in the proliferation of a subpopulation of inflammatory ILC2s [36]. Finally, IL-33 and IL-25 also increase basophil activation and migration in allergic asthma patients [37], and high levels of both cytokines have been reported in bronchoalveolar lavage fluid in asthma models [38].

TSLP is highly secreted by AECs in response to allergens, viruses, diesel extract particles, microbes, and helminths via Toll-like receptor (TLR) signalling [39]. Its secretion is also promoted by loss of E-cadherin after injury and exposure to T_H2 cytokines, such as IL-13 and IL-4 [40,41]. TSLP receptor (the heterodimer IL-7Rα/γc-chain) is highly expressed in DCs and ILC2s [42,43]. In mice, TSLP is able to induce expression of costimulatory molecules on DCs [44]. In combination with IL-33 and IL-25, TSLP also participates in recruitment and proliferation of ILC2 in the lungs, leading to the release of pro-T_H2 molecules such as IL-4, IL-5, IL-9, IL-13, and amphiregulin [45], which was recently shown to perpetuate allergic inflammation [46]. TSLP can also modulate several functions of MCs [47], including the release of proinflammatory cytokines such as IL-6, TNF-α, and IL-1β, but not cell degranulation [41]. Finally, TSLP has been associated with susceptibility to multiple allergic diseases by regulating basophil hematopoiesis [48].

AECs also release granulocyte-macrophage colony-stimulating factor (GM-CSF), CCL20 and CCL2 [49,50], IL-1α, and IL-4 or IL-13 [51] in response to house dust mite allergens (mite extract and Der p 1). These cytokines can induce chemotaxis of MCs and DCs in the epithelium, activation, and migration of DCs to lymph nodes, and polarization of T_H2 cells [52]. Human and mice bronchial epithelial cells can also produce IL-1α in response to allergen exposure and have an autocrine effect that potentiates the secretion of the aforementioned cytokines [53]. Eotaxins 1, 2, and 3 delivered by AECs are also able to induce activation of eosinophils and T_H2 in asthma [54]. In addition, allergen-exposed AECs secrete other alarmins, such as adenosine triphosphate, uric acid and amphoterin (HM-GB1) [55], which are generally released in stress and cell death responses. Increased levels of these molecules have also been reported in patients with asthma [56]. In conclusion, the secretory role of the airway epithelium in orchestrating innate and adaptive immune responses suggests that impaired epithelial barrier function may trigger uncontrolled and deleterious inflammatory processes, such as those observed in allergic reactions.

Aberrant immunochemical actions of the airway epithelium are ultimately determined by the maintenance of the structural integrity of the barrier. Thus, the barrier may be potentially altered by a primary cell-cell junction disruption or alternatively as a consequence of an epithelial remodeling process or epithelial-mesenchymal transition process, both of which involve cell-cell contact disassembly and an increase in the expression of mesenchymal-associated proteins such as α-smooth muscle actin, vimentin, and/or fibronectin [57-59]. The immediate effect of epithelial-mesenchymal transition on barrier function is easier access by inhaled antigens across a more permeable epithelial barrier, thus enabling their interaction with local immune cells. A repetitive injury resulting from chronic exposure to allergens may lead to persistent activation of airway repair processes or, in the worst case scenario, altered migration of progenitor cells and abnormal epithelial dedifferentiation, thus further contributing to unbalance the polarized secretion of the proinflammatory epithelium-derived molecules. Airway remodeling–derived inflammation in response to allergens has been widely associated with chronic respiratory diseases such as asthma [60,61] and has been shown to be even more persistent by means of a prolonged allergen challenge in mice [62-64]. Sustained allergen exposure also promotes the persistence of mucous cell hyperplasia in the murine airway wall [65], as well as smooth muscle remodeling in an experimental model of asthma [66].

Various features of a dysfunctional innate immune function of AECs appear to persist in cultures of cells from asthmatic patients, indicating underlying genetic and epigenetic mechanisms [67]. Polymorphisms in IL-6 [68], IL-4 [69], high-affinity IgE receptor [70], IL-4R [71], disintegrin and metalloproteinase 33 [72], and IL-13 [73] have been associated with epithelial dismantling and malfunctioning, especially in the context of asthma and chronic obstructive pulmonary disease [74,75]. In this sense, a high level of IL-13 in asthmatic patients has been involved in wall remodeling processes [76,77]. Moreover, some genetic variants of TSLP have been linked to asthma or allergic rhinitis [78]. The altered genes that appeared in exposed individuals have been implicated in pulmonary effects driven by environmental agents such as viruses, cigarette smoke, oxidants, and air pollution [79-81], explaining, in part, the higher susceptibility of these patients to the action of airborne insults (see below).

Lung and Redox Biology: Role in Respiratory Allergic Inflammation

Anatomically, the pulmonary epithelium is one of the cell structures most likely to suffer oxidative damage because of continuous exposure to oxidants present in the air, whether generated as part of normal metabolism or exogenously [1]. Oxidants are classified into reactive oxygen species (ROS) and reactive nitrogen species (RNS), and are widely characterized as highly unstable substances. The most physiologically significant ROS are the superoxide anion radical (O_2^-), hydroxyl radical (OH), nitric oxide (NO), and hydrogen peroxide (H_2O_2). NO and H_2O_2 can react immediately to form

© 2017 Esmon Publicidad

a highly reactive RNS form of peroxynitrite ($ONOO^-$) [82]. All these molecules play a relevant role in many cellular processes, such as proliferation, survival, airway remodelling, mucus secretion, and apoptosis and are also critical in the development of airway inflammatory processes [83].

Since all aerobic living forms suffer oxidative damage, the lungs present several antioxidant systems to maintain redox homeostasis. Under normal physiologic conditions, the balance between generation and elimination of ROS/RNS maintains the functional integrity of cell structures and the redox state of signalling proteins. However, prolonged exposure to oxidants can cause dysregulation of redox homeostasis, leading to "oxidative stress", which can in turn lead to cell death and has been proposed as the origin of a variety of airway diseases, such as allergic asthma (Figure 2) [84].

Endogenous oxidants are generated not only by mitochondrial respiration, but also by inflammation-activated cells such as eosinophils, neutrophils, monocytes, macrophages, and tissue-resident cells including endothelial, alveolar, and bronchial epithelial cells. As for the role of mitochondria in inflammation, oxidative stress may cause release to the cytosol of compounds such as damage-associated molecular pattern molecules, adenosine triphosphate, cardiolipins, and mitochondrial DNA, subsequently activating immune signalling cascades via intracellular activation of TLR agonists [85]. Mitochondrial dynamics are directly altered by the presence of airborne particles and protease allergens, leading to changes in membrane potential and proteosomal activity that ultimately leads to proapoptotic events [86,87]. However, the most important source of endogenous oxidants comes from the activation of inflammatory, immune, and structural cells by environmental components (including inhaled allergens), which in turn regulate the expression of specific genes for proinflammatory mediators and antioxidant protective enzymes via activation of redox-sensitive transcription factors such as activator protein-1 (AP-1) and NF-κB. In addition, inflammatory cells present a variety of oxidant-generating enzymatic systems that amplify the inflammatory response and oxidative stress initiated by exogenous insults, thus contributing to lung damage. Neutrophils, macrophages, and eosinophils produce O_2^-, NO, NO_2, and H_2O_2 by NADPH oxidase ($gp91^{phox}$-NOX2), eosinophil peroxidase (EPO), myeloperoxidase (MPO), and inducible NO synthase (iNOS) [88]. In AECs, NADPH oxidase dual oxidase 1 (DUOX1) catalyzes the generation of ROS and regulates IL-33 secretion and the subsequent T_H2-immune response to allergen challenge [89].

Besides having a direct deleterious effect on most of the cellular components, leading to lipid peroxidation of membrane phospholipid, depletion of intracellular tripeptide glutathione (γ-glutamyl-cysteinyl-glycine [GSH]), DNA damage, and amino acid modification in cellular proteins [90], ROS/RNS also have a critical role in the activation of redox/signalling pathways and transcription factors (see above). Modifications to proteins by physiological oxidants mainly involve reversible oxidation of cysteine residues, which act as cell redox sensors that regulate homeostasis and various biological processes, among them cell proliferation, migration, differentiation, and signalling, as well as gene transcription [5]. In contrast, protein modifications by exogenous oxidants are often associated with the pathogenesis of many human diseases, including asthma, heart disease, neurodegenerative disease, and cancer.

GSH, which contains a sulfhydryl group, is a critical antioxidant in the lung, in particular in the protection of airway epithelium against damage induced by oxidants and inflammation. GSH is the predominant antioxidant in airway cells, ranging from 1 to 11 mM depending on the subcellular compartment, and its concentration in the epithelial lining fluid (ELF) that bathes the entire surface of the lung, is over 100-fold higher than in plasma [91-93]. GSH is a key player in the maintenance of redox homeostasis in the lung, which is mainly defined by the ratio of the concentration of its reduced form to its disulphide form, GSH/GSSG [94]. Under normal conditions, the oxidized form represents less than 1% of the total GSH pool; however, alterations of the GSH/GSSG ratio in ELF have been described in patients with asthma and other inflammatory disorders such as cystic fibrosis. In this sense, depletion of GSH from the ELF activates inflammatory routes involving NFκB activation, thus playing a key role in the expression of proinflammatory genes and cytokine release [95]. In animal models, exposure to toxins, viruses, or allergens such as OVA decreased the total thiol content in bronchoalveolar lavage fluid, thus inducing epithelial apoptosis, cytokine release, and eosinophil influx. However, a higher GSSG content was observed, together with impaired activity of various enzymatic antioxidants such as superoxide dismutase (SOD), catalase, and thioredoxin [96,97]. Lower antioxidant activities, including those associated with GSH synthesis, have also been described in ELF and in cells of asthmatic patients. On the other hand, nuclear factor (erythroid-derived 2)–like 2 is a transcription factor that regulates the expression of phase II and antioxidant enzyme genes, for example, catalase, SOD, glutathione-S-transferase (GST), glutathione peroxidase (GPx), and glutathione synthetase, and is considered a feedback loop that is originally affected by dramatic changes in the GSH/GSSG ratio [1,97]. In this sense, GSTP1- and SOD-specific loci have been strongly associated with asthma and deficiencies in oxidant defenses, although their role remains unclear [98]. As for the protective role of GSH, it is noteworthy that GSH can also be reversibly incorporated into cysteine residues of proteins, through an enzymatic process called S-glutathionylation [99]. This process, which is catalyzed mainly by GSTs, protects oxidant-target proteins from being irreversibly oxidized, thereby avoiding their aberrant activation or loss of functionality through proteasome degradation [100]. This post-translational modification can alter the activity and function of specific transcription factors involved in inflammatory processes, such as the p65 and p50 subunits of NFκB, thus inhibiting their binding to DNA [101,102] and avoiding the expression of numerous proinflammatory genes. The regulatory inhibitory kappaB kinase beta may also undergo S-glutathionylation, thus allowing the inhibition of NFκB transactivation [103]. The expression of other inflammatory genes, such as c-Jun (AP-1), has also been reported to undergo S-glutathionylation [104]. Finally, the rate of S-glutathionylation is markedly lower in patients with asthma [105], thus reinforcing the hypothesis that associates the redox imbalance with the development of

© 2017 Esmon Publicidad

the pathological features of severe allergic asthma, including airway inflammation and epithelial barrier impairment.

Effect of Air Pollutants on the Airway Epithelium and Respiratory Allergies

Its anatomical and functional features make the lung the organ with the largest surface exposed to a wide range of air pollutants from natural sources or man-made activities, which have a harmful impact on human health and also on animals and plants. Air pollutants include volatile organic compounds, particulate matter (PM), gases, and metals [106], with carbon monoxide (CO), hydrocarbons, nitrogen dioxide (NO_2), PM, (SO_2), and ozone (O_3) being the most common and abundant. Whilst O_3 is formed in the earth's atmosphere by UV light reactions, CO, NO_2, and PM are generated from fossil fuel burning from motor vehicles, factories, gas heaters, cookers, and cigarette smoke, all of which are concentrated in urban areas. For example, in major cities, up to 90% of airborne PM consists of diesel exhaust particles, which are high-molecular-weight carbon-based entities (~100 nm) that can promote allergic airway inflammation and hyper-responsiveness [107-109].

Air pollutants can facilitate sensitization to aeroallergens by a direct effect on airway epithelium and largely contribute to respiratory allergic symptoms and to the pathogenesis of other chronic airway diseases, in particular chronic obstructive pulmonary disease [110,111]. Air pollutants act by increasing airway epithelial barrier permeability, inhibiting mucociliary clearance, and inducing AECs to secrete an array of inflammatory mediators such as chemokines, cytokines, eicosanoids, and adhesion molecules that recruit and activate DCs, ILC2s, and basophils, thus contributing to T_H2-type immunity. O_3 increases the release of IL-8, GM-CSF, TNF-α, and sICAM-1 on cultured human bronchial epithelial cells [112], while NO_2 enhances the secretion of leukotriene C4, CXCL8, GM-CSF, and TNF-α [113,114]. Moreover, diesel exhaust particles upregulate the mRNA levels of TSLP [115], which can promote maturation of myeloid DCs that support T_H2-type polarization [116]. Furthermore, numerous studies have shown that smokers exhibit impaired mucociliary clearance [117-120] because of the inhibitory effect of cigarette smoke compounds on the expression of genes involved in ciliogenesis [121]. In turn, an increase in barrier permeability may facilitate the access of aeroallergens to the submucosa and their interaction with resident DCs and ILC2s, as well as with recruited MCs, eosinophils, lymphocytes, and neutrophils [122].

The deleterious effect of air pollutants on airway epithelium has been attributed to oxidative stress [123]. Air pollutants can also generate ROS, which activates NF-κB signalling in the airway epithelium, leading to the secretion of the epithelial cytokines IL-1, IL-25, IL-33, GM-CSF, and TSLP, as well as other mediators. Subsequently a variety of cellular events are promoted and result in allergic sensitization to inhaled allergens [124,125]. O_3 [126], NO_2 [127], and cigarette smoke [128,129] induce epithelial cells to release ROS and RNS.

Another mechanism by which air pollutants contribute to respiratory allergies is by interacting with allergens, thus acting as carriers and adjuvants that modify the features of allergens, which in turn enhance the immune response to them. It has been shown that PM and diesel exhaust particles can carry allergens from pollen, cat, dog, and house dust mite [130]. Moreover, it has been reported that air pollution increases the allergenic potency of pollen [131-133]. In their model based on guinea pigs sensitized to *Zinnia* pollen, Chelregani et al [134] observed that pollen collected from polluted urban areas not only induced higher levels of serum IgE, but also increased eosinophil counts compared with nonpolluted pollen. Finally, growing evidence indicates that air pollutants can increase the production of allergens and proinflammatory mediators in pollens as a result of the plant adaptive response to environmental stress [131,135]. In addition, it has been shown that pollens are a source of oxidants [136]. Once pollen NADPH oxidases reach the airway epithelium, levels of ROS and GSSG in ELF increase. These NADPH oxidases, which originally participate in pollen germination and pollen tube formation, could contribute to the allergic airway inflammation induced by the allergen.

Funding

This study was supported by grant SAF2014-53209-R from the Ministerio de Economía y Competitividad and RIRAAF Network RD12/0013/0015 and ARADyAL Network RD16/0006/0014 from the ISCIII. JCL-R. is supported by a FPU fellowship from the Ministerio de Educación, Cultura y Deporte (Spain). SB is a fellow of the Juan de la Cierva program of the Ministerio de Economía y Competitividad (Spain).

Conflicts of Interest

The authors declare that they have no conflicts of interest.

References

1. Biswas SK, Rahman I. Environmental toxicity, redox signaling and lung inflammation: the role of glutathione. Mol Aspects Med. 2009;30(1-2):60-76.
2. Lambrecht BN, Hammad H. Allergens and the airway epithelium response: Gateway to allergic sensitization. J Allergy Clin Immunol. 2014;134(3):499-507.
3. von Mutius E. Gene-environment interactions in asthma. J Allergy Clin Immunol. 2009 Jan;123(1):3.
4. Gandhi VD, Vliagoftis H. Airway Epithelium Interactions with Aeroallergens: Role of Secreted Cytokines and Chemokines in Innate Immunity. Front Immunol. 2015;6(April):1-13.
5. Janssen-Heininger YMW, Mossman BT, Heintz NH, Forman HJ, Kalyanaraman B, Finkel T, et al. Redox-based regulation of signal transduction: principles, pitfalls, and promises. Free Radic Biol Med. 2008 Jul;45(1):1-17.
6. Kinnula VL, Crapo JD, Raivio KO. Generation and disposal of reactive oxygen metabolites in the lung. Lab Invest. 1995 Jul;73(1):3-19.
7. Finkel T. Signal transduction by reactive oxygen species. J Cell Biol. 2011 Jul;194(1):7-15.
8. Georas SN, Rezaee F. Epithelial barrier function: at the front line of asthma immunology and allergic airway inflammation.

© 2017 Esmon Publicidad

Vol. 134, The Journal of allergy and clinical immunology. 2014. p. 509-20.
9. Davies JA, Garrod DR. Molecular aspects of the epithelial phenotype. Bioessays. 1997 Aug;19(8):699-704.
10. Kojima T, Go M, Takano K, Kurose M, Ohkuni T, Koizumi J, et al. Regulation of tight junctions in upper airway epithelium. Biomed Res Int. 2013: 947072.
11. Ganesan S, Comstock AT, Sajjan US. Barrier function of airway tract epithelium. Tissue barriers. 2013;1(4):e24997.
12. Hallstrand TS, Hackett TL, Altemeier WA, Matute-Bello G, Hansbro PM, Knight DA. Airway epithelial regulation of pulmonary immune homeostasis and inflammation. Clin Immunol. 2014;151(1):1-15.
13. Gohy ST, Hupin C, Pilette C, Ladjemi MZ. Chronic inflammatory airway diseases: the central role of the epithelium revisited. Clin Exp Allergy. 2016.
14. Xue L, Salimi M, Panse I, Mjosberg JM, McKenzie ANJ, Spits H, et al. Prostaglandin D2 activates group 2 innate lymphoid cells through chemoattractant receptor-homologous molecule expressed on TH2 cells. J Allergy Clin Immunol. 2014 Apr;133(4):1184-94.
15. Hammad H, Lambrecht BN. Dendritic cells and epithelial cells: linking innate and adaptive immunity in asthma. Nat Rev Immunol. 2008;8(3):193-204.
16. Bartemes KR, Kita H. Dynamic role of epithelium-derived cytokines in asthma. Clin Immunol. 2012 Jun;143(3):222-35.
17. Lloyd CM, Saglani S. Epithelial cytokines and pulmonary allergic inflammation. Curr Opin Immunol. 2015;34:52-8.
18. Pawankar R, Hayashi M, Yamanishi S, Igarashi T. The paradigm of cytokine networks in allergic airway inflammation. Curr Opin Allergy Clin Immunol. 2015;15(1):41-8.
19. Mitchell PD, O'Byrne PM. Epithelial-Derived Cytokines in Asthma. Chest. 2017;151(6):1338-44.
20. Carriere V, Roussel L, Ortega N, Lacorre D-A, Americh L, Aguilar L, et al. IL-33, the IL-1-like cytokine ligand for ST2 receptor, is a chromatin-associated nuclear factor in vivo. Proc Natl Acad Sci U S A. 2007 Jan;104(1):282-7.
21. Luthi AU, Cullen SP, McNeela EA, Duriez PJ, Afonina IS, Sheridan C, et al. Suppression of interleukin-33 bioactivity through proteolysis by apoptotic caspases. Immunity. 2009 Jul;31(1):84-98.
22. Cohen ES, Scott IC, Majithiya JB, Rapley L, Kemp BP, England E, et al. Oxidation of the alarmin IL-33 regulates ST2-dependent inflammation. Nat Commun. 2015 Sep;6:8327.
23. Gour N, Lajoie S. Epithelial Cell Regulation of Allergic Diseases. Curr Allergy Asthma Rep. 2016 Sep;16(9):65.
24. Iwakura Y, Ishigame H, Saijo S, Nakae S. Functional specialization of interleukin-17 family members. Immunity. 2011 Feb;34(2):149-62.
25. Yagami A, Orihara K, Morita H, Futamura K, Hashimoto N, Matsumoto K, et al. IL-33 mediates inflammatory responses in human lung tissue cells. J Immunol. 2010 Nov;185(10):5743-50.
26. Besnard A-G, Togbe D, Guillou N, Erard F, Quesniaux V, Ryffel B. IL-33-activated dendritic cells are critical for allergic airway inflammation. Eur J Immunol. 2011 Jun;41(6):1675-86.
27. Kurowska-Stolarska M, Stolarski B, Kewin P, Murphy G, Corrigan CJ, Ying S, et al. IL-33 amplifies the polarization of alternatively activated macrophages that contribute to airway inflammation. J Immunol. 2009 Nov;183(10):6469-77.
28. Toy D, Kugler D, Wolfson M, Vanden Bos T, Gurgel J, Derry J, et al. Cutting edge: interleukin 17 signals through a heteromeric receptor complex. J Immunol. 2006 Jul;177(1):36-9.
29. Chang J, Xia Y-F, Zhang M-Z, Zhang L-M. IL-33 Signaling in Lung Injury. Transl Perioper pain Med. 2016;1(2):24-32.
30. Andrade M V, Iwaki S, Ropert C, Gazzinelli RT, Cunha-Melo JR, Beaven MA. Amplification of cytokine production through synergistic activation of NFAT and AP-1 following stimulation of mast cells with antigen and IL-33. Eur J Immunol. 2011 Mar;41(3):760-72.
31. Iikura M, Suto H, Kajiwara N, Oboki K, Ohno T, Okayama Y, et al. IL-33 can promote survival, adhesion and cytokine production in human mast cells. Lab Invest. 2007 Oct;87(10):971-8.
32. Sabatino G, Nicoletti M, Neri G, Saggini A, Rosati M, Conti F, et al. Impact of IL -9 and IL-33 in mast cells. J Biol Regul Homeost Agents. 2012;26(4):577-86.
33. Enoksson M, Lyberg K, Moller-Westerberg C, Fallon PG, Nilsson G, Lunderius-Andersson C. Mast cells as sensors of cell injury through IL-33 recognition. J Immunol. 2011 Feb;186(4):2523-8.
34. Blom L, Poulsen BC, Jensen BM, Hansen A, Poulsen LK. IL-33 induces IL-9 production in human CD4+ T cells and basophils. PLoS One. 2011;6(7):e21695.
35. Hongjia L, Caiqing Z, Degan L, Fen L, Chao W, Jinxiang W, et al. IL-25 promotes Th2 immunity responses in airway inflammation of asthmatic mice via activation of dendritic cells. Inflammation. 2014 Aug;37(4):1070-7.
36. Huang Y, Paul WE. Inflammatory group 2 innate lymphoid cells. Int Immunol. 2015;33(12):dxv044.
37. Salter BM, Oliveria JP, Nusca G, Smith SG, Tworek D, Mitchell PD, et al. IL-25 and IL-33 induce Type 2 inflammation in basophils from subjects with allergic asthma. Respir Res. 2016 Jan;17:5.
38. Beale J, Jayaraman A, Jackson DJ, Macintyre JDR, Edwards MR, Walton RP, et al. Rhinovirus-induced IL-25 in asthma exacerbation drives type 2 immunity and allergic pulmonary inflammation. Sci Transl Med. 2014 Oct;6(256):256ra134.
39. Mitchell PD, O'Byrne PM. Biologics and the lung: TSLP and other epithelial cell-derived cytokines in asthma. Pharmacol Ther. 2017;169:104-12.
40. Kato A, Favoreto SJ, Avila PC, Schleimer RP. TLR3- and Th2 cytokine-dependent production of thymic stromal lymphopoietin in human airway epithelial cells. J Immunol. 2007 Jul;179(2):1080-7.
41. Allakhverdi Z, Comeau MR, Jessup HK, Yoon B-RP, Brewer A, Chartier S, et al. Thymic stromal lymphopoietin is released by human epithelial cells in response to microbes, trauma, or inflammation and potently activates mast cells. J Exp Med. 2007 Feb;204(2):253-8.
42. Isaksen DE, Baumann H, Trobridge PA, Farr AG, Levin SD, Ziegler SF. Requirement for stat5 in thymic stromal lymphopoietin-mediated signal transduction. J Immunol. 1999 Dec;163(11):5971-7.
43. Park LS, Martin U, Garka K, Gliniak B, Di Santo JP, Muller W, et al. Cloning of the murine thymic stromal lymphopoietin (TSLP) receptor: Formation of a functional heteromeric complex requires interleukin 7 receptor. J Exp Med. 2000 Sep;192(5):659-70.
44. Pan G, Liang Y, Lu L, Chen X, Wang M, Wang L, et al. Blockage of thymic stromal lymphopoietin signaling improves acute

© 2017 Esmon Publicidad

lung injury in mice by regulating pulmonary dendritic cells. Int J Clin Exp Pathol. 2015;8(9):10698-706.
45. Halim TYF. Group 2 innate lymphoid cells in disease. Int Immunol. 2016 Jan;28(1):13-22.
46. Karta MR, Broide DH, Doherty TA. Insights into Group 2 Innate Lymphoid Cells in Human Airway Disease. Curr Allergy Asthma Rep. 2016;16(1):1-11.
47. Moon TC, St Laurent CD, Morris KE, Marcet C, Yoshimura T, Sekar Y, et al. Advances in mast cell biology: new understanding of heterogeneity and function. Mucosal Immunol. 2010 Mar;3(2):111-28.
48. Siracusa MC, Saenz SA, Hill DA, Kim BS, Headley MB, Doering TA, et al. TSLP promotes interleukin-3-independent basophil haematopoiesis and type 2 inflammation. Nature. 2011 Aug;477(7363):229-33.
49. Reibman J, Hsu Y, Chen LC, Bleck B, Gordon T. Airway epithelial cells release MIP-3alpha/CCL20 in response to cytokines and ambient particulate matter. Am J Respir Cell Mol Biol. 2003;28(22):648-54.
50. Pichavant M, Charbonnier A-S, Taront S, Brichet A, Wallaert B, Pestel J, et al. Asthmatic bronchial epithelium activated by the proteolytic allergen Der p 1 increases selective dendritic cell recruitment. J Allergy Clin Immunol. 2005 Apr;115(4):771-8.
51. Gour N, Wills-Karp M. IL-4 and IL-13 signaling in allergic airway disease. Cytokine. 2015.
52. Ito T, Wang Y-H, Duramad O, Hori T, Delespesse GJ, Watanabe N, et al. TSLP-activated dendritic cells induce an inflammatory T helper type 2 cell response through OX40 ligand. J Exp Med. 2005 Nov;202(9):1213-23.
53. Willart MAM, Deswarte K, Pouliot P, Braun H, Beyaert R, Lambrecht BN, et al. Interleukin-1alpha controls allergic sensitization to inhaled house dust mite via the epithelial release of GM-CSF and IL-33. J Exp Med. 2012 Jul;209(8):1505-17.
54. Coleman JM, Naik C, Holguin F, Ray A, Ray P, Trudeau JB, et al. Epithelial eotaxin-2 and eotaxin-3 expression: relation to asthma severity, luminal eosinophilia and age at onset. Thorax. 2012 Dec;67(12):1061-6.
55. Kono H, Rock KL. How dying cells alert the immune system to danger. Nat Rev Immunol. 2008 Apr;8(4):279-89.
56. Willart MAM, Lambrecht BN. The danger within: endogenous danger signals, atopy and asthma. Clin Exp Allergy. 2009 Jan;39(1):12-9.
57. Pain M, Bermudez O, Lacoste P, Royer P-J, Botturi K, Tissot A, et al. Tissue remodelling in chronic bronchial diseases: from the epithelial to mesenchymal phenotype. Eur Respir Rev. 2014 Mar;23(131):118-30.
58. Ozdamar B, Bose R, Barrios-Rodiles M, Wang H-R, Zhang Y, Wrana JL. Regulation of the polarity protein Par6 by TGFbeta receptors controls epithelial cell plasticity. Science. 2005 Mar;307(5715):1603-9.
59. Ikenouchi J, Matsuda M, Furuse M, Tsukita S. Regulation of tight junctions during the epithelium-mesenchyme transition: direct repression of the gene expression of claudins/occludin by Snail. J Cell Sci. 2003 May;116(Pt 10):1959-67.
60. Fehrenbach H, Wagner C, Wegmann M. Airway remodeling in asthma: what really matters. Cell Tissue Res. 2017 Mar;367(3):551-69.
61. Hogg J. Peripheral lung remodelling in asthma and chronic obstructive pulmonary disease. Vol. 24, The European respiratory journal. England; 2004. p. 893-4.
62. McMillan SJ, Lloyd CM. Prolonged allergen challenge in mice leads to persistent airway remodelling. Clin Exp Allergy. 2004 Mar;34(3):497-507.
63. Johnson JR, Roos A, Berg T, Nord M, Fuxe J. Chronic respiratory aeroallergen exposure in mice induces epithelial-mesenchymal transition in the large airways. PLoS One. 2011 Jan;6(1):e16175.
64. Masuda T, Tanaka H, Komai M, Nagao K, Ishizaki M, Kajiwara D, et al. Mast cells play a partial role in allergen-induced subepithelial fibrosis in a murine model of allergic asthma. Clin Exp Allergy. 2003 May;33(5):705-13.
65. Kumar RK, Herbert C, Foster PS. Expression of growth factors by airway epithelial cells in a model of chronic asthma: regulation and relationship to subepithelial fibrosis. Clin Exp Allergy. 2004 Apr;34(4):567-75.
66. Ramos-Barbon D, Presley JF, Hamid QA, Fixman ED, Martin JG. Antigen-specific CD4+ T cells drive airway smooth muscle remodeling in experimental asthma. J Clin Invest. 2005 Jun;115(6):1580-9.
67. Hiemstra PS, McCray PBJ, Bals R. The innate immune function of airway epithelial cells in inflammatory lung disease. Eur Respir J. 2015 Apr;45(4):1150-62.
68. Babusikova E, Jurecekova J, Jesenak M, Evinova A. Association of Gene Polymorphisms in Interleukin 6 in Infantile Bronchial Asthma. Arch Bronconeumol. 2017 Jul;53(7):381-6.
69. Micheal S, Minhas K, Ishaque M, Ahmed F, Ahmed A. IL-4 gene polymorphisms and their association with atopic asthma and allergic rhinitis in Pakistani patients. J Investig Allergol Clin Immunol. 2013;23(2):107-11.
70. Hizawa N, Yamaguchi E, Jinushi E, Konno S, Kawakami Y, Nishimura M. Increased total serum IgE levels in patients with asthma and promoter polymorphisms at CTLA4 and FCER1B. J Allergy Clin Immunol. 2001 Jul;108(1):74-9.
71. Slager RE, Otulana BA, Hawkins GA, Yen YP, Peters SP, Wenzel SE, et al. IL-4 receptor polymorphisms predict reduction in asthma exacerbations during response to an anti-IL-4 receptor alpha antagonist. J Allergy Clin Immunol. 2012 Aug;130(2):516-22.
72. Shah S, Rashid A, Shah ZA, Jan RA, Khan UH, Bhat IA, et al. A disintegrin and metalloprotease 33 polymorphism association with COPD in long-term tobacco smokers of the ethnic Kashmiri population of India. Lung India. 2015;32(3):220-4.
73. Xu Y, Li J, Ding Z, Li J, Li B, Yu Z, et al. Association between IL-13 +1923C/T polymorphism and asthma risk: a meta-analysis based on 26 case-control studies. Biosci Rep. 2017;37(1).
74. Reddy AJ, Kleeberger SR. Genetic polymorphisms associated with acute lung injury. Pharmacogenomics. 2009;10(9):1527-39.
75. Bierbaum S, Heinzmann A. The genetics of bronchial asthma in children. Respir Med. 2007;101(7):1369-75.
76. Yang G, Volk A, Petley T, Emmell E, Giles-Komar J, Shang X, et al. Anti-IL-13 monoclonal antibody inhibits airway hyperresponsiveness, inflammation and airway remodeling. Cytokine. 2004; 28(6):224-32.
77. Kumar RK, Herbert C, Yang M, Koskinen AML, McKenzie ANJ, Foster PS. Role of interleukin-13 in eosinophil accumulation

© 2017 Esmon Publicidad

and airway remodelling in a mouse model of chronic asthma. Clin Exp Allergy. 2002 Jul;32(7):1104-11.
78. Cianferoni A, Spergel J. The importance of TSLP in allergic disease and its role as a potential therapeutic target. Expert Rev Clin Immunol. 2014 Nov;10(11):1463-74.
79. Klingbeil EC, Hew KM, Nygaard UC, Nadeau KC. Polycyclic aromatic hydrocarbons, tobacco smoke, and epigenetic remodeling in asthma. Immunol Res. 2014 May;58(2-3):369-73.
80. Ho S-M. Environmental epigenetics of asthma: an update. J Allergy Clin Immunol. 2010 Sep;126(3):453-65.
81. Molfino NA, Coyle AJ. Gene-environment interactions in chronic obstructive pulmonary disease. Int J Chron Obstruct Pulmon Dis. 2008;3(3):491-7.
82. Comhair SAA, Erzurum SC. Redox control of asthma: molecular mechanisms and therapeutic opportunities. Antioxid Redox Signal. 2010 Jan;12(1):93-124.
83. Ckless K, Hodgkins SR, Ather JL, Martin R, Poynter ME. Epithelial, dendritic, and CD4(+) T cell regulation of and by reactive oxygen and nitrogen species in allergic sensitization. Biochim Biophys Acta. 2011 Nov;1810(11):1025-34.
84. Haddad JJ. Oxygen-sensing mechanisms and the regulation of redox-responsive transcription factors in development and pathophysiology. Respir Res. 2002;3:26.
85. Iyer D, Mishra N, Agrawal A. Mitochondrial Function in Allergic Disease. Curr Allergy Asthma Rep. 2017 May;17(5):29.
86. Gosens I, Post JA, de la Fonteyne LJJ, Jansen EHJM, Geus JW, Cassee FR, et al. Impact of agglomeration state of nano- and submicron sized gold particles on pulmonary inflammation. Part Fibre Toxicol. 2010 Dec;7(1):37.
87. Kipen HM, Gandhi S, Rich DQ, Ohman-Strickland P, Laumbach R, Fan Z-H, et al. Acute decreases in proteasome pathway activity after inhalation of fresh diesel exhaust or secondary organic aerosol. Environ Health Perspect. 2011 May;119(5):658-63.
88. Erzurum SC. New Insights in Oxidant Biology in Asthma. Ann Am Thorac Soc. 2016 Mar;13 Suppl 1:S35-9.
89. Hristova M, Habibovic A, Veith C, Janssen-Heininger YMW, Dixon AE, Geiszt M, et al. Airway epithelial dual oxidase 1 mediates allergen-induced IL-33 secretion and activation of type 2 immune responses. J Allergy Clin Immunol. 2016 May;137(5):1545-56.e11.
90. Hoffman S, Nolin J, McMillan D, Wouters E, Janssen-Heininger Y, Reynaert N. Thiol redox chemistry: role of protein cysteine oxidation and altered redox homeostasis in allergic inflammation and asthma. J Cell Biochem. 2015 Jun;116(6):884-92.
91. Moss M, Guidot DM, Wong-Lambertina M, Ten Hoor T, Perez RL, Brown LA. The effects of chronic alcohol abuse on pulmonary glutathione homeostasis. Am J Respir Crit Care Med. 2000 Feb;161(2.1):414-9.
92. Mudway IS, Stenfors N, Blomberg A, Helleday R, Dunster C, Marklund SL, et al. Differences in basal airway antioxidant concentrations are not predictive of individual responsiveness to ozone: a comparison of healthy and mild asthmatic subjects. Free Radic Biol Med. 2001 Oct;31(8):962-74.
93. Nadeem A, Chhabra SK, Masood A, Raj HG. Increased oxidative stress and altered levels of antioxidants in asthma. J Allergy Clin Immunol. 2003 Jan;111(1):72-8.
94. Fitzpatrick AM, Jones DP, Brown LAS. Glutathione redox control of asthma: from molecular mechanisms to therapeutic opportunities. Antioxid Redox Signal. 2012 Jul;17(2):375-408.
95. Yang S-R, Chida AS, Bauter MR, Shafiq N, Seweryniak K, Maggirwar SB, et al. Cigarette smoke induces proinflammatory cytokine release by activation of NF-kappaB and posttranslational modifications of histone deacetylase in macrophages. Am J Physiol Lung Cell Mol Physiol. 2006 Jul;291(1):L46-57.
96. Nadeem A, Masood A, Siddiqui N. Oxidant--antioxidant imbalance in asthma: scientific evidence, epidemiological data and possible therapeutic options. Ther Adv Respir Dis. 2008 Aug;2(4):215-35.
97. Sahiner UM, Birben E, Erzurum S, Sackesen C, Kalayci O. Oxidative stress in asthma. World Allergy Organ J. 2011 Oct;4(10):151-8.
98. Schroer KT, Gibson AM, Sivaprasad U, Bass SA, Ericksen MB, Wills-Karp M, et al. Downregulation of glutathione S-transferase pi in asthma contributes to enhanced oxidative stress. J Allergy Clin Immunol. 2011 Sep;128(3):539-48.
99. Dalle-Donne I, Rossi R, Giustarini D, Colombo R, Milzani A. S-glutathionylation in protein redox regulation. Free Radic Biol Med. 2007 Sep;43(6):883-98.
100. Mallis RJ, Hamann MJ, Zhao W, Zhang T, Hendrich S, Thomas JA. Irreversible thiol oxidation in carbonic anhydrase III: protection by S-glutathiolation and detection in aging rats. Biol Chem. 2002;383(3-4):649-62.
101. Qanungo S, Starke DW, Pai H V, Mieyal JJ, Nieminen A-L. Glutathione supplementation potentiates hypoxic apoptosis by S-glutathionylation of p65-NFkappaB. J Biol Chem. 2007 Jun;282(25):18427-36.
102. Pineda-Molina E, Klatt P, Vazquez J, Marina A, Garcia de Lacoba M, Perez-Sala D, et al. Glutathionylation of the p50 subunit of NF-kappaB: a mechanism for redox-induced inhibition of DNA binding. Biochemistry. 2001 Nov;40(47):14134-42.
103. Reynaert NL, van der Vliet A, Guala AS, McGovern T, Hristova M, Pantano C, et al. Dynamic redox control of NF-kappaB through glutaredoxin-regulated S-glutathionylation of inhibitory kappaB kinase beta. Proc Natl Acad Sci U S A. 2006 Aug;103(35):13086-91.
104. Rahman I, Gilmour PS, Jimenez LA, MacNee W. Oxidative stress and TNF-alpha induce histone acetylation and NF-kappaB/AP-1 activation in alveolar epithelial cells: potential mechanism in gene transcription in lung inflammation. Mol Cell Biochem. 2002;234-235(1-2):239-48.
105. Jiang L, Diaz PT, Best TM, Stimpfl JN, He F, Zuo L. Molecular characterization of redox mechanisms in allergic asthma. Ann Allergy Asthma Immunol. 2014 Aug;113(2):137-42.
106. Akimoto H. Global Air Quality and Pollution. Science. 2003;302(5651):1716-9.
107. Yang SN, Hsieh CC, Kuo HF, Lee MS, Huang MY, Kuo CH, et al. The effects of environmental toxins on allergic inflammation. Allergy, Asthma Immunol Res. 2014;6(6):478-84.
108. Levetin E, Van de Water P. Environmental contributions to allergic disease. Curr Allergy Asthma Rep. 2001;1:506-14.
109. Kelly FJ, Fussell JC. Air pollution and airway disease. Clin Exp Allergy. 2011;41(8):1059-71.
110. Provost EB, Chaumont A, Kicinski M, Cox B, Fierens F, Bernard A, et al. Serum levels of club cell secretory protein (Clara) and

© 2017 Esmon Publicidad

short- and long-term exposure to particulate air pollution in adolescents. Environ Int. 2014;68:66-70.
111. Dietert RR, DeWitt JC, Germolec DR, Zelikoff JT. Breaking patterns of environmentally influenced disease for health risk reduction: Immune perspectives. Environ Health Perspect. 2010;118(8):1091-9.
112. Rusznak C, Devalia JLL, Sapsford RJJ, Davies RJJ. Ozone-induced mediator release from human bronchial epithelial cells <I>in vitro</I> and the influence of nedocromil sodium. Eur Respir J. 1996;9(11):2298-305.
113. Devalia JL, Campbell AM, Sapsford RJ, Rusznak C, Quint D, Godard P, et al. Effect of nitrogen dioxide on synthesis of inflammatory cytokines expressed by human bronchial epithelial cells in vitro. Am J Respir Cell Mol Biol. 1993;9(3):271-8.
114. Devalia JL, Sapsford RJ, Cundell DR, Rusznak C, Campbell AM, Davies RJ. Human bronchial epithelial cell dysfunction following in vitro exposure to nitrogen dioxide. Eur Respir J. 1993;6(9):1308-16.
115. Bleck B, Grunig G, Chiu A, Liu M, Gordon T, Kazeros A, et al. MicroRNA-375 regulation of thymic stromal lymphopoietin by diesel exhaust particles and ambient particulate matter in human bronchial epithelial cells. J Immunol. 2013;190(7):3757-63.
116. Bleck B, Tse DB, Jaspers I, Curotto MA, Lafaille D, Reibman J, et al. Diesel exhaust particle-exposed human bronchial epithelial cells induce dendritic cell maturation. J Immunol. 2006;176(12):7431-7.
117. Vastag E, Matthys H, Kohler D, Gronbeck L, Daikeler G. Mucociliary clearance and airways obstruction in smokers, ex-smokers and normal subjects who never smoked. Eur J Respir Dis Suppl. 1985;139:93-100.
118. Goodman RM, Yergin BM, Landa JF, Golivanux MH, Sackner MA. Relationship of smoking history and pulmonary function tests to tracheal mucous velocity in nonsmokers, young smokers, ex-smokers, and patients with chronic bronchitis. Am Rev Respir Dis. 1978 Feb;117(2):205-14.
119. Lourenço R V., Klimek MF, Borowski CJ. Deposition and clearance of 2 micron particles in the tracheobronchial tree of normal subjects--smokers and nonsmokers. J Clin Invest. 1971;50(7):1411-20.
120. Camner P, Philipson K. Tracheobronchial clearance in smoking-discordant twins. Arch Environ Health. 1972 Jul;25(1):60-3.
121. Brekman A, Walters MS, Tilley AE, Crystal RG. FOXJ1 prevents cilia growth inhibition by cigarette smoke in human airway epithelium in vitro. Am J Respir Cell Mol Biol. 2014;51(5):688-700.
122. Lambrecht BN, Hammad H. The immunology of the allergy epidemic and the hygiene hypothesis. Nat Immunol. 2017;(18):1076-83.
123. D'Amato G, Holgate ST, Pawankar R, Ledford DK, Cecchi L, Al-Ahmad M, et al. Meteorological conditions, climate change, new emerging factors, and asthma and related allergic disorders. A statement of the World Allergy Organization. World Allergy Organ J. 2015;8(1):25.
124. Bleck B, Tse DB, Gordon T, Ahsan MR, Reibman J. Diesel exhaust particle-treated human bronchial epithelial cells upregulate Jagged-1 and OX40 ligand in myeloid dendritic cells via thymic stromal lymphopoietin. J Immunol. 2010 Dec;185(11):6636-45.
125. Brandt EB, Myers JMB, Ryan PH, Hershey GKK. Air pollution and allergic diseases. Curr Opin Pediatr. 2015 Dec;27(6):724-35.
126. Song H, Tan W, Zhang X. Ozone induces inflammation in bronchial epithelial cells. J Asthma. 2011 Feb;48(1):79-83.
127. Tunnicliffe WS, Burge PS, Ayres JG. Effect of domestic concentrations of nitrogen dioxide on airway responses to inhaled allergen in asthmatic patients. Lancet (London, England). 1994 Dec;344(8939-8940):1733-6.
128. Ishikawa S, Ito S. Repeated whole cigarette smoke exposure alters cell differentiation and augments secretion of inflammatory mediators in air-liquid interface three-dimensional co-culture model of human bronchial tissue. Toxicol In Vitro. 2017 Feb;38:170-8.
129. Comer DM, Elborn JS, Ennis M. Inflammatory and cytotoxic effects of acrolein, nicotine, acetylaldehyde and cigarette smoke extract on human nasal epithelial cells. BMC Pulm Med. 2014 Mar;14:32.
130. Ormstad H, Johansen B V, Gaarder PI. Airborne house dust particles and diesel exhaust particles as allergen carriers. Clin Exp Allergy. 1998 Jun;28(6):702-8.
131. Senechal H, Visez N, Charpin D, Shahali Y, Peltre G, Biolley J-P, et al. A Review of the Effects of Major Atmospheric Pollutants on Pollen Grains, Pollen Content, and Allergenicity. ScientificWorldJournal. 2015;2015:940243.
132. Schiavoni G, D'Amato G, Afferni C. The dangerous liaison between pollens and pollution in respiratory allergy. Ann Allergy Asthma Immunol. 2017 Mar;118(3):269-75.
133. Bartra Tomás J, Mullol J, Del Cuvillo A, Dávila I, Ferrer M, Jáuregui I, et al. Air pollution and allergens. J Investig Allergol Clin Immunol. 2007;17(2):3-8.
134. Chehregani A, Maide A, Gholami M, Ali Shariatzadeh M, Nassiri H. Increasing allergy potency of Zinnia pollen grains in polluted areas. Ecotoxicol Environ Saf. 2004;58(2):267-72.
136. Boldogh I, Bacsi A, Choudhury BK, Dharajiya N, Alam R, Hazra TK, et al. ROS generated by pollen NADPH oxidase provide a signal that augments antigen-induced allergic airway inflammation. J Clin Invest. 2005 Aug;115(8):2169-7.

Manuscript received July 26, 2017; accepted for publication September 21, 2017.

E Batanero

Departamento de Bioquímica y Biología Molecular I
Facultad de Ciencias Químicas
Universidad Complutense, Madrid, Spain
E-mail: ebataner@ucm.es

© 2017 Esmon Publicidad

Effects of Ole e 1 on Human Bronchial Epithelial Cells Cultured at the Air-Liquid Interface

López-Rodríguez JC[1], Solís-Fernández G[1], Barderas R[2], Villalba M[1], Batanero E[1]

[1]*Departamento de Bioquímica y Biología Molecular I, Facultad de Ciencias Químicas. Universidad Complutense de Madrid, Madrid, Spain*

[2]*UFIEC, National Institute of Health Carlos III, Majadahonda, Madrid, Spain*

J Investig Allergol Clin Immunol 2018; Vol. 28(3): 186-189
doi: 10.18176/jiaci.0227

Key words: Air-liquid interface culture. Airway epithelium. Cell differentiation. Ole e 1. Olive pollen.

Palabras clave: Cultivo en interfase aire-líquido. Epitelio de las vías aéreas. Diferenciación celular. Ole e 1. Polen de olivo.

Airway epithelium is a highly regulated first protective barrier against inhaled substances including respiratory viruses, bacteria, air pollutants, cigarette smoke, and allergens, which have easy access to the airway mucosae [1]. For several decades, dysfunction of airway epithelium has been increasingly linked to airway inflammatory diseases such as asthma, chronic obstructive pulmonary disease, and cystic fibrosis [2]. Furthermore, growing evidence suggests that impaired epithelium can be the cause, rather than the consequence, of inflammatory disease [3,4] and that the nature of the host immune response is strongly determined by the state of the epithelium at the time of contact with the inhaled substances [5].

In this study, we describe the effect of Ole e 1, the main allergen of olive pollen, on bronchial epithelium throughout the differentiation process. Primary normal human bronchial epithelial cells (NHBE) from 2 female donors (age, 40 and 44 years; nonsmokers) (Lonza) were cultured at the air-liquid interface (ALI) in differentiation B-ALI-D medium (Lonza) according to the manufacturer's instructions to obtain a pseudostratified barrier with a mucociliary phenotype that represents one of the best in vitro cell models mimicking the complexity of human airway epithelium. NHBE cells were apically exposed to purified Ole e 1 (25 µg/mL) in B-ALI-D medium for 16 hours on days 7 and 21 at the ALI; these time points correspond to undifferentiated and differentiated epithelium, respectively.

Exposure of differentiating NHBE cells to Ole e 1 did not impair establishment of the epithelial barrier and its physical properties, as assessed using transepithelial electrical resistance (TEER) measurements and ultrastructural analysis based on transmission electron microscopy (TEM). No significant changes in TEER—an indirect measure of apical junctional complex (AJC) formation—were observed in response to exposure to Ole e 1 at day 7 or at day 21 at the ALI, regardless of the donor (Figure, A). Consistent with

 © 2018 Esmon Publicidad

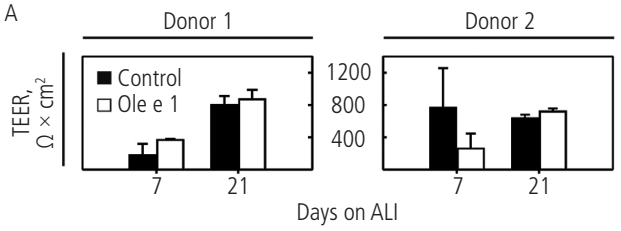

Figure, A. Exposure to Ole e 1 did not impair establishment of the epithelial barrier or apical junctional complex formation, although it did alter the cytokine secretion profile in differentiating NHBE cells from 2 donors at day 7 and 21 on ALI. TEER values are the mean (SD) of triplicate determinations on a given well (n=5). TEER indicates transepithelial electrical resistance; NHBE, normal human bronchial epithelial cells.

TEER values, TEM micrographs revealed a normal epithelial structure in differentiating NHBE cells after exposure to Ole e 1 compared with untreated control cells and detected interdonor variability (Figure, B). At day 7, undifferentiated cultures showed 2-3 layers of cells with scattered microvilli at the apical surface, while at day 21 these formed a structural and functional barrier characterized by the presence of ciliated cells (note the cross-sections of the ciliary axonemes in the Figure, B) and secretory cells with a vesicle-enriched cytosol. In addition, junctional protein expression studies using immunofluorescence labeling showed that exposure to Ole e 1 did not disrupt barrier integrity, since no alterations were detected in the AJC structures in differentiating NHBE cells, apart from the variations between donors (Figure, C). At day 7 on ALI, in control and exposed NHBE cells, E-cad and ZO-1 (canonical proteins of adherens junctions [AJ] and tight junctions [TJ], respectively) were diffusely organized within the cytoplasm and at the plasma membrane, becoming localized in the plasma membrane at the cell-cell contact sites on day 21, thus indicating formation of AJCs. Western blot analysis confirmed that allergen exposure did not affect

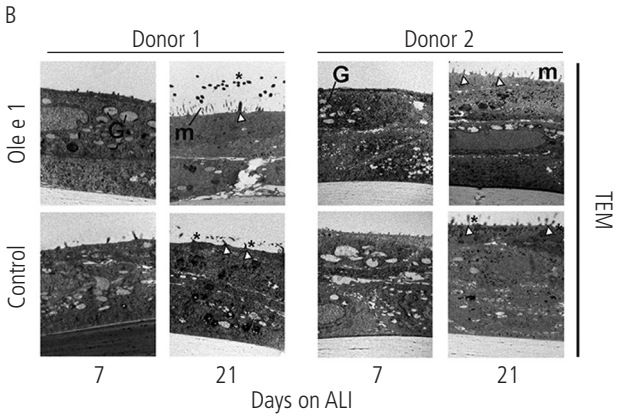

Figure, B. Exposure to Ole e 1 did not impair establishment of the epithelial barrier or apical junctional complex formation, although it did alter the cytokine secretion profile in differentiating NHBE cells from 2 donors at day 7 and 21 on ALI. TEM micrographs showing cilia and the axoneme (white arrowhead), microvilli (m), and goblet (G) cells. Note the cross-sections of the ciliary axoneme (*). Magnification, ×10-20K. ALI indicates air-liquid interface; TEM, transmission electron microscopy; NHBE, normal human bronchial epithelial cells.

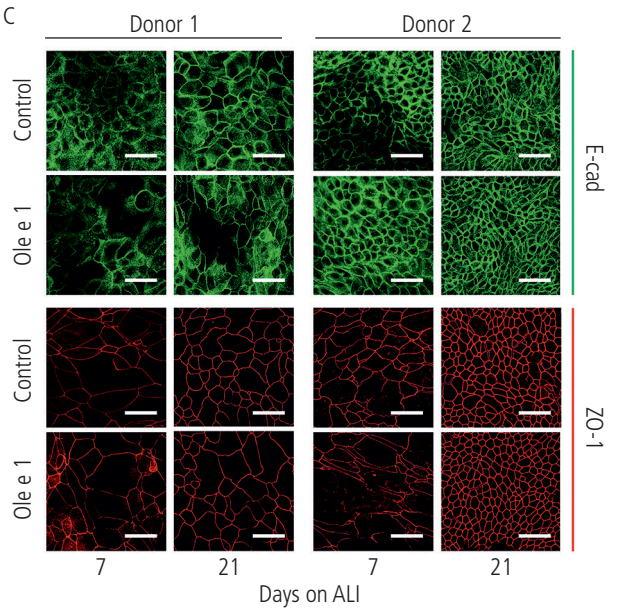

Figure, C. Exposure to Ole e 1 did not impair establishment of the epithelial barrier or apical junctional complex formation, although it did alter the cytokine secretion profile in differentiating NHBE cells from 2 donors at day 7 and 21 on ALI. Confocal laser scanning microscopy analysis for E-cadherin (green) and ZO-1 (red) proteins. Representative Z-stacks are shown. Scale bar = 25 µm. ALI indicates air-liquid interface; NHBE, normal human bronchial epithelial cells.

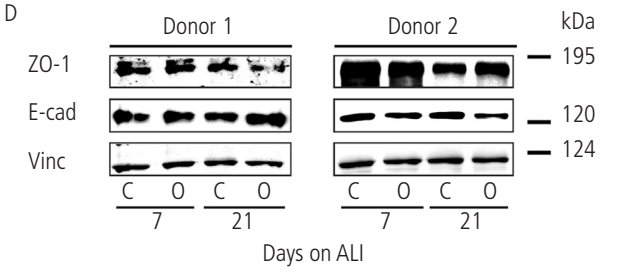

Figure, D. Exposure to Ole e 1 did not impair establishment of the epithelial barrier or apical junctional complex formation, although it did alter the cytokine secretion profile in differentiating NHBE cells from 2 donors at day 7 and 21 on ALI. Western blotting analysis for the expression of E-cadherin (E-cad) and ZO-1. Ole e 1–exposed cells (O) and control cells (C). Vinculin (Vinc) was used as a lane loading control. Molecular weights of proteins are indicated in kDa. Representative Western blotting of 2 replicates is shown. ALI indicates air-liquid interface; NHBE, normal human bronchial epithelial cells.

expression of major AJ and TJ proteins in the course of NHBE differentiation (Figure, D). Interestingly, protein levels of ZO-1 and E-cadherin were similar between day 7 and day 21 of NHBE differentiation, suggesting that the establishment of an epithelial barrier is more likely due to the reorganization of E-cadherin and ZO-1 into AJC structures than to an increase in their levels.

Moreover, the effect of exposure to Ole e 1 on the epithelial cell populations emerging from differentiating NHBE cells at the ALI was determined using polymerase chain reaction with specific cell type markers: *CC-10* for Club cells, *FOXJ1*

© 2018 Esmon Publicidad

E

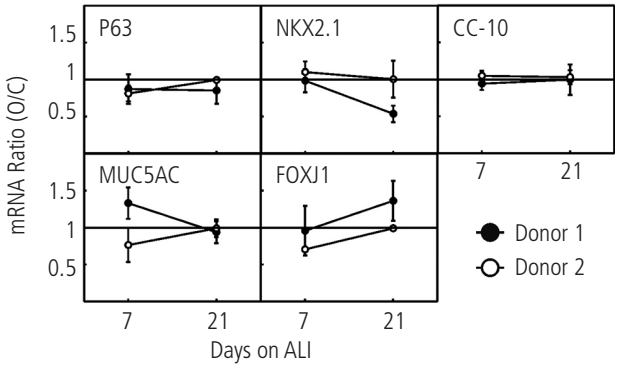

Figure, E. Exposure to Ole e 1 did not impair establishment of the epithelial barrier or apical junctional complex formation, although it did alter the cytokine secretion profile in differentiating NHBE cells from 2 donors at day 7 and 21 on ALI. mRNA levels of specific epithelial cell markers after exposure of NHBE cells to Ole e 1 (O) compared with control cells (C). Relative mRNA levels of CC-10 (Club cell), FOXJ1 (ciliated cells), MUC5AC (goblet cells), NKX2.1 (progenitor cells), and P63 (basal cells) were determined by semiquantitative reverse transcription polymerase chain reaction and expressed as a fold-change of control values after normalization using GAPDH as a housekeeping control. A ≥2-fold change was considered significant. Data shown are mean (SD) of 3 replicates. ALI indicates air-liquid interface; NHBE, normal human bronchial epithelial cells.

for ciliated cells, *MUC5AC* for goblet cells, *NKX2.1* as a lung-committed marker, and *P63* for basal cells (Figure, E). In control NHBE cells, the expression levels of *FOXJ1*, *MUC5AC*, and *NKX2.1* mRNA changed during the course of differentiation at the ALI. We did not observe significant alterations in any of the transcript levels studied upon exposure to Ole e 1, except for the decrease in *NKX2.1* mRNA levels at day 21 at the ALI in donor 1.

F

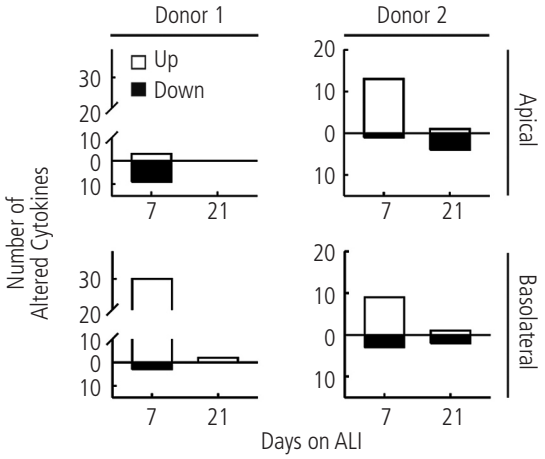

Figure, F. Exposure to Ole e 1 did not impair establishment of the epithelial barrier or apical junctional complex formation, although it did alter the cytokine secretion profile in differentiating NHBE cells from 2 donors at day 7 and 21 on ALI. Cytokine secretion profile as determined by antibody microarray analysis. Bar graphs indicate the number of significantly altered cytokines that displayed ≥2-fold changes compared with control cells in the apical and basolateral compartments of NHBE cultures. NHBE indicates normal human bronchial cells; TEER, transepithelial electrical resistance; TEM, transmission electron microscopy; ALI, air-liquid interface.

Finally, a RayBio Human Cytokine Antibody Array 5 (RayBiotech) analyzed with the GenePix Pro 7.1 software (Molecular Devices) was used to assess whether exposure to Ole e 1 affected the levels of cytokines secreted from differentiating NHBE cells (Figure, F). Interestingly, the number of altered cytokines secreted by undifferentiated cells (day 7 at the ALI) exposed to Ole e 1 was higher when compared with differentiated NHBE cells (day 21 at the ALI), which showed only a few modified mediators from both the apical and the basolateral sides of the culture, regardless of the donor (Online Supplementary Tables S1, S2, and S3). In general, undifferentiated cells displayed a greater number of upregulated cytokines on the basolateral side than on the apical side. These included cytokines that have been previously described in asthma and allergic inflammation. For example, there was a 7.82-fold increase in apical secretion of IP-10/CXCL10 in donor 1. Basolateral secretion of TARC/CCL17 was also upregulated (2.25-fold increase) in this donor. In contrast, the apical release of MCP-1 was upregulated (4.83-fold increase) after exposure to the allergen in donor 2. Thus, the altered cytokine profile obtained showed strong dependence on the donor. Only 3 cytokines were found to be shared by donor 1 and donor 2. IGFBP4 was upregulated, especially on the basolateral side (4.98-6.46-fold increase). Leptin secretion was upregulated on the basolateral and apical sides of donor 1 and donor 2, respectively; in contrast, MIG/CXCL9 was downregulated (0.29-0.39 fold increase) on the apical side. This finding suggests that cytokine outcomes may be related to the cellular state of differentiation at the time of allergen exposure, possibly owing to the significant changes in gene expression that take place during the differentiation process of NHBE cells [6,7]. The heterogeneity observed on the cytokines secreted by airway epithelial cells upon interaction with an allergen would provide a variety of microenvironments that support the activation/maturation of various immune cells and, consequently, the final host immune response. In addition, important differences in cytokine patterns were also observed between the 2 donors, both in the number and in the type of cytokine secreted, indicating that the response was also strongly influenced by donor features, as indicated in previous reports [8,9]. Interdonor variability is one of the main disadvantages of using primary NHBE cells cultured at the ALI for research, as it hinders interpretation of results. Thus, our study supports the idea that both the donor and the state of differentiation of bronchial epithelial cells have a major influence on the immune response to Ole e 1.

Disruption of airway epithelial AJCs by environmental proteases could facilitate penetration of the allergen through the epithelium and access to immune cells, thus contributing to the initiation and exacerbation of allergic diseases. Given that Ole e 1, which is not a protease, stimulated NHBE cells to release cytokines without disrupting epithelial integrity, it is likely that the mechanism involved in the sensitization and/or the development of allergic reactions to this allergen is protease-independent. A protease-independent mechanism has been described for several allergens, including allergens from pollens and house dust mite [10].

In this study, we demonstrated that Ole e 1 allergen induced the release of a plethora of cytokines from NHBE cells

 © 2018 Esmon Publicidad

cultured at the ALI, which is affected both by the differentiation status of the cells at the time of exposure and donor features. Additionally, our findings highlight the importance of using a well-characterized model of human airway for allergy-related research.

Supplementary data

Supplementary data are available at Journal of Investigational Allergology and Clinical Immunology online.

Acknowledgments

We thank Mª Luisa García and Ana Vicente from the ICTS National Electron Microscopy Center for assistance with electron microscopy and Sara Abián from the Complutense University for her excellent technical support.

Funding

The study was supported by grants from the Spanish Ministry of Economy and Competitiveness SAF2014-53209-R (MV and RB) and RIRAAF Network RD12/0013/0015 (MV) from the ISCIII. JCL-R is supported by an FPU fellowship from the Spanish Ministry of Education, Culture, and Sport.

Conflicts of Interest

The authors declare that they have no conflicts of interest.

Previous Presentations

Some of the data from this study were presented in poster format at the European Academy of Allergy and Clinical Immunology (EAACI) Congress, Vienna, Austria. June 2016

References

1. Hallstrand TS, Hackett TL, Altemeier WA, Matute-Bello G, Hansbro PM, Knight DA. Airway epithelial regulation of pulmonary immune homeostasis and inflammation. Clin Immunol. 2014;151:1-15.
2. Rezaee F, Georas SN. Breaking barriers: New insights into airway epithelial barrier function in health and disease. Am J Respir Cell Mol Biol. 2014;50:857-69.
3. Mattila P, Joenväärä S, Renkonen J, Toppila-Salmi S, Renkonen R. Allergy as an epithelial barrier disease. Clin Transl Allergy. 2011;1:5.
4. Loxham M, Davies DE, Blume C. Epithelial Function and Dysfunction in Asthma. Clin Exp Allergy. 2014;44:1299-313.
5. Bulek K, Swaidani S, Aronica M, Li X. Epithelium: the interplay between innate and Th2 immunity. Immunol Cell Biol. 2010;88:257-68.
6. Ross AJ, Dailey LA, Brighton LE, Devlin RB. Transcriptional profiling of mucociliary differentiation in human airway epithelial cells. Am J Respir Cell Mol Biol. 2007;37:169-85.
7. Martinez-Anton A, Sokolowska M, Kern S, Davis AS, Alsaaty S, Taubenberger JK, et al. Changes in microRNA and mRNA expression with differentiation of human bronchial epithelial cells. Am J Respir Cell Mol Biol. 2013;49:384-95.
8. Min KA, Rosania GR, Shin MC. Human airway primary epithelial cells show distinct architectures on membrane supports under different culture conditions. Cell Biochem Biophys. 2016;74:191-203.
9. Blume C, Davies DE. In vitro and ex vivo models of human asthma. Eur J Pharm Biopharm. 2013;84:394-400.
10. Kauffman HF, Tamm M, Timmerman JAB, Borger P. House dust mite major allergens Der p 1 and Der p 5 activate human airway-derived epithelial cells by protease-dependent and protease-independent mechanisms. Clin Mol Allergy. 2006;4:5.

Manuscript received July 18, 2017; accepted for publication January 14, 2018.

Eva Batanero
Departamento de Bioquímica y Biología Molecular I
Facultad de Ciencias Químicas
Universidad Complutense de Madrid
Madrid, Spain
E-mail: ebataner@ucm.es

© 2018 Esmon Publicidad

SUPPLEMENTAL TABLES

Effects of Ole e 1 allergen on human bronchial epithelial cells cultured at air-liquid interface (No. JIACI-D-17-00149)

Juan C. López-Rodríguez[1], Guillermo Solís-Fernández[1], Rodrigo Barderas[2], Mayte Villalba[1], Eva Batanero[1]

[1]Departamento de Bioquímica y Biología Molecular I, Facultad de Ciencias Químicas. Universidad Complutense de Madrid, Madrid (Spain)

[2]UFIEC, National Institute of Health Carlos III, Majadahonda, Madrid (Spain)

Corresponding author*:*

Eva Batanero (ebataner@ucm.es)

Departamento de Bioquímica y Biología Molecular I, Facultad de Ciencias Químicas. Universidad Complutense de Madrid, Madrid (Spain).

J Investig Allergol Clin Immunol 2018; Vol. 28(3)
doi: 10.18176/jiaci.0227

© 2018 Esmon Publicidad

Table S1. Differentially expressed cytokines in culture media of NHBE cells exposed to Ole e 1 at day 7 on ALI from Donor 1.

Cytokine	Description	Gene ID	UniProt Ref	Alternative name*	Side	Fold Change†
ANG	Angiogenin (EC 3.1.27.-)	283	P03950	ANG, RNASE5	Apical	0.49
BDNF	Brain-derived neurotrophic factor	627	P23560	Abrineurin	Basal	5.36
CCL23	Myeloid progenitor inhibitory factor 1	6368	P55773	MPIF, MIP3	Basal	2.05
Flt-3Ligand	Fms-related tyrosine kinase 3 ligand	2323	P49771	Flt3L	Basal	>10
Fracktalkine	Fractalkine (C-X3-C motif chemokine 1)	6376	P78423	CX3CL1, FKN	Basal	5.39
FGF4	Fibroblast growth factor 4	2249	P08620	HST-1	Apical	2.24
FGF6	Fibroblast growth factor 6	2251	P10767	HST2, HBGF-6	Basal	2.32
FGF7	Fibroblast growth factor 7	2252	P21781	KGF,HBGF7	Basal	2.95
FGF9	Fibroblast growth factor 9	2254	P31371	GAF, HBGF-9	Basal	4.23
GCP-2	Granulocyte chemotactic protein 2 (C-X-C motif chemokine 6)	6372	P80162	CXCL6	Basal	2.53
G-CSF	Granulocyte colony-stimulating factor (Pluripoietin)	1440	P09919	CSF3, C17orf3	Basal	0.01
HGF	Hepatocyte growth factor (Hepatopoietin-A)	3082	P14210	HPTA	Apical	0.5
IGFBP4	Insulin-like growth factor-binding protein 4	3487	P22692	IBP4	Apical/Basal	2.04/4.98
IL-1β	Interleukin-1 beta (IL-1 beta) (Catabolin)	3553	P01584	IL-1B, IL-1 F2	Basal	2.54
IL-5	Interleukin-5	3567	P05113	TRF	Apical/Basal	0.37/0.25
IL-7	Interleukin-7	3574	P13232		Apical/Basal	0.01/0.24
IL-15	Interleukin-15	3600	P40933		Basal	2.45
IL-16	Interleukin-16	3603	Q14005	LCF	Basal	3.16
IP-10	C-X-C motif chemokine 10 (10 kDa interferon gamma-induced protein)	3627	P02778	CXCL10, INP10	Basal	7.82
LEPTIN	Leptin (Obese protein)	3952	P41159	LEP	Basal	7.05
LIF	Leukemia inhibitory factor	3976	P15018	HILDA	Basal	8.08
LIGHT	Tumor necrosis factor ligand superfamily member 14	8740	O43557	TNFSF14	Basal	9.52
M-CSF	Macrophage colony-stimulating factor 1	1435	P09603	CSF1	Apical	0.32

© 2018 Esmon Publicidad

MCP-1	Monocyte chemoattractant protein 1	6347	P13500	CCL2, MCAF	Basal	2.53
MCP-4	Monocyte chemoattractant protein 4	6357	Q99616	CCL13	Basal	3.74
MDC	Macrophage-derived chemokine (C-C motif chemokine 22)	6367	O00626	CCL22	Apical	0.21
MIG	C-X-C motif chemokine 9 (Monokine induced by interferon-gamma)	4283	Q07325	CXCL9	Apical/Basal	0.29/>10
MIP-1δ	C-C motif chemokine 15 (Chemokine CC-2)	6359	Q16663	CCL15, MIP5	Apical	0.5
OPG	Tumor necrosis factor receptor superfamily member 11B (Osteoprotegerin)	4982	O00300	TNFRSF11B	Basal	5.89
OPN	Osteopontin (Bone sialoprotein 1)	6696	P10451	SPP1, BNSP	Basal	5.21
PARC	Pulmonary and activation-regulated chemokine	6362	P55774	CCL18, AMAC-1	Apical/Basal	2.63/6.02
PDGF BB	Platelet-derived growth factor subunit B	5155	P01127	PDGFB, PDGF2	Basal	4.33
PLGF	Placenta growth factor	5228	P49763	PGF, PGFL	Basal	3.73
RANTES	C-C motif chemokine 5 (Eosinophil chemotactic cytokine)	6352	P13501	CCL5	Apical	0.45
SDF-1	Stromal cell-derived factor 1 (C-X-C motif chemokine 12)	6387	P48061	CXCL12 alpha	Basal	2.38
TARC	Thymus and activation-regulated chemokine (C-C motif chemokine 17)	6361	Q92583	CCL17, SCYA17	Basal	2.25
TGFβ1	Transforming growth factor beta-1	7040	P01137	LAP	Basal	2.45
TGFβ2	Transforming growth factor beta-2	7042	P61812	BSC-1, G-TSF	Basal	3.07
TGFβ3	Transforming growth factor beta-3	7043	P10600		Basal	2.55
VEGF	Vascular endothelial growth factor A	7422	P15692	VEGFA	Basal	2.07

*Alternative names are used for a protein (UniProt accesion number).

[†]Values over 2-fold changes were considered biological relevant. Those values with fold changes higher than 10 are represented as >10-fold change. Since it is a semi-quantitative technique, >10-fold change probably is more likely to be an actual change.

© 2018 Esmon Publicidad

Table S2. Differentially expressed cytokines in culture media of NHBE cells exposed to Ole e 1 at day 7 on ALI from Donor 2.

Cytokine	Description	Gene ID	UniProt Ref	Alternative name*	Side	Fold Change†
I-309	C-C motif chemokine 1 (Small-inducible cytokine A1)	6346	P22362	TCA3, CCL1	Apical	3.83
IGFBP4	Insulin-like growth factor-binding protein 4	3487	P22692	IBP4	Apical/Basal	2.80/6.46
IFNγ	Interferon gamma	3458	P01579	IFNG	Apical/Basal	2.04/5.53
IL-1α	Interleukin-1 alpha (Hematopoietin-1)	3552	P01583	IL-1A, IL-1 F1	Apical	3.57
IL-2	Interleukin-2	3558	P60568	TCGF	Basal	2.60
IL-4	Interleukin-4	3565	P05112	BSF1, Pitrakinra	Apical/Basal	2.12/2.70
IL-5	Interleukin-5	3567	P05113	TRF	Basal	2.58
IL-6	Interleukin-6	3569	P05231	BSF2, CDF	Basal	2.84
IL-7	Interleukin-7	3574	P13232		Basal	2.23
IL-10	Interleukin-10	3586	P22301	CSIF	Apical/Basal	>10/3.92
IL-12p40/70	Interleukin-12 subunit alpha	3592	P29459	NKSF1, IL-12A	Apical	4.33
IL-13	Interleukin-13	3596	P35225	NC30	Basal	4.53
IL-15	Interleukin-15	3600	P40933		Apical	4.41
LEPTIN	Leptin (Obese protein)	3952	P41159	LEP	Apical	4.77
MCP-1	Monocyte chemoattractant protein 1	6347	P13500	CCL2, MCAF	Apical	4.83
MCP-2	Monocyte chemoattractant protein 2	6355	P80075	CCL8	Apical/Basal	3.30/0.44
MCP-3	Monocyte chemoattractant protein 3	6354	P80098	CCL7, MARC	Apical	3.18
MIG	C-X-C motif chemokine 9 (Monokine induced by interferon-gamma)	4283	Q07325	CXCL9	Apical/Basal	0.39/0.02
MIP-1δ	C-C motif chemokine 15 (Chemokine CC-2)	6359	Q16663	CCL15, MIP5	Apical	3.57
SDF-1	Stromal cell-derived factor 1 (C-X-C motif chemokine 12)	6387	P48061	CXCL12 alpha	Basal	0.15

*Alternative names are used for a protein (UniProt accesion number).

†Values over 2-fold changes were considered biological relevant. Those values with fold changes higher than 10 are represented as >10-fold change. Since it is a semi-quantitative technique, >10-fold change probably is more likely to be an actual change.

© 2018 Esmon Publicidad

Table S3. Differentially expressed cytokines in culture media of NHBE cells exposed to Ole e 1 at day 21 on ALI from Donors 1 and 2.

Cytokine	Description	Gene ID	UniProt Ref	Alternative name*	Side	Fold Change†
IGFBP1[1]	Insulin-like growth factor-binding protein 1	3484	P08833	IGF1, IBP1	Basal	2.16
MIP-3α[1]	Macrophage inflammatory protein 3 alpha	6364	P78556	CCL20, LARC	Basal	2.52
FGF7[2]	Fibroblast growth factor 7	2252	P21781	KGF,HBGF7	Apical	0.5
GROα[2]	Growth-regulated alpha protein (C-X-C motif chemokine 1)	2919	P09341	CXCL1, NAP3	Basal	0.37
I-309[2]	C-C motif chemokine 1 (Small-inducible cytokine A1)	6346	P22362	TCA3, CCL1	Basal	0.46
IL-4[2]	Interleukin-4	3565	P05112	BSF1, Pitrakinra	Apical	0.35
IL-6[2]	Interleukin-6	3569	P05231	BSF2, CDF	Basal	>10
MCP-1[2]	Monocyte chemoattractant protein 1	6347	P13500	CCL2, MCAF	Apical	0.38
MIG[2]	C-X-C motif chemokine 9 (Monokine induced by interferon-gamma)	4283	Q07325	CXCL9	Apical	4.32
TGFβ1[2]	Transforming growth factor beta-1	7040	P01137	LAP	Apical	0.48

*Alternative names are used for a protein (UniProt accesion number.)

†Values over 2-fold changes were considered biological relevant. Those values with fold changes higher than 10 are represented as >10-fold change. Since it is a semi-quantitative technique, >10-fold change probably is more likely to be an actual change.

[1]Donor 1 and[2]Donor 2.

© 2018 Esmon Publicidad